UNCLASSIFIED

AD NUMBER

AD492300

NEW LIMITATION CHANGE

TO

Approved for public release, distribution unlimited

FROM

Distribution authorized to U.S. Gov't. agencies and their contractors; Administrative/Operational use; 20 July 1951. Other requests shall be referred to Naval Ordnance Systems Command, Washington DC.

AUTHORITY

DoDD 5230.24, 18 Mar 1987

THIS PAGE IS UNCLASSIFIED

[redacted]

NTIS

NAVORD REPORT 1493

Cop. 10

AD-49 2300

THE MATHEMATICAL THEORY OF AIRBORNE FIRE CONTROL

This document [illegible] for public release [illegible] distribution is unlimited.

A BUREAU OF ORDNANCE PUBLICATION

OCT 22 1952

NAVORD REPORT 1493

THE MATHEMATICAL THEORY OF AIRBORNE FIRE CONTROL

BY

KAJ L. NIELSEN, Ph.D.
Head, Mathematics Division,
U. S. NAVAL ORDNANCE PLANT, INDIANAPOLIS

and

JAMES F. HEYDA, Ph.D.
Assistant Head, Mathematics Division,
U. S. NAVAL ORDNANCE PLANT, INDIANAPOLIS

For sale by the Superintendent of Documents, U. S. Government Printing Office, Washington 25, D. C. — Price $2.00

20 July 1951

DEPARTMENT OF THE NAVY
BUREAU OF ORDNANCE
WASHINGTON 25, D. C.

20 July 1951

NAVORD REPORT 1493

THE MATHEMATICAL THEORY OF AIRBORNE FIRE CONTROL

1. NAVORD Report 1493 presents, in unclassified form, the mathematical theory of aircraft fire control as developed in the present state of the art. It is intended that this book will serve as a basic text for use by schools or individuals desiring background theory in the field of aircraft fire control.

2. This publication does not supersede any existing publication.

E. M. BLOCK
Head of Aviation Ordnance Branch
Research and Development Division
Bureau of Ordnance
Navy Dept., Washington, D. C.

CONTENTS

Chapter		Page
	PREFACE	xiii
1.	AEROBALLISTICS	1

PART 1. REVIEW OF FUNDAMENTALS

1.1	Introduction	1
1.2	The Coordinate Systems	1
1.3	The Trajectory	2
1.4	The General Problem of the Trajectory	3
1.5	The Force System	5
1.6	The Stability of the Projectile	7
1.7	The Equations of Motion	8
1.8	The Siacci Method	9

PART 2. THE BALLISTICS OF AERIAL GUNNERY

1.9	Aerial Gunnery	11
1.10	Dimensionless Ballistic Coefficient	15
1.11	The Motion of Small Arms Projectiles Fired from Aircraft	16
1.12	Ballistic Computations for Aerial Gunnery	23
1.13	Bullet Firing Tables	25
1.14	Bomb Ballistics	27
1.15	Rocket Ballistics	27
2.	DEFLECTION THEORY FOR AIR-TO-AIR GUNNERY	29
2.1	Introduction	29
2.2	Actual and Relative Motions	29
2.3	Fixed Gun-Platform — Linear Target Motion	30
2.4	Moving Gun-Platform — Fixed Target	31
2.5	Moving Gun-Platform — Moving Target on a Straight Line	32
2.6	Kinematic Lead and Bullet Trail	35
2.7	Determination of the Kinematic Lead	37
2.8	The General Case in Three-Dimensional Space	38
2.8.1	Introduction	38
2.8.2	The Muzzle Velocity Vector V_0	38
2.8.3	An Expansion for the Projectile Range R	39
2.8.4	Lead Equation in Vector Form	40
2.8.5	The Ballistic Factors q and l	41
2.8.6	The Terms Containing V_G and Q in Equation (2.43)	41
2.8.7	Resolution of the Ownship Velocity Relative to the Ownship Axes	42
2.8.8	The Windage Jump Vector J	43
2.8.9	Lead Angle Equations for Azimuth-Elevation Top Deck Turret	45
2.9	An Example	51

Chapter *Page*

3. PURSUIT COURSES 57
3.1 Introduction 57
3.2 The Space Course for a Pure Pursuit Attack 57
3.3 The Space Course for a Lead Pursuit Attack 64
3.4 Equations of the Relative Course 65
3.5 Time as a Parameter 72
3.6 The Acceleration of the Fighter Caused by the Curvature of His Space Course 73
3.6.1 Maximum Acceleration 76
3.7 Aerodynamic Pursuit Course 77
3.8 Attack in a Vertical Plane 77
3.9 The Determination of the Aircraft Constants 80
3.10 Dimensionless Form 82
3.11 Examples 82
3.12 The Three-Dimensional Equations 89
3.13 Minimum Radius of Turn 91
3.14 Collision or Interception Courses 93

4. THEORY OF LEAD COMPUTING SIGHTS 97
4.1 Introduction 97
4.2 Essential Elements of a Fire Control System 97
4.3 Disturbed and Director Systems 97
4.4 Types of Tracking Controls and Their Peculiarities 98
4.5 Smoothing of Input Data 99
4.6 A Generic Lead Formula for the Coplaner Case 101
4.7 The Basic Differential Equation of a Typical Gyro Sight 102
4.8 Solving the Basic Equation — Interpretation 104
4.9 Transient Behavior 105
4.10 Operational Stability 105
4.11 Amplification of Gun Motion with Respect to Sight Motion 106
4.12 Choice of the Sight Parameter $\underline{a}$ 107
4.13 The Basic Differential Equation Including Trail 107

5. GYROSCOPIC LEAD COMPUTING SIGHTS 111
5.1 Some Preliminary Ideas from Dynamics 111
5.2 Theory of the Gyroscope 112
5.3 Use of a Gyro to Produce Kinematic Lead 116
5.4 The Eddy-Current Constrained Gyro 116
5.5 An Optical Linkage 119
5.6 Free, Constrained, and Captured Gyros and Their Uses 122

6. BOMBING 123
6.1 Introduction 123

A. HIGH-LEVEL BOMBING
6.2 Vacuum Trajectory 123
6.3 Air Trajectory Under No Wind 125
6.4 Drift and Target Motion 128
6.5 Mechanization 130

Chapter *Page*

B. LOW-LEVEL BOMBING
6.6 Impracticability in Range Angle Aiming at Low Altitudes 130
6.7 The Angular Rate Principle 131
6.8 Mechanization 132

C. DIVE OR GLIDE BOMBING
6.9 Introduction 132
6.10 Angular Rate of Sight Line (Vacuum Case) 133
6.11 Mechanization, Using Angular Rate 134
6.12 Correction of Angular Rate for Trail 134

D. TOSS BOMBING
6.13 Basic Release Conditions for a Stationary Target 135
6.14 An Approximate Solution for the Release Time 138
6.15 Air Resistance in Toss Bombing 141

7. ROCKETRY 145
7.1 Introduction 145
7.2 Methods of Launching Airborne Rockets 145
7.3 Coordinate Systems 146
7.4 Qualitative Discussion of Trajectories 147
7.5 Illustrations of the Effects on Rocket Trajectories 151
7.6 The Sighting Problem 161
7.7 Determination of Sighting Tables 166
7.8 Basic Principles of a Rocket Sight 168
7.9 A Rocket Sight Based on Equation (7.25) 168
7.10 A Rate Gyro Rocket Sight 171
7.11 General Theory of Rocket Tossing 172
7.12 A Specialized Equation for Pull-up Time in Rocket Tossing 175
7.13 Rocket Tossing with no Time Delay 178
7.14 Spin-Stabilized Aircraft Rockets 179
7.15 Air-to-Air Rocketry 179

8. GLOSSARY OF NOTATION 181
8.1 Introduction 181
8.2 General Definitions 181
8.3 Definitions of Symbols for Chapter 1 182
8.4 Definitions of Symbols for Chapter 2 184
8.5 Definitions of Symbols for Chapter 3 186
8.6 Definitions of Symbols for Chapter 4 187
8.7 Definitions of Symbols for Chapter 5 188
8.8 Definitions of Symbols for Chapter 6 189
8.9 Definitions of Symbols for Chapter 7 191

Appendix A. VECTOR OPERATIONS 193
A.1 Vector Algebra — Addition and Subtraction 193
A.2 Vector Algebra — Scalar and Vector Products 194
A.3 Vector Calculus — The Derivative 195
A.4 Time Derivative of a Vector Referred to a Rotating Frame of Reference 196

Chapter *Page*

Appendix B. CONVERSION TABLES 198

B.1 Introduction 198
Conversion Table — Knots to MPH to FT/SEC 198
Conversion Table — MPH to FT/SEC to KNOTS 199
Conversion Table — FT/SEC to MPH to KNOTS 199
Conversion Table — DEGREES to MILS 200
Conversion Table — MILS to DEGREES 201
Constants 202
Chart of Altitude Versus Speed 203
Nomogram for Calculating Rate of Decrease of Aititude in a Dive 204

BIBLIOGRAPHY 205

ILLUSTRATIONS

Figure		Page
1.	The Aeroballistic Problem	xiv
2.	Coordinate System	1
3.	Coordinate Systems	2
4.	Trajectories	3
5.	Trajectory Showing Deflection	4
6.	Plane of Yaw	5
7.	Forces Acting on a Projectile	6
8.	The Force System of a Top	6
9.	Pseudo Velocity	10
10.	Aeroballistics	11
11.	Spherical Δ on Unit Sphere	13
12.	Vector Diagram of V_ω, u_ω, V_G	13
13.	Bullet Coordinates	14
14.	Lateral and Vertical Deflections	15
15.	Vibration Motion	17
16.	Initial Conditions of Vibratory Motion	18
17.	i_1, i_2 — System	20
18.	Direction Cosines of $u_{\omega F}$	23
19.	Air-to-Air Gunnery	28
20.	Air Courses of Gun and Target	29
21.	Path of T Relative to G	30
22.	Fixed Gun vs. Moving Target	30
23.	Moving Gun vs. Fixed Target	32
24.	Moving Gun vs. Rectilinear Target Motion	33
25.	Determination of ω and $\dot{r}$	34
26.	Ballistic Deflections	35
27.	Aereal Approximation	37
28.	Siacci Coordinates	38
29.	Gun and Target Space Paths	39
30.	First and Second Order Bias Errors	40
31.	Ownship Axes	42
32.	Attack and Skid Angles	42
33.	Initial Yaw Angle	44
34.	The General Case in Three Dimensions	44
35.	Right Spherical Triangle	45
36.	Orientation of the Unit Vector **n**	47
37.	Resolution of the Vector $\mathbf{e}_0$	48
38.	Particular Case — Computation of Lead Angles	51
39.	Fundamental Angles	53
40.	Pursuit Course	56
41.	Coordinates	58
42.	Coordinates for Pure Pursuit	59
43.	Pure Pursuit Course Example	61
44.	Vector Diagram	63
45.	Polar Coordinate System for a Deviated Pursuit	64
46.	Vector Diagram	65
47.	Ballistic Triangle	68

Figure *Page*
48. Pure Pursuit Course Example 70
49. Lead Pursuit Course Example 72
50. Acceleration Circles 75
51. Force Diagram 78
52. Angles for Pure Pursuit 79
53. Velocity Diagram 80
54. Initial Value of γ — Example 1 84
55. Aerodynamic Lead Pursuit Course Example 85
56. Initial Value of γ — Example 2 87
57. Aerodynamic Lead Pursuit Course Example 88
58. A Three-Dimensional Situation 89
59. Force System 90
60. Force System 91
61. Buffet Region 92
62. Minimum Radius of Turn 93
63. Collision Course 94
64. Collision Course Example 95
65. Lead Computing Sight 96
66. Director System 97
67. Disturbed System 98
68. Graph of the Weight Function $e^{t/K}$ 100
69. The Kinematic Lead 102
70. The Gyro Axis as a Computing Line 103
71. Ballistic, Kinematic, and Total Lead Angles 108
72. Gyroscopic Lead Computing Sight 110
73. Moment of a Force About a Point 111
74. Rotating Solid of Revolution 112
75. Circular Disk Gyroscope 113
76. Gyroscopic Precession 113
77. Use of a Rate Gyro to Determine Lead 115
78. Using Fixed Reference Line 115
79. The Gyro Axis as a Computing Line 115
80. Gyro Dome, Axle, and Mirror 117
81. Motion of Gun with Respect to Gyro Spin Axis 117
82. Precessing Forces Introduced Electromagnetically 118
83. Optical System of the Sight Head 119
84. Reticle and Stadiametric Ranging Disk — Radial Slits 121
85. Reticle and Stadiametric Ranging Disk — Spiral Slits 121
86. Stadiametric Ranging 121
87. Geometry of Stadiametric Ranging 121
88. Dive Bombing 123
89. Glide Bombing 123
90. Vacuum Trajectory — Bomb 124
91. Vacuum and Air Trajectories — Bomb 125
92. The Bombing Mil 127
93. Drift Angle and Trail 128
94. The Bombing Problem — Three-Dimensional View 129
95. Low-Level Bombing 131
96. Dive Bombing 133

Figure		Page
97.	Toss Bombing	136
98.	Air and Vacuum Trajectories	141
99.	Complex Armament Installation	144
100.	Coordinate System	146
101.	Angle of Attack	147
102.	Drop-Launching Conditions	149
103.	Retro-Launching Conditions	150
104.	Gravity Drop Comparison	151
105.	Effect of Dive Angle	152
106.	Effect of Launching Speed	153
107.	Range Misestimation	154
108.	Effect of Rocket Temperature	155
109.	Effective Launcher Line in Lateral Plane	156
110.	Skid	157
111.	Effect of Angle of Attack	157
112.	Nosing Over or Pulling Up	158
113.	Curve of Approach	159
114.	Wind and Target Motion	160
115.	Trajectory Drop, ψ	161
116.	Rate of Change of σ	162
117.	Target Moving in Range	164
118.	Kinematic Lead — Stationary Target	165
119.	Azimuth Target Motion	166
120.	Voltage Computer — Wiring Diagram	169
121.	Instantaneous Diagram for the Sighting Problem — Elevation Plane (Magnitude of Angles are Exaggerated)	170
122.	Rocket Tossing (Greatly Exaggerated)	173
123.	Velocity Diagram at D	175
124.	Rocket Tossing with No Time Delay	177
125.	Vector Parallelogram	193
126.	Scalar Triple Product	195
127.	Vector Differentiation	195
128.	Unit Vector and Its Derivative	196
129.	Time Derivative of a Vector Referred to a Rotating Frame	197
130.	Airspeed vs. Altitude	203
131.	Nomogram for Calculating Rate of Decrease of Altitude in a Dive	204

PREFACE

This book is a consolidation of the tremendous amount of work done on the subject during World War II by innumerable investigators. It may be used as a basic text on aviation fire control principles for use in the training of officers in the military academies, in ordnance courses of Reserve Officers' Training Programs at universities and colleges, and in indoctrination courses at Armed Forces line schools. It also may be used to great advantage by scientists and engineers engaged in research and development in the field of aviation fire control in military establishments and in the laboratories of academic or industrial institutions under the auspices of the government.

The text presupposes a knowledge by the reader of the mathematics taught in the usual undergraduate college calculus course. A familiarity with vector analysis also is desirable in following the development of the theory but is not essential to an understanding of the principles and the conclusions. The main vector operations employed in this text are defined and briefly explained in Appendix A.

The specialized nomenclature and notation adopted in this book represent a deliberate attempt at much-needed standardization in this branch of military science and considerable effort has been expended in endeavoring to harmonize the conflicting opinions and usages encountered among the various principals and pioneers. The commonly accepted standard mathematical symbolization has been adhered to generally and any deviation rigorously defined. Numerous diagrams and examples have been freely included to illustrate important concepts.

It is to be noted that this book does not, as a good text book should, contain problems the solution of which is designed to impress upon the student the principles expounded. The omission is partly motivated by expedience but is mainly the result of the authors' opinion that the instructors using the book as a text would be in the best position to formulate problems commensurate with students' requirements and available time. It is hoped that such problems can eventually be compiled, to provide a sequel to this volume.

This text, like most comprehensive text books, includes the work of many contributors to the theory. Although the authors are among the list of contributors, their present role is chiefly that of expositors. In the exercise of this function, it is impracticable to make specific acknowledgment of the contributions of the large number of scientists who played a part in the development of the theory of aviation fire control, since most of their work was done, and its publication remains, under military security regulations which restrict dissemination of the information. It is, accordingly, with regret that only passive credit can be accorded these anonymous scientists who contributed so much both to the theory and the military applications, and whose original work has been "borrowed" in writing this book.

It is possible, however, to give credit to those who gave direct aid in the preparation of this book. Thus, the authors gratefully acknowledge their indebtedness to their associates in the Research Department at the Naval Ordnance Plant in Indianapolis for their criticisms and suggestions and to the officials in the Bureau of Ordnance for their encouragement and cooperation. In particular, the authors are grateful to Dr. L. E. Ward of the Naval Ordnance Test Station at Inyokern, California, and Dr. Martha Cox of the Naval Ordnance Plant, Indianapolis, who contributed much to the original manuscript. They also are indebted to Mrs. Mary Kelso and Mrs. Nannie Twineham who did most of the computational work and to Mrs. Janet Edwards and Mrs. Eunice Stultz who prepared the manuscript.

J. F. HEYDA.
K. L. NIELSEN.

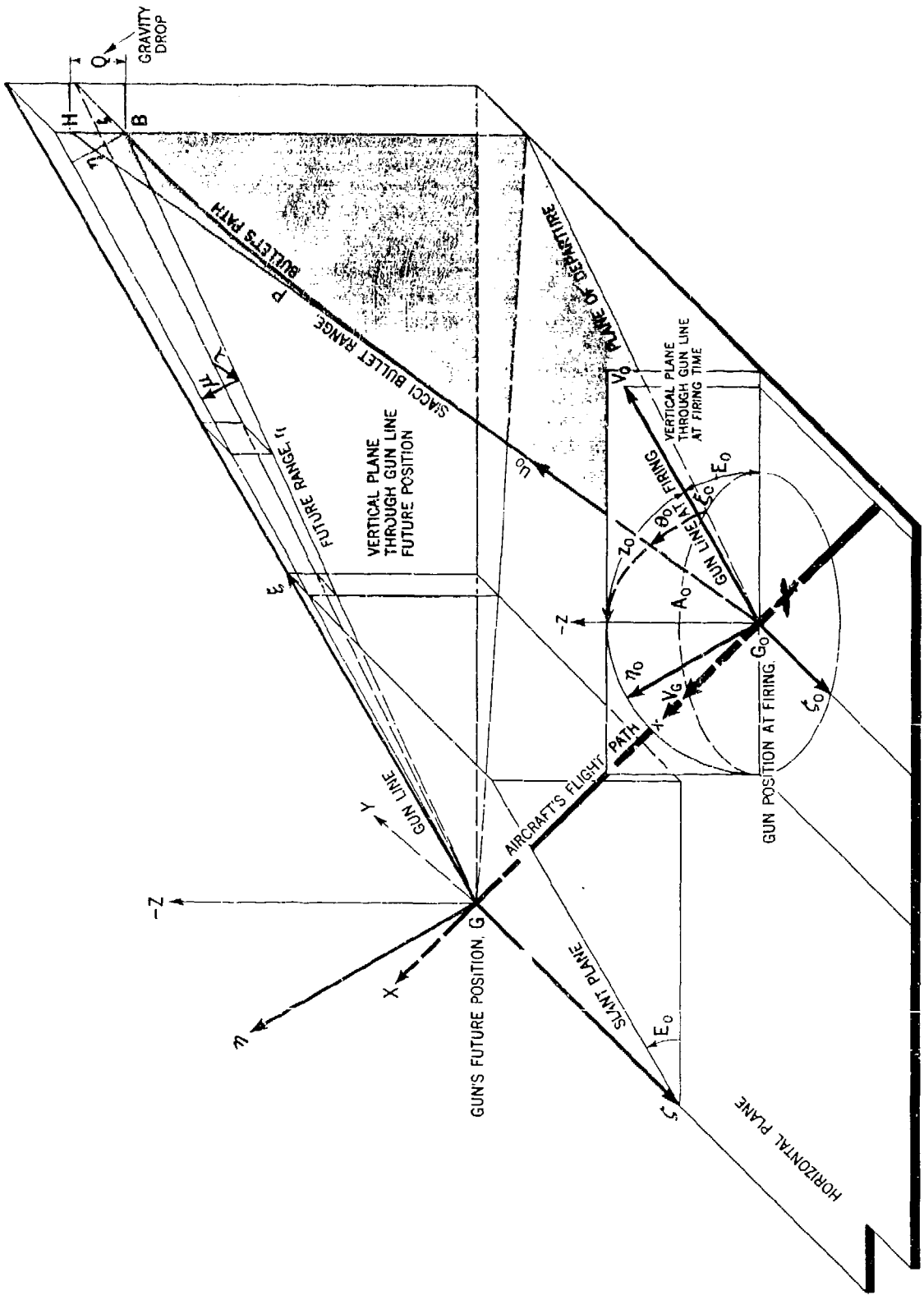

Figure 1. — The Aeroballistic Problem

Chapter I

AEROBALLISTICS

PART I. REVIEW OF FUNDAMENTALS

1.1 Introduction

In order to aim a projectile toward a point so that it will collide with a target at that point, it is necessary to know the motion of the projectile as it travels the required distance to the point. Ballistics is the science which is concerned with the motion of projectiles. It is, therefore, appropriate to begin the theory of fire control with a consideration of ballistics. The theory of ballistics is usually separated into two distinct parts:

(1) Interior ballistics, which is concerned with the motion of the projectile while it is still in the bore of the gun.

(2) Exterior ballistics, which is concerned with the motion of the projectile after it leaves the muzzle.

Although no discussion can be complete without considering both parts, in the theory of fire control we are primarily interested in exterior ballistics.

In fire control theory the term projectile may refer to any missile such as a bullet, rocket, bomb, etc., which is projected at a target. The projecting mechanism will henceforth be called the gun. Since the motion of a projectile depends upon many factors such as its shape, size, weight, initial and subsequent velocities, etc., any general theory of the motion of projectiles must be specialized for particular projectiles. The clearest approach is to develop the theory for bullets and make the necessary changes for rockets, bombs, and other projectiles.

A detailed treatment of the theory of ballistics is beyond the scope of this book. This chapter will consider only the fundamental principles and will indicate methods for the determination of the necessary data. Since this book is primarily concerned with airborne fire control, all computations will be specialized to aerial gunnery and the ballistics for aerial gunnery will henceforth be termed Aeroballistics.

1.2 The Coordinate Systems

In order to describe the motion of a projectile it is necessary to have a reference coordinate system. Let X, Y, Z be a right-hand set of mutually orthogonal axes with their origin at the muzzle of the gun and such that the (X,Y)-plane is horizontal and the Z-axis points vertically downward. This rectangular coordinate system is shown in figure 2.

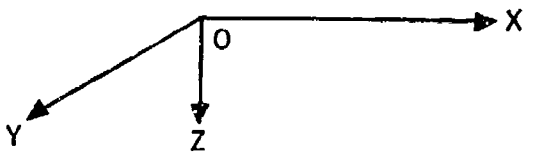

Figure 2. — Coordinate System

If the gun is mounted in a moving aircraft, this rectangular coordinate system is then moving with the gun and its axes can be defined more closely as follows:

the X-axis coincides with the Armament Datum Line and is positive forward;

the Y-axis coincides with the aircraft's lateral axis and is positive along the starboard wing;

the Z-axis coincides with the aircraft vertical axis and is positive downward.

The motion of the projectile can be described in terms of its (X,Y,Z) coordinates. However, if the gun is moving it also is necessary to have a coordinate system which is fixed in the air mass at the instant of fire. Let x, y, z be a set of axes parallel to X, Y, Z but at rest in the air mass and such that the origins of the two systems coincide at the instant of projectile release. For a gun located on the surface of the earth, the (x,y)-plane is tangent to the earth at the origin and is often called the datum plane.

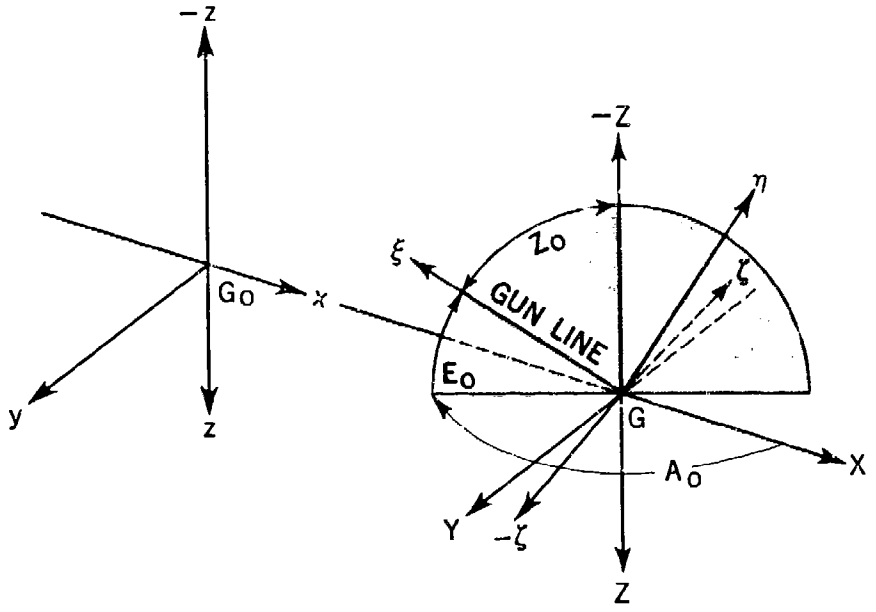

Figure 3. — Coordinate Systems

It is convenient to have still a third set of rectangular axes, ξ, η, ζ, moving with the gun and such that:

- ξ is along the gun bore axis;
- η is in a vertical plane through the gun bore axis and directed away from the ground; and,
- ζ is in a horizontal plane and directed so that the ordered set $|\xi, \eta, \zeta|$ forms a right-handed system of coordinates.

All three coordinate systems are shown in figure 3. The airplane is assumed to be flying in a horizontal plane and the angle of attack of the Armament Datum Line is ignored. The restrictions imposed by these assumptions will be discussed in section 1.9, Aerial Gunnery.

The above choice of systems of coordinate axes differs from the usual choice employed in surface ballistics. However, it coincides with the adopted standards in the discussions of aircraft theories and, since we are primarily concerned with aeroballistics, it is thought to be an advantageous system. It is hoped that this change of notation will not cause too much confusion for the student of ballistics.

1.3 The Trajectory

The trajectory is the curve in space traced by the center of gravity of the projectile as it moves through the air. The origin of the trajectory is the position of the center of gravity of the projectile at the instant of release. The tangent to the trajectory at its origin is the line of departure, and the vertical plane through the line of departure is the plane of departure. The angle that the line of departure makes with the horizontal is the initial angle of inclination of the trajectory and is also called the angle of departure; it is denoted by θ_o.

If the coordinates of the center of gravity of the projectile are specified uniquely at any time t after release, the trajectory is completely described. Thus the trajectory is defined by

$$X = X(t)$$
$$Y = Y(t)$$
$$Z = Z(t)$$

where $X(t)$, $Y(t)$, $Z(t)$ denote functions of time t. These functions must, of course, be zero when $t = 0$. The coordinates of the center of gravity of the projectile may be expressed in terms of the coordinate systems (X, Y, Z) or (ξ, η, ζ), but, for reference to inertial space, these coordinates must be transformed to the space coordinates x, y, z.

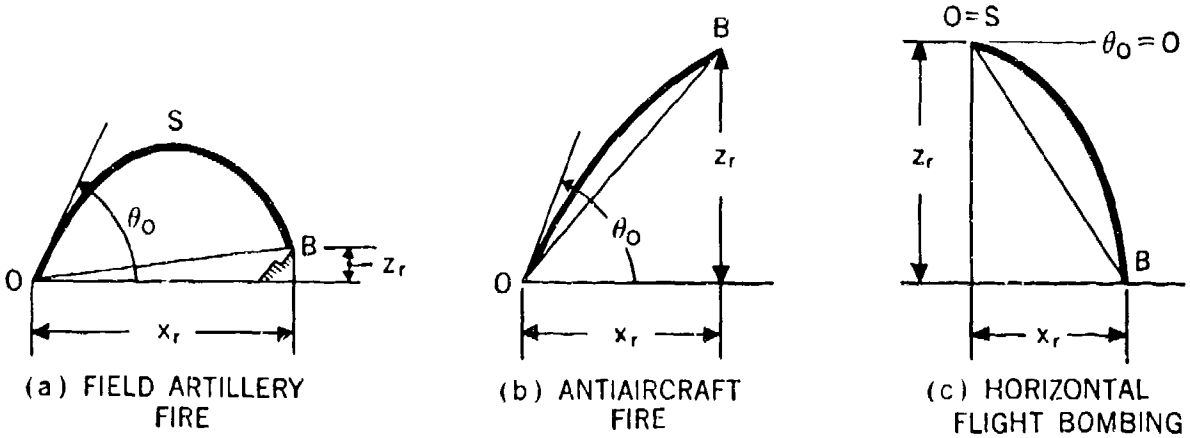

Figure 4. — Trajectories

In general, there are four factors which determine the trajectory:

(a) The position of the origin,
(b) the conditions of projection,
(c) the ballistic characteristics of the projectile, and
(d) the characteristics of the air through which it passes.

The projections on the plane of departure of three typical trajectories are illustrated in figure 4, where (a) shows field artillery fire, (b) antiaircraft fire, and (c) horizontal flight bombing.

If we limit our attention to the plane of departure and consider it to be coincident with the x, z-plane, the following quantities are often referred to as the elements of the trajectory.

O — the origin.
B — the point of impact or the point of burst.
S — the summit of the trajectory.
OS — the ascending branch.
SB — the descending branch.
OB — the slant range.
θ_0 — the initial angle of inclination.
x_r — the horizontal range.
z_r — the altitude of impact.

It is to be noted that in antiaircraft fire the projectile usually bursts before the summit is reached and thus the entire trajectory is in the ascending branch. In horizontal bombing, the summit is the origin of the trajectory and the entire trajectory is in the descending branch.

Figure 4 shows only the projections on the plane of departure, taken to be the (x, z)-plane for these illustrations. Actually, the trajectory may not lie entirely in this plane but also may have a projection in the (x,y)-plane. The y value at the point of impact, y, is called the deflection and that part of it which is not due to the wind is called drift. The three-dimensional picture is illustrated in figure 5.

1.4 The General Problem of the Trajectory

The calculation of the trajectory of a projectile of given characteristics under given initial conditions forms the primary problem of exterior ballistics. In order to state the problem specifically let us consider a stationary gun and let the gun bore axis lie in the (x,z)-plane. Let us further adopt the following notation.

(x, y, z) = Coordinates of the center of gravity of the projectile at any time t.
(x_0, y_0, z_0) = initial values; i.e., at $t = O$.
θ_0 = initial angle of inclination, angle from x-axis to the line of departure.
v_0 = initial velocity of the projectile.
v_x, v_y, v_z = components of the projectile velocity in the directions of the coordinate axes at any time t.

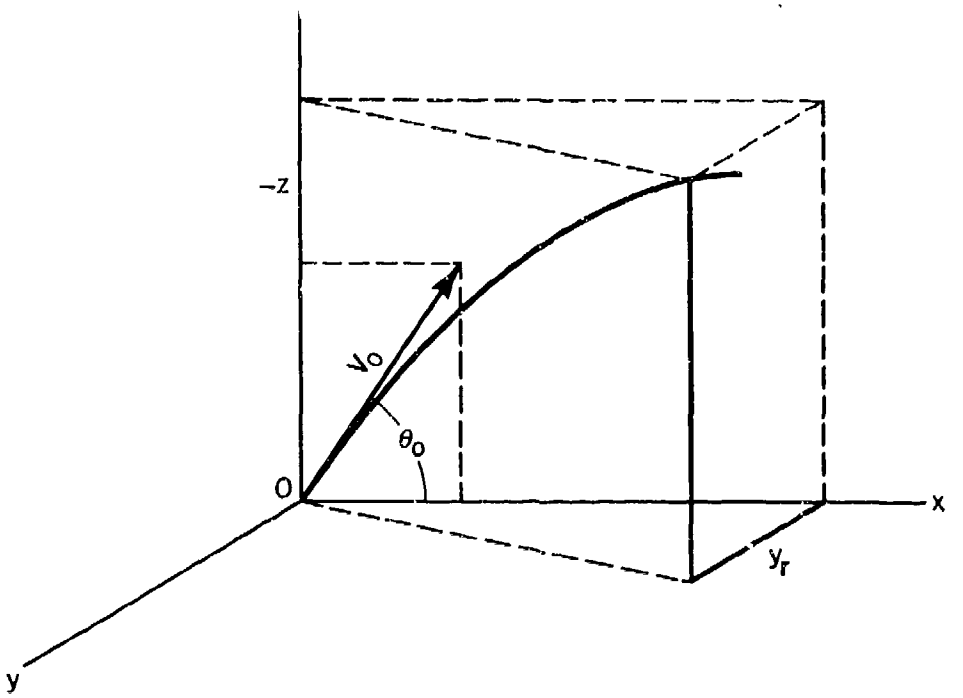

Figure 5. — Trajectory Showing Deflection

m = mass of the projectile.
F_x, F_y, F_z = components of the force acting on the projectile.

The problem is to find the x, y, z coordinates as functions of the time, t. As the initial step in its solution we use Newton's second law of motion,

Force = Mass × Acceleration, and apply it for each component direction. Thus,

$$(1.1) \quad m\frac{dv_x}{dt} = F_x,\ m\frac{dv_y}{dt} = F_y,\ m\frac{dv_z}{dt} = F_z,$$

where

$$\frac{dv_x}{dt},\ \frac{dv_y}{dt},\ \text{and}\ \frac{dv_z}{dt}$$

are the components of acceleration. Since

$$v_x = \frac{dx}{dt},\ v_y = \frac{dy}{dt},\ \text{and}\ v_z = \frac{dz}{dt},$$

the equations (1.1) may be written

$$(1.2) \quad \begin{cases} m\dfrac{d^2x}{dt^2} = F_x, \\ m\dfrac{d^2y}{dt^2} = F_y, \\ m\dfrac{d^2z}{dt^2} = F_z. \end{cases}$$

[In this and subsequent work, the earth's rotation is neglected.]

The problem is then two-fold: first, to find the components of the force and, secondly, to solve the system (1.2), which is a system of second order differential equations. The solution of the system (1.2) depends upon the form in which the force components, F_x, F_y, and F_z, can be expressed. The initial values of the variables, namely,

$$x_o = y_o = z_o = O,$$
$$v_{x_o} = v_o \cos\theta_o,$$
$$v_{z_o} = -v_o \sin\theta_o,$$
$$v_{y_o} = O,$$

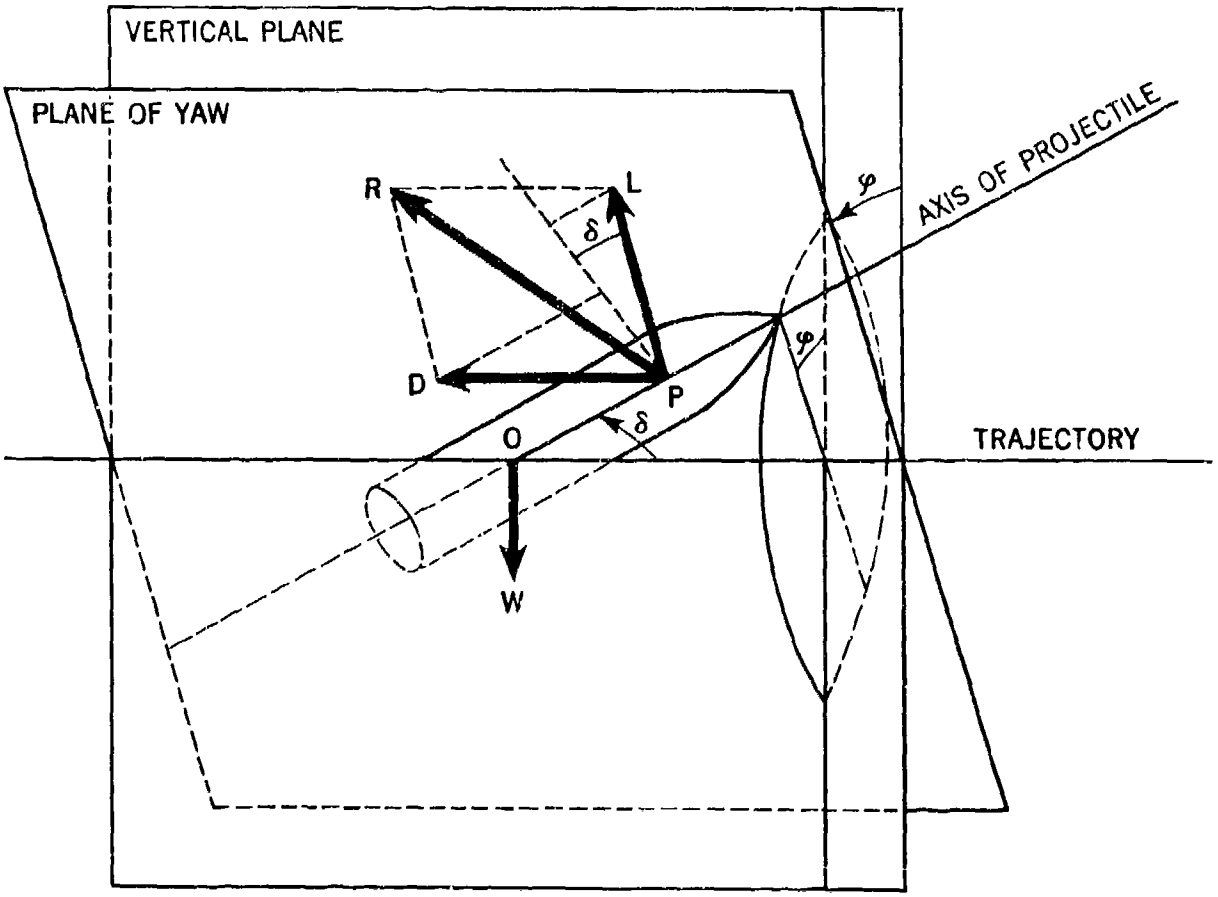

Figure 6. — Plane of Yaw

are used to determine the constants of integration. However, the determination of the force components is not a simple matter and requires, in fact, approximate methods.

For the sake of simplicity in future work, the following notational convention is made.

Convention: A dot placed above any variable denotes the derivative of that variable with respect to time; two dots denote the second derivative with respect to time, etc. Thus,

$$\dot{x} = \frac{dx}{dt}; \quad \ddot{\theta} = \frac{d^2\theta}{dt^2}, \quad \dddot{y} = \frac{d^3y}{dt^3}.$$

1.5 The Force System

A projectile is generally a solid of revolution which has an axis of symmetry, or such a body with symmetrically placed fins; this axis of symmetry is referred to as the axis of the projectile. A projectile will move through the air with its axis at an angle δ with the direction of motion; this angle is called the angle of yaw. The plane which includes the axis of the projectile and the tangent to the trajectory is called the plane of yaw. This plane makes an angle φ, called the angle of orientation, with the vertical plane through the tangent to the trajectory. See figure 6.

Let O be the location of the center of gravity and P the location of the center of pressure. The center of pressure is the point at which the resultant of the aerodynamic forces is applied. The following forces are acting on the projectile and are shown in figure 7.

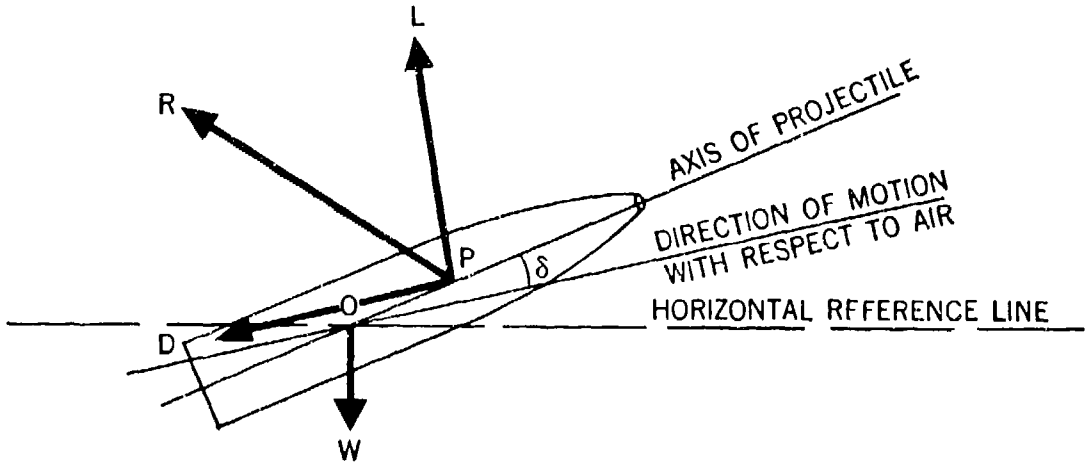

Figure 7. — Forces Acting on a Projectile

W = the weight of the projectile, acting at the center of gravity; it has its line of action parallel to the vertical plane through the gun bore axis and thus has no x or y components since the x,y-plane is taken to be horizontal. Its components are, therefore, O, O, mg.

R = a retardation force acting on the projectile due to the resistance of the atmosphere. The line of action of this air resistance is considered to lie in the plane of yaw and has its origin at the center of pressure which is usually ahead of the center of gravity. The force R is decomposed into two components D and L.

D = the drag or head resistance. This force originates at the center of pressure and has a direction parallel and opposite to the direction of motion.

L = the cross wind force. This force originates at the center of pressure and is directed perpendicular to the direction of motion. In aerodynamics this is the usual lift force.

It is well known from the principles of mechanics that the forces acting on a rigid body may be replaced by a single resultant force with a certain line of action and a couple tending to cause rotation about this line of action. Here, the resultant force is R and its line of action is in the plane of yaw. The couple is very small and often neglected. However, due to the fact that the center of pressure, P, is ahead of the center of gravity, O, there exists an overturning moment M of R about O. This moment, M, is caused by the component of R which is in the plane of yaw and perpendicular to the axis of the projectile. This component is usually called the normal force and is denoted by N_R. The moment arm is the distance OP.

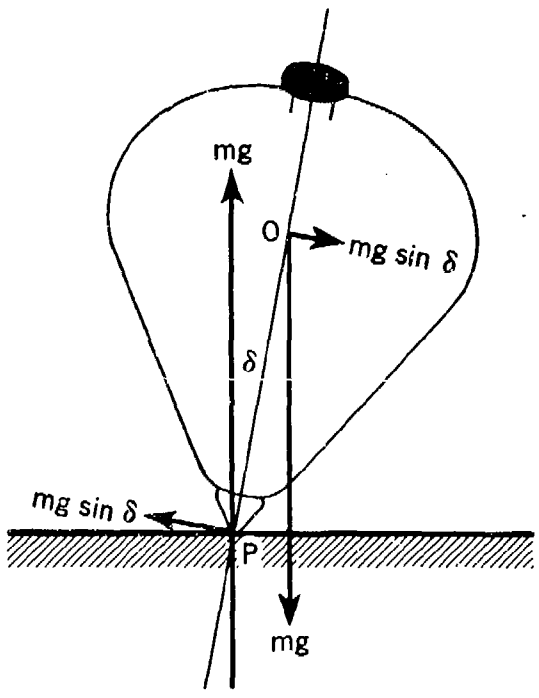

Figure 8. — The Force System of a Top

In order to obtain expressions for the forces D and L and the moment M, we must enter the theory of aerodynamics. Since it is beyond the scope of this book to develop this theory in detail, we shall simply draw from it the following expressions:

$$(1.3)\quad \begin{cases} D = K_D \rho_a d^2 V^2, \\ L = K_L \rho_a d^2 V^2 \sin \delta, \\ M = K_M \rho_a d^3 V^2 \sin \delta, \end{cases}$$

where K_D, K_L, and K_M are called the drag, cross wind force, and moment coefficients. These coefficients are dimensionless* and are functions of the parameters

$$\frac{\rho_a V d}{\sigma}, \frac{V}{a}, \text{ and } \delta,$$

where the new symbols are defined as follows:

d = diameter of the projectile;
ρ_a = air density;
V = projectile velocity relative to the air;
a = speed of sound in air;
σ = viscosity of the air.

In aerodynamic theory, the first parameter is called the **Reynolds number** and the second is the **Mach number**. Extensive experiments are conducted at proving grounds to determine the above coefficients for a given projectile shape and position of the center of gravity.

The velocity V is the vector difference of the projectile velocity v which is with respect to the ground, and the wind velocity w with respect to the ground. Thus the components of V are given by

$$V_x = v_x - w_x,\ V_y = v_y - w_y, \text{ and } V_z = v_z - w_z.$$

1.6 The Stability of the Projectile

In general, projectiles have the center of pressure ahead of the center of gravity. The air force then creates a moment which tends to overturn the projectile or causes the projectile to tumble. In order to prevent this tumbling, fins may be attached to the tail of the projectile, thereby bringing the center of pressure to the rear of the center of gravity whence the air moment becomes a righting moment instead of an overturning one. This is usually done in the case of bombs and rockets. A second method to prevent tumbling is to spin the projectile about its longitudinal axis, a procedure which is generally applied to bullets and shells and occasionally to rockets. The projectile then becomes not only an aerodynamic body but also a gyroscopic body.*

The general gyroscopic action of a projectile may best be compared with that of a spinning top. Consider a top spinning on a flat smooth surface and let the contact point be at P, the center of gravity at O, and let δ be the angle between the vertical and the axis of the top. The force system is shown in figure 8. It is easily seen that the component of the force due to gravity which is normal to the axis of the top is $mg \sin \delta$. The overturning moment is then given by

$$M = \kappa \sin \delta$$

where the moment factor κ is $(\overline{PO})\ (mg)$. It is well known that if the top is spinning rapidly enough, the axis of the top will continue to move near the vertical in spite of any outside interference. When this is the case the motion of the axis about the vertical is said to be stable. As the top loses its spin, its axis "falls away" from the vertical and the top tumbles; the motion is then said to be unstable. The condition for stability is given by the inequality

$$\frac{A^2 N^2}{4B\kappa} > 1$$

where A is the axial moment of inertia, B is the moment of inertia about the transverse axis through the center of gravity, N is the spin in radians per second, and κ is the moment factor. The same condition is true for a projectile. The factor $A^2N^2/4B\kappa$ is called the stability factor and is denoted by x. For a projectile, the moment factor κ is given by (see equation (1.3))

$$\kappa = K_M \rho_a d^3 V^2$$

and the spin at the muzzle, N, is given by

*That the coefficients are dimensionless can be seen by a dimensional analysis of equations (1.3); e.g.,

$$\frac{(m)\ (ft)}{(sec)^2} = K_D \frac{m}{(ft)^3} \frac{(ft)^2}{} \frac{(ft)^2}{(sec)^2} = K_D \frac{(m)\ (ft)}{(sec)^2}$$

*For a more detailed description of the behavior of a gyroscope see Chapter 5.

$$(1.4) \quad N = \frac{2\pi V_o}{nd}$$

where V_o is the muzzle velocity and n is the number of calibers for one turn of the rifling. Caliber is used here as a unit of length equal to the diameter of the gun bore, d. The stability factor for a projectile is then given by

$$(1.5) \quad s = \frac{\pi^2 A^2 V_o^2}{\pi^2 B K_M \rho_a d^5 V^2}$$

and $s >$ for 1/stable motion. If $s < 1$, the flight of the projectile becomes erratic and is very similar to the "wobbling" of a top as its motion becomes unstable. The stability factor, s, is a dimensionless quantity.

It is to be noted that the overturning moment is a function of the angle of yaw and becomes zero if the yaw is zero. It has been determined experimentally that the yaw near the gun results from the clearance of the projectile in the bore and tends to dampen out in time. At some distance from the gun the curvature of the trajectory becomes considerable and a relatively steady precessional yaw is caused by this curvature. At first, the axis of the projectile tends to point above the trajectory and thus a moment arises which causes the axis of the projectile with right-hand spin to precess like a gyroscope* toward the right of the trajectory. If the angle of departure is not too great, the projectile continues to point to the right so that the plane of yaw is approximately horizontal and the orientation angle is nearly 90°. Since the cross wind force L lies in the plane of yaw and the projectile points to the right of the trajectory, L will push the projectile to the right and produce the phenomenon of drift.

For large angles of departure, the angle of yaw becomes greater and the cross wind force has appreciable components along all three coordinate axes.

Extensive measurements under conditions for which the cross wind force can be assumed to be perpendicular to the X axis have shown that $\sin \delta$ can be approximated by

$$(1.6) \quad \sin \delta = \frac{ANg \cos \theta}{K_M \rho_a d^3 V^3}$$

*See Chapter 5.

where θ is the angle of inclination of the tangent to the trajectory. The stability of a projectile is usually assured by making the spin N sufficiently large. However, equation (1.6) places a warning not to make N too large since an increase in N increases the yaw.

1.7 The Equations of Motion

A form of the equations of motion of the projectile can be obtained by substituting the components of the forces into (1.2). The couple which tends to cause a rotation about the line of action of R will be neglected. The magnitudes of D and L are given by equations (1.3). The directions of D and L can be obtained from figure 7. D is parallel and opposite to the direction of motion. The components of $-D$ are then given by its magnitude times the direction cosines of the line of motion. Since the vector V coincides in direction with the line of motion, these direction cosines may be written,

$$\frac{V_x}{V}, \quad \frac{V_y}{V}, \text{ and } \frac{V_z}{V},$$

so that the components of D are

$$-D\frac{V_x}{V}, \quad -D\frac{V_y}{V}, \text{ and } D\frac{V_z}{V}.$$

The general direction of L depends upon the angle of orientation, φ. However, for projectiles which have their angles of departure less than about 45°, the cross wind force may be assumed to be in the same direction as the Y-axis. Under these assumptions the equations of motion then become

$$(1.7) \begin{cases} m\ddot{x} = -D\dfrac{V_x}{V}; \\ m\ddot{y} = -D\dfrac{V_y}{V} + L; \\ m\ddot{z} = +D\dfrac{V_z}{V} + mg. \end{cases}$$

If we now approximate $\cos \theta$ in equation (1.6) by V_x/V, we can substitute (1.6) into (1.3) and obtain

$$(1.8)\quad L = AN\frac{g}{d}\frac{K_L}{K_M}\frac{V_x}{V^2}.$$

The substitution of (1.3) into (1.7) then gives in units of mass, length, and time.

$$(1.9)\quad \begin{cases} \ddot{x} = -\dfrac{K_D\rho_a d^2 V}{m} V_x \\ \ddot{y} = -\dfrac{K_D\rho_a d^2 V}{m} V_y + \dfrac{AN}{m}\dfrac{g}{d}\dfrac{K_L}{K_M}\dfrac{V_x}{V^2} \\ \ddot{z} = \dfrac{K_D\rho_a d^2 V}{m} V_z + g \end{cases}$$

This system of differential equations must be handled by approximate methods. However, before discussing such methods, it is appropriate at this point to stop and consider two factors which enter into the consideration of the above system. The first of these is the atmosphere. The forces and the moment depend upon the wind and the air density. The wind components w_x, w_y, and w_z are determined as functions of the altitude which, for guns located on the ground, is a distance along z. The density ρ_a can be determined by pressure and temperature measurements; however, it is usually obtained from an assumed standard structure of the atmosphere. The standard structure assumes that the density is an exponential function of the altitude,

$$\rho_a = \rho_o e^{-hy}$$

where ρ_o is the reference density, taken to be .07513 lb/ft^3, and h is a constant equal to .0000316 per foot.*

The second factor for consideration arises from the manner in which the drag coefficient K_D is determined. K_D is usually found as a function of V/a for a given projectile shape, by measurements on a projectile at zero yaw. The drag function itself is determined by test firings of a standard projectile. The performance of a given projectile which differs from the standard projectile may then be estimated by the introduction of a form factor, i, which compares the given projectile with the standard one. If the drag coefficient for the standard projectile is denoted by K_{D_s}, the form factor is defined by

$$i = K_D/K_{D_s}$$

and in effect provides an average correction to the drag coefficient of the standard projectile. A new constant C, called the ballistic coefficient, is now defined as

$$C = \frac{W}{id^2} = \frac{mg}{id^2}$$

and this factor is used in equation (1.9).

In practice, the form factor i and the drag coefficient K_D are seldom determined. Actually, the ballistic coefficient, C, is determined from test firings which relate the performance of the projectile to that of the standard projectile to which it is most similar.

1.8 The Siacci Method*

This method modifies the differential equations of motion so that it becomes possible to solve them in terms of quadratures. The modification consists in assuming a constant average value for the air density and introducing a pseudo velocity u, defined as the vertical projection of the remaining velocity upon the line of departure. The remaining velocity is the actual velocity of the projectile at any point on the trajectory.

It is easily seen from figure 9 that

$$(1.10)\quad u\cos\theta_o = v\cos\theta \text{ or } u = v\cos\theta\ \sec\theta_o.$$

If the plane of departure is in the (x, z)-plane, then we also have

$$u = v_x \sec\theta_o \quad\text{or}\quad v_x = u\cos\theta_o.$$

A drag function for a standard projectile of a given type may be determined experimentally as a function of the remaining velocity. Under conditions of no wind $(V = v)$ we may then write

$$(1.11)\quad F(v) = K_D v$$

and the first equation of (1.9) becomes

$$(1.12)\quad \ddot{x} = \dot{v}_x = -\frac{\rho_a}{C}F(v)v_x.$$

*We have changed the units from mass to pounds.

*For a more detailed discussion of the Siacci method, see any standard text book on ballistics.

From the above definition of u we have

$$(1.13)\quad \begin{cases} v_x = u\cos\theta_o, \\ dv_x = du\cos\theta_o, \\ \dot{v}_x = \dfrac{dv_x}{dt} = \dfrac{dv_x}{dx}\dfrac{dx}{dt} = \dfrac{dv_x}{dx}v_x \\ \quad = \dfrac{du}{dx}v_x\cos\theta_o, \end{cases}$$

so that

$$(1.14)\quad \ddot{x} = \frac{du}{dx}v_x\cos\theta_o = -\frac{\rho_a}{C}F(v)v_x$$

or

$$(1.15)\quad \frac{dx}{du} = -\frac{C\cos\theta_o}{\rho_a F(v)}.$$

If now the Siacci assumption is made that $\rho_a F(v)$ can be replaced by $\rho_o G(u)$, equation (1.15) then becomes

$$(1.16)\quad dx = -\frac{C\cos\theta_o}{\rho_o}\frac{du}{G(u)},$$

and can be integrated. The integral

$$(1.17)\quad S(u) = -\int\frac{du}{G(u)}$$

is called the Siacci space function and is evaluated and tabulated for a range of predetermined values of u and initial conditions.

Similarly, three other functions may be obtained, the inclination function $I(u)$, the altitude function $A(u)$ and the time function $T(u)$. These functions are completely defined by

$$(1.18)\quad \begin{cases} I'(u) = -\dfrac{2g}{u^2G(u)} \\ A'(u) = -\dfrac{I(u)}{G(u)} \\ T'(u) = -\dfrac{1}{uG(u)} \end{cases}$$

and given initial values. The prime denotes the derivative with respect to u.

The procedure for solving the problem of the trajectory then reduces to the determination of the drag function $G(u)$, the tabulation of the four Siacci functions, and then the substitution of these values into the equations of motion. This process will be specialized to the case of aerial gunnery.

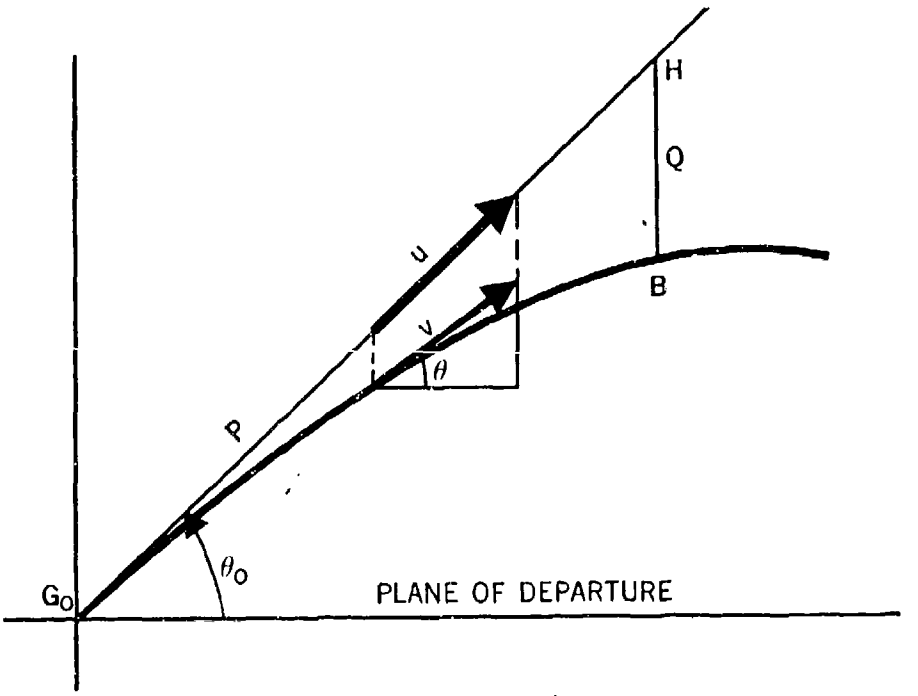

Figure 9. — Pseudo Velocity

PART 2. THE BALLISTICS OF AERIAL GUNNERY

1.9 Aerial Gunnery

This book is primarily concerned with the firing of projectiles from aircraft in flight. The fact that the gun is moving through the air in a specified direction and with an appreciable velocity adds further complications to the problem. On the other hand, projectiles fired from an aircraft move only over relatively short ranges and the maximum ordinate of the trajectory is not too great. This enables one to ignore the change of the density during the flight of the projectile and also to ignore the drift.

Figure 10 illustrates the general situation for aerial gunnery under the assumption that

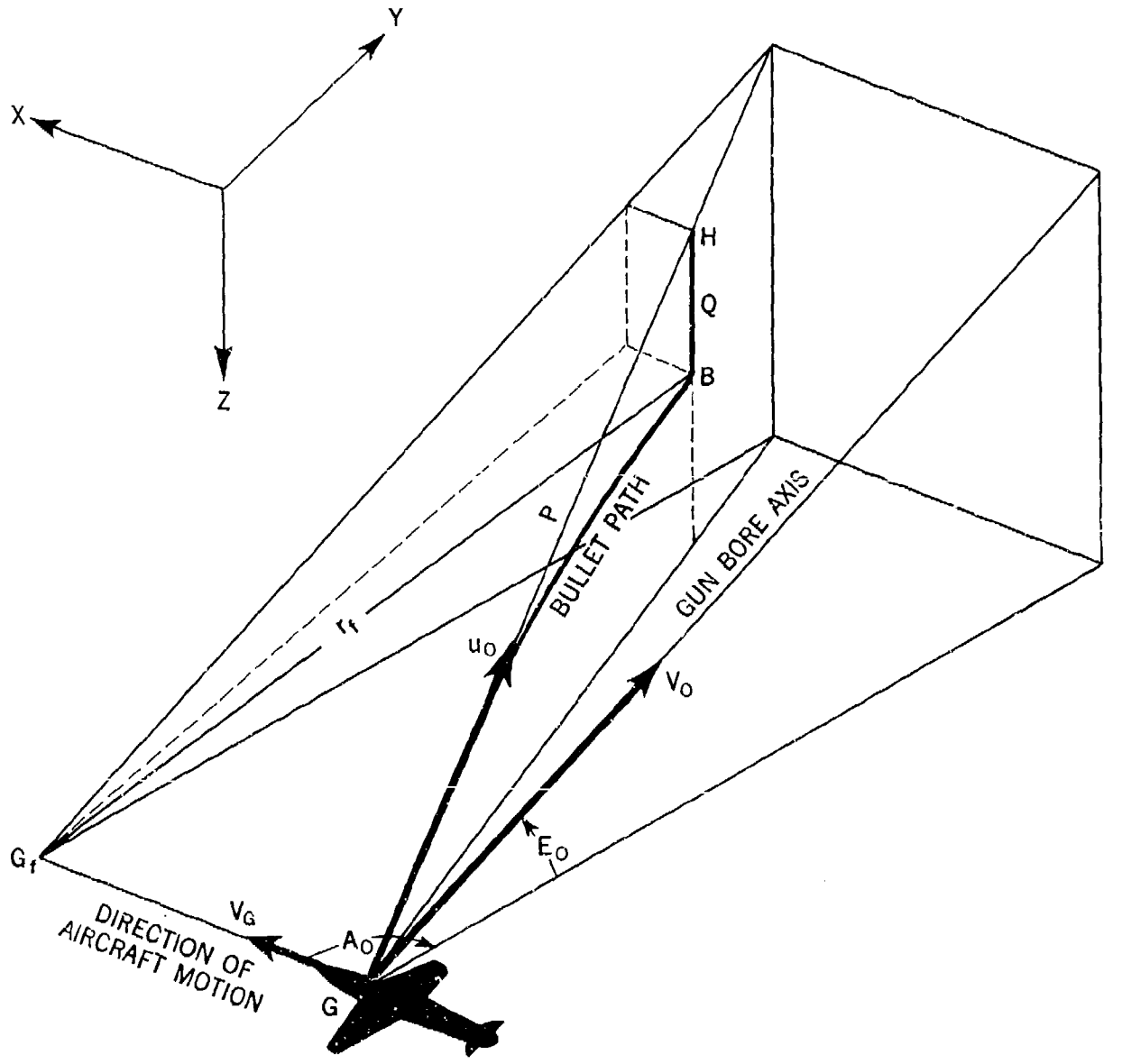

Figure 10. — Aeroballistics

the airplane is flying a straight-line unaccelerated course in a horizontal plane. Should the airplane maneuver, due account must be taken of the dive, bank, and yaw angles of the airplane and of whatever accelerations may be present. The path of the projectile can still be computed; however, the force components along the axes of a chosen coordinate system would involve the above mentioned angles. Present day firing tables are computed with the above assumptions and the maneuvering of the airplane is considered in the sighting problem. Consequently, we shall limit our ballistic discussion to that pictured in figure 10.

Let

A_o be the azimuth angle of the gun bore measured in the (X, Y)-plane from X through Y;

Z_o be the zenith angle of the gun bore;

E_o be the elevation angle of the gun bore measured positively from the horizontal plane toward the zenith;

$\mathbf{V}_G$ be the gun velocity (i.e., aircraft's true airspeed); taken to be along the X-axis;

$\mathbf{V}_o$ be the muzzle velocity of the projectile, relative to the X, Y, Z coordinate axes.

$\mathbf{u}_o$ be the initial velocity of the projectile; it is the resultant of $\mathbf{V}_o$ and $\mathbf{V}_G$.

t_f be the time of flight of the projectile.

P be the Siacci coordinate; it is the distance along the line of departure from the origin of the x, y, z system to a point H which is vertically above the projectile. The projectile is considered to be moving without drift.

Q be the Siacci coordinate, which is the vertical distance from H to the projectile.

r_f be the distance between the muzzle of the gun and the projectile at any instant t; it is called the slant range or future range and, in firing tables, is denoted by D.

Consider again the three coordinate systems described in section 1.2, The Coordinate Systems.

The direction cosines of the bore of the gun in the (X, Y, Z) coordinate systems are given by

$$\cos A_o \sin Z_o,\ \sin A_o \sin Z_o, \text{ and } \cos Z_o$$

and the initial components of the velocity of the projectile in the (x, y, z) system are

$$(1.19)\quad \begin{cases} u_x = V_o \cos A_o \sin Z_o + V_G, \\ u_y = V_o \sin A_o \sin Z_o, \text{ and} \\ u_z = -V_o \cos Z_o. \end{cases}$$

It follows then that the initial true airspeed of the projectile is given by

$$\begin{aligned} u_o^2 &= u_x^2 + u_y^2 + u_z^2 \\ &= V_o^2 \cos^2 A_o \sin^2 Z_o + 2V_oV_G \cos A_o \sin Z_o \\ &\qquad + V_G^2 + V_o^2 \cos^2 Z_o \\ &\qquad + V_o^2 \sin^2 A_o \sin^2 Z_o \\ &= V_o^2 \left[\sin^2 Z_o(\cos^2 A_o + \sin^2 A_o) + \cos^2 Z_o\right] \\ &\qquad + 2V_oV_G \cos A_o \sin Z_o + V_G^2, \end{aligned}$$

$$(1.20)\quad u_o^2 = V_o^2 + 2V_oV_G \cos A_o \sin Z_o + V_G^2.$$

After a time of flight t_f the Siacci coordinates of the projectile are P and Q and X, Y, Z coordinates may be found in the following manner. The right spherical triangles shown in figure 11 yield the following relations

$$(1.21)\quad \begin{cases} \cos \tau = \cos E_o \cos A_o = \sin Z_o \cos A_o, \\ \sin \psi = \sin E_o / \sin \tau = \cos Z_o / \sin \tau, \\ \sin \theta_o = \sin \nu \sin \psi, \\ \cos \nu = \cos \theta_o \cos A'. \end{cases}$$

The vector diagram of figure 12 yields

$$(1.22)\quad \sin \nu = \frac{V_o}{u_o} \sin \tau$$

so that

$$(1.23)\quad \sin \theta_o = \frac{V_o}{u_o} \cos Z_o.$$

The coordinates x, y, z of the projectile are given by

$$(1.24)\quad \begin{cases} x = P' \cos A' = P \cos \theta_o \cos A' \\ \quad = P \cos \nu, \\ y = P' \sin A' = P \cos \theta_o \sin A', \\ -z = P \sin \theta_o - Q \end{cases}$$

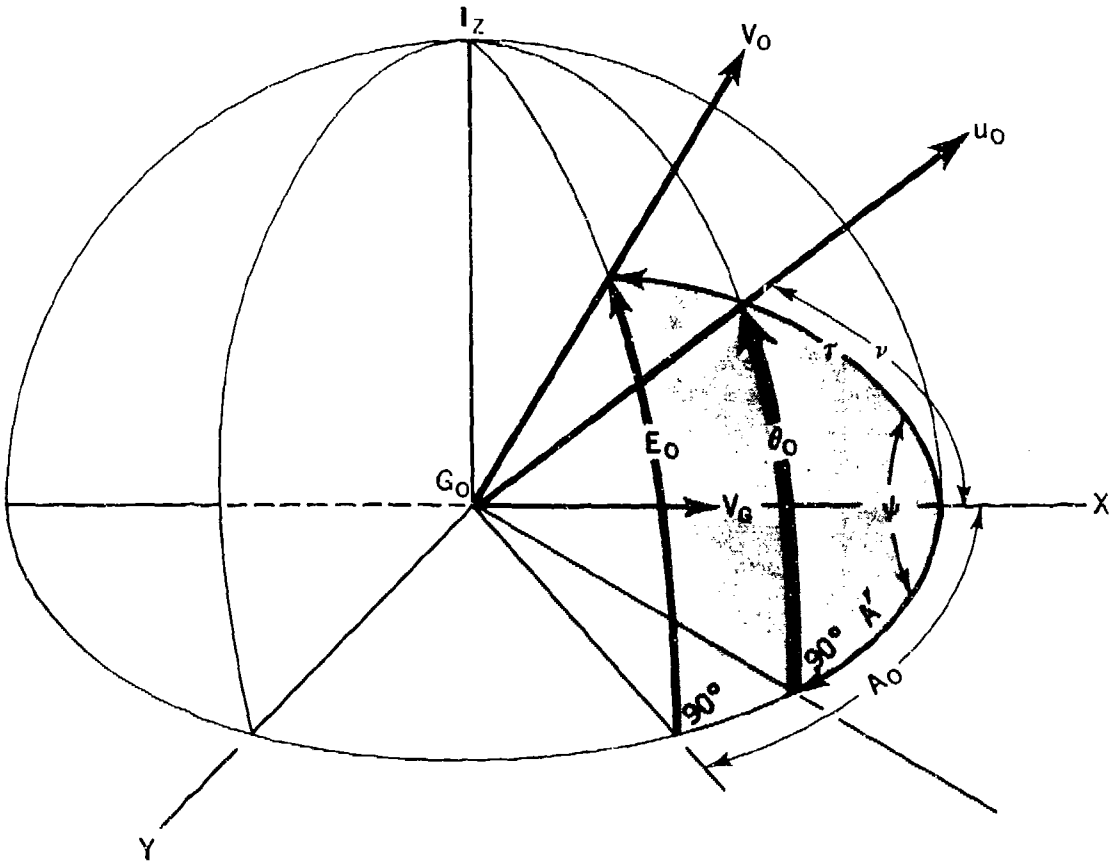

Figure 11. — Spherical Δ on Unit Sphere

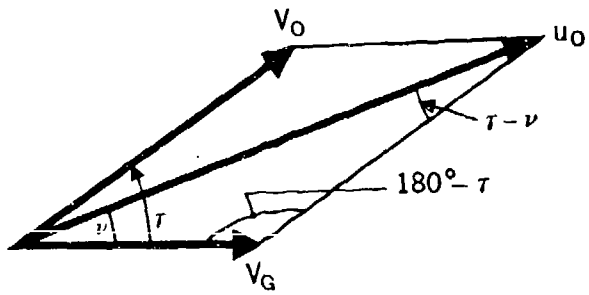

Figure 12. — Vector Diagram of V_o, u_o, V_G

The coordinates X, Y, Z of the projectile in the moving frame of reference, figure 13, are related to x, y, z by

(1.25) $X = x - V_G t_f$, $Y = y$, and $Z = z$

since the aircraft is assumed to be moving horizontally along the x-axis.

Upon combining (1.19), (1.23), (1.24), and (1.25) we find the coordinates of the projectile at any time t to be

$$(1.26)\quad \begin{cases} X = \dfrac{P}{u_o}(V_G + V_o \sin Z_o \cos A_o) - V_G t_f, \\[2ex] Y = P\dfrac{V_o}{u_o} \sin Z_o \sin A_o, \\[2ex] -Z = P\dfrac{V_o}{u_o} \cos Z_o - Q. \end{cases}$$

The relation of the rectangular coordinates ξ, η, ζ, which are moving with the aircraft (see section 1.2), to X, Y, Z coordinates is given by the following scheme:

	X	Y	$-Z$
ξ	$\sin Z_o \cos A_o$	$\sin Z_o \sin A_o$	$\cos Z_o$
η	$-\cos Z_o \cos A_o$	$-\cos Z_o \sin A_o$	$\sin Z_o$
ζ	$-\sin A_o$	$\cos A_o$	O

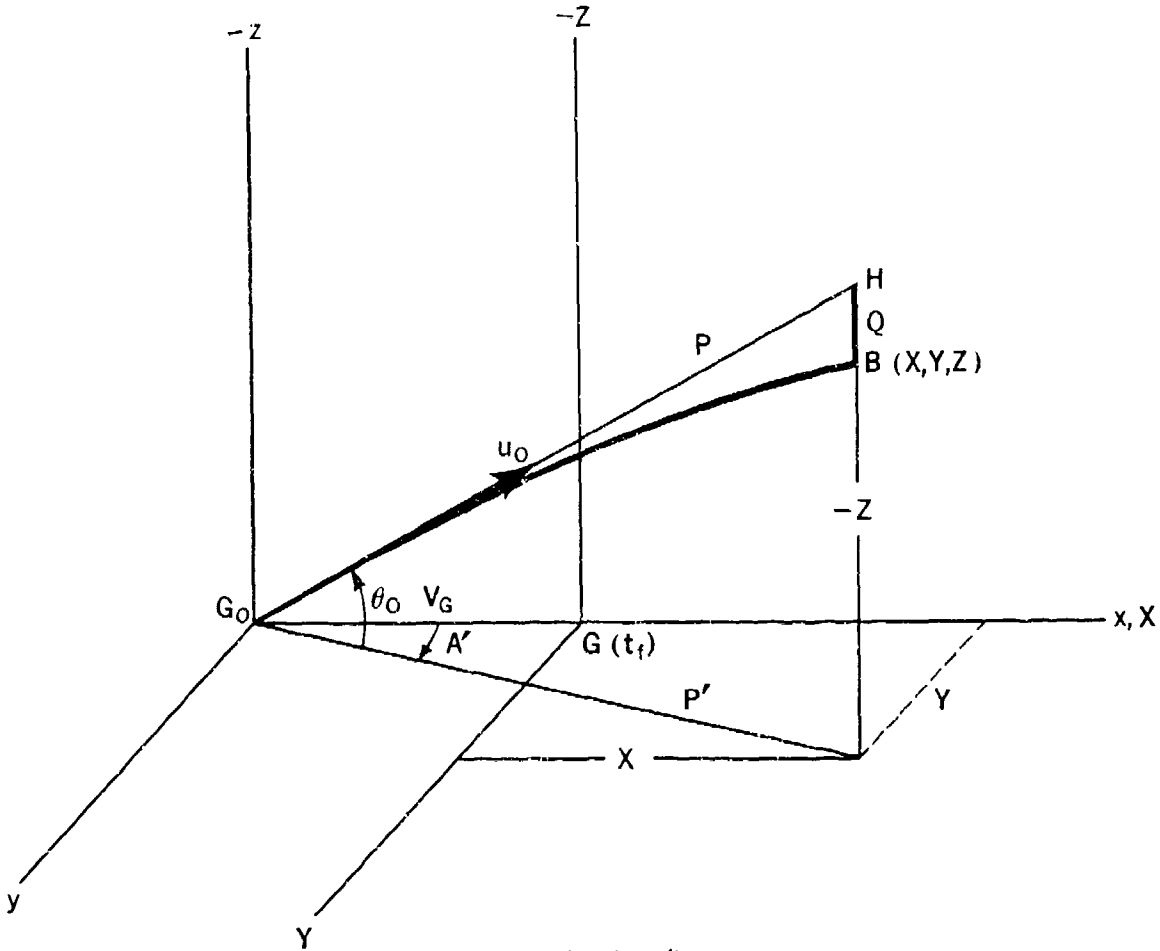

Figure 13. — Bullet Coordinates

Thus the ξ, η, ζ coordinates of the projectile are given by

$$(1.27)\quad \begin{cases} \xi = P\dfrac{V_o}{u_o} - Q\cos Z_o \\ \qquad + V_G\left(\dfrac{P}{u_o} - t_f\right)\sin Z_o \cos A_o, \\ \eta = -V_G\left(\dfrac{P}{u_o} - t_f\right)\cos Z_o \cos A_o \\ \qquad - Q\sin Z_o, \\ \zeta = -V_G\left(\dfrac{P}{u_o} - t_f\right)\sin A_o. \end{cases}$$

The slant range r_f is now given by

$$(1.28)\quad r_f^2 = \xi^2 + \eta^2 + \zeta^2.$$

In aerial gunnery the primary ballistic problem is to determine:

(a) the time of flight, t_f, and
(b) the gravity drop, Q,

for a given P. They are, of course, dependent upon the following quantities:

$$(1.29)\quad \begin{cases} \rho = \text{the relative air density } \rho_a/\rho_o, \\ V_G = \text{true airspeed of the aircraft}, \\ V_o = \text{muzzle velocity of the gun}, \\ Z_o = \text{zenith angle of the gun line}, \\ A_o = \text{azimuth angle of the gun line}, \\ P = \text{the Siacci coordinate}. \end{cases}$$

Values of t_f and Q may be computed for given values of the quantities (1.29) and tabulated. The usual procedure, however, is to tabulate t_f and Q at fixed interval values of these quantities. It is customary to replace P by r_f in this tabulation.

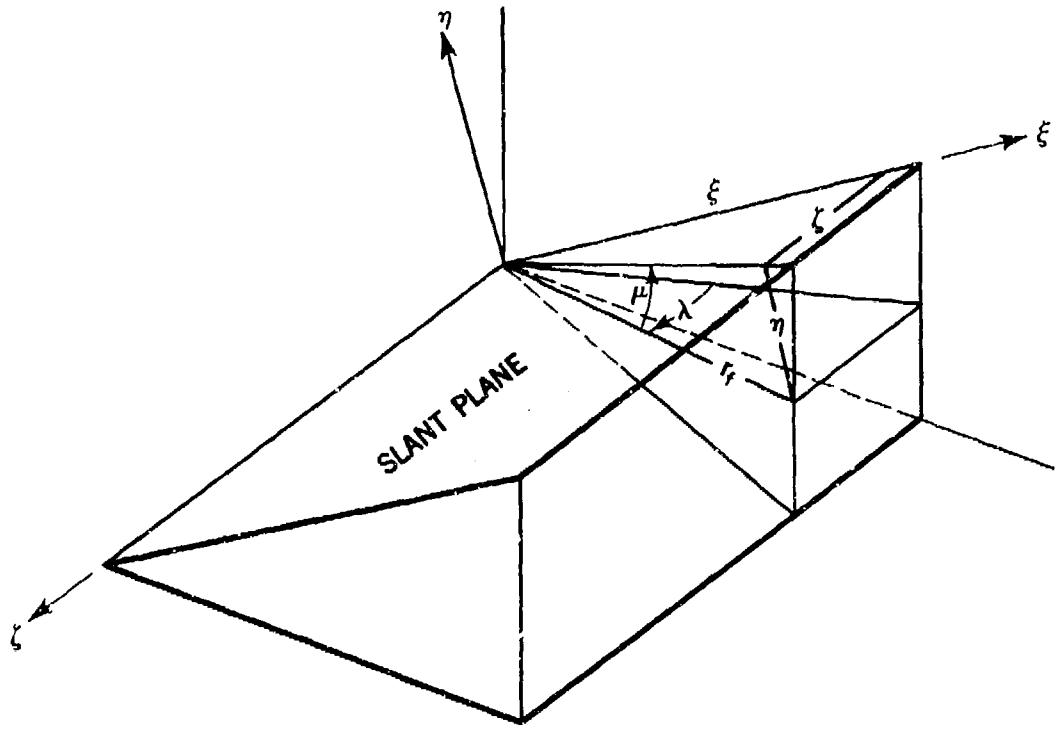

Figure 14. — Lateral and Vertical Deflections

Although the computation of t_f and Q forms the primary problem, two other terms also are of interest and are tabulated; namely,

λ = the lateral deflection,

= the angle between the gun-projectile line and the vertical plane through the gun bore; it is positive when the gun-projectile line is to the right of this vertical plane when viewed from the gun. It is an instantaneous relative position angle.

μ = the vertical deflection,

= the angle between the gun-projectile line and the "slant plane" through the gun bore and perpendicular to the vertical plane through the gun bore; it is positive when the gun-projectile line lies above the slant plane. It also is an instantaneous relative position angle.

These angles are shown in figure 14. It is easily seen that their values may be computed from the formulas

$$(1.30)\quad \begin{cases} \sin\lambda = \zeta/r_f, \\ \sin\mu = \eta/r_f. \end{cases}$$

1.10 Dimensionless Ballistic Coefficient

The ballistic coefficient defined in section 1.7 is not a dimensionless quantity. A more mathematically logical treatment of the development of the Siacci method for aerial gunnery is obtained by defining a dimensionless ballistic coefficient. Let the subscript s denote quantities related to the standard projectile of a given type, then we may define

$$(1.31)\quad C_n = \frac{\dfrac{W}{W_s}}{\dfrac{K_D}{K_{D_s}}\left(\dfrac{d}{d_s}\right)^2} = \frac{\dfrac{W}{W_s}}{i\left(\dfrac{d}{d_s}\right)^2}$$

to be the dimensionless ballistic coefficient for a type n projectile.

The first equation of (1.9) under conditions of

no wind may now be written (units in pounds, length, seconds)

$$\ddot{x} = -\frac{K_D \rho_a}{mg} d^2 v v_x$$

$$= -\rho \frac{K_D}{K_{D_s}} \frac{W_s}{W} \left(\frac{d}{d_s}\right)^2 \left[\frac{\rho_0 K_{D_s} d_s^2 v}{W_s}\right] v_x$$

$$= -\rho \frac{\frac{K_D}{K_{D_s}} \left(\frac{d}{d_s}\right)^2}{\frac{W}{W_s}} \left[\frac{\rho_0 K_{D_s} v}{\frac{W_s}{d_s^2}}\right] v_x$$

$$= -\frac{\rho}{C_n} \left[\frac{\frac{\rho_0}{W_s} K_{D_s} v}{d_s^2}\right] v_x$$

$$(1.32) \quad \ddot{x} = -\frac{\rho}{C_n} G_n(v)\, v_x$$

where

$$(1.33) \quad G_n(v) = \frac{\rho_0 K_{D_s} v}{m_s/d_s^2}$$

is the drag function, for the standard type n projectile, determined from test firings as a function of the velocity v.

In aerial gunnery, the trajectory is nearly flat and consequently we may use the Siacci approximation,

$$v \doteq u \text{ and } G_n(v) \doteq G_n(u)$$

and equation (1.32) becomes

$$(1.34) \quad \ddot{x} = -\frac{\rho}{C_n} G(u)\, v_x.$$

In section 1.8 we saw that if the (x, z)-plane is the plane of departure, then

$$v_x = u \cos \theta_0 \qquad \text{or} \qquad u = v_x \sec \theta_0$$

from which we get by a differentiation

$$(1.35) \quad \frac{du}{dt} = \dot{v}_x \sec \theta_0$$

$$= -\frac{\rho}{C_n} G_n(u)\, v_x \sec \theta_0 \text{ since } \dot{v}_x = \ddot{x}$$

$$= -\frac{\rho}{C_n} G_n(u)\, u.$$

Since $u = dP/dt$, we have

$$\frac{du}{dt} = -\frac{\rho}{C_n} G_n(u) \frac{dP}{dt}$$

or

$$(1.36) \quad dP = -\frac{C_n}{\rho} \frac{du}{G_n(u)}.$$

Equation (1.36) may be integrated to give the Siacci range, P,

$$(1.37) \quad P = -\frac{C_n}{\rho} \int_{u_0}^{u} \frac{du}{G_n(u)} = \frac{C_n}{\rho}(S - S_0),$$

where S is the Siacci space function

$$(1.38) \quad S = -\int_{u}^{U} \frac{du}{G_n(u)}, \qquad (U > u_0).$$

The time of flight may be obtained by integrating equation (1.35)

$$(1.39) \quad t_f = -\frac{C_n}{\rho} \int_{u_0}^{u} \frac{du}{u\, G_n(u)} = \frac{C_n}{\rho}(T - T_0),$$

where T is the Siacci time function

$$(1.40) \quad T = -\int_{u}^{U} \frac{du}{u\, G_n(u)}, \qquad (U > u_0).$$

1.11 The Motion of Small Arms Projectiles Fired from an Aircraft

The effect of the yaw on the drag of a small arms projectile is an important factor in the motion of these projectiles when fired from a

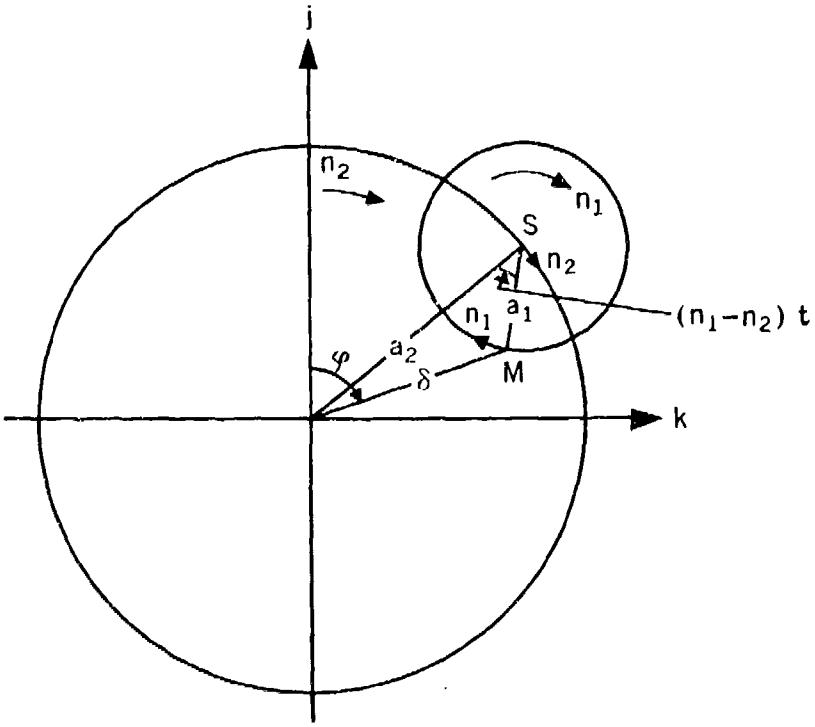

Figure 15. — Vibration Motion

moving aircraft. It is accounted for by the approximation that the drag force due to yaw is proportional to the square of the yaw angle for small yaw angles. The first problem then is to find an expression for the square of the yaw angle, δ. This expression is found by considering the gyroscopic motion of bullets fired from an aircraft; the drift is ignored and only the vibratory motion of the center of gravity about the mean trajectory is considered. The mean trajectory is a particle trajectory that differs from the actual trajectory only by periodic terms.

The detailed solution of the vibratory motion is beyond the scope of this book. (For the theory of vibrations, see any standard book on mechanics; for the complete theory, on which this discussion is based, consult reference (2) of the bibliography in the back of this book.) The presentation here will be more or less along intuitive lines.

Let j and k be the rectangular components of the yaw. Then the theory of vibrations shows that the motion is given by a linear combination of

(1.41) $\cos n_1 t$, $\sin n_1 t$, $\cos n_2 t$, and $\sin n_2 t$

with four coefficients that are slowly varying functions of time and in which n_1 and n_2 are solutions of the associated frequency equation and take the forms

$$(1.42)\quad \begin{cases} n_1 = \dfrac{AN}{2B}(1+p) \\[2ex] n_2 = \dfrac{AN}{2B}(1-p) \end{cases}$$

where

$$(1.43)\quad p = \sqrt{1-(1/s)}$$

and the quantities A, B, N, and s are defined in section 1.6.

If we ignore the gradual variation of the coefficients, then (j, k) may be considered to be the rectangular coordinates of a point M which is rotating in a clockwise direction at an angular rate n_1 in a circular path of radius a_1. The center of this circular path, S, rotates clockwise around the origin at an angular rate n_2 and describes a

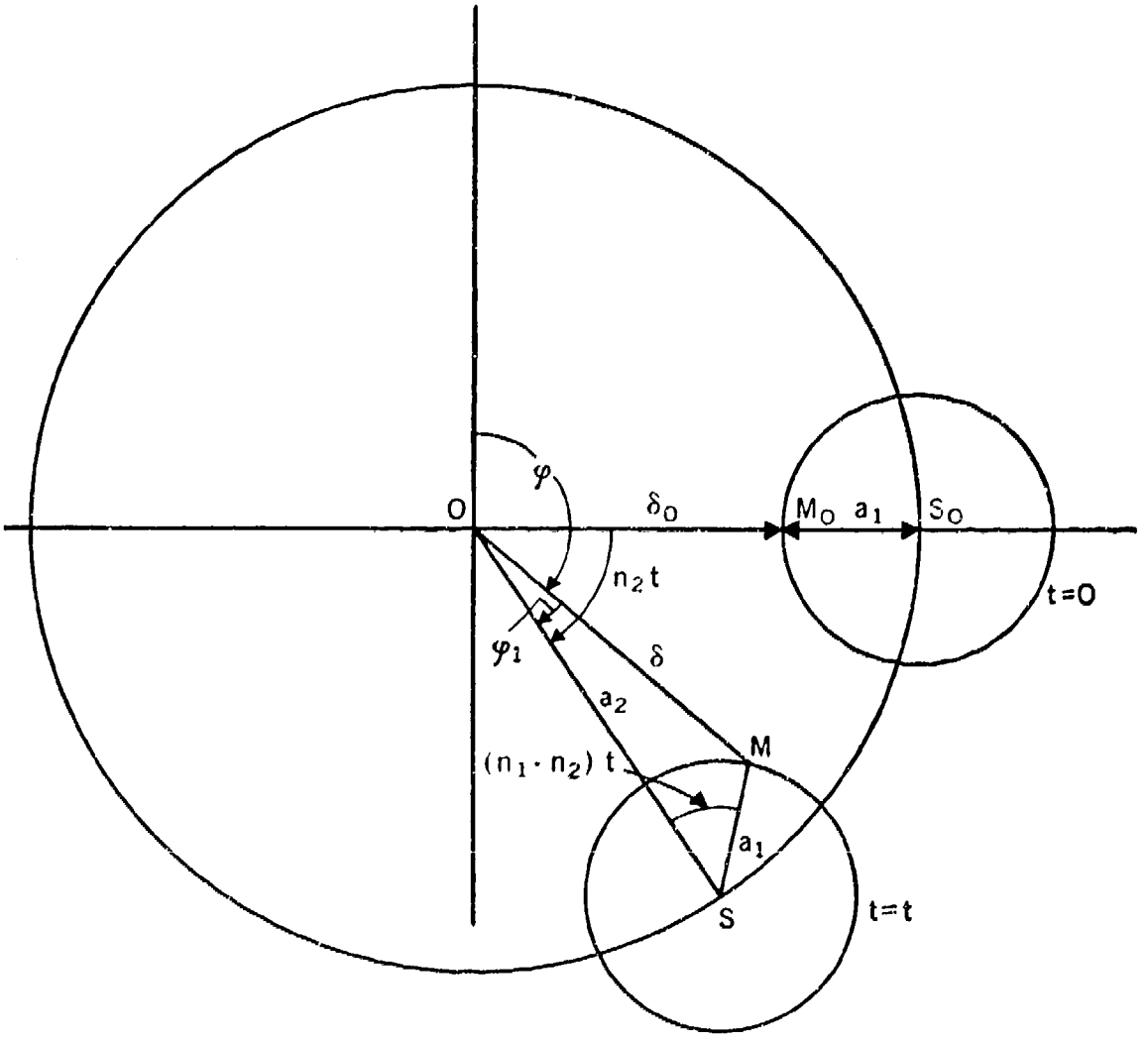

Figure 16. — Initial Conditions of Vibratory Motion

circle of radius a_2. The clockwise angle from the j-axis to the radius vector of M is the angle of orientation of yaw, φ, and the distance of M from the origin may be represented by the angle of yaw, δ. The configuration is shown in figure 15, from which it is seen by the law of cosines that

$$(1.44) \quad \delta^2 = a_1^2 + a_2^2 - 2a_1a_2 \cos (n_1 - n_2)t$$

if the time is measured from a suitable instant and the algebraic signs of n_1 and n_2 are taken into consideration.

The rotation in the circle of radius a_1 may be called the nutation, and the rotation in the circle of radius a_2 may be called the precession; the resultant of these two is the complete yawing motion. The slow variation of the coefficients of the periodic terms in this vibratory motion consists of arbitrary constant factors multiplied by damping factors. We may consider a_1 to be the amplitude of the nutation and a_2 the amplitude of the precession. The rates of variation or of damping of the amplitudes may be experimentally determined.

For small arms bullets, the two damping factors have been shown experimentally to be equal and may be expressed by

$$(1.45) \quad p^{-1/2} \; e^{-\rho_a c_1 P}$$

where P should be the actual distance the bullet has travelled but which is here taken to be the Siacci P. The constant c_1 may be experimentally determined and is given by

$$(1.46) \quad c_1 = \frac{d^4 K_H}{2B} + \frac{d^2 K_L}{2m}$$

where K_H is the yawing moment coefficient.

Let us consider a projectile which starts its motion with an initial angle of yaw δ_o, the angle of orientation equal to 90°, and such that the initial values of the time derivatives of δ and φ are zero; that is, initially $t = O$, $\delta = \delta_o$, $\varphi = 90°$, $\dot{\varphi} = \dot{\delta} = O$. Figure 16 pictures the situation at $t = O$ and also at some time t.

Let φ_1 be the angle between OM and OS, then from figure 16, we have

$$n_2 t = \varphi - 90° + \varphi_1$$

and upon differentiating with respect to t

$$n_2 = \dot{\varphi} + \dot{\varphi}_1 .$$

At $t = O$ we considered $\dot{\varphi} = O$ so that initially

$$n_2 = \dot{\varphi}_1 .$$

If we apply the law of sines to triangle OMS, we obtain

$$a_1 \sin [180° - \varphi_1 - (n_1 - n_2) t] = a_2 \sin \varphi_1$$

or

$$a_1 \sin [\varphi_1 + (n_1 - n_2)\, t] = a_2 \sin \varphi_1 .$$

Differentiating this equation with respect to time, we have

$$a_1 [\dot{\varphi}_1 + (n_1 - n_2)] \cos [\varphi_1 + (n_1 - n_2)\, t] = a_2 \dot{\varphi}_1 \cos \varphi_1 .$$

Thus, at $t = O$ we have

$$a_1 [\dot{\varphi}_1 + (n_1 - n_2)] = a_2 \dot{\varphi}_1$$

or, since $\dot{\varphi}_1 = n_2$ at $t = O$,

$$a_1 n_1 = a_2 n_2 .$$

It is easily seen from figure 16 that

$$\delta_o = a_2 - a_1$$

so that we have two simultaneous equations

$$(1.47) \begin{cases} \delta_o = a_2 - a_1 \\ a_1 n_1 = a_2 n_2 \end{cases}$$

whence we may solve for the initial values of a_1 and a_2,

$$(1.48) \begin{cases} a_{10} = \dfrac{n_2 \delta_o}{n_1 - n_2} \\ a_{20} = \dfrac{n_1 \delta_o}{n_1 - n_2} . \end{cases}$$

The substitution of (1.42) into (1.48) yields

$$(1.49) \begin{cases} a_{10} = \dfrac{(1 - p_o)\, \delta_o}{2p_o} , \\ a_{20} = \dfrac{(1 + p_o)\, \delta_o}{2p_o} , \end{cases}$$

where p_o is the initial value of p. Since the damping factor is common to both, we have a_1 and a_2 given at all times by

$$(1.50) \begin{cases} a_1 = \dfrac{(1 - p_o)\, \delta_o}{2p_o} \left[\dfrac{p_o}{p} \right]^{1/2} e^{-\rho_a c_1 P} , \\ a_2 = \dfrac{(1 + p_o)\, \delta_o}{2p_o} \left[\dfrac{p_o}{p} \right]^{1/2} e^{-\rho_a c_1 P} , \end{cases}$$

where $p_o^{1/2}$ is the arbitrary constant factor multiplying the damping factor. The mean value of δ^2 averaged over a single period of δ^2 is

$$(1.51) \quad \begin{aligned} \bar{\delta}^2 &= a_1^2 + a_2^2 \\ &= \delta_o^2 \frac{1 + p_o^2}{2p_o^2} \left(\frac{p_o}{p} \right) e^{-2\rho_a c_1 P} \\ &= \delta_o^2 \frac{s_o - \frac{1}{2}}{s_o - 1} \left(\frac{p_o}{p} \right) e^{-2\rho_a c_1 P} \end{aligned}$$

where the last equation is obtained by making use of equation (1.43). The variation of the stability s along the trajectory is approximated by

$$(1.52) \quad \frac{p_o}{p} = e^{\frac{-\rho_a d^2}{s_o - 1} \cdot \frac{1}{m} K_D P}$$

The mean value of δ^2 is then finally given by

$$(1.53) \quad \bar{\delta}^2 = \delta_o^2 \frac{s_o - \frac{1}{2}}{s_o - 1} \; e^{-2\rho_a (c_1 + c_2) P}$$

988995 O - 62 - 3

where

$$(1.54) \quad c_2 = \frac{d^2}{2(s_o - 1)m} K_D .$$

The yaw of the projectile has two effects upon the trajectory. First, yaw makes the drag greater than it would be if no yaw were present and, secondly, it introduces the so-called windage jump. At the instant of firing to starboard, the tangent to the instantaneous trajectory points higher than the tangent to the mean trajectory, in other words, the tangent to the mean trajectory is lower than the bore of the gun by an angle ϵ; this angle is called the windage jump. The windage jump for a given bullet depends essentially on the initial angle of yaw and the initial air speed of the bullet. It can be shown that ϵ is given by

$$(1.55) \quad \epsilon = \frac{AN}{md} \frac{K_L}{K_M} \frac{\delta_o}{u_o}$$

where K_L and K_M are again the force and overturning moment coefficients. The effect of the windage jump upon the trajectory may be considered as a differential correction and thus the motion of the projectile will be studied first by neglecting the windage jump.

The effect of the yaw on the drag may be accounted for by applying a modified drag force coefficient for the standard projectile. Using the approximation that the drag force due to yaw is proportional to the square of the yaw angle for small yaw angles, we may write

$$(1.56) \quad K_{D_\delta} = K_{D_o} (1 + K_{D\delta} \bar{\delta}^2)$$

where

K_{D_o} = drag coefficient for zero yaw angle;

$K_{D\delta}$ = yaw drag coefficient;

$\bar{\delta}^2$ = mean value of δ^2 discussed above.

If this expression for K_{D_δ} is substituted into equation (1.33), we have a new drag function, G_δ, which makes allowance for the yaw of the projectile,

$$(1.57) \quad G_\delta = G_n (1 + K_{D\delta} \bar{\delta}^2)$$

where G_n is the experimentally determined drag function for zero yaw for a type n projectile.

Let i_1, i_2 be a set of rectangular axes fixed in the air, lying in the plane of departure with i_1 horizontal and i_2 vertical. The origin is the position of the gun at the instant of firing. It is easily seen from figure 17 that

$$(1.58) \begin{cases} P = i_1 \sec \theta_o \\ Q = i_1 \tan \theta_o - i_2. \end{cases}$$

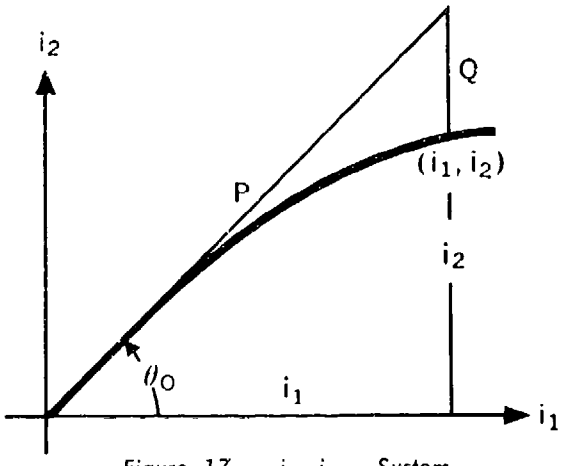

Figure 17.—i_1, i_2—System

For the equations of motion of the projectile, taking account of the influence of gravity and drag, we have equation (1.32) and a similar equation in the z direction, where $\ddot{x}$ and v_x are replaced by $\ddot{i}_1$ and $\dot{i}_1$; $-\ddot{z}$ and $-v_z$ are replaced by $\ddot{i}_2$ and $\dot{i}_2$, and the drag function is corrected for yaw by formula (1.57). Thus,

$$(1.59) \begin{cases} \ddot{i}_2 = -\rho \dfrac{G_n}{C_n} (1 + \bar{\delta}^2 K_{D\delta}) \dot{i}_2 - g , \\ \ddot{i}_1 = -\rho \dfrac{G_n}{C_n} (1 + \bar{\delta}^2 K_{D\delta}) \dot{i}_1 , \end{cases}$$

where

ρ is the relative air density,

G_n is the appropriate drag function for zero yaw,

C_n is the appropriate ballistic coefficient, and

$K_{D\delta}$ is the yaw drag coefficient.

From equations (1.58) we have

$$(1.60) \begin{cases} i_1 = P \cos \theta_o , \\ i_2 = P \sin \theta_o - Q ; \end{cases}$$

$$(1.61)\quad \begin{cases} \dot{i}_1 = \dot{P}\cos\theta_o, \\ \dot{i}_2 = \dot{P}\sin\theta_o - \dot{Q}. \end{cases}$$

$$(1.62)\quad \begin{cases} \ddot{i}_1 = \ddot{P}\cos\theta_o, \\ \ddot{i}_2 = \ddot{P}\sin\theta_o - \ddot{Q}. \end{cases}$$

Equations (1.59) may therefore be written in the following form

$$(1.63)\quad \begin{cases} \ddot{P}\sin\theta_o - \ddot{Q} + \rho\dfrac{G_n}{C_n}(1+\bar{\delta}^2 K_{D\delta})\cdot \\ \qquad (\dot{P}\sin\theta_o - \dot{Q}) + g = O, \\ \ddot{P}\cos\theta_o + \rho\dfrac{G_n}{C_n}(1+\bar{\delta}^2 K_{D\delta})\cdot \\ \qquad \dot{P}\cos\theta_o = O. \end{cases}$$

or

$$(1.64)\quad \begin{cases} \ddot{Q} + \rho\dfrac{G_n}{C_n}(1+\bar{\delta}^2 K_{D\delta})\,\dot{Q} = g + \sin\theta_o\cdot \\ \qquad [\ddot{P} + \rho\dfrac{G_n}{C_n}(1+\bar{\delta}^2 K_{D\delta})\,\dot{P}], \\ \ddot{P} + \rho\dfrac{G_n}{C_n}(1+\bar{\delta}^2 K_{D\delta})\,\dot{P} = O. \end{cases}$$

Recall that $u = \dot{P}$ so that $\ddot{P} = \dot{u} = \dfrac{du}{dt}$. The second equation of (1.64) then takes the form

$$(1.65)\quad du + \rho\frac{G_n}{C_n}(1+\bar{\delta}^2 K_{D\delta})\,dP = O,$$

or

$$(1.66)\quad \frac{du}{dP} = -\rho\frac{G_n}{C_n}(1+\bar{\delta}^2 K_{D\delta}) = \frac{d\dot{P}}{dP}.$$

Since G_n is a function of u, we divide (1.65) by G_n and rewrite to get

$$-\frac{du}{G_n} = \frac{\rho}{C_n}(1+\bar{\delta}^2 K_{D\delta})\,dP.$$

We have now separated the variables and we can integrate to find

$$(1.67)\quad -\int_{u_o}^{u}\frac{du}{G_n} = \frac{\rho}{C_n}\int_{P_o}^{P}(1+\bar{\delta}^2 K_{D\delta})\,dP$$

$$= \frac{\rho}{C_n}\left[\int_{P_o}^{P} dP + K_{D\delta}\int_{P_o}^{P}\bar{\delta}^2\,dP\right]$$

The integral on the left-hand side of equation (1.67) yields the Siacci Space function S for the drag function G [see equation (1.17)]. On the right-hand side we have from equation (1.53)

$$(1.68)\quad \frac{\rho}{C_n}P'\Big]_{P_o}^{P} + \frac{\rho}{C_n}K_{D\delta}\int_{P_o}^{P}\left(\delta_o^2\frac{s_o-\frac{1}{2}}{s_o-1}\,e^{-2\rho_a(c_1+c_2)P'}\right)dP'$$

where P' is a dummy variable used to indicate the value of P at any point in the interval of integration. The initial value of $P = P_o$ is zero and the initial value of $S = S_o$ is the value of S at u_o. Let

$$(1.69)\quad c = (c_1 + c_2)\,\rho_o$$

where ρ_o is the standard air density. We can now evaluate the integral of (1.68) and upon substitution of the initial values we finally have from (1.67)

$$(1.70)\quad S = S_o + \frac{\rho}{C_n}P + K\left(1 - e^{-2\rho c P'}\right),$$

where

$$(1.71)\quad K = \frac{1}{2C_n c}K_{D\delta}\,\delta_o^2\frac{s_o-\frac{1}{2}}{s_o-1}.$$

The value of t for a given Siacci coordinate P may now be found in the following manner. The constants necessary for the given projectile such as K_D, $K_{D\delta}$, c, c_1, c_2, etc., are determined experimentally. A drag function $G_n(u)$ also is determined from measurements, and the Siacci space function S is tabulated for this drag function by numerical integration of (1.17). Then, under given firing conditions of A_o, Z_o, V_o

and V_G, the Siacci function S is obtained from (1.70) at given values of P. Values of u are then found from tables of S for these values of S and since

$$u = \dot{P} = \frac{dP}{dt},$$

we have

$$dt = \frac{1}{u}\, dP$$

so that

$$(1.72) \qquad t_f = \int_0^P \frac{1}{u}\, dP'$$

where the prime is again a dummy index.

To obtain Q, we return to the first equation of (1.64). Upon the substitution of the second equation of (1.64) and (1.66) into this equation it reduces to

$$(1.73) \qquad \ddot{Q} - \frac{d\dot{P}}{dP}\dot{Q} = g\,.$$

The latter equation is a linear differential equation in $\dot{Q}$ which may be integrated to obtain

$$(1.74) \qquad \left.\frac{\dot{Q}}{\dot{P}}\right]_0^{t_f} = g \int_0^{t_f} \frac{dt'}{\dot{P}}\,.$$

Since $\dot{Q} = O$ at $t = O$, $\dot{P} = u = u_o$ at $t = O$, $dt' = dP'/u$, and $P = P$ at $t = t_f$, we have

$$(1.75) \qquad \dot{Q} = gu \int_0^P \frac{dP'}{u^2}$$

where the prime is again a dummy index. A second integration yields, since $Q = O$ at $t = O$,

$$(1.76) \qquad Q = g \int_0^{t_f} \left[u \int_0^P u^{-2}\, dP'\right] dt$$

or

$$(1.77) \qquad Q = g \int_0^P \int_0^{P'} u^{-2}\, dP''\, dP'$$

where again dummy variables of integration are used, with the evaluation of t_f and Q for given values of P from equations (1.26) or (1.27) and a transformation to the x, y, z coordinate system.

The effect of the windage jump upon the trajectory is small and is applied to the trajectory by an approximate differential correction. The windage jump changes the direction of the line of departure by adding to the vector $\mathbf{u}_o$ a vector $\mathbf{J}$ whose magnitude is $u_o\epsilon$ and which is directed at right angles to the plane containing $\mathbf{V}_G$ and $\mathbf{V}_o$, in a sense such that vectors in the directions of $\mathbf{V}_G$, $\mathbf{V}_o$, $\mathbf{J}$ form an ordered right-handed triad. Since it is perpendicular to the plane containing $\mathbf{V}_G$ and since $\mathbf{V}_G$ is assumed to be directed along the X-axis, the vector $\mathbf{J}$ is perpendicular to the X-axis and its direction cosine with respect to X is zero. Since this vector also is perpendicular to $\mathbf{V}_o$, it is easily seen, by referring to figure 11, that its direction cosines with respect to the other axes can be found from the diagram of figure 18 in which V_o' is the projection of V_o upon the (Y,Z)-plane.

They are thus $\sin\psi$ and $\cos\psi$. Formulas (1.21) then furnish the direction cosines for the x, y, z system in the form

$$(1.78) \qquad \begin{aligned} &O,\ \cos Z_o/(1 - \sin^2 Z_o \cos^2 A_o)^{\frac{1}{2}}, \\ &\sin Z_o \sin A_o/(1 - \sin^2 Z_o \cos^2 A_o)^{\frac{1}{2}}. \end{aligned}$$

The components in the x, y, z system are these direction cosines multiplied by $u_o\epsilon$.

The windage jump does not alter the magnitude of $\mathbf{u}_o$; its effect is to increase the X, Y, Z coordinates of the projectile by the x, y, z components multiplied by the time factor P/u_o. We thus have the increments

$$(1.79) \qquad \begin{cases} \Delta x = O\,; \\ \Delta y = P\epsilon \cos Z_o/(1 - \sin^2 Z_o, \cos^2 A_o)^{\frac{1}{2}}\,; \\ \Delta z = P\epsilon \sin Z_o \sin A_o/(1 - \sin^2 Z_o \cos^2 A_o)^{\frac{1}{2}}. \end{cases}$$

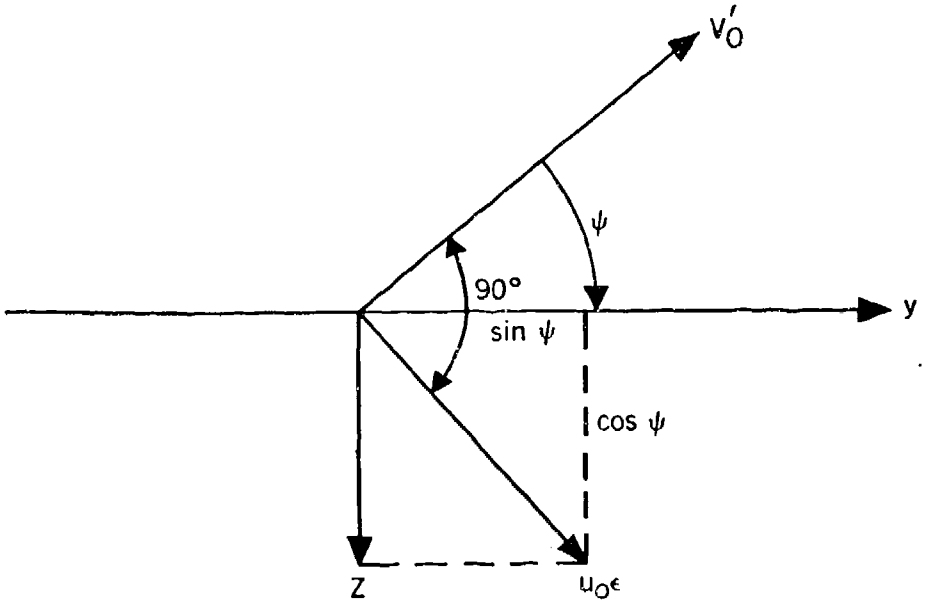

Figure 18. — Direction Cosines of $u_0\epsilon$

It follows then that the increments on ξ, η, ζ are

$$(1.80)\quad \begin{cases} \Delta\xi = O, \\ \Delta\eta = -P_\epsilon\,(1 - \sin^2 Z_o \cos^2 A_o)^{-\frac{1}{2}} \cdot [\sin^2 Z_o \sin A_o + \cos^2 Z_o \sin A_o] \\ \quad = -P_\epsilon\,(1 - \sin^2 Z_o \cos^2 A_o)^{-\frac{1}{2}} \cdot (\sin A_o)\,, \\ \Delta\zeta = P_\epsilon \cos Z_o \cos A_o\,(1 - \sin^2 Z_o \cdot \cos^2 A_o)^{-\frac{1}{2}}\,. \end{cases}$$

The resulting effect on r_f is small and will be neglected. We are then concerned only with the small increases in λ and μ which are represented by $\delta\lambda$ and $\delta\mu$. The initial yaw angle may be regarded as $\tau - \nu$ of figure 10 so that

$$(1.81)\quad \sin\delta_o = \frac{V_G}{u_o}\sin\tau\,.$$

Since the theory is based on a small angle δ_o we may put δ_o equal to its sine for the following approximation:

$$(1.82)\quad \delta_o^2 = V_G^2\,(1 - \sin^2 Z_o \cos^2 A_o)/u_o^2$$

or

$$(1.83)\quad (1 - \sin^2 Z_o \cos^2 A_o)^{\frac{1}{2}} = \delta_o u_o / V_G\,.$$

Upon using (1.30) and (1.80), the increments on λ and μ are then approximated by

$$(1.84)\quad \begin{cases} \delta\lambda = \dfrac{P}{r_f}\,\epsilon\,\dfrac{V_G}{\delta_o u_o}\cos Z_o \cos A_o\,, \\ \delta\mu = -\dfrac{P}{r_f}\,\epsilon\,\dfrac{V_G}{\delta_o u_o}\sin A_o\,. \end{cases}$$

Substituting (1.55) into (1.84) yields

$$(1.85)\quad \begin{cases} \delta\lambda = b\,\dfrac{P}{r_f}\,\dfrac{V_G}{u_o^2}\cos Z_o \cos A_o\,, \\ \delta\mu = -\,b\,\dfrac{P}{r_f}\,\dfrac{V_G}{u_o^2}\sin A_o \end{cases}$$

where

$$(1.86)\quad b = \frac{AN}{md}\,\frac{K_L}{K_M}\,.$$

1.12 Ballistic Computations for Aerial Gunnery

Ballistic data is computed and presented in firing tables. For aerial gunnery, the computation is based upon the theory developed in the

last section, the computational steps for which may be summarized briefly as follows:

(1) Determination of the drag function $G_n(u)$ for a projectile of given type by test firings.

(2) Determination of the corresponding Siacci Space function $S(u)$. See equation (1.17).

(3) Determination of the ballistic constants K_L, K_M, K_D, $K_D\delta$, V_o, s_s, c', c'', b, and C_n for the specific projectile from experimental data. $c' = c_1\rho_o$ and $c'' = \rho_o d^2 K_D/2m$ are determined instead of c_1 and c_2. The quantity s_s is the value of the stability factor s near the muzzle of a stationary gun in air of standard density. It is experimentally determined in such a manner that it may be used in step 7 below.

(4) Choose values of the variables, each from one of the following intervals and hold these values constant throughout a given computation:

$O \leq \rho \leq 1.$ $\quad O \leq Z_o \leq 180°$

$O \leq V_G \leq 600$ mi/hr. $\quad O \leq A_o \leq 180°$

$O \leq P \leq 10{,}000$ ft. $\quad$ Starboard side.

The computations for the port side are the same except that the lateral deflections change signs.

(5) Compute u_o:

$$u_o^2 = V_o^2 + 2V_G V_o \sin Z_o \cos A_o + V_G^2.$$

(6) Compute δ_o^2:

$$\delta_o^2 = \frac{V_G^2}{u_o^2}(1 - \sin^2 Z_o \cos^2 A_o) \text{ in radians.}$$

(7) Compute s_o:

$$s_o = V_o^2 s_s / p u_o^2 .$$

(8) Compute c:

$$c = c' + \frac{c''}{s_o - 1}.$$

(9) Compute K:

$$K = \frac{1}{2C_n c} K_D\delta \, \delta_o^2 \frac{s_o - .5}{s_o - 1}.$$

(10) Compute S for a given sequence of P taken at even intervals:

$$S = S_o + \frac{\rho}{C_n} P + K(1 - e^{-2\rho c P})$$

where S_o is the value of the Siacci space function at u_o and is found from the Siacci Space Function Table.

(11) Find u from the Siacci Space Function Table using the values of S from (10), and then compute $1/u$ and $1/u^2$.

(12) Compute the time of flight t_f:

$$t_f = \int_0^P \frac{1}{u} dP'$$

by a numerical integration having given $1/u$, the integrand, at evenly spaced intervals of P.

(13) Compute Q:

$$Q = g \int_0^P \int_0^{P'} \left(\frac{1}{u}\right)^2 dP'' \, dP'$$

by a numerical integration. This is simply a procedure of finding the second primitive.

(14) Compute ξ, η, ζ:

$$\xi = P\frac{V_o}{u_o} - Q\cos Z_o + V_G\left(\frac{P}{u_o} - t_f\right)\sin Z_o \cos A_o,$$

$$\eta = -V_G\left(\frac{P}{u_o} - t_f\right)\cos Z_o \cos A_o - Q\sin Z_o,$$

$$\zeta = -V_G\left(\frac{P}{u_o} - t_f\right)\sin A_o.$$

(15) Compute r_f:

$$r_f^2 = \xi^2 + \eta^2 + \zeta^2.$$

(16) Compute λ and μ:

$$\sin\lambda = \frac{\zeta}{r_f} \text{ and } \sin\mu = \frac{\eta}{r_f}.$$

(17) Compute $\delta\lambda$ and $\delta\mu$:

$$\delta\lambda = b\frac{V_G}{u_o^2}\frac{P}{r_f}\cos Z_o \cos A_o,$$

$$\delta\mu = -b\frac{V_G}{u_o^2}\frac{P}{r_f}\sin A_o.$$

The computation gives values of t_f, λ, μ, $\delta\lambda$, and $\delta\mu$ for evenly spaced values of P and corresponding computed values of r_f at the chosen values of the variables mentioned in (4) above. These quantities can then be put in terms of evenly spaced values of r_f by graphical interpolation or by any other convenient method of interpolation. This is the usual form for tabulating data in aircraft firing tables.

The units in which the tables are computed are feet, radians, mils, and seconds. The units in which the tables are published are usually yards, miles per hour, mils, and seconds. The mil used here is the military mil defined to be 1/6400 of a revolution.

1.13 Bullet Firing Tables

In order to further illustrate the computation and use of firing tables let us consider a small portion of a bullet firing table. A certain 20-mm projectile has the following ballistic characteristics:

$s_s = 2.85$; $c' = .0015488$ ft.$^{-1}$;

$C_n = .510$; $c'' = .0000978$ ft.$^{-1}$;

$K_D\delta = 16.4$; $b = 86{,}600$ mils/ft/sec.;

$V_o = 2750$ ft/sec.

Consider the following values of the variables:

$V_G = 300$ mi./hr. $= 440$ ft./sec.

$\rho = .8$

$A_o = 45° = 800$ mils

$Z_o = 22.5° = 400$ mils

$g = 32.174$ ft./sec^2.

P was chosen at intervals of 1000 ft. For the integration, 9-point Lagrangian integration coefficients were used. The quantity A represents the first integral of $1/u^2$ and B is the second integral; i.e., B is the integral of A. The interpolation for evenly spaced intervals of r_f was done graphically. The windage jump corrections, $\delta\lambda$, and $\delta\mu$, are nearly constant for r_f and are usually tabulated for all r_f. The constancy can be seen by the check made at the two extremes. The evenly spaced intervals for r_f are given in yards, everything else is in feet. λ and μ are obtained in mils by simply multiplying their sines by 1020.

Table 1.1 Computation of Firing Tables

P	$2\rho cP$	$e^{-2\rho cP}$	S	u	$\frac{1}{u}\times 10^{+3}$	t_f	$\frac{1^2}{u}\times 10^{+6}$
0	0	1	4224.264	2900.162	.34481	0	.11889
1000	2.55248	.077888263	6036.468	2456.784	.40704	.37874	.16568
2000	5.10496	.006066582	7624.067	2098.867	.47645	.81870	.22700
3000	7.65744	.000472516	9194.171	1777.268	.56266	1.33695	.31659
4000	10.20992	.000036803	10762.913	1489.775	.67124	1.95149	.45057
5000	12.7624	.000002867	12331.549	1242.493	.80483	2.68828	.64775
6000	15.31488	.000000223	13900.177	1074.132	.93098	3.55875	.86673
7000	17.86736	.000000017	15468.804	983.271	1.01701	4.53598	1.03432
8000	20.41984	.000000001	17037.431	911.952	1.09655	5.59012	1.20242

P	$A\times 10^{+3}$	B	Q	$t_f-\frac{P}{u_o}$	$V_G\left(t_f-\frac{P}{u_o}\right)$
0	0	0	0	0	0
1000	.145342	.070032	2.2532	.033930	14.92918
2000	.338967	.306882	9.8736	.129080	56.79527
3000	.608321	.773153	24.8754	.302525	133.11120
4000	.986850	1.559572	50.1777	.572258	251.79355
5000	1.531335	2.802213	90.1584	.964237	424.26407
6000	2.290161	4.694521	151.0415	1.489900	655.55608
7000	3.216363	7.449026	239.6650	2.122321	933.82126
8000	4.355123	11.235351	361.4862	2.831657	1245.92894

P	ξ	η	ζ	r_f	$\sin\lambda$	$\sin\mu$	λ	μ
0	0	0	0	0	0	0	0	0
1000	942.101	8.891	10.557	942.202	.011204	.009436	11.43	9.6
2000	1871.955	33.325	40.160	1872.682	.021445	.017795	21.87	18.15
3000	2785.667	77.440	94.124	2788.332	.033756	.027772	34.43	28.33
4000	3678.399	145.290	178.045	3685.570	.048308	.039421	49.27	40.21
5000	4543.014	242.662	300.000	4559.371	.065798	.053222	67.11	54.29
6000	5372.402	370.462	463.548	5405.073	.085761	.068539	87.48	69.91
7000	6163.449	518.334	660.312	6220.353	.106153	.083328	108.28	84.99
8000	6914.669	675.609	881.005	7003.232	.125799	.096471	128.31	98.40

r_f	400	800	1200	1600	2000
t_f	.49	1.11	1.89	2.92	4.26
λ	14	29	48	73	102.5
μ	12	24	39	59	81
$\delta\lambda$	3.1	—	—	—	3.4
$\delta\mu$	−3.4	—	—	—	−3.7

Firing tables are usually massive. A small portion of one table is presented here for future reference.

Table 1.2

Firing Table. Without Windage Jump																
$\rho = .4$							$V_o = 2750$ ft/sec.					$V_G = 450$ mi/hr.				
		t_f seconds					μ mils					λ mils				
Z mils	A mils	D (yds)*					D (yds)*					D (yds)*				
		400	800	1200	1600	2000	400	800	1200	1600	2000	400	800	1200	1600	2000
1200	0	.47	1.00	1.61	2.33	3.22	3	6	8	12	15	0	0	0	0	0
	400	.47	1.00	1.61	2.33	3.20	3	5	7	10	12	6	12	18	26	36
	800	.47	1.01	1.62	2.32	3.16	2	3	4	4	5	12	23	35	49	66
	1200	.48	1.02	1.62	2.30	3.08	0	−1	−2	−4	−6	20	34	48	65	84
	1600	.48	1.02	1.60	2.26	2.98	−3	−6	−9	−14	−18	25	40	55	71	88
	2000	.48	1.00	1.57	2.18	2.85	−6	−11	−16	−22	−28	22	35	47	60	74
	2400	.47	.98	1.52	2.10	2.72	−9	−15	−22	−28	−36	15	24	32	41	50
	2800	.46	.96	1.48	2.04	2.63	−9	−17	−24	−31	−39	9	13	17	21	26
	3200	.46	.94	1.46	2.00	2.58	−9	−17	−24	−31	−39	0	0	0	0	0
1600	0	.46	.99	1.60	2.31	3.18	−3	−6	−10	−16	−23	0	0	0	0	0
	400	.46	.99	1.60	2.31	3.17	−3	−6	−10	−16	−23	6	11	18	26	35
	800	.47	1.00	1.61	2.31	3.13	−3	−6	−10	−16	−22	12	22	34	48	64
	1200	.48	1.01	1.61	2.28	3.05	−3	−6	−10	−15	−21	20	34	48	64	82
	1600	.48	1.02	1.60	2.24	2.95	−3	−6	−10	−15	−20	25	40	54	70	87
	2000	.47	.99	1.55	2.16	2.81	−3	−6	−10	−14	−18	21	34	46	58	72
	2400	.46	.97	1.50	2.07	2.67	−3	−6	−9	−13	−17	13	22	30	39	47
	2800	.46	.94	1.45	1.99	2.56	−3	−6	−9	−12	−16	7	12	16	20	24
	3200	.45	.92	1.42	1.95	2.51	−3	−6	−9	−12	−15	0	0	0	0	0

*$D = r_f$

1.14 Bomb Ballistics

In bombing from an aircraft at ground targets, the bomb is released without any projecting force and allowed to fall. As it travels through the air, it is acted upon by the forces of gravity and air resistance. The bomb is, of course, given an initial velocity which is the true airspeed of the aircraft. If a wind is blowing, it also will act upon the bomb and will cause it to drift with respect to the ground, and this drift becomes a serious factor in bombing.

The force system for a bomb is similar to that of the general projectile already discussed. A bomb, however, is not given a spin but is equipped instead with symmetrical fins which serve to bring the center of pressure behind the center of gravity, thus making the bomb stable.

The same coordinate system that was used before also can be used for bombing, except that the origin is now located at the summit of the trajectory and the trajectory has only a descending branch.

In general, the theory is the same. We shall consider the theory of bombing in chapter 6.

1.15 Rocket Ballistics

In the firing of rockets from aircraft, the rocket is propelled during its burning time and thereafter falls freely like a bomb. Thus a rocket acts like both a bullet and a bomb. The forces acting on a rocket are the same as those on any other projectile. However, the changing of its projecting velocity during the course of its travel causes added peculiarities. The ballistics of a rocket will be discussed in chapter 7 where the theory of rocket firing will be considered in detail.

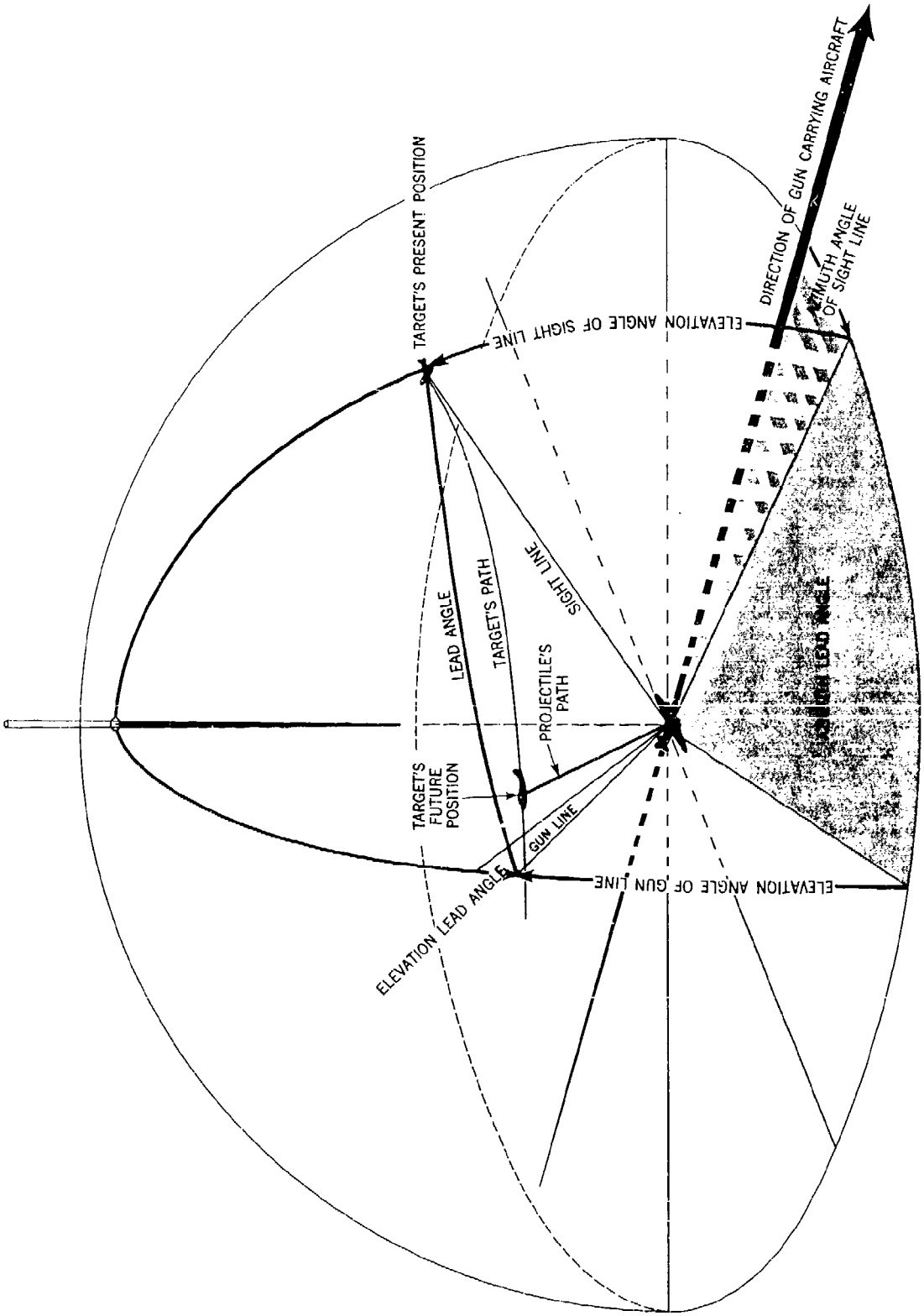

Figure 19. — Air-to-air Gunnery

Chapter 2

DEFLECTION THEORY FOR AIR-TO-AIR GUNNERY

2.1 Introduction

In the main, the present chapter will be concerned with the problem of successfully aiming a moving gun at a moving target so as to secure a hit. Since it is only in special circumstances that the gun will be pointed directly at the target, of immediate concern to us will be the development of formulas expressing the angle by which the gun-bore axis must be deflected from the gun-target line at the instant of fire in terms of kinematic and ballistic factors continuously measurable at the gun. This angle is known as the angle of lead or, more briefly, the lead angle. The gun will be thought of as mounted on a platform, called the gun-platform, and hereafter denoted by the letter G; while the target, denoted by T, will be a fighter aircraft attacking G. The gun platform G may be considered to be a bomber or turreted fighter with flexible guns, i.e., guns the direction of whose fire is in general unrestricted. By motion of G or T we shall mean motion with respect to the air mass, so that the concept of absolute wind need not be taken into account here. An object will be fixed in space if it has no motion with respect to the air mass.

2.2 Actual Motion and Relative Motion

The actual path in space traced by T, and viewed by an observer fixed at O, is in general a very different appearing curve when viewed from the moving point G. Thus, if G flies straight and level and T flies along just abreast of G, an observer at O sees T describe a straight line, whereas to the gunner at G the target T will appear to hang stationary off his beam. In general, the path of T as seen from O is called the "air course" of T whereas the path as viewed from G is spoken of as the "relative course." By way of illustration, figure 20 shows air courses of G and T, supposed coplanar, with corresponding positions of G and T indicated for consecutive seconds. The angle τ measured from G's

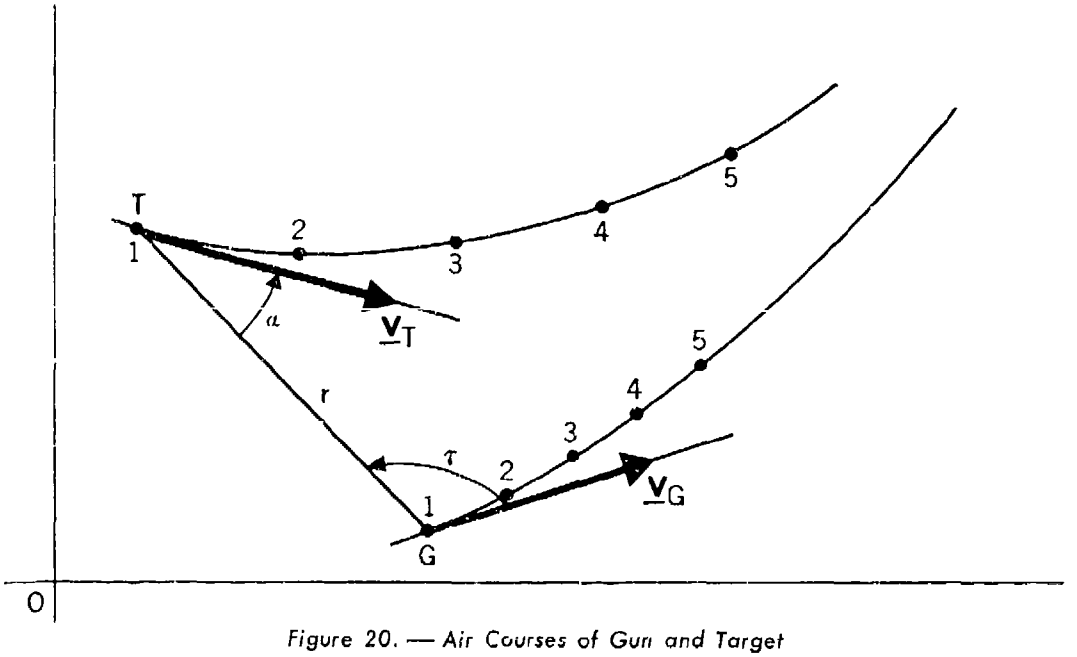

Figure 20. — Air Courses of Gun and Target

bow to the gun-target line GT, is called the angle-off of the target or simply the angle-off. The approach angle α, measured at the present position of the target, is formed by the tangent to the target's path and the gun-target line. More precisely, it is defined as the directed angle from $-\mathbf{r}$ to $\mathbf{V}_T$. The distance GT, denoted by r, is the present range of the target. The curve drawn in figure 21 represents the path of T relative to G and may be obtained by plotting on polar coordinate paper the points (r, τ) associated with each G position and drawing a smooth curve through these points. In figure 20, the points were plotted assuming constant tangential speeds for both T and G, that is to say, the magnitudes V_T, V_G of the velocity vectors $\mathbf{V}_T$, $\mathbf{V}_G$ are constant. Hence, it is important to notice that while on the air courses equal distances are covered in equal times, along the relative course this is no longer true. The velocity of T relative to G is in fact $\mathbf{V}_T - \mathbf{V}_G$ whose magnitude, as can be easily verified from figure 20, is

$$(2.1) \quad |\mathbf{V}_T - \mathbf{V}_G| = \sqrt{V_G^2 + V_T^2 + 2V_G V_T \cos(\alpha + \tau)}.$$

This magnitude is dependent on α and τ and hence is, in general, not constant.

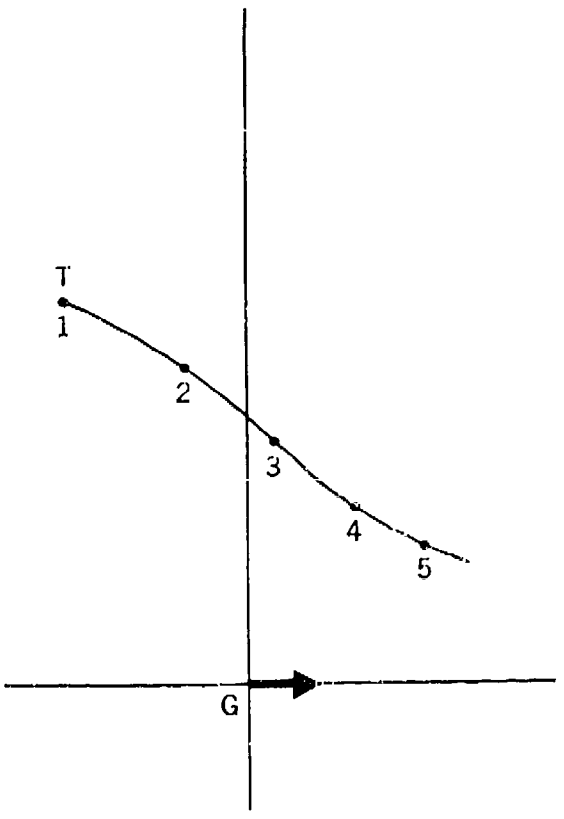

Figure 21. — Path of T Relative to G

2.3 Case I—Fixed Gun-Platform—Linear Target Motion

This case is essentially that which obtains in antiaircraft fire, but, as will be seen, it also applies to the fighter pilot's problem of correctly aiming forward-firing guns. The basic aiming allowance here is for the target's motion during the projectile's time in flight and is called the kinematic lead. Additional slight modifications of the gun bore's position must be made to allow for gravity drop. In this paragraph we shall consider the kinematic lead only, reserving gravity drop corrections for later cases of which this case can be considered to be a particular instance.

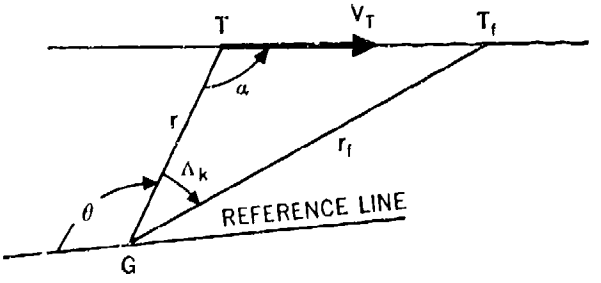

Figure 22. — Fixed Gun vs. Moving Target

In figure 22, suppose that T traverses line TT_f with constant speed V_T. T_f represents the position of the target at the time of impact with a suitably aimed projectile and will be referred to as the future position of the target. Similarly, r_f will be called the future range. The angle Λ_k, measured positively in a clockwise direction when viewed from above, is then the required kinematic deflection. Letting t_f be the time of flight of the bullet over the range r_f, and V_f be the mean velocity of the bullet over this range, then in triangle GTT_f the Law of Sines yields

$$\frac{\text{Sin } \Lambda_k}{\text{Sin } \alpha} = \frac{TT_f}{r_f} = \frac{V_T t_f}{V_f t_f} = \frac{V_T}{V_f},$$

whence,

$$(2.2) \quad \sin \Lambda_k = \frac{V_T}{V_f} \sin \alpha .$$

If the lead angle Λ_k is small, we can replace $\sin \Lambda_k$ by Λ_k, provided Λ_k is measured in radians, with resulting error less $\frac{1}{6} \Lambda_k^3$. Equation (2.2), considered from the standpoint of a lead-computing sight, is not of much value since the quantities V_T, α would not be directly available as inputs. If we resolve the vector $\mathbf{V}_T$ into components along and perpendicular to GT, then the perpendicular component may be written

$$(2.3) \quad V_T \sin \alpha = r\omega = r \frac{d\theta}{dt} = r\dot{\theta}$$

wherein ω is the angular rate of the line GT in rad/sec and θ is its angular coordinate referred to a fixed reference line through G. Combining (2.3) and (2.2) we may write

$$(2.4) \quad \sin \Lambda_k = \frac{r\omega}{V_f} .$$

In order to put (2.4) into an approximate form involving only present data, let us introduce the velocity V_r, which represents the mean velocity if the bullet had to cover r instead of r_f. Then,

$$\sin \Lambda_k = \frac{V_r}{V_f} \cdot \frac{r\omega}{V_r} = \frac{V_r}{V_f} \cdot t\omega$$

where t is the present time of flight, that is, the bullet's time of flight over the range r. Since for small Λ_k, r and r_f differ very little, the factor $\frac{V_r}{V_f}$ is close to 1 and we have, as a useful approximation, the formula

$$(2.5) \quad \Lambda_k = t\omega .$$

The fighter pilot's problem of correctly aiming forward-firing guns is then taken care of approximately by (2.4), wherein V_f is replaced by a new mean velocity arising out of the fact that the projectile's muzzle velocity has been augmented by the velocity of the aircraft. Thus, as far as the mathematics of the situation is concerned, the pilot might as well be sitting in a balloon firing bullets of higher muzzle velocity.

2.4 Case 2—Moving Gun-Platform —Fixed Target

This case — which might properly be called the strafing case — is, mathematically speaking, the complement of the fixed gun versus moving target case. There are, however, important physical differences. In Case 1, the path of the bullet is an extension of the bore axis, a fact which is no longer true here as is evident from figure 23. The muzzle velocity $\mathbf{V}_o$ of the bullet is compounded with the gun-platform velocity $\mathbf{V}_G$ according to the parallelogram law to give a resultant velocity $\mathbf{u}_o$ of the bullet with respect to the air mass. We shall refer to $\mathbf{u}_o$ as the initial velocity of the bullet and to the parallelogram $GABC$ as the firing parallelogram.

Under the assumption that the bullet travels a straight line, it is evident from the figure that, to hit the fixed target T, it is sufficient to aim the gun so that the arrow GB will be pointing directly towards T at the time of fire. Neglecting gravity drop as before, we find from triangle GAB that

$$\frac{\sin \Lambda}{\sin \tau} = \frac{AB}{GA} = \frac{GC}{GA} = \frac{V_G}{V_o},$$

whence

$$(2.6) \quad \sin \Lambda = \frac{V_G}{V_o} \sin \tau .$$

The path of the gun platform is shown as a curved line in figure 23, for the sake of generality. Actually, the individual bullet is only concerned with the tangential velocity $\mathbf{V}_G$ at the instant of fire. What the gun-platform does after the bullet leaves it, no longer affects the motion of the bullet.

From (2.6), we note that bullet direction is determined by $\mathbf{V}_o$ and $\mathbf{V}_G$ and, except for gravity

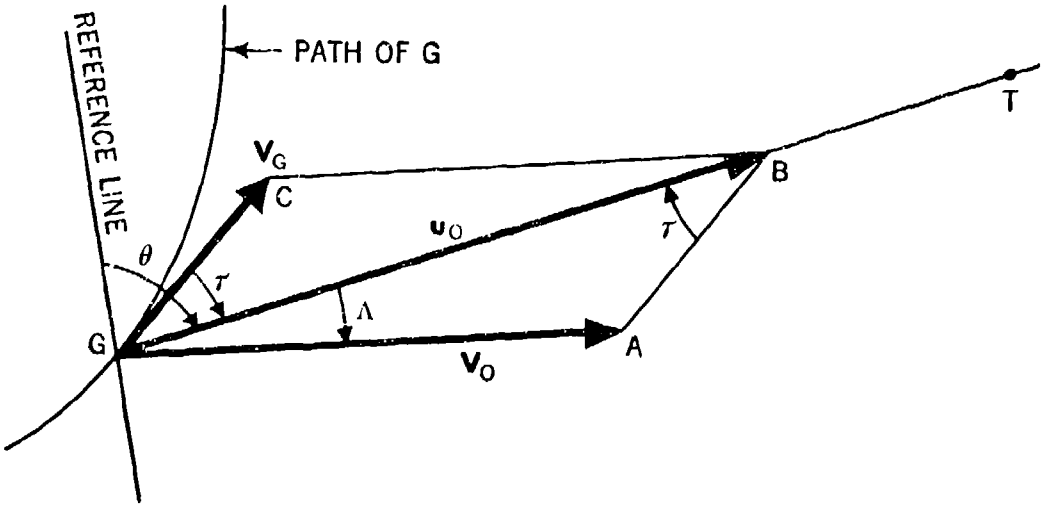

Figure 23. — Moving Gun vs. Fixed Target

drop, is independent of bullet range GT. This contrasts with Case 1 of the fixed gun-platform — moving target, where bullet direction was dependent on V_f (cf. Equation (2.2)), which in turn depended on the bullet range GT_f. In the present case, the only effect of range is that a more distant target will be hit a little later.

The ratio

$$\frac{V_G \sin \tau}{V_o} = \frac{\text{speed of gun-platform in a direction perpendicular to the gun-target line}}{\text{muzzle speed of bullet}}$$

appears frequently in the theory of aerial gunnery and is called the own-speed deflection. Hence we may say that for a fixed target, the sine of the lead angle is given by the own-speed deflection.

Equation (2.6) can be rewritten involving $r = GT$ and $\dot{\theta} = \omega$. Thus,

$$(2.7) \quad \sin \Lambda = \frac{r\omega}{V_o},$$

a form involving mechanizable inputs.

As far as the actual and relative motions are concerned, we remark that in space, GT rotates about T as a pivot, but, as the gunner at G sees things, G is fixed and T is drifting backwards with angular rate ω.

2.5 Case 3—Moving Gun-Platform—Moving Target on a Straight Line

In this section we shall combine Cases 1 and 2 and permit both platform and target to move. We shall assume, for simplicity at this point, that the air courses of G and T are coplanar and that the air course of T is in fact a straight line traversed with constant speed. Gravity drop will again be neglected.

Referring to figure 24, G, T are the present positions of gun and target, that is, the positions at the instant of fire; GT_f is the air course of the bullet (bullet range), T_f is the future position of T (position at time of impact with the bullet) and t_f is the time taken for the bullet to cover the range GT_f. The broken lines represent auxiliary constructions necessary for the following derivation:

$$\sin \Lambda = \frac{FA}{V_o} = \frac{BD - BE}{V_o}$$

$$= \frac{V_G \sin \tau - u_o \sin \varphi}{V_o}$$

or

$$(2.8) \quad \sin \Lambda = \frac{V_G}{V_o} \sin \tau - \frac{u_o}{V_o} \sin \varphi,$$

a form useful for computational purposes.

From triangle GTT_f we have by the Law of Sines

$$\sin\varphi = \frac{V_T t_f}{GT_f}\sin\alpha = \frac{V_T}{\dfrac{GT_f}{t_f}}\sin\alpha$$

$$= \frac{V_T}{\bar{u}}\sin\alpha = \frac{qV_T}{u_o}\sin\alpha\,,$$

where

$$q = \frac{u_o}{\bar{u}} = \frac{\text{initial speed of bullet}}{\text{average speed of bullet}} > 1\,.$$

Equation (2.8) may now be written

$$\text{(2.9)}\quad \sin\Lambda = \frac{V_G}{V_o}\sin\tau - \frac{qV_T}{V_o}\sin\alpha\,.$$

The quantity q defined above is a measure of bullet slowdown. Indeed, the average bullet speed is obtained by multiplying the initial speed u_o by $\frac{1}{q}$. An interpretation of q in terms of t_f also can be given. Letting $GT_f = R$ we have

$$\text{(2.10)}\quad q = \frac{u_o}{\bar{u}} = \frac{u_o t_f}{R} = \frac{t_f}{\dfrac{R}{u_o}} = \frac{t_f}{t_o}$$

$$= \frac{t_o + lt_o}{t_o}\,, \qquad l > O\,,$$

wherein t_o represents the time required for the bullet to cover R in a vacuum. From (2.10),

$$\text{(2.11)}\quad q = \frac{u_o t_f}{R} = 1 + l$$

and

$$t_f = t_o + lt_o = qt_o\,,$$

which shows that l represents the proportion by which the time of flight has been increased due to the slowdown of the bullet.

Assuming angles to be measured positively as indicated by the arrows in figure 24, we can now see how (2.9) can be regarded as a combination of the formulas (2.2) and (2.6) of the two previous cases of fixed gun-platform vs. fixed target. The first term of (2.9) tells the gunner to aim to the rear to make allowance for his own speed while the second term tells

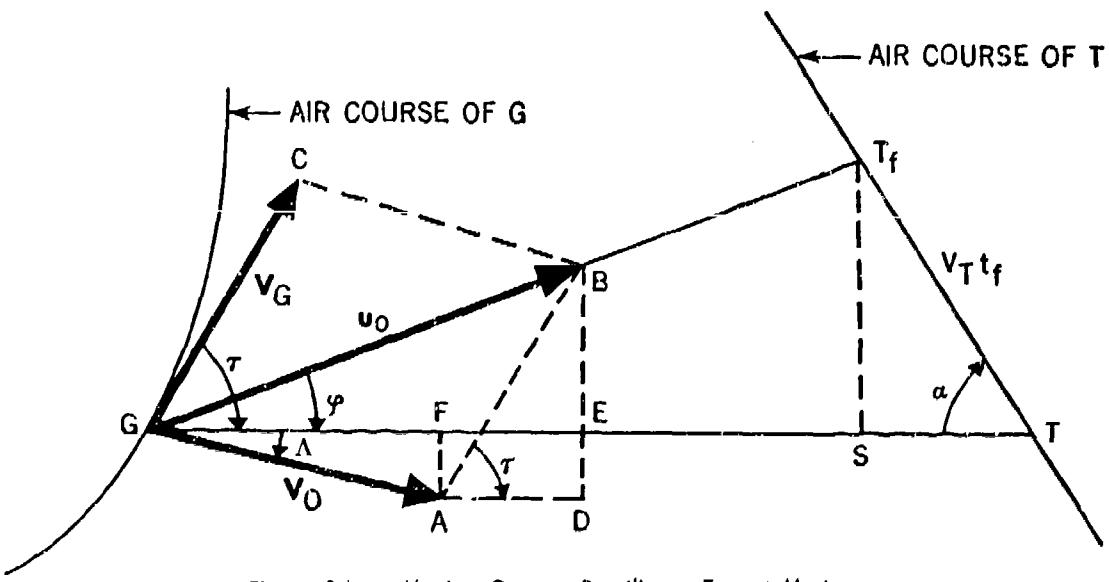

Figure 24. — Moving Gun vs. Rectilinear Target Motion

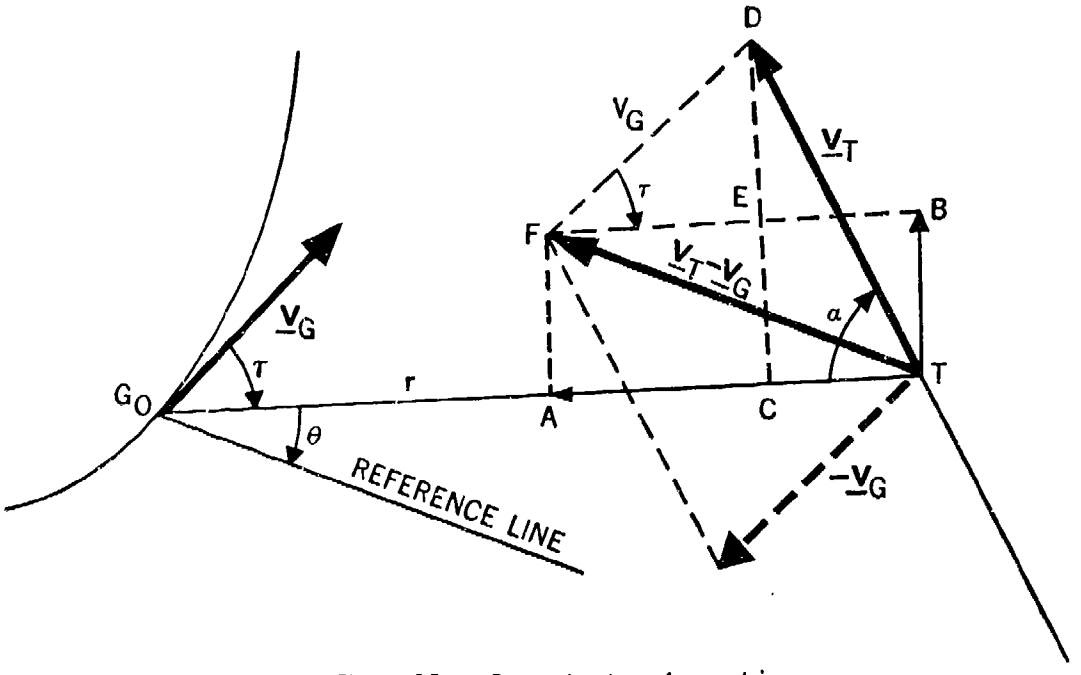

Figure 25. — Determination of ω and $\dot{r}$

him to pull the gun forward (backwards if the target is receding) to allow for target motion.

As before, the lead angle Λ also can be expressed in terms of the angular rate ω of the gun-target line GT and the present range r. To derive a formula for ω, we make use of the relative velocity concept introduced in section 2.2. In figure 25, the velocity of T relative to G is the vector $\mathbf{V}_T - \mathbf{V}_G$. Assuming clockwise angular motion as positive and linear measurements on GT positive when directed from G towards T, we have, upon resolving this vector into components perpendicular to and along G_oT:

$$\begin{aligned} -r\dot{\theta} = -r\omega &= TB = CD - ED \\ &= V_T \sin\alpha - V_G \sin\tau \end{aligned}$$

or

$$(2.12) \qquad r\omega = V_G \sin\tau - V_T \sin\alpha .$$

A useful formula for range rate $\dot{r}$ is obtained by considering the component of $\mathbf{V}_T - \mathbf{V}_G$ on G_oT:

$$\begin{aligned} \dot{r} &= -AT = -AC - CT \\ &= -V_G \cos\tau - V_T \cos\alpha \end{aligned}$$

or

$$(2.13) \qquad \dot{r} = -(V_G \cos\tau + V_T \cos\alpha).$$

Although figure 25 is drawn for straight line target motion, it is obvious that the formulas (2.12) and (2.13) hold in general since $\mathbf{V}_T$ at only one point is involved in their derivations.

Eliminating in succession τ and α from (2.9) and (2.12), we find

$$(2.14) \qquad \sin\Lambda = \frac{r\omega}{V_o} - l\frac{V_T}{V_o}\sin\alpha ;$$

and

$$(2.15) \qquad \sin\Lambda = q\frac{r\omega}{V_o} - l\frac{V_G}{V_o}\sin\tau .$$

In order to interpret these equations, observe that if there were no slowdown of the bullet, we would have $l = O$ and then $\sin\Lambda$ would be given by

$$(2.16) \qquad \sin\Lambda = \frac{r\omega}{V_o} = \frac{V_G}{V_o}\sin\tau - \frac{V_T}{V_o}\sin\alpha .$$

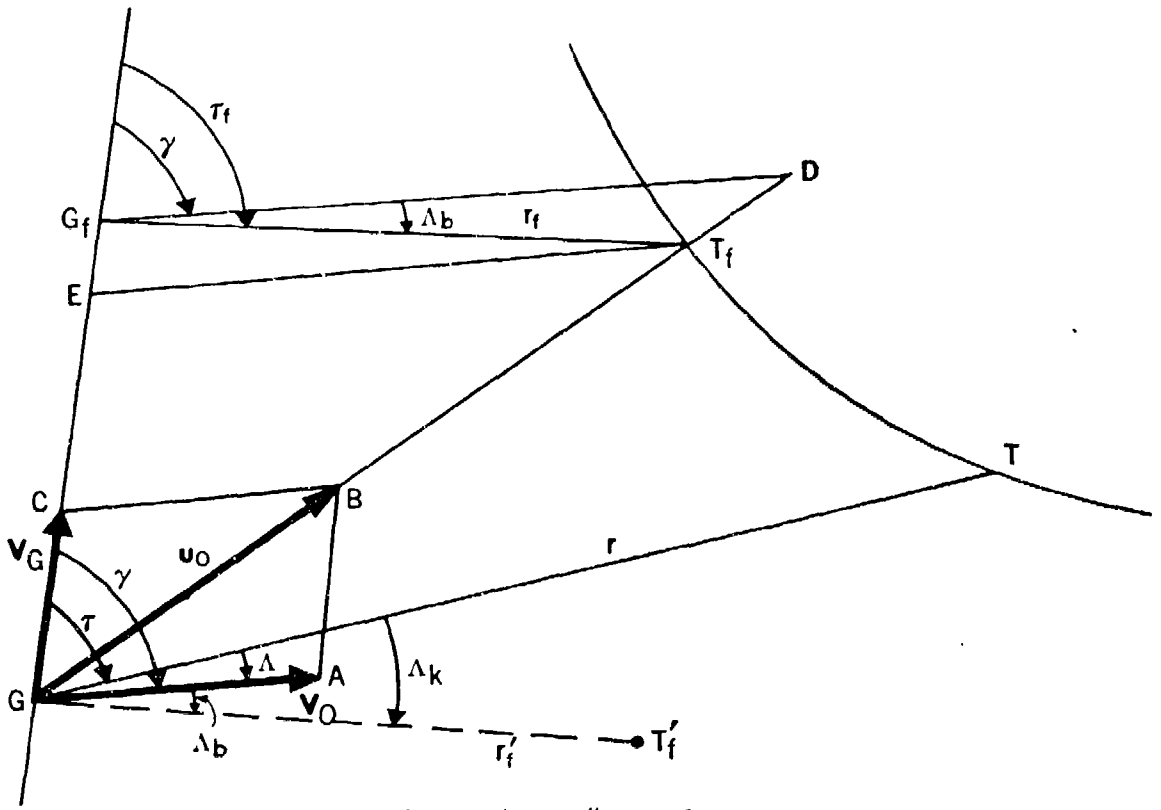

Figure 26. — Ballistic Deflections

Rewriting (2.9) as

$$\sin \Lambda = \frac{V_G}{V_o} \sin \tau - \frac{V_T}{V_o} \sin \alpha$$

$$- \frac{lV_T}{V_o} \sin \alpha$$

we see, by comparing it with (2.16), that bullet slowdown alters the lead term *sin* Λ by the amount

$$l \frac{V_T}{V_o} \sin \alpha .$$

2.6 Kinematic Lead and Bullet Trail

To simplify matters, we shall assume that the gun traverses a straight line with constant speed, the target path being unrestricted. Again we consider only the two-dimensional case with both air courses lying in the same mathematical plane and gravity effect on the bullet negligible. In figure 26, G and T are the positions of the gun-platform and target at the time of fire. Their positions at the time of impact of the bullet with T are denoted by G_f and T_f. Then the distance G_fT_f from the gun to the target at the time of impact is called the future range of the target and is denoted by r_f. The firing parallelogram is $GABC$ as before. The angles-off of the gun and sight line are γ and τ, respectively, and their difference $\gamma - \tau$ is by definition the total lead angle Λ.

The bullet leaves the gun with velocity $\mathbf{V}_o$ relative to the gun and with velocity $\mathbf{u}_o = \mathbf{V}_o + \mathbf{V}_G$ with respect to the air mass. We shall suppose that the effect of air resistance on the bullet can be accounted for by a drag force, parallel to the direction of motion, and acting on the bullet at its center of gravity. (As ex-

plained in chapter 1, this assumption is valid, to within a small initial correction called the windage jump, for explaining the motion of the bullet in flight.) The effect, then, of air resistance is a mere slowing down of the bullet along its air course, GT_f. From figure 26 and the results of the last section we note that, for a time of flight of t_f seconds, the bullet range GT_f is equal to the vacuum bullet range GD ($= u_o t_f$) multiplied by the slowdown factor $\frac{1}{q}$.

Thus, $GT_f = u_o t_f / q$. If air resistance were lacking, the bullet would always have a velocity component $\mathbf{V}_G$ in the direction of the gun's motion, so that a person stationed at G would always see the bullet moving along a line which would be a mere extension of the gun bore. In other words, in a vacuum the relative path of the bullet would be the straight line GA. But, because of air resistance the observer at G sees the bullet "curve toward the rear" since the bullet, so to speak, no longer keeps up with the gun. This curved path is, in fact, traced by the point T_f', whose polar coordinates are (r_f', τ_f'), as it moves along the line GT_f with speed $\frac{u_o}{q'}$.

The angle DG_fT_f, measured from the bore axis of the gun to the future range line, is called the bullet trail or lateral deflection of the bullet. It is the same as angle AGT_f' appearing in the lower part of the figure, where the line G_fT_f has been redrawn in the position GT_f'. We shall denote bullet trail by Λ_b. The angle TGT_f' is called the kinematic lead, referred to by the symbol Λ_k. It is the lead arising from the relative motion of the two aircraft and, in the absence of ballistic effects, is coincident with the total lead. In general, as is evident from figure 26, we have

$$(2.17) \qquad \Lambda = \Lambda_k - \Lambda_b .$$

We proceed to derive some formulas for Λ_b for the situation depicted in figure 26. The Law of Sines applied to triangle EG_fT_f yields:

$$\frac{\sin \Lambda_b}{EG_f} = \frac{\sin \gamma}{G_fT_f} = \frac{\sin \tau_f}{ET_f} .$$

Since ET_f is drawn parallel to $G_fD = V_o t_f$, triangles GET_f and GG_fD are similar. Thus we find that

$$EG_f = \frac{lV_G t_f}{q}, \quad ET_f = \frac{V_o t_f}{q},$$

whence

$$(2.18) \qquad \sin \Lambda_b = \frac{lV_G t_f \sin \gamma}{q r_f} = \frac{lV_G}{qV_f} \sin \gamma ,$$

where

$$v_f = \frac{r_f}{t_f} .$$

Similarly,

$$(2.19) \qquad \sin \Lambda_b = \frac{lV_G}{V_o} \sin \tau_f .$$

The quantity V_f appearing in (2.18) represents the average speed of the bullet over the future range. An approximate formula for this quantity is found by applying the Law of Cosines to triangle EG_fT_f. Thus:

$$r_f^2 = EG_f^2 + ET_f^2 - 2(EG_f)\ (ET_f) \cos \gamma$$

or

$$V_f^2 = \frac{1}{q^2} [V_o^2 + l^2V_G^2 - 2lV_oV_G \cos \gamma]$$

$$= \frac{1}{q^2} [(V_o - lV_G \cos \gamma)^2 + l^2V_G^2 \sin^2 \gamma] .$$

Since $V_G << V_o$, the term $l^2V_G^2 \sin^2 \gamma$ is, for most attack data, generally negligible, so that approximately

$$(2.20) \qquad V_f \doteq \frac{V_o - lV_G \cos \gamma}{q}$$

and

$$(2.21) \qquad \sin \Lambda_b \doteq \frac{lV_G}{V_o - lV_G \cos \gamma} \sin \gamma .$$

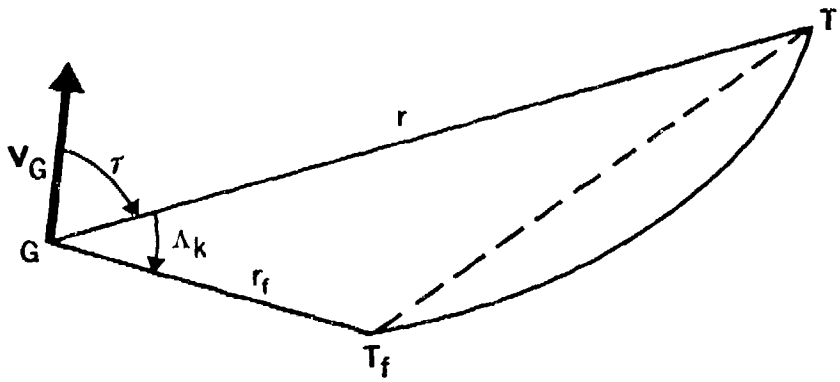

Figure 27. — Aereal Approximation

2.7 Determination of the Kinematic Lead

The angle Λ_k in figure 26 can be determined readily using the relative path of T. An arc of this path traversed by T during the time of flight t_f is shown in figure 27. Since the path of G is here assumed to be a straight line, we have immediately $\omega = \dot{\tau}$. It should be borne in mind that this is no longer true for curvilinear gun-platform air courses. In the latter case, to $\dot{\tau}$ must be added the angular rate of turn of the gun-platform itself.

To find an approximate expression for $\sin \Lambda_k$ we note that:

Area of triangle $TGT_f \doteq$ Area of Sector TGT_f,

or

$$(2.22) \quad \tfrac{1}{2} r r_f \sin \Lambda_k = \tfrac{1}{2} \int_0^{t_f} r^2 \omega dt \; ; \quad (\omega dt = d\tau).$$

The expression $r^2\omega$ can be interpeted physically as the angular momentum of a unit mass placed at point T and moving with T with respect to the moving origin G. We shall denote it by M and refer to it as the angular momentum of the sight line. Let $M(t) = r^2\omega$ at variable time t and let $M = M(O)$.

Expanding $M(t)$ in a Maclaurin's series we may rewrite (2.22) as

$$(2.23) \quad r r_f \sin \Lambda_k = \int_0^{t_f} [M + t\dot{M} + \ldots] dt$$

$$\doteq M t_f + \tfrac{1}{2} \dot{M} t_f^2$$

where $\dot{M} = \dot{M}(t)]_t = O$, etc., and terms of higher order have been neglected. This yields finally the form

$$(2.24) \quad \sin \Lambda_k = \frac{t_f}{r r_f} (M + \tfrac{1}{2} t_f \dot{M})$$

or if (2.20) be employed for $V_f = r_f / t_f$,

$$(2.25) \quad \sin \Lambda_k = \frac{q \; (M + \tfrac{1}{2} t_f \dot{M})}{r \; [V_o - l V_G \cos \gamma]}$$

The approximation (2.22) assumes that the time of flight is small and that the curvature of the relative path is not large.

When the air courses of gun and target are both straight lines, $\dot{M}$ is identically zero and the angular momentum is then constant. To prove this let us write M in the form $r(r\omega)$. We then have, by differentiation with respect to the time,

$$\dot{M} = \dot{r}(r\omega) + r\frac{d}{dt}(r\omega) .$$

Using the relations for $\dot{r}$ and $r\omega$ given by equations (2.13) and (2.12), we find

$$\dot{M} = -r\,V_G\,(\omega - \dot{\tau})\cos\tau$$
$$-\,r\,V_T\,(\omega + \dot{\alpha})\cos\alpha .$$

Since the gun-platform is on a linear path, $\omega = \dot{\tau}$. Moreover, although the angles τ and α are themselves variable, their sum is constant and equal, in fact, to the supplement of the angle of intersection of the two straight line paths. Hence,

$$\omega + \dot{\alpha} = \dot{\tau} + \dot{\alpha} = \frac{d}{dt}(\tau + \alpha) = O .$$

Substituting into the last expression for $\dot{M}$, we obtain $\dot{M} = O$ as desired.

2.8 Case 4—The General Case in Three-Dimensional Space

2.8.1 Introduction

In the preceding sections, lead formulas were derived under the simplifying assumption that the gun-platform and the target moved in a fixed plane, the so-called plane of action. In this, the general case, we shall allow the gun and target paths to be any flyable paths in space. Moreover, the additional corrections in the lead formulas that must be made to take into account ownship acceleration, projectile drop due to gravity, angles of attack and skid, angles of bank and dive, and the secondary ballistic correction due to windage jump, will be accounted for. A general vector equation for the lead will be derived first. This equation, valid for all gun turret coordinate systems, will then be specialized, by way of illustration, for the case where the gun-carrying aircraft is a bomber with an azimuth-elevation top deck turret. An example illustrating the computation of lead angles for a specific tactical situation concludes the study. It should be emphasized that, throughout this chapter, gun and target speeds are assumed constant.

2.8.2 The Muzzle Velocity Vector $\mathbf{V}_o$

As noted in Chapter 1, the windage jump vector $\mathbf{J}$ is perpendicular to the plane of $\mathbf{V}_o$ and $\mathbf{V}_G$ and has the direction of $\mathbf{V}_G \times \mathbf{V}_o$. The initial velocity $\mathbf{u}_o$ is then

$$(2.26) \qquad \mathbf{u}_o = \mathbf{V}_G + \mathbf{V}_o + \mathbf{J}.$$

Thus we find that

$$(2.27) \qquad \mathbf{V}_o = \mathbf{u}_o - \mathbf{V}_G - \mathbf{J}.$$

From figure 28, showing the present and future positions of the gun and target, respectively, we note that the Siacci coordinates $\mathbf{P}$ and $\mathbf{Q}$ of the point T_f have the directions, respectively, of $\mathbf{u}_o$ and $\mathbf{n}$, where $\mathbf{n}$ is a unit vector directed vertically downward.

Hence,

$$\mathbf{u}_o = \frac{u_o}{P}\mathbf{P} = \frac{u_o}{P}(\mathbf{R} - \mathbf{Q}) ,$$

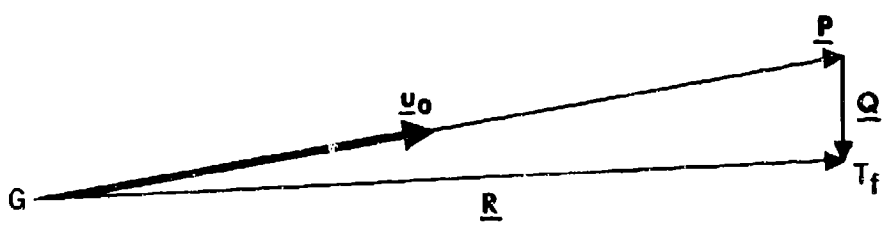

Figure 28. — Siacci Coordinates

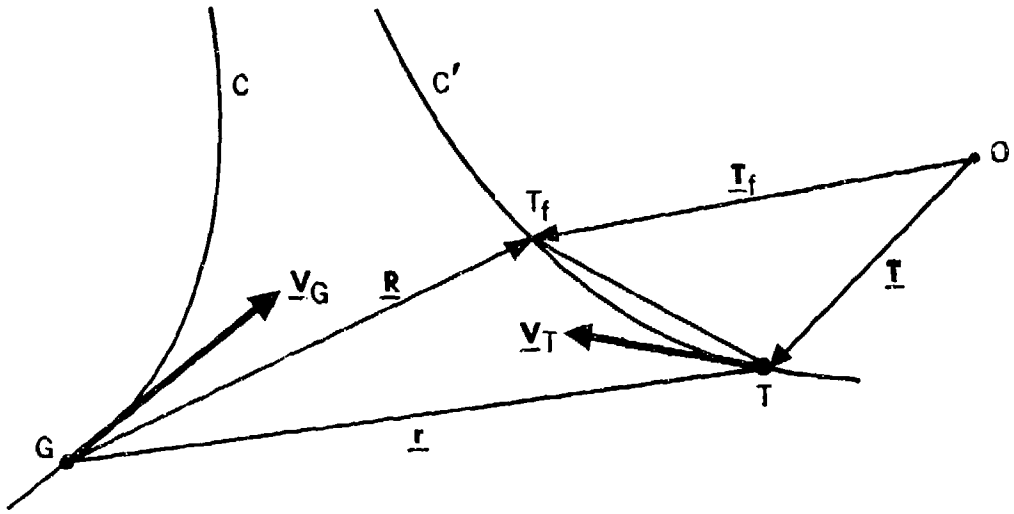

Figure 29. — Gun and Target Space Paths

and thus from (2.27) we find that

$$(2.28)\quad \mathbf{V}_o = \frac{u_o}{P}\mathbf{R} - \mathbf{V}_G - \mathbf{J} - \mathbf{w}\,,$$

wherein the gravity drop component is

$$(2.29)\quad \mathbf{w} = \frac{u_o Q}{P}\mathbf{n}\,.$$

2.8.3 An Expansion for the Projectile Range R

Consider the situation as depicted in figure 29. Here C, C' are the space paths of ownship and target, respectively; G and T are their present positions while T_f is the target future position. Vectors $\mathbf{r}$ and $\mathbf{R}$ are the present and projectile ranges; $\mathbf{T}$ and $\mathbf{T}_f$ are position vectors, relative to the fixed point O, of points T and T_f. Finally, $\mathbf{V}_G$ and $\mathbf{V}_T$ vectors denote the gun and target velocities at points G and T, respectively.

From the figure we note that

$$(2.30)\quad \mathbf{R} = \mathbf{r} + \vec{TT_f} = \mathbf{r} + \mathbf{T}_f - \mathbf{T}.$$

If we assume that $t = O$ corresponds to the instant of fire, then $\mathbf{T}(t$ will represent the position vector of an arbitrary point on the TT_f; $\mathbf{T}(t_f) = \mathbf{T}_f$ and $\mathbf{T}(o) = \mathbf{T}$. Upon expanding $\mathbf{T}(t)$ in a Maclaurin's series and evaluating it at $t = t_f$, we find

$$(2.31)\quad \mathbf{T}_f = \mathbf{T} + t_f\dot{\mathbf{T}} + \frac{t_f^2}{2}\ddot{\mathbf{T}} + \ldots\,,$$

where $\dot{\mathbf{T}} = \dot{\mathbf{T}}(t)]_t = O$, etc.

Since $\dot{\mathbf{T}} = \mathbf{V}_T$ and $\ddot{\mathbf{T}} = \dot{\mathbf{V}}_T$, we may rewrite (2.31) in the form

$$(2.32)\quad \mathbf{T}_f - \mathbf{T} = t_f\mathbf{V}_T + \frac{t_f^2}{2}\dot{\mathbf{V}}_T + \ldots\,,$$

and hence obtain from (2.30) the following basic expansion for the projectile range $\mathbf{R}$:

$$(2.33)\quad \mathbf{R} = \mathbf{r} + t_f\mathbf{V}_T + \frac{t_f^2}{2}\dot{V}_T + \ldots\,.$$

An aircraft fire control computer of the director type, i.e., one where information gained by positioning the radar antenna (line of sight) is sent to the computer which then computes the proper gun orders, is said to be of the first (second) order if the first two (three) and only the first two (three) terms of the right-hand member of equation (2.33) are accounted for in

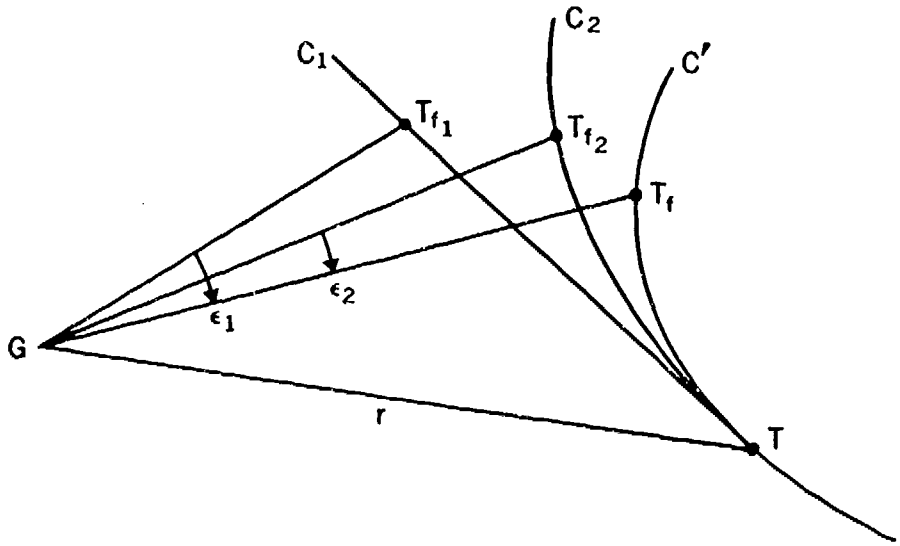

Figure 30. — First and Second Order Bias Errors

evaluating the lead angle. Thus, a first order computer uses target position and velocity data only, and is based on the relation

$$(2.34) \quad \mathbf{R} = \mathbf{r} + t_f \, \mathbf{V}_T,$$

which represents, for varying values of V_T and t_f, the vector equation of the line tangent to the target path at the instant of fire. For this reason, a first order computer is sometimes referred to as a linear predictor. A second order computer, in addition to target position and velocity data, employs target acceleration and is based on the equation

$$(2.35) \quad \mathbf{R} = \mathbf{r} + t_f \, \mathbf{V}_T + \frac{t_f}{2} \dot{\mathbf{V}}_T .$$

Geometrically, the vector relation (2.35) represents, for varying t_f and V_T, a parabola tangent to the target path at the instant of fire. Hence, a second order or parabolic predictor partially accounts for target course curvature by replacing the arc TT_f of the target path by the parabolic arc

$$(2.36) \quad \mathbf{R} = \mathbf{r} + t \, \mathbf{V}_T + \frac{t^2}{2} \dot{\mathbf{V}}_T , \quad O < t \leq t_f .$$

These facts are illustrated in figure 30 in which C_1, C_2 and C' represent, respectively, the tangent line to the target path, the parabolic arc (2.36), and the target path itself. The angles ε_1 and ε_2 represent, respectively, the aiming errors present in first and second order computers due to neglect of higher order terms in the expansion (2.33).

In the present study, we shall base the development of lead angle formulas upon the second order expansion (2.35). It will be noted that this expansion involves target velocity and acceleration relative to the air mass, quantities not directly measurable at ownship. However, since target velocity (acceleration) relative to the air mass is the sum of target velocity (acceleration) relative to ownship plus ownship velocity (acceleration) relative to the air mass, in symbols

$$(2.37) \quad \mathbf{V}_T = \dot{\mathbf{r}} + \mathbf{V}_G , \quad \dot{\mathbf{V}}_T = \ddot{\mathbf{r}} + \dot{\mathbf{V}}_G ,$$

we can express $\mathbf{R}$ in terms of the directly measurable quantities $\dot{\mathbf{r}}$, $\ddot{\mathbf{r}}$, $\mathbf{V}_G$, $\dot{\mathbf{V}}_G$.

Thus

$$(2.38) \quad \mathbf{R} = \mathbf{r} + t_f (\dot{\mathbf{r}} + \mathbf{V}_G) + \frac{t_f^2}{2} (\ddot{\mathbf{r}} + \dot{\mathbf{V}}_G) .$$

2.8.4 Lead Equation in Vector Form

Let us define $\mathbf{e}$ and $\mathbf{e}_o$ as unit vectors possessing the directions of $\mathbf{r}$ and $\mathbf{V}_o$, respectively.

Then the acute angle directed from $\mathbf{e}$ to $\mathbf{e}_o$ is the total lead angle, Λ. Since

$$\sin \Lambda = |\mathbf{e} \times \mathbf{e}_o|,$$

we shall be concerned with the total lead vector, $\mathbf{e} \times \mathbf{e}_o$. Dividing (2.28) by V_o we obtain for $\mathbf{e}_o$ the expression

$$(2.39) \quad \mathbf{e}_o = \frac{u_o}{P V_o} \mathbf{R} - \frac{\mathbf{V}_G}{V_o} - \frac{\mathbf{J}}{V_o} - \frac{\mathbf{w}}{V_o}$$

Substituting $\mathbf{R}$ from (2.38) we have

$$(2.40) \quad \mathbf{e}_o = \frac{u_o}{PV_o} [\mathbf{r} + t_f(\dot{\mathbf{r}} + \mathbf{V}_G) + \tfrac{1}{2} t_f^2 (\ddot{\mathbf{r}} + \dot{\mathbf{V}}_G)] - \frac{\mathbf{V}_G}{V_o} - \frac{\mathbf{J}}{V_o} - \frac{\mathbf{w}}{V_o}$$

The total lead vector $\mathbf{e} \times \mathbf{e}_o$ may now be written by forming the vector product $\mathbf{r} \times \mathbf{e}_o / r$, since $\mathbf{r} = r\mathbf{e}$. The result is

$$(2.41) \quad \mathbf{e} \times \mathbf{e}_o = \frac{u_o t_f}{rPV_o} [\mathbf{r} \times \dot{\mathbf{r}} + \mathbf{r} \times \mathbf{V}_G + \tfrac{1}{2} t_f(\mathbf{r} \times \ddot{\mathbf{r}} + \mathbf{r} \times \dot{\mathbf{V}}_G)] - \frac{\mathbf{r} \times \mathbf{V}_G}{rV_o} - \frac{\mathbf{r} \times \mathbf{J}}{rV_o} - \frac{\mathbf{r} \times \mathbf{w}}{rV_o}.$$

Introducing the quantity

$$(2.42) \quad q = 1 + l = \frac{u_o t_f}{P}$$

and recalling the definition of $\mathbf{w}$ given in (2.29), we may rewrite equation (2.41) in the form

$$(2.43) \quad \mathbf{e} \times \mathbf{e}_o = \frac{q}{rV_o} \left[\mathbf{r} \times \dot{\mathbf{r}} + \tfrac{1}{2} t_f(\mathbf{r} \times \ddot{\mathbf{r}}) + \tfrac{1}{2} t_f(\mathbf{r} \times \dot{\mathbf{V}}_G) - \mathbf{r} \times \left(\frac{\mathbf{Q}}{t_f} \right) \right] + \frac{l\mathbf{r} \times \mathbf{V}_G}{rV_o} - \frac{\mathbf{r} \times \mathbf{J}}{rV_o}.$$

2.8.5 The Ballistic Factors q and l

The interpretations of the ballistic quantities q and l given by (2.42) are essentially those given earlier in equation (2.10) et seq. There is a slight difference due to the fact that we do not here assume that the bullet moves in a straight line. The quantity $t_o = P/u_o$ now represents the time of flight in vacuum of a projectile having the same Siacci coordinate P as the projectile under consideration. From the relations

$$t_f = qt_o = t_o + lt_o$$

it is seen that l is the factor by which the time of flight has been increased due to bullet slowdown. Moreover,

$$q = \frac{t_f}{t_o} = \frac{\text{time of flight in air}}{\text{time of flight in vacuum}} > 1 .$$

A second interpretation for q can be obtained if we observe that the quantity $\bar{u} = Pt_f$ is the average speed of the projectile along its Siacci range P. For a bullet moving at high speed, this quantity is a very good approximation of its true average speed. Since

$$q = \frac{u_o}{\bar{u}} = \frac{\text{initial speed of bullet}}{\text{average speed of bullet on its Siacci range}},$$

it follows that the bullet is slowed down by approximately l/q, due to the action of air resistance.

2.8.6 The Terms Containing $\dot{\mathbf{V}}_G$ and Q in Equation (2.43)

The terms,

$$(2.44) \quad \frac{t_f}{2} (\mathbf{r} \times \dot{\mathbf{V}}_G) - \mathbf{r} \times \frac{\mathbf{Q}}{t_f},$$

appearing in equation (2.43), can be rewritten so that when linear accelerometers are used the dominant part of the second term is included with the first. We note firstly that $\mathbf{Q}/t_f$ can be written as

$$(2.45) \quad \frac{\mathbf{Q}}{t_f} = \frac{t_f}{2}(\mathbf{g} - F\mathbf{n}) ,$$

where $\mathbf{g}$ is the acceleration due to gravity and F is a correction term, depending on projectile type, air density, and time of flight. Combining equations (2.44) and (2.45) and denoting the difference $\mathbf{V}_G - \mathbf{g}$ by $\mathbf{a}$, we can write (2.44) in the form

$$(2.46) \quad \frac{t_f}{2}\mathbf{r} \times \mathbf{a} + \frac{Ft_f}{2}\mathbf{r} \times \mathbf{n} .$$

2.8.7 Resolution of the Ownship Velocity Relative to the Ownship Axes

We begin by introducing a right-handed system of mutually perpendicular unit vectors $\mathbf{i}_G$, $\mathbf{j}_G$, $\mathbf{k}_G$ related to ownship as shown in figure 31. These vectors are fixed relative to ownship. The vector $\mathbf{i}_G$ is directed forward along the longitudinal axis; the vector $\mathbf{j}_G$ is directed along the starboard wing; the vector $\mathbf{k}_G = \mathbf{i}_G \times \mathbf{j}_G$ then completes the coordinate system. We shall in the future refer to this as the ownship system.

In order to resolve the ownship velocity $\mathbf{V}_G$ relative to the ownship system of axes, we define first the angles of attack and skid. Figure 32 shows these angles, with the attack angle α_2 and the skid angle α_3 both positively oriented. (The numerical subscripts $_1$, $_2$, $_3$ on the letter α indicate corresponding angular rotations about the $\mathbf{i}_G$ (roll), $\mathbf{j}_G$ (pitch), $\mathbf{k}_G$ (yaw)-axes, respectively.) More precisely, we have the following definitions:

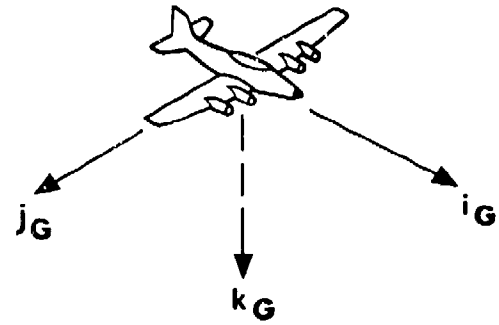

Figure 31. — Ownship Axes

(a) the angle of attack, α_2, is the acute angle from the longitudinal axis $\mathbf{i}_G$ to the projection of $\mathbf{V}_G$ upon the $(\mathbf{i}_G, \mathbf{k}_G)$-plane; α_2 is positive if $\mathbf{V}_G$ is below the $(\mathbf{i}_G, \mathbf{j}_G)$-plane.

(b) the angle of skid, α_3, is the acute angle from the longitudinal axis $\mathbf{i}_G$ to the projection of $\mathbf{V}_G$ upon the $(\mathbf{i}_G, \mathbf{j}_G)$-plane; α_3 is positive to starboard.

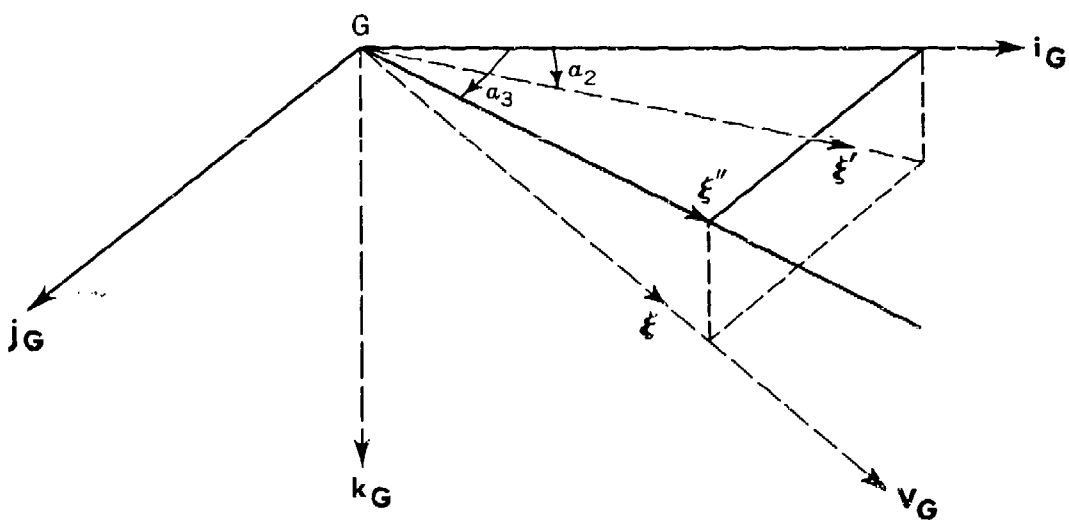

Figure 32. — Attack and Skid Angles

To resolve $\mathbf{V}_G$ into components along the roll, pitch, and yaw axes, each component a function of α_2 and α_3, let us consider the unit vector $\boldsymbol{\xi} = \mathbf{V}_G/V_G$. From figure 32, the unit vectors $\boldsymbol{\xi}'$, $\boldsymbol{\xi}''$ are given by

$$\boldsymbol{\xi}' = \mathbf{i}_G \cos \alpha_2 + \mathbf{k}_G \sin \alpha_2$$

$$\boldsymbol{\xi}'' = \mathbf{i}_G \cos \alpha_3 + \mathbf{j}_G \sin \alpha_3.$$

If we denote $\boldsymbol{\xi}$ by

$$(2.47) \quad \boldsymbol{\xi} = B_1 \mathbf{i}_G + B_2 \mathbf{j}_G + B_3 \mathbf{k}_G,$$

then,

$$\boldsymbol{\xi} \cdot \boldsymbol{\xi}' = B_1 \cos \alpha_2 + B_3 \sin \alpha_2$$

$$\boldsymbol{\xi} \cdot \boldsymbol{\xi}'' = B_1 \cos \alpha_3 + B_2 \sin \alpha_3.$$

However, since the angles which $\boldsymbol{\xi}$ makes with $\boldsymbol{\xi}'$ and $\mathbf{j}_G$ are complementary, and the same is true of the angles which $\boldsymbol{\xi}$ makes with $\boldsymbol{\xi}''$ and $\mathbf{k}_G$, we have

$$\boldsymbol{\xi} \cdot \boldsymbol{\xi}' = \sqrt{1 - (\boldsymbol{\xi} \cdot \mathbf{j}_G)^2} = \sqrt{1 - B_2^2}$$

$$\boldsymbol{\xi} \cdot \boldsymbol{\xi}'' = \sqrt{1 - (\boldsymbol{\xi} \cdot \mathbf{k}_G)^2} = \sqrt{1 - B_3^2},$$

and hence,

$$(2.48) \quad \begin{cases} B_1 \cos \alpha_2 + B_3 \sin \alpha_2 = \sqrt{1 - B_2^2} \\ B_1 \cos \alpha_3 + B_3 \sin \alpha_3 = \sqrt{1 - B_3^2} \end{cases}.$$

If now we combine the relations (2.48) with the fundamental one,

$$B_1^2 + B_2^2 + B_3^2 = 1,$$

the quantities B_1, B_2, B_3 can be obtained as the simultaneous solution of the system of three equations. The actual solution is left to the reader. Our result is found to be

$$(2.49) \quad \mathbf{V}_G = NV_G \, (\mathbf{i}_G \cos \alpha_2 \cos \alpha_3 + \mathbf{j}_G \cos \alpha_2 \sin \alpha_3 + \mathbf{k}_G \sin \alpha_2 \cos \alpha_3),$$

where

$$(2.50) \quad N = (1 - \sin^2 \alpha_2 \sin^2 \alpha_3)^{-1/2}.$$

2.8.8 The Windage Jump Vector J

In Chapter 1, it was shown that the windage jump vector $\mathbf{J}$ has magnitude $b\,\delta_o$, where b is a constant depending on the ammunition (see equations (1.55) and (1.86)) and δ_o is the initial yaw angle of the projectile, shown in figure 33. Moreover, the direction of $\mathbf{J}$ is the same as that of $\mathbf{V}_G \times \mathbf{V}_o$. Since δ_o is a small angle, we see from figure 33 that to a good approximation

$$(2.51) \quad \delta_o = V_G \frac{\sin \tau_o}{u_o} \text{ (radians)}.$$

Hence,

$$(2.52) \quad J = \frac{bV_G}{u_o} \sin \tau_o \text{ (yds/sec)}.$$

Since the direction of $\mathbf{J}$ is that of $\mathbf{V}_G \times \mathbf{V}_o$, we have, equating unit vectors,

$$\frac{1}{J}\mathbf{J} = \frac{\mathbf{V}_G \times \mathbf{V}_o}{V_G V_o \sin \tau_o}.$$

Thus, using (2.52) we obtain the following vector expression for $\mathbf{J}$:

$$(2.53) \quad \mathbf{J} = \frac{b}{u_o V_o} (\mathbf{V}_G \times \mathbf{V}_o).$$

For the 20-mm M97 projectile, $\mathbf{V}_o = 2680$ ft/sec and $b = 102.4$ ft/sec. From equation (2.43) we see that the maximum contribution of $\mathbf{J}$ to the total lead $|\mathbf{e} \times \mathbf{e}_o| = \sin \Lambda$ is

$$(J)_{max}/V_o.$$

Equation (2.52) shows that J will be a maximum when $\dfrac{\sin \tau_o}{u_o}$, considered as a function of τ_o, is a maximum. But from figure 33 we note that

$$\frac{\sin \tau_o}{u_o} = \frac{\sin (\tau_o - \delta_o)}{V_o}.$$

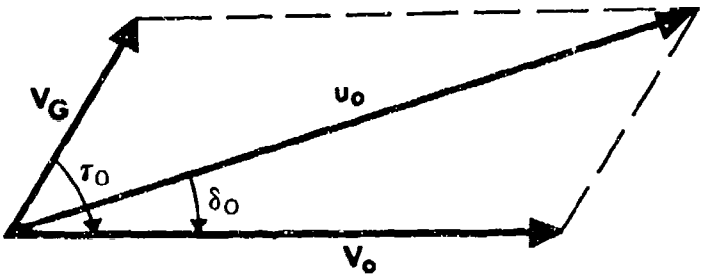

Figure 33. — Initial Yaw Angle

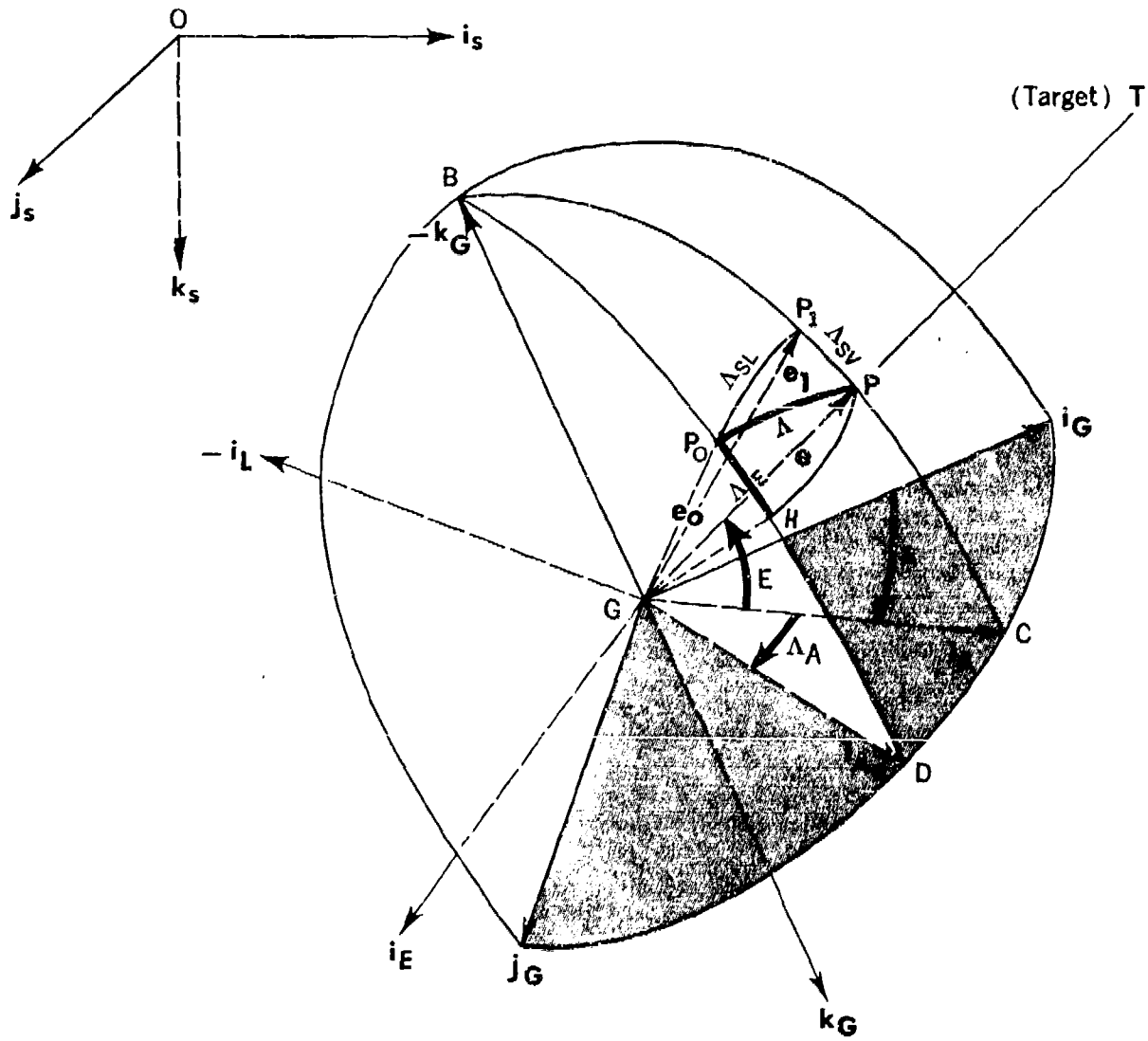

Figure 34. — The General Case in Three Dimensions

Thus, the maximum value of $\dfrac{\sin \tau_o}{u_o}$ is $\dfrac{1}{V_o}$,

achieved when $\tau_o = \dfrac{\pi}{2} + \delta_o$.

Hence,

$$(2.54) \qquad (J)_{max}/V_o = \frac{bV_G}{V_o^2} \times 1000 \text{ mils}$$

is the maximum contribution in mils to the total lead angle Λ, this maximum being achieved for the gun angle-off τ_o, slightly greater than 90°. For 20-mm M97 ammunition and $V_G =$ 250 yds/sec, we find this maximum to be 10 mils.

It should be noted from equation (2.52) that windage jump is negligible for fixed forward-firing gunnery or for moderate gun angles-off τ_o, i.e., $\tau_o \leq 15°$.

2.8.9 Lead Angle Equations for Azimuth-Elevation Top Deck Turret

2.8.9.1. ORIENTATION—In figure 34 $[\mathbf{i}_s, \mathbf{j}_s, \mathbf{k}_s]$ is a right-handed set of unit vectors with origin O fixed relative to the air mass, the vector $\mathbf{k}_s$ being directed vertically downward. The ownship coordinate system is shown relative to the octant of a unit sphere and is purposely positioned in a dived-and-banked orientation relative to the space axes $\mathbf{i}_s, \mathbf{j}_s, \mathbf{k}_s$. The sight line unit vector $\mathbf{e}$ is determined by the angular coordinates A, E, measured positively as shown. Angle A is in the ownship azimuth plane determined by the vectors $\mathbf{i}_G, \mathbf{j}_G$; angle E lies in the ownship vertical plane determined by $\mathbf{k}_G$ and the terminal side of A. If the corresponding angular coordinates of the gun-bore-axis unit vector $\mathbf{e}_o$ are designated by A_o, E_o, then the azimuth and elevation lead angles, Λ_A and Λ_E, for which we seek formulas, are defined by

$$(2.55) \qquad \Lambda_A = A_o - A, \quad \Lambda_E = E_o - E\,.$$

These lead angles are shown in figure 34 as angles CGD and HGP_o. The plane of the circular arc $\widehat{PH}$ is parallel to the ownship azimuth plane, so that arc PH is an arc of a small circle. The total lead angle Λ, of which Λ_A and Λ_E are the desired components, is of course the angle PGP_o between $\mathbf{e}$ and $\mathbf{e}_o$.

Since, as will be seen, the auxiliary angles Λ_{SL}, Λ_{SV}, can be found more directly from the input data than the lead angles themselves, we shall express Λ_A and Λ_E in terms of Λ_{SL}, Λ_{SV}. The latter angles are known as the sight lateral and sight vertical angles, respectively. They are defined geometrically as follows: A plane is passed through $\mathbf{e}_o$ perpendicular to the ownship vertical plane (i.e., the plane of $\mathbf{e}$ and $\mathbf{k}_G$) and intersecting the latter in the unit vector $\mathbf{e}_1$. The sight lateral angle Λ_{SL} is then defined as the acute angle between the vectors $\mathbf{e}_o$ and $\mathbf{e}_1$. Similarly, the sight vertical angle Λ_{SV} is defined as the angle between the vectors $\mathbf{e}$ and $\mathbf{e}_1$

2.8.9.2. RELATIONSHIP BETWEEN THE ANGLES Λ_A, Λ_E and Λ_{SL}, Λ_{SV} — If we apply Napier's Rules for right spherical triangles to triangle BP_1P_o of figure 34, in which face angle P_1BP_o is Λ_A, side $\widehat{BP_o}$ is $90° - E_o$, side $\widehat{P_1B}$ is $90° - (E + \Lambda_{SV})$, and side $\widehat{P_1B_o}$ is Λ_{SL}, we obtain (see figure 35)

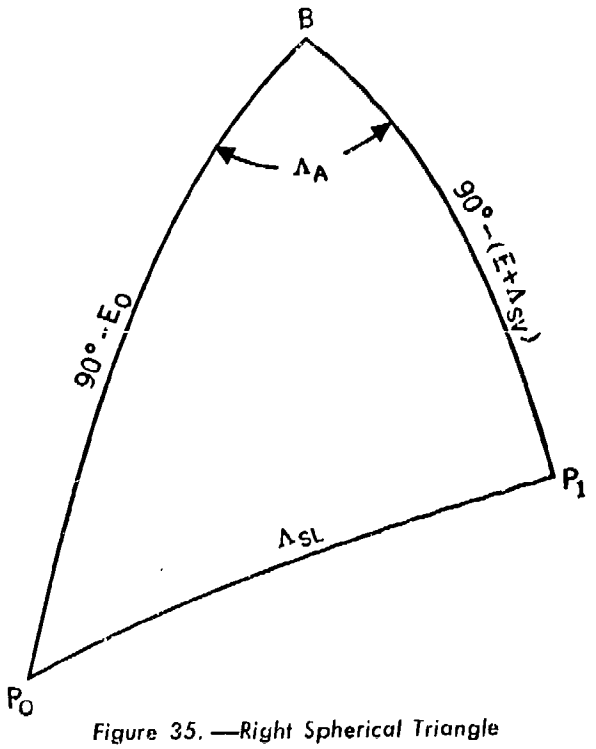

Figure 35.—Right Spherical Triangle

(2.56) $\sin \Lambda_{SL} = \sin \Lambda_A \cos E_o$

(2.57) $\sin E_o = \cos \Lambda_{SL} \sin (E + \Lambda_{SV})$.

In view of (2.55), these equations may be rewritten as

(2.58) $\sin \Lambda_{SL} = \sin \Lambda_A \cos (E + \Lambda_E)$

(2.59) $\sin (E + \Lambda_E) = \cos \Lambda_{SL} \sin (E + \Lambda_{SV})$.

2.8.9.3 THE SIGHT COORDINATE SYSTEM—In our work we shall assume that the radar antenna, directed along the gun-target line $\mathbf{r} = r\mathbf{e}$, tracks the target perfectly. The direction of the radar antenna then coincides continuously with that of the sight line vector $\mathbf{e}$. Since the angular velocity $\boldsymbol{\omega}$ of the sight line relative to space is represented by a vector perpendicular to $\mathbf{e}$, it is convenient to resolve $\boldsymbol{\omega}$ into components along perpendicular axes lying in a plane normal to $\mathbf{e}$. These axes are denoted in figure 34 by the unit vectors $\mathbf{i}_E$ and $\mathbf{i}_L$ and defined as follows: $\mathbf{i}_E$ is normal to $\mathbf{e}$ and so oriented as to coincide with $\mathbf{j}_G$ when $\mathbf{e}$ is directed along $\mathbf{i}_G$; the vector $\mathbf{i}_L$ is then completely defined by $\mathbf{i}_L = \mathbf{e} \times \mathbf{i}_E$. The three axes, $[\mathbf{e}, \mathbf{i}_E, \mathbf{i}_L]$ are thus mutually perpendicular and constitute a moving right-hand frame of reference which we shall refer to hereafter as the sight coordinate system. The angular velocity of this system relative to inertial space will be noted by $\boldsymbol{\Omega}_S$.

2.8.9.4. RESOLUTION OF THE VECTORS $\mathbf{r} \times \dot{\mathbf{r}}$ AND $\mathbf{r} \times \ddot{\mathbf{r}}$ — These vectors, appearing in the basic vector lead equation (2.43), give essentially the angular momentum and the time rate of change of angular momentum of a unit target mass relative to the moving origin G (See figure 34).

Designating $\mathbf{r} \times \dot{\mathbf{r}}$ by $\mathbf{M}$, we have

$$\mathbf{M} = r\,\mathbf{e} \times (\dot{r}\,\mathbf{e} + r\,\dot{\mathbf{e}}) = r^2\mathbf{e} \times \dot{\mathbf{e}} = r^2\boldsymbol{\omega}.$$

Hence, if we denote $\boldsymbol{\omega}$ by

(2.60) $\boldsymbol{\omega} = \omega_L \mathbf{i}_L + \omega_E \mathbf{i}_E$,

we may write

(2.61) $\mathbf{M} = M_L \mathbf{i}_L + M_E \mathbf{i}_E$,

where

(2.62) $M_L = r^2\omega_L$, $M_E = r^2\omega_E$.

The vector $\dot{\mathbf{M}} = \mathbf{r} \times \ddot{\mathbf{r}}$ is then, by known rules of vector analysis (see Appendix A), given by

(2.63) $$\dot{\mathbf{M}} = \frac{\delta \mathbf{M}}{\delta t} + \boldsymbol{\Omega}_S \times \mathbf{M}$$

where the first term of the right member indicates a time derivative taken with respect to the sight coordinate system. Thus,

(2.64) $$\frac{\delta \mathbf{M}}{\delta t} = \dot{M}_L \mathbf{i}_L + \dot{M}_E \mathbf{i}_E.$$

If we denote the component of $\boldsymbol{\Omega}_S$ in the direction of $\mathbf{e}$ by ω_e, then, since the angular velocity $\boldsymbol{\Omega}_S$ differs from the angular $\boldsymbol{\omega}$ of the sight line by a rotation about the sight line, we may write

(2.65) $\boldsymbol{\Omega}_S = \omega_e\,\mathbf{e} + \boldsymbol{\omega}$

Moreover, since $\boldsymbol{\omega} \times \mathbf{M} = O$, we find that

(2.66) $\boldsymbol{\Omega}_S \times \mathbf{M} = \omega_e\ \mathbf{e} \times \mathbf{M}$.

Substituting $\mathbf{M}$ from (2.61) into (2.66) and combining with (2.64) as indicated by (2.63), we obtain finally

(2.67) $\dot{\mathbf{M}} = (\dot{M}_L + M_E\omega_e)\,\mathbf{i}_L + (\dot{M}_E - M_L\omega_e)\,\mathbf{i}_E$.

The angular rates ω_L, ω_E, ω_e can be obtained physically by attaching gyroscopes with properly oriented spin axes to the rigid system of axes $\mathbf{i}_L$, $\mathbf{i}_E$, $\mathbf{e}$, where $\mathbf{e}$ is along the radar antenna.

2.8.9.5 RESOLUTION OF THE UNIT VECTOR $\mathbf{n}$ RELATIVE TO THE OWNSHIP AXES—This vector, first introduced in equation (2.29), is directed vertically downward and is located relative to the ownship system of axes by means of the bank and dive angles, β and δ. Figure 36 shows the basic coordinate system in both the "unbanked and undived" orientation, $(\mathbf{i}_G', \mathbf{j}_G', \mathbf{k}_G')$, and the "banked and dived" orientation, $(\mathbf{i}_G, \mathbf{j}_G, \mathbf{k}_G)$. The triad $(\mathbf{i}_G, \mathbf{j}_G', \mathbf{k}_G'')$ corresponds to the

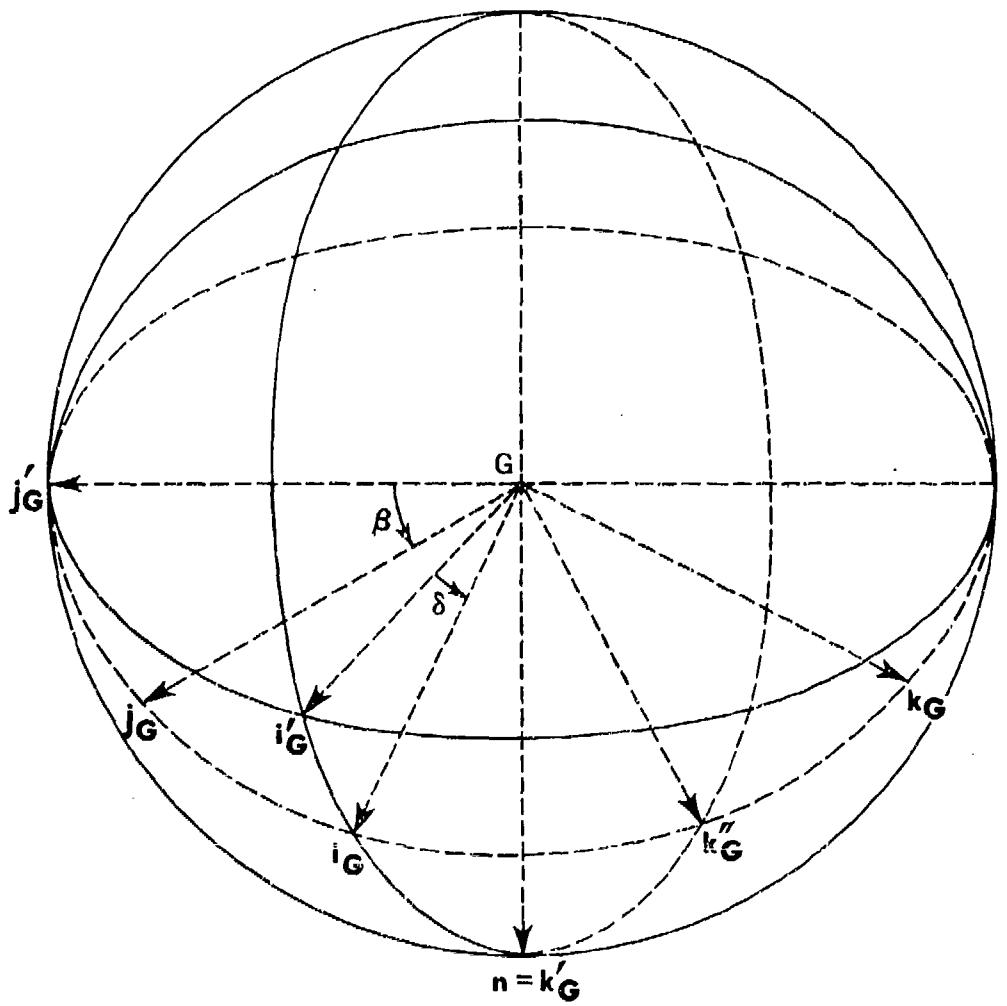

Figure 36. — Orientation of the Unit Vector n

case of bank zero and dive δ. Angles β and δ are positive as shown.

From figure 36 it is evident that,

$$\mathbf{n} = \mathbf{k}_G'' \cos\delta + \mathbf{i}_G \sin\delta.$$

$$\mathbf{k}_G'' = \mathbf{k}_G \cos\beta + \mathbf{j}_G \sin\beta.$$

and hence, that

$$\text{(2.68)} \quad \mathbf{n} = \mathbf{i}_G \sin\delta + \mathbf{j}_G \sin\beta \cos\delta + \mathbf{k}_G \cos\beta \cos\delta.$$

2.8.9.6 Resolution of the Total Lead Vector, $\mathbf{e} \times \mathbf{e}_o$—In figure 34, we note that in the circular sector GP_1P_o,

$$\text{(2.69)} \quad \mathbf{e}_o = \cos\Lambda_{SL}\, \mathbf{e}_1 + \sin\Lambda_{SL}\, \mathbf{i}_E.$$

This follows from observing that, since the radar antenna directed along $\mathbf{e}$ moves in an azimuth-elevation system of coordinates, the vector $\mathbf{i}_E$ is perpendicular to the plane of angle E. The relation (2.69) can be seen more clearly from figure 37, which shows the sector GP_1P_o isolated from the rest of figure 34.

Hence, we find that

$$\mathbf{e} \times \mathbf{e}_o = \cos\Lambda_{SL}\, \mathbf{e} \times \mathbf{e}_1 + \sin\Lambda_{SL}\, \mathbf{e} \times \mathbf{i}_E;$$

or, since

$$\mathbf{e} \times \mathbf{e}_1 = \mathbf{i}_E \sin \Lambda_{SV}, \quad \mathbf{e} \times \mathbf{i}_E = \mathbf{i}_L$$

that

$$(2.70) \quad \mathbf{e} \times \mathbf{e}_o = \mathbf{i}_E \sin \Lambda_{SV} \cos \Lambda_{SL} + \mathbf{i}_L \sin \Lambda_{SL}.$$

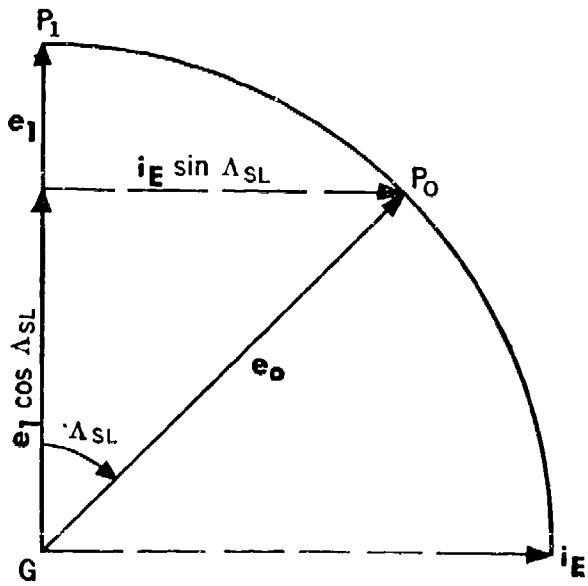

Figure 37. — Resolution of the Vector $\mathbf{e}_o$

2.8.9.7 A SUMMARY OF THE VECTOR TERMS OF EQUATION (2.43)—We list here the individual vector terms of the fundamental vector lead equation (2.43), each expressed in terms of the component vectors $\mathbf{e}$, $\mathbf{i}_L$, $\mathbf{i}_E$. For convenience, equation (2.43) is rewritten here in a slightly modified form as equation (2.71).

$$(2.71) \quad \mathbf{e} \times \mathbf{e}_o = \frac{q}{rV_o}\left[\mathbf{M} + \frac{t_f}{2}\dot{\mathbf{M}} + \frac{t_f}{2}\mathbf{r} \times \mathbf{a} + \frac{Ft_f}{2}\mathbf{r} \times \mathbf{n}\right] + \frac{l}{rV_o}\mathbf{r} \times \mathbf{V}_G - \frac{\mathbf{r} \times \mathbf{J}}{rV_o}$$

$$(2.72) \quad \mathbf{e} \times \mathbf{e}_o = \mathbf{i}_E \sin \Lambda_{SV} \cos \Lambda_{SL} + \mathbf{i}_L \sin \Lambda_{SL}$$

$$(2.73) \quad \mathbf{M} = M_L \mathbf{i}_L + M_E \mathbf{i}_E$$

$$(2.74) \quad \dot{\mathbf{M}} = (\dot{M}_L + M_E \omega_e)\mathbf{i}_L + (\dot{M}_E - M_L \omega_e)\mathbf{i}_E$$

$$(2.75) \quad \mathbf{r} = r\mathbf{e}$$

$$(2.76) \quad \mathbf{a} = a_1 \mathbf{i}_G + a_2 \mathbf{j}_G + a_3 \mathbf{k}_G.$$

In order to express $\mathbf{a}$ in the sight coordinate system $[\mathbf{e}, \mathbf{i}_E, \mathbf{i}_L]$, it is necessary to resolve each of the vectors $\mathbf{i}_G$, $\mathbf{j}_G$, $\mathbf{k}_G$, in this system. From figure 34 we note first that

$$\mathbf{e} = \mathbf{i}_A \cos E - \mathbf{k}_G \sin E$$

$$\mathbf{i}_A = \mathbf{i}_G \cos A + \mathbf{j}_G \sin A.$$

Hence,

$$(2.77) \quad \mathbf{e} = \mathbf{i}_G \cos A \cos E + \mathbf{j}_G \sin A \cos E - \mathbf{k}_G \sin E.$$

Similarly,

$$(2.78) \quad \mathbf{i}_L = \mathbf{i}_G \cos A \sin E + \mathbf{j}_G \sin A \sin E + \mathbf{k}_G \cos E$$

$$(2.79) \quad \mathbf{i}_E = -\mathbf{i}_G \sin A + \mathbf{j}_G \cos A.$$

For ease of inversion the equations (2.77), (2.78) and (2.79) can be represented symbolically by the following table of direction cosines.

(2.80)

	$\mathbf{e}$	$\mathbf{i}_L$	$\mathbf{i}_E$
$\mathbf{i}_G$	$\cos A \cos E$	$\sin A \sin E$	$-\sin A$
$\mathbf{j}_G$	$\sin A \cos E$	$\sin A \sin E$	$\cos A$
$\mathbf{k}_G$	$-\sin E$	$\cos E$	O

By way of illustration we see from the table that

$$(2.81)\quad \mathbf{i}_G = \mathbf{e}\cos A\cos E + \mathbf{i}_L\cos A\sin E - \mathbf{i}_E\sin A.$$

Combining equations (2.76) and (2.80) we obtain

$$(2.82)\quad \mathbf{a} = \mathbf{e}(a_1\cos A\cos E + a_2\sin A\cos E - a_3\sin E)$$
$$+\mathbf{i}_L(a_1\cos A\sin E + a_2\sin A\sin E + a_3\cos E)$$
$$+\mathbf{i}_E(-a_1\sin A + a_2\cos A).$$

From (2.75) and (2.82) there results

$$(2.83)\quad \mathbf{e}\times\mathbf{a} = \mathbf{i}_E(-a_1\cos A\sin E - a_2\sin A\sin E - a_3\cos E) + \mathbf{i}_L(a_2\cos A - a_1\sin A).$$

Also, from (2.68) and (2.80) we have

$$(2.84)\quad \mathbf{n} = \mathbf{e}(\sin\delta\cos A\cos E + \sin\beta\cos\delta\sin A\cos E - \cos\beta\cos\delta\sin E)$$
$$+\mathbf{i}_L(\sin\delta\cos A\sin E + \sin\beta\cos\delta\sin A\sin E + \cos\beta\cos\delta\cos E)$$
$$+\mathbf{i}_E(-\sin\delta\sin A + \sin\beta\cos\delta\cos A).$$

$$(2.85)\quad \mathbf{r}\times\mathbf{n} = r\,[\mathbf{i}_E(-\sin\delta\cos A\sin E - \sin\beta\cos\delta\sin A\sin E - \cos\beta\cos\delta\cos E) + \mathbf{i}_L(-\sin\delta\sin A + \sin\beta\cos\delta\cos A)].$$

In evaluating the vectors $\mathbf{r}\times\mathbf{V}_G$ and $\mathbf{r}\times\mathbf{J}$, appearing in (2.71), we make the simplifying assumption that the attack and skid angles, α_2 and α_3 can be neglected. This is a reasonable assumption in that the aircraft for which the present lead angle equations are being written is considered to be a heavy, relatively non-maneuverable bomber. We assume then that $\mathbf{V}_G = V_G\mathbf{i}_G$. Hence,

$$(2.86)\quad -\mathbf{r}\times\mathbf{V}_G = rV_G\,[\mathbf{i}_E\cos A\sin E + \mathbf{i}_L\sin A].$$

From (2.53) and (2.75) we note that

$$\mathbf{r}\times\mathbf{J} = \frac{b\,V_G\,r}{u_o}\,\mathbf{e}\times(\mathbf{i}_G\times\mathbf{e}_o).$$

However, vector $\mathbf{i}_G\times\mathbf{e}_o$, with the aid of figure 34, becomes

$$\mathbf{i}_G\times\mathbf{e}_o = \mathbf{i}_G\times(\mathbf{i}_{A_o}\cos E_o - \mathbf{k}_G\sin E_o)$$
$$= \mathbf{k}_G\sin A_o\cos E_o + \mathbf{j}_G\sin E_o.$$

Hence,

$$\mathbf{e}\times(\mathbf{i}_G\times\mathbf{e}_o) = \sin A_o\cos E_o\,(\mathbf{e}\times\mathbf{k}_G) + \sin E_o\,(\mathbf{e}\times\mathbf{j}_G);$$

but from (2.80) we find

$$\mathbf{e}\times\mathbf{j}_G = -\mathbf{i}_E\sin A\sin E + \mathbf{i}_L\cos A$$

$$\mathbf{e}\times\mathbf{k}_G = -\mathbf{i}_E\cos E.$$

Thus, we arrive finally at the vector expression

$$(2.87)\quad \mathbf{r}\times\mathbf{J} = \frac{bV_Or}{u_o}\,[\mathbf{i}_E(-\sin A_o\cos E_o\cos E - \sin E_o\sin A\sin E) + \mathbf{i}_L\sin E_o\cos A].$$

2.8.9.8 Lead Angle Equations for Azimuth-Elevation Top Deck Turret—Upon taking the $\mathbf{i}_E$ and $\mathbf{i}_L$ components of the individual vector terms of equation (2.71), we arrive at the final lead equations. They are:

$$\sin \Lambda_{SV} \cos \Lambda_{SL} = \frac{q}{rV_o} \left[M_E + \frac{t_f}{2} (\dot{M}_E - M_L \omega_e) \right] \tag{2.88}$$

$$- \frac{qt_f}{2V_o} (a_1 \cos A \sin E + a_2 \sin A \sin E + a_3 \cos E)$$

$$- \frac{Fqt_f}{2V_o} (\sin \beta \cos \delta \sin A \sin E + \sin \delta \cos A \sin E + \cos \beta \cos \delta \cos E)$$

$$- \frac{lV_G}{V_o} \cos A \sin E + \frac{bV_G}{u_o V_o} (\sin A_o \cos E_o \cos E + \sin E_o \sin A \sin E)$$

$$\sin \Lambda_{SL} = \frac{q}{rV_o} \left[M_L + \frac{t_f}{2} (\dot{M}_L + M_E \omega_e) \right] \tag{2.89}$$

$$+ \frac{qt_f}{2V_o} (a_2 \cos A - a_1 \sin A) - \frac{Fqt_f}{2V_o} (\sin \delta \sin A - \sin \beta \cos \delta \cos A)$$

$$- \frac{lV_G}{V_o} \sin A - \frac{bV_G}{u_o V_o} \sin E_o \cos A ,$$

where

$$\sin \Lambda_{SL} = \sin \Lambda_A \cos E_o \tag{2.90}$$

$$\sin E_o = \cos \Lambda_{SL} \sin (E + \Lambda_{SV}) \tag{2.91}$$

$$A_o = A + \Lambda_A, \quad E_o = E + \Lambda_E , \tag{2.92}$$

and

$$M_L = r^2 \omega_L, \quad M_E = r^2 \omega_E. \tag{2.93}$$

The basic computer inputs are:

range, r

angular velocity components of the sight coordinate system: ω_L, ω_E, ω_e

linear acceleration of ownship, components a_1, a_2, a_3

bank and dive angles, β and δ

true airspeed, V_G

angular coordinates of the line of sight, A and E

muzzle velocity, V_o

windage jump constant, b.

All other quantities appearing in the equations are derived from these basic inputs. The quantities q and t_f in particular are usually obtained from empirical formulas giving these quantities as functions of basic inputs. The manner in which t_f is obtained theoretically has already been considered in chapter 1.

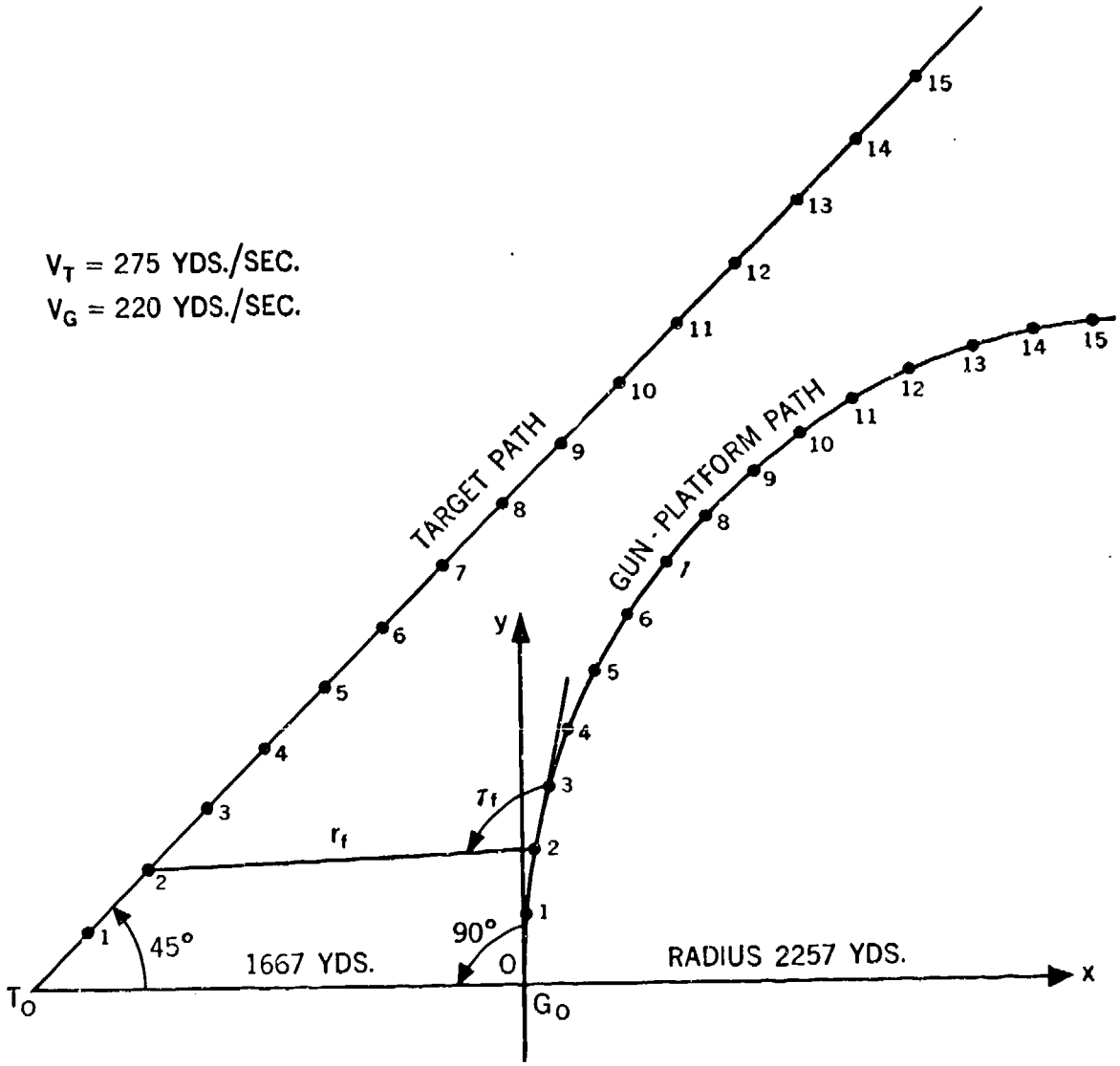

Figure 38. — Particular Case — Computation of Lead Angles

Finally, we note that the quantity u_o, appearing in the windage jump terms, can be found from (see figure 33)

$$u_o^2 = V_o^2 + V_G^2 + 2V_G V_o \cos \tau_o,$$

or, in terms of the angular coordinates of the gun bore axis, from

$$u_o^2 = V_o^2 + V_G^2 + 2V_G V_o \cos A_o \cos E_o. \tag{2.94}$$

2.9 An Example

By way of illustrating the computation of lead angles in a particular case, let us consider the coplanar attack shown in figure 38. Here, the target traverses a straight line with a speed constantly 275 yds/sec. and the gun-platform sweeps out a circle of radius 2257 yards, traveling with constant tangential speed of 220 yds/sec. At time $t = O$ their positions are G_o, T_o with $G_oT_o = 1667$ yards; the initial approach

988995 O - 53 - 5

angle of the target is 45° while the angle-off of the target is 90°. The position of G, T are shown for a time interval of 15 seconds. Since the firing tables, as was explained in Chapter 1, give t_f as a function of the future range, r_f, it is most convenient to assume these positions as future positions and the times indicated on the figure as impact times. Gravity drop will be neglected in our computations.

The lead angle formula (2.15), which applies here, can be written in the form

$$(2.95) \quad \sin \Delta = \frac{qM}{rV_o} - \frac{lV_G}{V_o} \sin \tau, \quad M = r^2\omega .$$

We shall take ownship speed V_G to be 220 yds/sec and the projectile muzzle velocity V_o to be 2750 yds/sec. With coordinate axes xOy, chosen as indicated, we write down first of all the parametric equations giving the future coordinates (x_{G_f}, y_{G_f}), (x_{T_f}, y_{T_f}) as functions of the impact times t_i. Thus,

$$(2.96) \begin{cases} x_{G_f} = 2257\ [1 - \cos \psi_i] \\ y_{G_f} = 2257 \sin \psi_i \end{cases}$$

$$\psi_i = \frac{V_G}{2257} t_i = .09745\ t_i$$

$$(2.97) \begin{cases} x_{T_f} = -1667 + \dfrac{275\ t_i}{\sqrt{2}} \\ x_{T_f} = \dfrac{275\ t_i}{\sqrt{2}} \end{cases}$$

$$t_i = 0,1,2,\ldots\ldots.15 .$$

Future ranges corresponding to these positions are then found from

$$(2.98) \quad r_f = \sqrt{(x_{G_f} - x_{T_f})^2 + (y_{G_f} - y_{T_f})^2} .$$

Since the input variables to equation (2.95) are measured at the instant of fire t, it is necessary to compute t_f in order that t may be found from

$$(2.99) \quad t = t_i - t_f .$$

The firing tables list times of flight as a function of present gun angle-off γ, present zenith angle of the gun (angle between gun-bore axis and the vertical), future range r_f, relative air density ρ, and speed of gun-platform V_G. In our coplanar case of horizontal flight, the zenith angle is constantly 90° (1600 mils), $V_G = 220$ yds/sec and ρ will be taken to be 0.4, which corresponds to an altitude of approximately 29,000 feet. Therefore, to obtain t_f from the tables we need to know the present gun angle-off γ. In lieu of this quantity, which is not now known, we use τ_f, the future sight-line angle-off, and thus obtain from the tables approximate values of t_f to be used in (2.99). The angle τ_f can be read from a carefully drawn figure or else computed directly from

$$(2.100) \quad \tan \tau_f = \frac{m_f \tan \psi_i - 1}{m_f + \tan \psi_i} ,$$

$$m_f = \frac{y_{G_f} - y_{T_f}}{x_{G_f} - x_{T_f}} .$$

With the approximate value of t_f thus obtained, one computes, knowing t and the present coordinates (x_G, y_G), (x_T, y_T), the projectile range R by using t in place of t_i in (2.96) and (2.97) and then employing the distance formula for R,

$$(2.101) \quad R = \sqrt{(x_{T_f} - x_G)^2 + (y_{T_f} - y_G)^2} .$$

To find the angle γ we need to know the angles μ, ν, ψ_i, as is evident from the firing parallelogram drawing shown in figure 39. The actual chain of relations that leads to γ is as follows: (angles are measured positively in a clockwise direction)

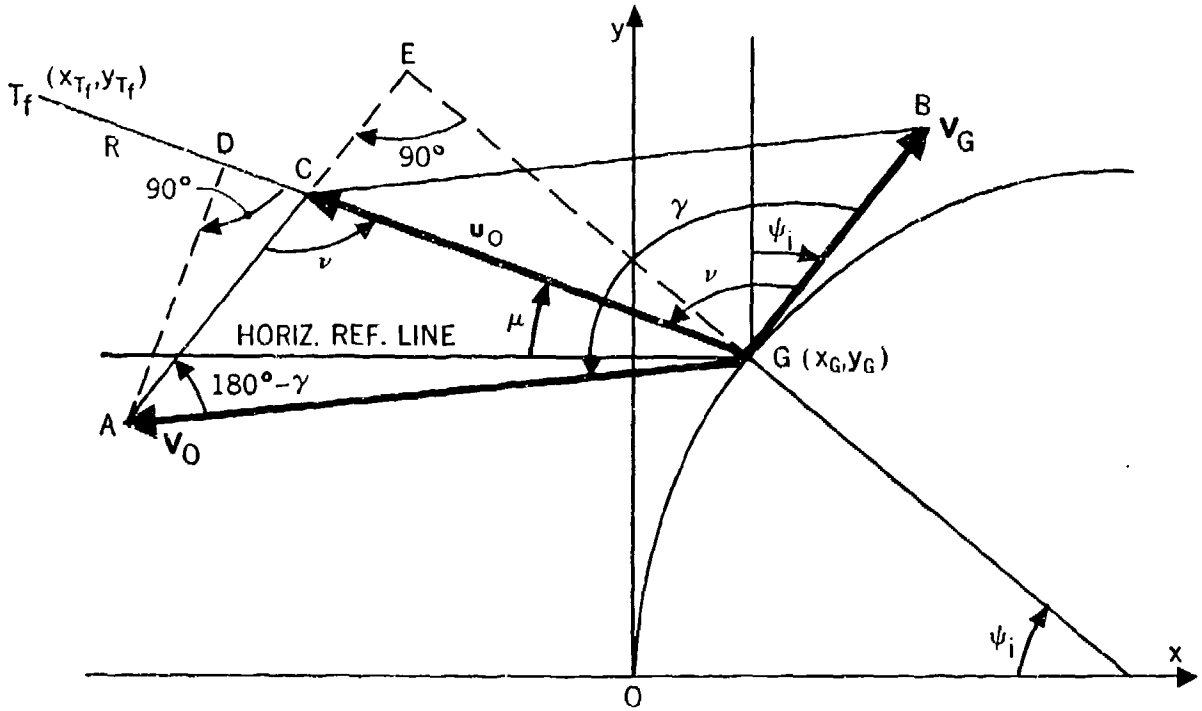

Figure 39. — Fundamental Angles

$$(2.102) \quad \sin \mu = \frac{y_{T_f} - y_G}{R} \; ;$$

$$(2.103) \quad \nu = -90^\circ + \mu - \psi_i \; ;$$

$$u_o = GC = GD - CD =$$

$$\sqrt{GA^2 - AD^2} - AC \cos (180^\circ - \nu)$$

or

$$(2.104) \quad u_o = V_G \cos \nu + \sqrt{V_o^2 - V_G^2 \sin^2 \nu} \; .$$

Finally, we note that

$$CE = AE - AC$$

or

$$u_o \cos (180^\circ - \nu) = V_o \cos (180^\circ - \gamma) - V_G,$$

which may be written

$$(2.105) \quad \cos \gamma = \frac{u_o \cos \nu - V_G}{V_o} \; .$$

Once γ has been determined from (2.105), a more accurate t_f may be obtained by using this value of γ in the firing tables. This leads, via the chain of equations just written, to a more accurate γ. If this iterative process be continued, both t_f and γ can be found accurately to as many decimal places as the original data warrants.

Using this accurately determined t_f in (2.99), we now find values of the gun and target coordinates at the time of fire from

$$(2.106) \quad \begin{cases} \psi = \dfrac{V_G}{2257} t \, , \\ x_G = 2257 \, [1 - \cos\psi], \; y_G = 2257 \sin \psi \, , \\ x_T = -1667 + \dfrac{275t}{\sqrt{2}} \, , \quad y_T = \dfrac{275t}{\sqrt{2}} \, . \end{cases}$$

With this information we can now find the input quantities r, τ, M, q, l. We have

$$(2.107) \quad r = \sqrt{(x_G - x_T)^2 + (y_G - y_T)^2}\ ;$$

$$(2.108) \quad \tan\tau = \frac{m\tan\psi - 1}{m + \tan\psi}, \quad m = \frac{y_G - y_T}{x_G - x_T}.$$

The quantity m in (2.108) represents the slope of the sight line referred to the fixed axes xOy in figure 39. Hence the angular rate of rotation ω of the sight line is

$$\omega = \frac{d}{dt}\,[\arctan m]$$

and

$$M = r^2\omega = r^2 \frac{d}{dt}\,[\arctan\left(\frac{y_G - y_T}{x_G - x_T}\right)]\ ,$$

which simplifies to

$$(2.109) \quad M = (x_G - x_T)\ (\dot{y}_G - \dot{y}_T) - (y_G - y_T)\ (\dot{x}_G - \dot{x}_T)\ .$$

The dotted quantities in (2.109) are the time derivatives of the corresponding ones in (2.106). Finally, knowing u_o, t_f, and R from (2.101), we compute q from the known relation

$$(2.110) \quad q = \frac{u_o t_f}{R}\ .$$

The lead angle Λ can now be determined from (2.95).

The results have been computed for this example and are exhibited in table 2.1. Distances are in yards, time in seconds, ω in radians per second, Λ in mils.

Table 2.1

Values At Time of Fire

Dimensions: yards, seconds, degrees, mils

t_i	t_f	t	r_f	R	u_o	r	τ(deg)	M	q	l	ω	ν(deg)	A(mils)
0	2.39	−2.39	1666.667	1805.618	1007.043	2193.076	75.087	29082	1.3335	0.3335	.0060	59.886	58
1	2.06	−1.06	1483.134	1548.888	975.548	1883.921	83.303	40078	1.2975	0.2975	.0113	68.141	41
2	1.79	0.21	1321.369	1323.385	944.048	1626.314	91.360	42398	1.2769	0.2769	.0160	76.162	30
3	1.56	1.44	1180.979	1137.331	911.168	1408.475	99.524	38679	1.2498	0.2498	.0195	84.511	22
4	1.37	2.63	1061.169	984.302	879.856	1230.480	107.515	30923	1.2246	0.2246	.0204	92.625	18
5	1.20	3.80	960.778	861.321	849.890	1084.100	115.306	20431	1.1841	0.1841	.0174	100.721	16
6	1.08	4.92	878.442	764.471	824.508	968.594	122.443	8574	1.1648	0.1648	.0091	107.993	22
7	0.99	6.01	812.913	691.048	804.575	877.714	128.716	− 4009	1.1526	0.1526	−.0052	114.097	34
8	0.92	7.08	763.500	637.924	790.567	808.649	133.755	−16686	1.1463	0.1463	−.0255	118.669	51
9	0.88	8.12	730.555	604.668	782.359	758.662	137.330	−29212	1.1386	0.1386	−.0508	121.487	70
10	0.86	9.14	715.795	591.033	780.018	727.338	139.262	−41338	1.1350	0.1350	.0781	122.311	92
11	0.87	10.13	722.177	598.296	782.973	715.369	139.623	−52769	1.1385	0.1385	−.1031	121.271	113
12	0.91	11.09	753.185	629.033	789.660	723.917	138.734	−64155	1.1424	0.1424	−.1224	118.975	133
13	0.99	12.01	811.749	684.303	798.632	753.677	137.127	−74955	1.1554	0.1554	−.1320	116.004	151
14	1.11	12.89	899.413	764.695	807.804	803.896	135.341	−85526	1.1726	0.1726	−.1323	113.079	166
15	1.26	13.74	1016.212	870.114	814.998	873.797	133.774	−96219	1.1802	0.1802	−.1260	110.854	174

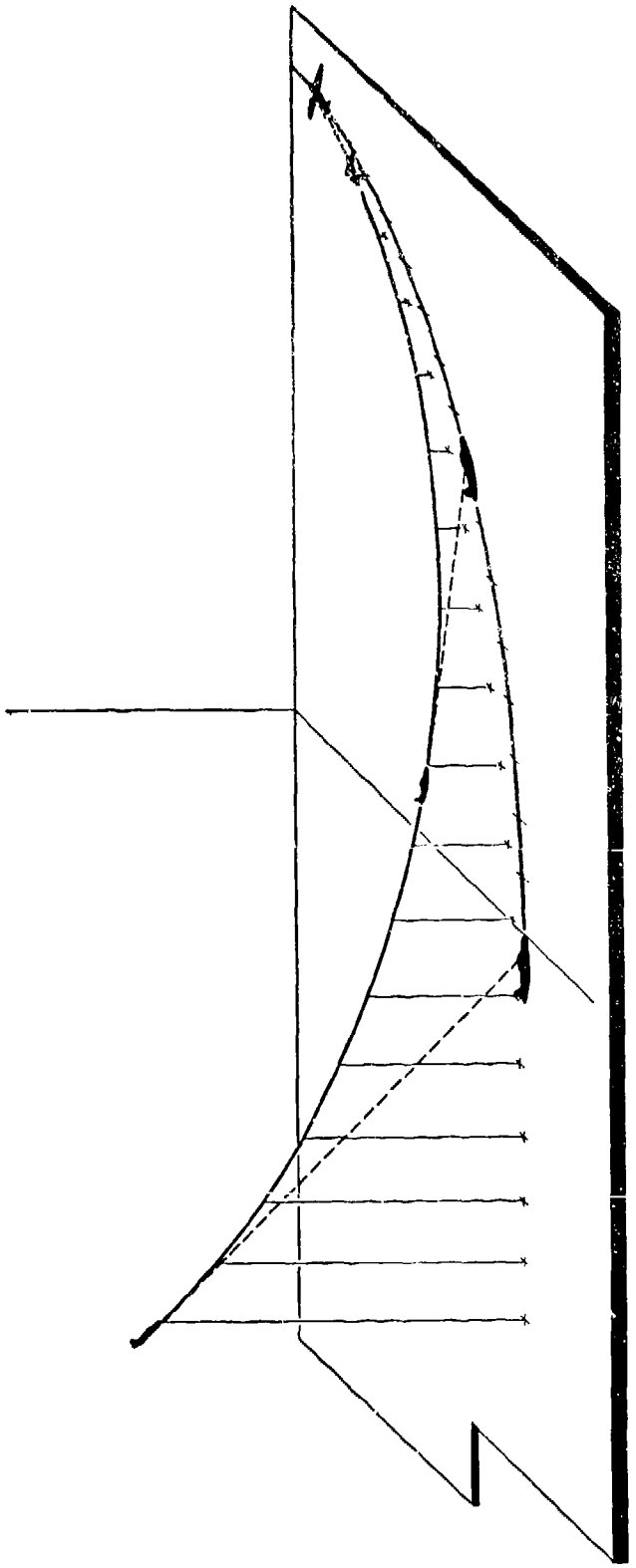

Figure 40. — Pursuit Course

Chapter 3

PURSUIT COURSES

3.1 Introduction

The problem of determining the equation of a curve of pursuit is a classical problem in mathematics. Historically it dates back to the time of Leonardo da Vinci. One classical statement of the problem was to determine a dog's course as the dog runs toward its master who is walking along a straight path. The military aspects of the problem were brought into prominence in connection with aircraft combat wherein one aircraft is attacked by another possessing guns capable of being fired in a fixed direction only. In order for the one aircraft to keep the other under continuous fire, it must fly some kind of a pursuit course. The problem appears again with the invention of homing missiles which continuously change heading under radio, optical, or acoustic guidance unwillingly supplied by the target.

The importance of pursuit courses in air-to-air combat is two-fold. The attacker, flying an aircraft equipped with fixed guns, must understand such a course in order to determine whether or not his aircraft can fly the required flight path. He also must rely upon his knowledge of this flight path to give him inputs to his fire control system. The defender uses his knowledge of the flight path to determine the future positions of the attacker and thus establishes the required leads for his guns.

In aircraft combat there are four kinds of pursuit courses. To be specific, let us consider a fighter aircraft equipped with fixed guns in combat with a bomber equipped with flexible guns. Thus, we consider the bomber to be pursued and the fighter to be the pursuer. The fighter's guns are assumed to point in the direction of its flight.

If the fighter pilot flies his airplane in such a way that his guns are always pointed directly at the bomber, he is said to fly a pure pursuit course. In such a course, the mush of the airplane and the lead that the guns must have are ignored. If the bomber is flying a straight and level course, the fighter's motion lies in a geometric plane with the bomber's course and this plane is called the plane of action.

If the lead is taken into consideration, that is, if the fighter flies so that his guns are always directed at a point ahead of the bomber by the required amount to secure a hit, and the mush of the airplane is ignored, then he is said to fly a lead pursuit course.

If the fighter flies his airplane in such a way that his guns are always pointed directly at the bomber and his flight path is determined from the angle of attack and other aerodynamic considerations, he is said to fly an aerodynamic pursuit course.

If the fighter flies his airplane in such a manner that his guns are always pointed ahead of the bomber by the amount required to score a hit, and his flight path is determined by aerodynamic considerations, then he is said to fly an aerodynamic lead pursuit course.

The complexity of the courses increases in the order defined above and thus it is advantageous to consider the simpler pure pursuit first.

3.2 The Space Course for a Pure Pursuit Attack

In analyzing pursuit courses, there are two types of courses to consider; one is the actual space course traversed by the combating aircraft and the other is the path of the one aircraft relative to the other. Let us begin by considering the space course and let it be referred to a set of rectangular coordinate axes which lie in the plane of action. See figures 41 and 42.

Let (x_B, y_B) and (x_F, y_F) be the coordinates of the bomber and the fighter, respectively, at any time t. Since the fighter is the pursuer, we

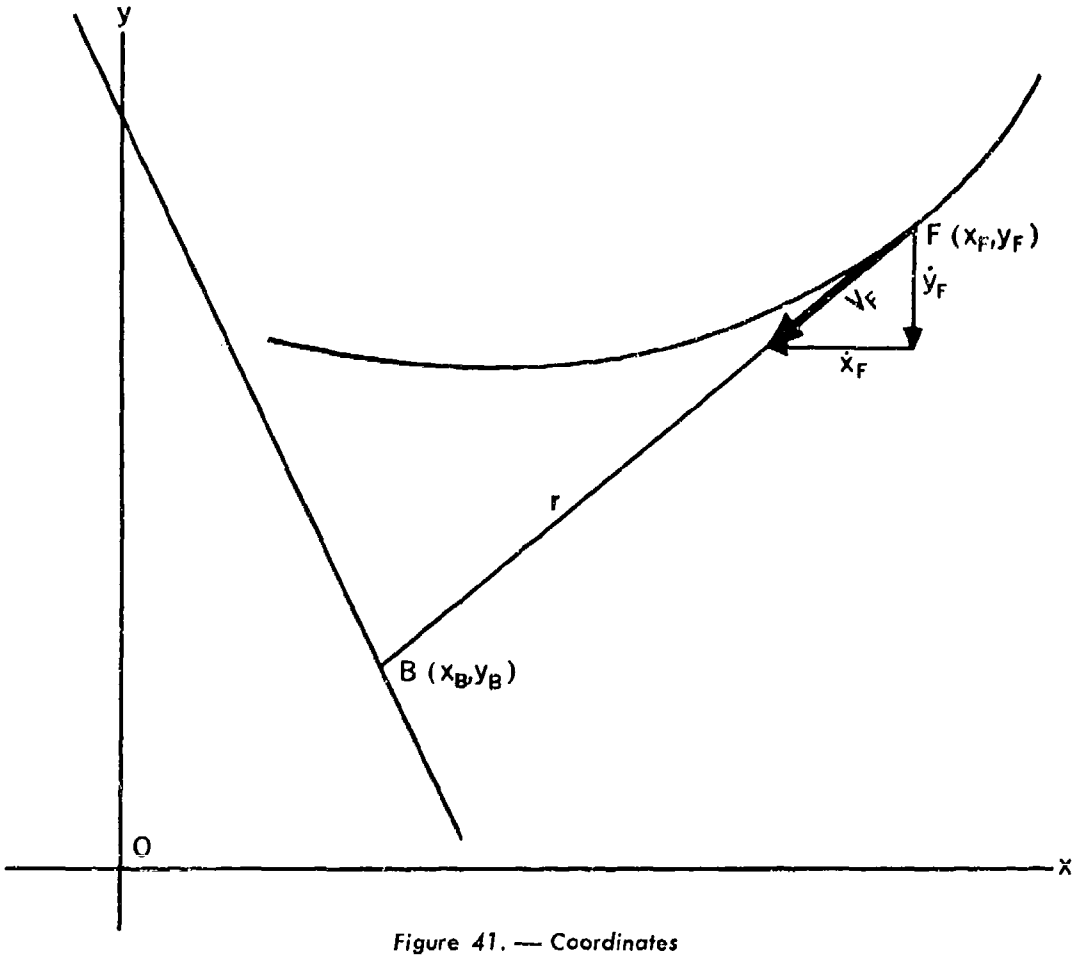

Figure 41. — Coordinates

are seeking expressions for his coordinates in terms of known quantities. The definition of a pure pursuit course specifies that the equation of the tangent to the fighter's path must be satisfied by the bomber's coordinates. Thus, the equation for a straight line yields

$$(3.1) \quad (y_B - y_F) = m\,(x_B - x_F),$$

where m is the slope of the tangent line. The slope of the tangent line is, of course, the derivative at any point on the fighter's path and, consequently,

$$(3.2) \quad m = \frac{dy_F}{dx_F} = \frac{\dot{y}_F}{\dot{x}_F},$$

so that equation (3.1) becomes

$$(3.3) \quad y_B - y_F = \frac{\dot{y}_F}{\dot{x}_F}\,(x_B - x_F)$$

or

$$(3.4) \quad \dot{y}_F = \dot{x}_F\,\frac{y_B - y_F}{x_B - x_F}.$$

It is easily seen that the forward velocity of the fighter, V_F, is given by

$$(3.5) \quad \dot{x}_F^2 + \dot{y}_F^2 = V_F^2.$$

The substitution of (3.4) into (3.5) yields

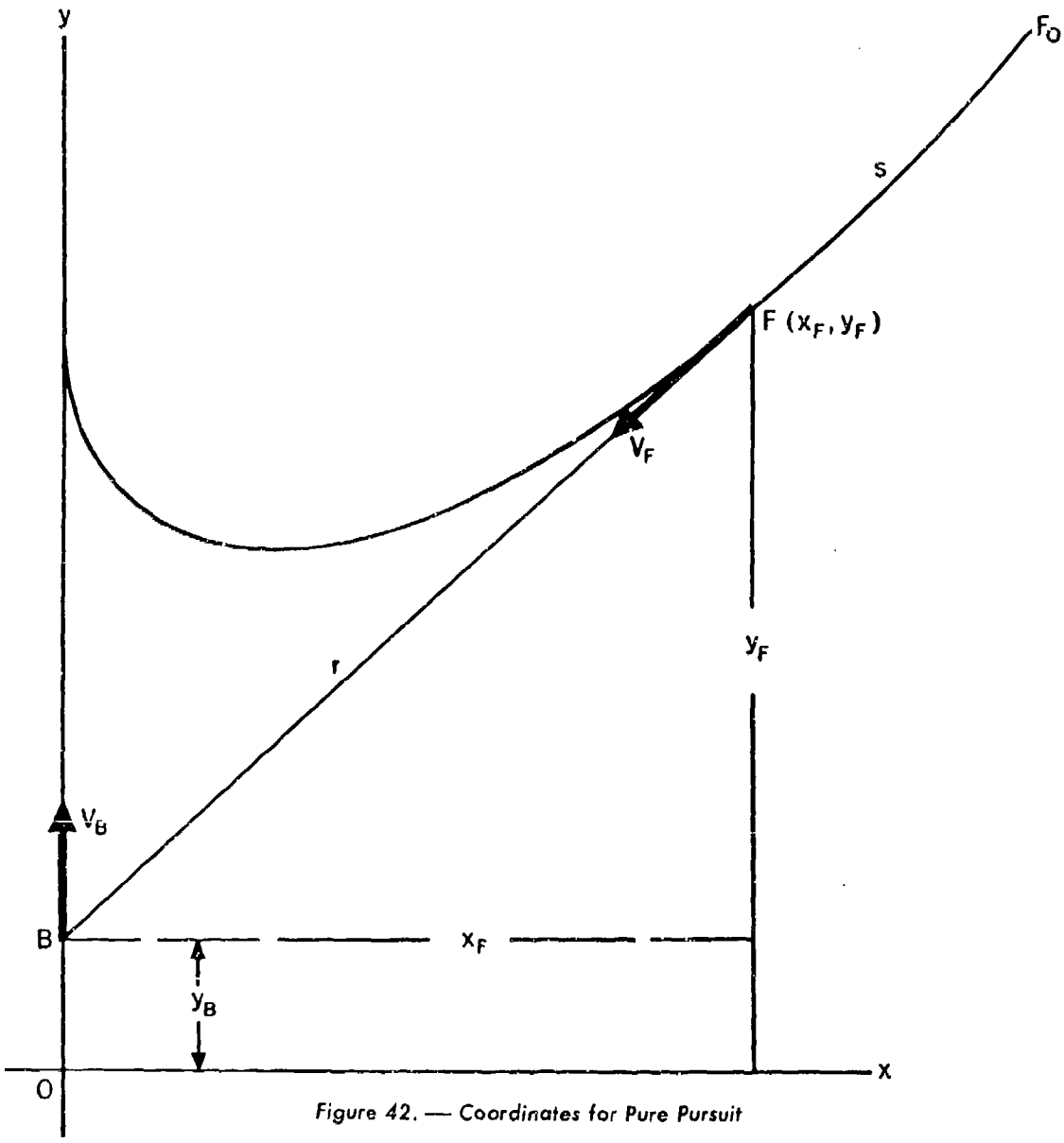

Figure 42. — Coordinates for Pure Pursuit

$$(3.6) \quad \dot{x}_F^2 \left[1 + \left(\frac{y_B - y_F}{x_B - x_F} \right)^2 \right] = V_F^2$$

or, upon simplifying,

$$(3.7) \quad \dot{x}_F^2 = V_F^2 \left[\frac{(x_B - x_F)^2}{(x_B - x_F)^2 + (y_B - y_F)^2} \right]$$

$$= V_F^2 \frac{(x_B - x_F)^2}{r^2} ,$$

where

$$(3.8) \quad r^2 = (x_B - x_F)^2 + (y_B - y_F)^2 .$$

The quantity r is the range between the bomber and the fighter at any time t. Equation (3.7), therefore, yields an expression for the time derivative of the fighter's x-coordinate,

$$(3.9) \quad \dot{x}_F = \frac{V_F}{r} (x_B - x_F) ;$$

similarly, from equation (3.4) we have

$$(3.10) \quad \dot{y}_F = \frac{V_F}{r}(y_B - y_F) .$$

Equations (3.9) and (3.10) form a system of differential equations which describes the motion of the fighter in terms of the coordinates of the bomber, the fighter's velocity and the range. The right-hand side of both equations are thus functions of time, t, the independent variable. For certain restricted cases, these differential equations may be solved explicitly; however, in general, it will be necessary to solve this system numerically.

As a special case, let the course of the bomber be taken along the positive y-axis and let its coordinates be (O,O) at $t = O$. Let the coordinates of the fighter at $t = O$ be given by (x_{F_0}, y_{F_0}). Let us further assume that the bomber and fighter are both flying at constant speeds, V_B and V_F, respectively. The situation is illustrated in figure 42. In this case, it is possible to obtain y as a function of x analytically. Since $x_B = O$ and $y_B = V_B t$ we have from equation (3.1)

$$(3.11) \quad V_B t - y_F = -\frac{dy_F}{dx_F} x_F .$$

Since the bomber coordinates are specified, we may for convenience drop the subscripts F and write (3.11) in the form

$$(3.12) \quad y = V_B t + y'x, \text{ where } y' = \frac{dy}{dx} .$$

The variable t may now be eliminated by use of the relation

$$(3.13) \quad s = V_F t \text{ or } t = s/V_F ,$$

where s is the arc length along the fighter's path. Equation (3.12) then becomes

$$(3.14) \quad y = cs + y'x, \text{ where } c = V_B/V_F .$$

This equation may now be differentiated with respect to x to yield

$$(3.15) \quad xy'' = c\sqrt{1 + y'^2}$$

or

$$(3.16) \quad \frac{y''}{\sqrt{1 + y'^2}} = \frac{C}{x} ,$$

since $s' = -\sqrt{1 + y'^2}$.

Performing the integration in equation (3.16) we find

$$ln\left(y' + \sqrt{1 + y'^2}\right) = ln\, x^c + ln\, k ,$$

or

$$(3.17) \quad y' + \sqrt{1 + y'^2} = k\, x^c ,$$

where k is a constant of integration which may be determined from the initial conditions $x = x_0$, $y' = y_0/x_0$.

Equation (3.17) is now solved for y' to give

$$(3.17a) \quad y' = \tfrac{1}{2}\left[kx^c - \frac{1}{kx^c} \right]$$

and integrated again to give

$$(3.18) \quad y = \tfrac{1}{2}\left[k\frac{x^{1+c}}{1+c} - \frac{1}{k}\frac{x^{1-c}}{1-c} \right] + C, \text{ if } c \neq 1,$$

$$= \tfrac{1}{2}\left[k\frac{x^2}{2} - \frac{1}{k}\, ln\, x \right] + C, \text{ if } c = 1.$$

Thus we have y as an explicit function of x and the pursuit course of the fighter is determined.

As an illustration, the space course was computed for the following set of conditions:

$V_B = 220$ yds/sec.	$V_F = 275$ yds/sec.
$x_{B_0} = y_{B_0} = 0$.	$x_{F_0} = 500$, $y_{F_0} = 1000$.

First we obtain $c = .8$, $k = .029362086$, $C = 706.7422$.

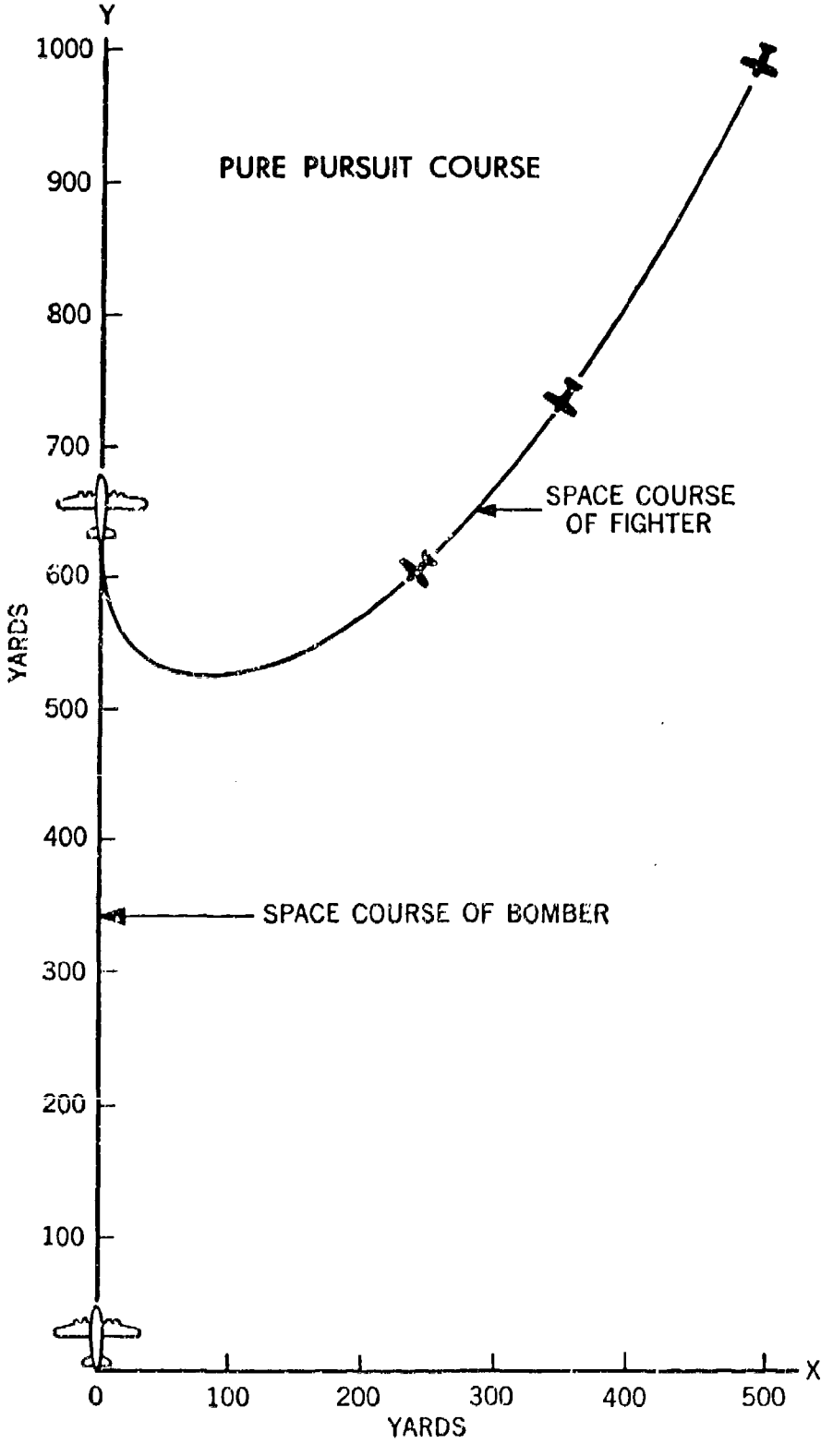

Figure 43. — Pure Pursuit Course Example

The values of the coordinates are given in table 3.1 and the course is shown in figure 43. The course also was computed by a numerical solution of equations (3.9) and (3.10). A Runge-Kutta method of solution was used with $\Delta t = .2$. The values are shown in table 3.2.

Table 3.1

Pure Pursuit Course

$$y = .008156135\, x^{1.8} - 85.143817\, x^{.2} + 706.7422$$

$V_B = 220$ yds/sec.; $V_F = 275$ yds/sec.; $c = .8$; $x_{F_0} = 500$ yds; $y_{F_0} = 1000$ yds.

x	y	t	x	y	t
500	1000	0	45	532.15	2.52
450	904.52	.39	40	534.92	2.54
400	818.26	.75	35	538.28	2.56
350	741.58	1.09	30	542.36	2.59
300	674.90	1.39	25	548.34	2.61
250	618.81	1.66	20	553.52	2.64
200	574.14	1.91	15	561.47	2.68
150	542.17	2.12	10	572.39	2.72
100	525.34	2.32	5	589.41	2.78
50	529.88	2.50	0	706.74	—

Table 3.2

Pure Pursuit Course

$$\dot{x}_F = -\frac{V_F}{r} x_F; \qquad \dot{y}_F = \frac{V_F}{r}(y_B - y_F)\,;\; y_B = V_B t$$

Initial Conditions Same as for table 3.1

t	y_B	x_F	y_F	r	$\dot{x}_F$	$\dot{y}_F$
0	0	500	1000		−123.0	−246.0
.2	44	475	951	1024	−127.6	−243.6
.4	88	449	903	930	−132.7	−240.8
.6	132	422	855	837	−138.6	−237.5
.8	176	393	808	744	−145.4	−233.4
1.0	220	364	761	652	−153.3	−228.3
.2	264	332	716	561	−162.7	−221.9
.4	308	298	673	471	−174.1	−212.9
.6	352	262	631	383	−188.2	−200.6
.8	396	223	593	297	−206.0	−182.2
2.0	440	179	559	216	−229.0	−152.3
.2	484	131	534	140	−257.0	− 97.8
.4	528	77	524	77	−274.7	13.6
.6	572	29	544	39	−199.3	189.5
.8	616	7	591	26	− 73.9	264.9
3.0	660	1	645	15	− 11.1	274.8
3.1	682	—	673	9	− 9.2	274.8
3.2	704	—	700	—	—	275

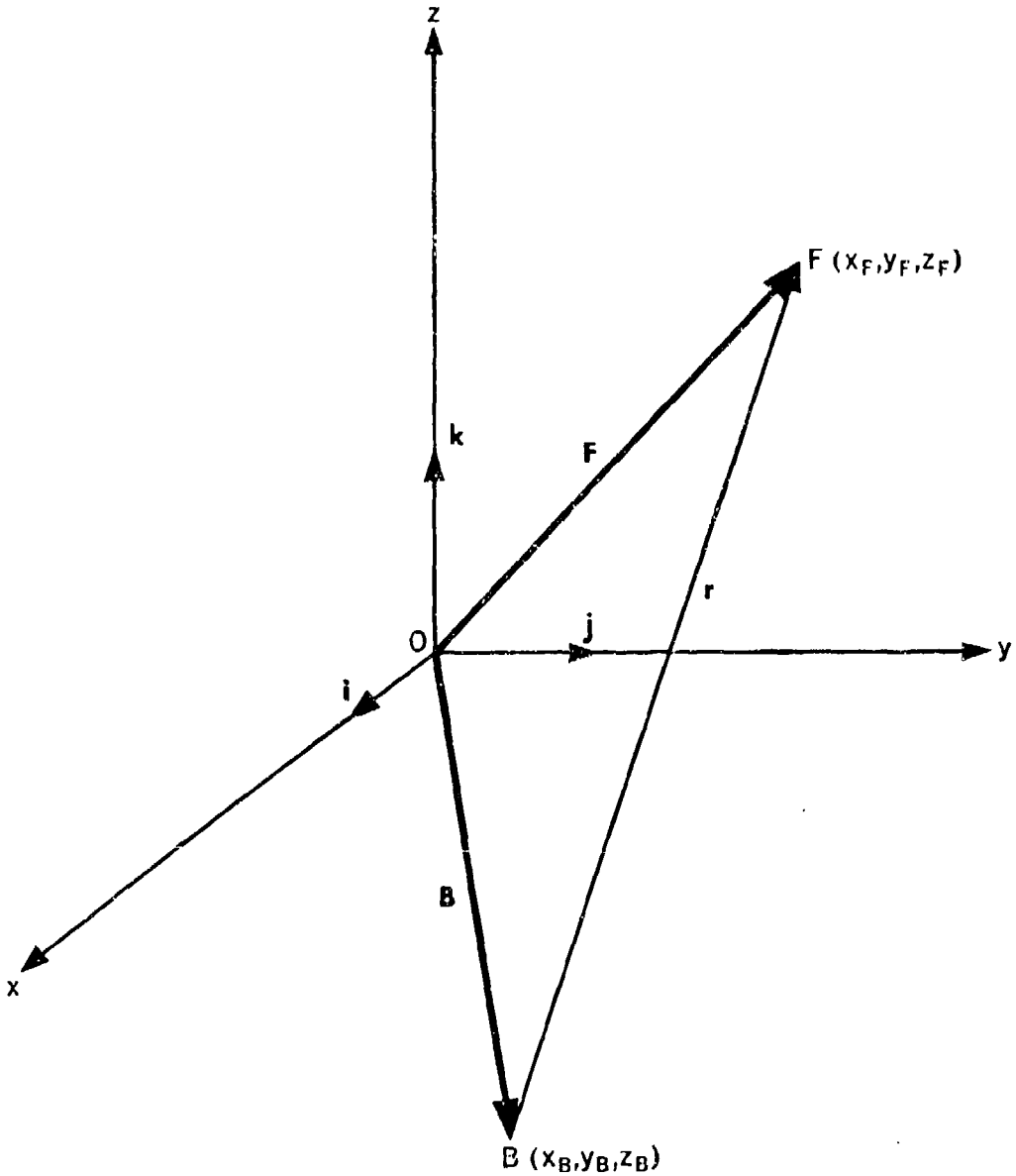

Figure 44. — Vector Diagram

The extension of equations (3.9) and (3.10) to a three-dimensional rectangular coordinate system (x, y, z) is straight forward. We now have (x_B, y_B, z_B) and (x_F, y_F, z_F) representing the coordinates of the bomber and fighter, respectively. The differential equations which now define the fighter's motion are given by the following system:

$$(3.19)\quad \begin{cases} \dot{x}_F = \dfrac{V_F}{r}(x_B - x_F)\,, \\[2ex] \dot{y}_F = \dfrac{V_F}{r}(y_B - y_F)\,, \\[2ex] \dot{z}_F = \dfrac{V_F}{r}(z_B - z_F)\,, \end{cases}$$

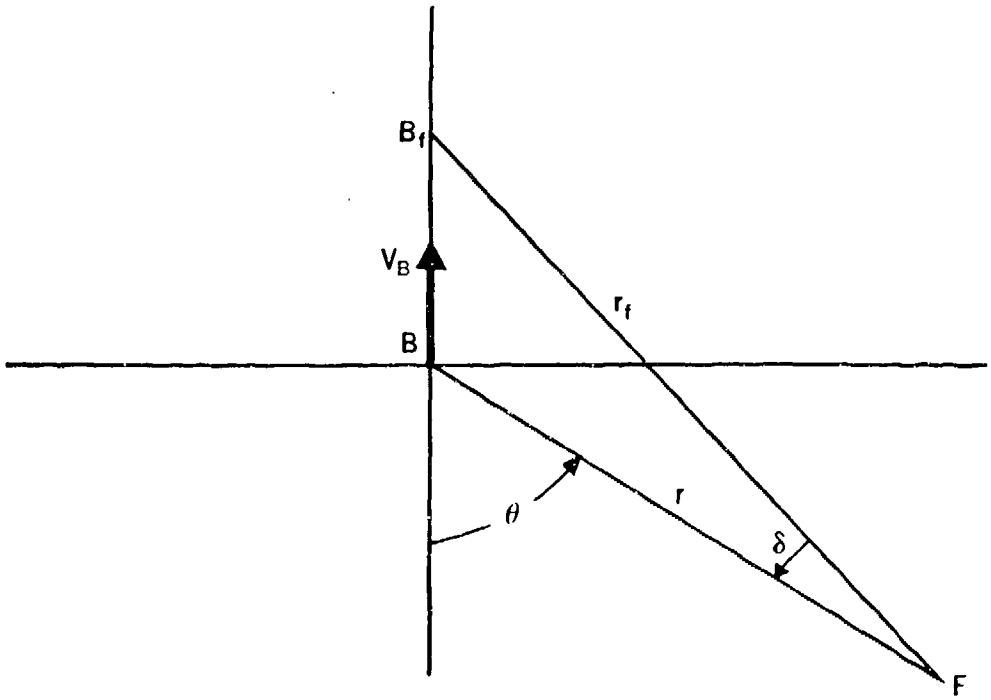

Figure 45. — Polar Coordinate System for a Deviated Pursuit

where

$$(3.20)\quad r^2 = (x_B - x_F)^2 + (y_B - y_F)^2 + (z_B - z_F)^2$$

and

$$(3.21)\quad \dot{x}_F^2 + \dot{y}_F^2 + \dot{z}_F^2 = V_F^2 .$$

Equations (3.19) are easily derived if we use vectors. Let **i**, **j**, **k** be unit vectors along the x, y, z axes, respectively, see figure 44. Then the vectors from the origin to the fighter's position and bomber position are

$$(3.22)\quad \mathbf{F} = x_F\mathbf{i} + y_F\mathbf{j} + z_F\mathbf{k},$$

$$(3.23)\quad \mathbf{B} = x_B\mathbf{i} + y_B\mathbf{j} + z_B\mathbf{k}.$$

The range vector is

$$(3.24)\quad \mathbf{r} = \mathbf{F} - \mathbf{B} = (x_F - x_B)\,\mathbf{i} + (y_F - y_B)\,\mathbf{j} + (z_F - z_B)\,\mathbf{k}.$$

Differentiating **F** we have

$$(3.25)\quad \dot{\mathbf{F}} = \mathbf{V}_F = \dot{x}_F\mathbf{i} + \dot{y}_F\mathbf{j} + \dot{z}_F\mathbf{k}.$$

For a pursuit course

$$(3.26)\quad \mathbf{V}_F = -\frac{V_F}{r}\mathbf{r} = -\frac{V_F}{r}\Big[(x_F - x_B)\,\mathbf{i} + (y_F - y_B)\,\mathbf{j} + (z_F - z_B)\,\mathbf{k}\Big].$$

If we now combine (3.25) and (3.26) and write the components we have the system (3.19).

3.3 The Space Course for a Lead Pursuit Attack

The differential equation of the pursuit curve with lead in rectangular coordinates can be derived in a manner similar to that of the last section. However, the equations are very ineffi-

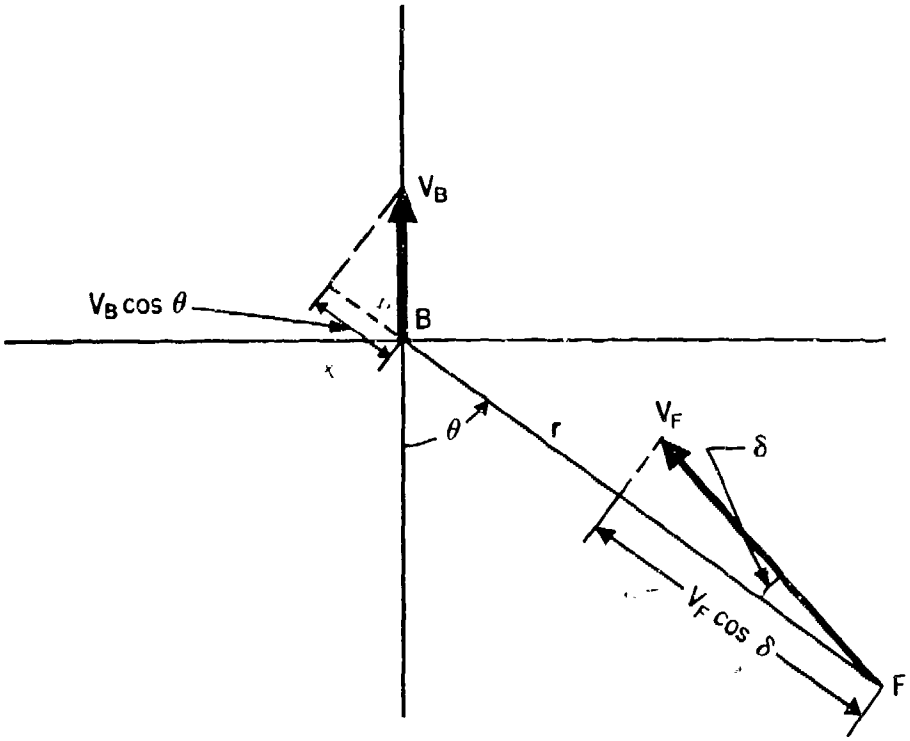

Figure 46. — Vector Diagram

cient and the most desirable approach is to obtain the relative course of the pursuer and then to convert to the space course if it is needed. As was pointed out in section 2.2, in a relative course the origin of the coordinate system moves with the bomber so that the relative coordinates are simply the space coordinates of the fighter less the bomber's coordinates at any time t. Thus, if X_F, Y_F, Z_F, are the fighter's relative coordinates, then

$$(3.27)\quad \begin{cases} X_F = x_F - x_B, \\ Y_F = y_F - y_B, \\ Z_F = z_F - z_B. \end{cases}$$

It is then clear that if the fighter's relative coordinates and the bomber's space coordinates are known, then the fighter's space coordinates could be found by solving (3.27) for x_F, y_F, and z_F.

3.4 Equations of the Relative Course

In the mechanization of fire control equipment it is the relative course of the pursuer which is of the greatest importance. This relative course is best described in terms of a polar coordinate system which has its origin at the bomber. Let us, therefore, choose such a system and measure the angle, θ, from the stern end of the longitudinal axis of the aircraft. See figure 45.

Pursuit courses with lead have often been called deviated pursuit courses, a more general term than lead pursuit courses. Thus, the angle at which the fighter aircraft is flying away from the direct line to the bomber is called the angle of deviation, δ. This angle is, of course, the lead angle in an exact lead pursuit course. The deviation angle is specified separately as some function of θ and r. If $\delta = O$, we have a pure pursuit and if δ is a constant, we have a fixed lead pursuit.

The polar radius r also is the present range at any time t. From the vector diagram of figure 46, it is clear that the rate of change of the range is

$$(3.28) \quad \frac{dr}{dt} = \dot{r} = -V_F \cos\delta + V_B \cos\theta ,$$

and the transverse component of relative velocity is given by

$$(3.29) \quad r\frac{d\theta}{dt} = r\dot{\theta} = V_F \sin\delta - V_B \sin\theta .$$

If we divide equation (3.28) by (3.29) we obtain

$$(3.30) \quad \frac{dr}{r} = \frac{V_F \cos\delta + V_B \cos\theta}{V_F \sin\delta - V_B \sin\theta} d\theta$$

$$= \frac{-\cos\delta + c\cos\theta}{\sin\delta - c\sin\theta} d\theta .$$

This equation is integrable for various deviation functions. If $\delta = O$; i.e., pure pursuit, we have

$$\frac{dr}{r} = \frac{-1 + c\cos\theta}{-c\sin\theta} d\theta$$

$$= \left(\frac{1}{c} csc\,\theta - \cot\theta \right) d\theta$$

and,

$$ln\, r = \frac{1}{c} ln \tan \tfrac{1}{2}\theta - ln \sin\theta + ln\, r_o ,$$

$$= ln \frac{\tan^{1/c} \frac{1}{2}\theta}{\sin\theta} + ln\, r_o ,$$

or,

$$(3.31) \quad r = r_o \frac{\tan^{1/c} \frac{1}{2}\theta}{\sin\theta} ;$$

where r_o includes all constants of integration. It is easily seen that if we let $\theta = 90°$, $r_o = r$ or, in other words, r_o is the range on the beam; that is, the fighter is directly abeam of the bomber. Equation (3.31), is then, the polar equation for a relative pure pursuit course. This may be changed to rectangular coordinates by the usual transformation equations

$$(3.32) \quad \begin{cases} X = r\sin\theta, \\ Y = -r\cos\theta, \end{cases}$$

if we choose the X, Y axes as shown in figure 45.

For a variable lead pursuit it is first necessary to determine the deviation function. Let us, therefore, consider the ballistic triangle of figure 47.

The law of sines applied to triangle FBB_F yields

$$(3.33) \quad \sin\delta = \frac{BB_f}{r_f} \sin\theta .$$

Let t_f be the time of flight of the bullet over the future range r_f and $\bar{u}$ be the average speed of the bullet. Then we have

$$(3.34) \quad BB_f = V_B\, t_f$$

and

$$(3.35) \quad r_f = \bar{u}\, t_f .$$

Substitution into (3.33) yields

$$(3.36) \quad \sin\delta = c_1 \sin\theta ,$$

where

$$(3.37) \quad c_1 = \frac{V_B}{\bar{u}}.^{*}$$

Straight substitution into equation (3.30) yields

$$(3.38) \quad \frac{dr}{r} = \frac{\sqrt{1 - c_1^2 \sin^2 \theta} + c \cos \theta}{(c_1 - c) \sin \theta} d\theta ,$$

which may be reduced to

$$(3.39) \quad \frac{dr}{r} = \frac{1}{c - c_1}\left[\sqrt{csc^2 \theta - c_1^2}\, d\theta - c \cot \theta \, d\theta\right].$$

This equation may be integrated; the first integral on the right-hand side, however, needs some manipulation. Let us make the substitution

$$z = c_1 \frac{\cos \theta}{\cos \delta} \quad \text{or} \quad z \cos \delta = c_1 \cos \theta .$$

The differential relation

$$dz \cos \delta - z \sin \delta \, d\delta = - c_1 \sin \theta \, d\theta$$

may be solved for $d\theta$ with the aid of the fact that from $\sin \delta = c_1 \sin \theta$ we have $d\delta = z d\theta$. Thus we have

$$dz \cos \delta = (z^2 \sin \delta - c_1 \sin \theta) \, d\theta$$

$$= (z^2 - 1) \, c_1 \sin \theta \, d\theta$$

or

$$d\theta = \frac{1}{z^2 - 1} \frac{\cos \delta}{c_1 \sin \theta} dz$$

$$= \frac{1}{z^2 - 1} \frac{\sqrt{1 - c_1^2}}{\sqrt{c_1^2 - z^2}} dz .$$

To obtain the last expression, we need to prove the identity

$$\frac{\cos \delta}{c_1 \sin \theta} = \frac{\sqrt{1 - c_1^2}}{\sqrt{c_1^2 - z^2}},$$

which is more easily accomplished by working on the right-hand side, making the substitution for z. The integral $\int [csc^2 \theta - c_1^2]^{\frac{1}{2}} \, d\theta$ then becomes

$$I_1 = \int [csc^2 \theta - c_1^2]^{\frac{1}{2}} \, d\theta = \int \frac{\cos \delta}{\sin \delta} d\theta$$

$$= (c_1^2 - 1) \, c_1 \int \frac{dz}{(c_1^2 - z^2)\,(1 - z^2)},$$

which may be solved by the usual method of partial fractions to give

$$I_1 = ln\left[\left(\frac{c_1 - z}{c_1 + z}\right)^{\frac{1}{2}} \left(\frac{1 + z}{1 - z}\right)^{c_1/2}\right].$$

For convenience in writing, let $c_2 = c - c_1$. The integration of equation (3.39) then yields

*We assume now that c_1 is a constant; this is not precisely true since $\bar{u}$ is a function of the range. However, it is a usable approximation.

988995 O - 52 - 6

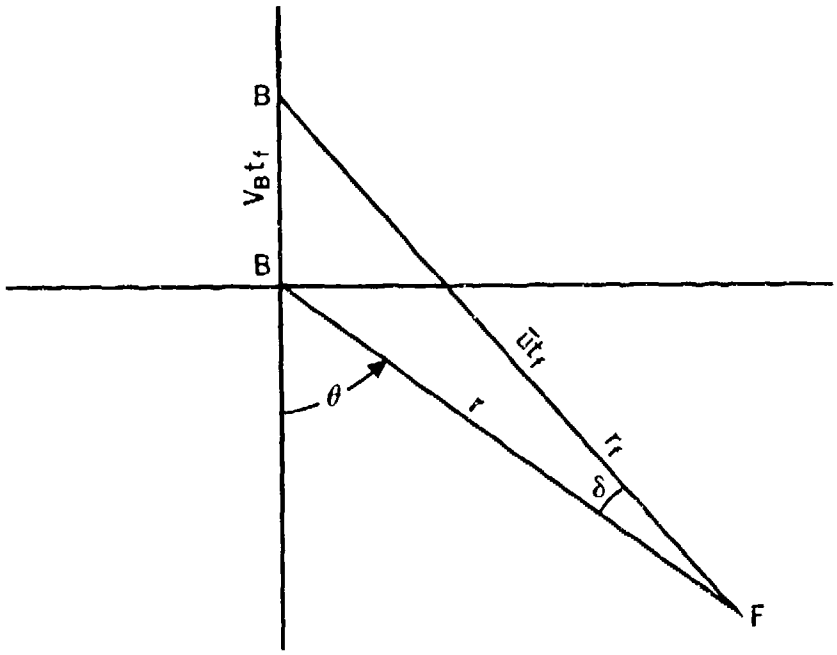

Figure 47. — Ballistic Triangle

$$(3.40)\qquad ln\frac{r}{r_o}=\frac{1}{c_2}\left[ln\left(\frac{c_1-z}{c_1+z}\right)\left(\frac{1+z}{1-z}\right)^{c_1}\right]^{\frac{1}{2}}-\frac{c}{c_2}\,ln\sin\theta$$

or

$$(3.41)\qquad r=r_o\left\{\left[\left(\frac{\cos\delta-\cos\theta}{\cos\delta+\cos\theta}\right)\left(\frac{\cos\delta+c_1\cos\theta}{\cos\delta-c_1\cos\theta}\right)^{c_1}\right]^{\frac{1}{2}}\frac{1}{\sin^c\theta}\right\}^{1/c_2},$$

where r_o is again the constant of integration that becomes the range on the beam.

If δ is small, a useful approximation is obtained by letting $\cos\delta=1$, and if we insert this approximation and the expression (3.36) into equation (3.30), we have

$$\frac{dr}{r}=\frac{-1+c\cos\theta}{(c_1-c)\sin\theta}\,d\theta$$

$$=\frac{1}{c-c_1}(csc\,\theta-c\cot\theta)\,d\theta$$

which may be integrated to give

$$ln\frac{r}{r_o}=\frac{1}{c-c_1}(ln\tan\tfrac{1}{2}\theta-c\,ln\sin\theta)$$

whence

$$(3.42)\qquad r=r_o\left(\frac{\tan\frac{1}{2}\theta}{\sin^c\theta}\right)^{1/(c-c_1)}$$

or

$$(3.43)\qquad r^{c-c_1}=r_o^{c-c_1}\left(\frac{\tan\frac{1}{2}\theta}{\sin^c\theta}\right).$$

This is the approximation which was made in most of the analyses carried out during World War II.

In the above equations, r_o is the constant of integration which needs to be determined. If we let $\theta=90°$ in the above equations, we see that $r=r_o$ or, in other words, r_o is the range on the beam.

Table 3.3
Example of Relative Course in Pure Pursuit

$$r = r_o \frac{\tan^{1.25} \frac{1}{2}\theta}{\sin\theta}$$

$r_o = 82.274314$; $c = .8$; $1/c = 1.25$; $V_F = 275$, $V_B = 220$

Units: yds., sec., degrees

$X = r \sin\theta$; $Y = -r\cos\theta$

θ	r	X	Y
150	853.5	426.8	739.2
140	452.7	291.0	346.8
130	278.7	213.5	179.2
120	188.8	163.5	94.4
110	136.7	128.5	46.8
100	104.0	102.5	18.1
90	82.3	82.3	0
80	67.1	66.1	−11.7
70	56.1	52.7	−19.2
60	47.8	41.4	−23.9
50	41.4	31.7	−26.6
40	36.2	23.3	−27.7
30	31.7	15.9	−27.5
20	27.5	9.4	−25.8
10	22.5	3.9	−22.1
0	——	0	0

Table 3.4
Example of Relative Course in Deviated Pursuit

$\cos\delta \doteq 1$

$$r = r_o \left(\frac{\tan\frac{1}{2}\theta}{\sin^c\theta}\right)^{\frac{1}{c-c_1}}$$

Units: degrees, yards, seconds.

$r_o = 1000$; $c = 2/3$; $c_1 = 1/10$, $\theta_o = 90°$, $V_F = 220$

θ	r (yds)	X (yds)	Y (yds)	a (gees)
90°	1000	1000	0	2.56
80°	747.1	735.7	−129.7	3.31
70°	573.7	539.1	−196.2	4.05
60°	449.3	389.1	−224.6	4.68
50°	356.0	272.7	−228.8	5.15
40°	282.6	181.7	−216.5	5.37
30°	221.2	110.1	−191.6	5.28
20°	165.3	56.5	−155.3	4.80
10°	106.5	18.5	−104.9	3.76
0°	0	0	0	——

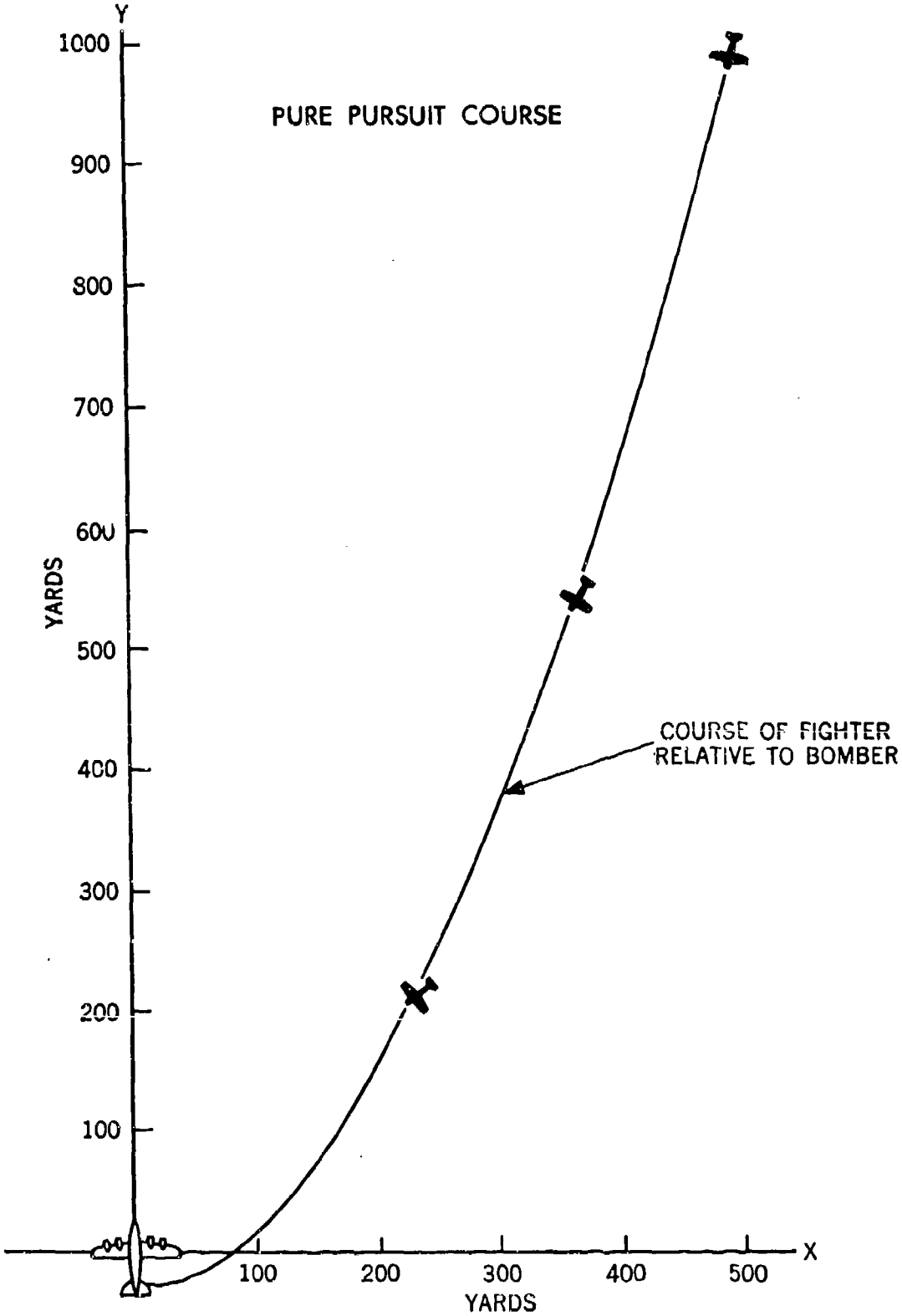

Figure 48. — Pure Pursuit Course Example

Table 3.5

Example of Relative and Space Course in Deviated Pursuit

$\cos \delta \doteq 1$

$$\dot{r} = -\frac{220}{3}\left[\ 3-2\cos\theta\ \right]$$

$$\dot{\theta} = -\frac{374}{3}\left[\frac{\sin\theta}{r}\right]$$

Same Conditions and units as for table 3.4

t	θ	r	X	Y	y_B	y_F
0	90.000	1000	1000	0	0	0
.4	87.012	913.5	912.3	− 47.6	58.7	11.1
.8	83.743	830.2	825.3	− 90.5	117.3	26.8
1.0	81.992	789.9	782.1	−110.0	146.7	36.6
1.2	80.159	750.4	739.4	−128.3	176.0	47.7
1.4	78.239	711.9	697.0	−145.1	205.3	60.2
1.6	76.229	674.4	655.0	−160.5	234.7	74.1
1.8	74.123	637.9	613.6	−174.5	264.0	89.5
2.0	71.920	602.5	572.7	−187.0	293.3	106.4
2.2	69.614	568.1	532.5	−197.9	322.7	124.8
2.4	67.205	534.9	493.1	−207.2	352.0	144.8
2.6	64.690	502.9	454.6	−215.0	381.3	166.3
2.8	62.069	472.0	417.0	−221.1	410.7	189.6
3.0	59.342	442.4	380.5	−225.6	440.0	214.4
3.2	56.513	413.9	345.2	−228.4	469.3	241.0
3.4	53.587	386.7	311.2	−229.6	498.7	269.1
3.6	50.571	360.7	278.6	−229.1	528.0	298.9
3.8	47.473	336.0	247.6	− 227.1	557.3	330.2
4.0	44.308	312.4	218.2	−223.5	586.7	363.1
4.2	41.090	289.9	190.6	−218.5	616.0	397.5
4.4	37.838	268.6	164.8	−212.1	645.3	433.2
4.6	34.572	248.2	140.9	−204.4	674.7	470.3
4.8	31.315	228.9	118.9	−195.5	704.0	508.5
5.0	28.092	210.3	99.0	−185.6	733.3	547.8
5.2	24.927	192.6	81.2	−174.6	762.7	588.0
5.4	21.848	175.5	65.3	−162.9	792.0	629.1
5.6	18.878	159.0	51.4	−150.5	821.3	670.9
5.8	16.042	143.0	39.5	−137.4	850.7	713.2
6.0	13.370	127.4	29.4	−123.9	880.0	756.1
6.2	10.869	112.0	21.1	−110.0	909.3	799.3
6.4	8.568	96.9	14.4	− 95.9	938.7	842.8
6.6	6.485	82.0	9.26	− 81.5	968.0	886.5
6.8	4.641	67.2	5.44	− 67.0	997.3	930.3
7.0	3.055	52.5	2.80	− 52.4	1026.7	974.2
7.2	1.751	37.8	1.15	− 37.8	1056.0	1018.2
7.4	.764	23.1	.31	− 23.1	1085.3	1062.2
7.6	.187	8.5	0	− 8.5	1114.7	1106.2

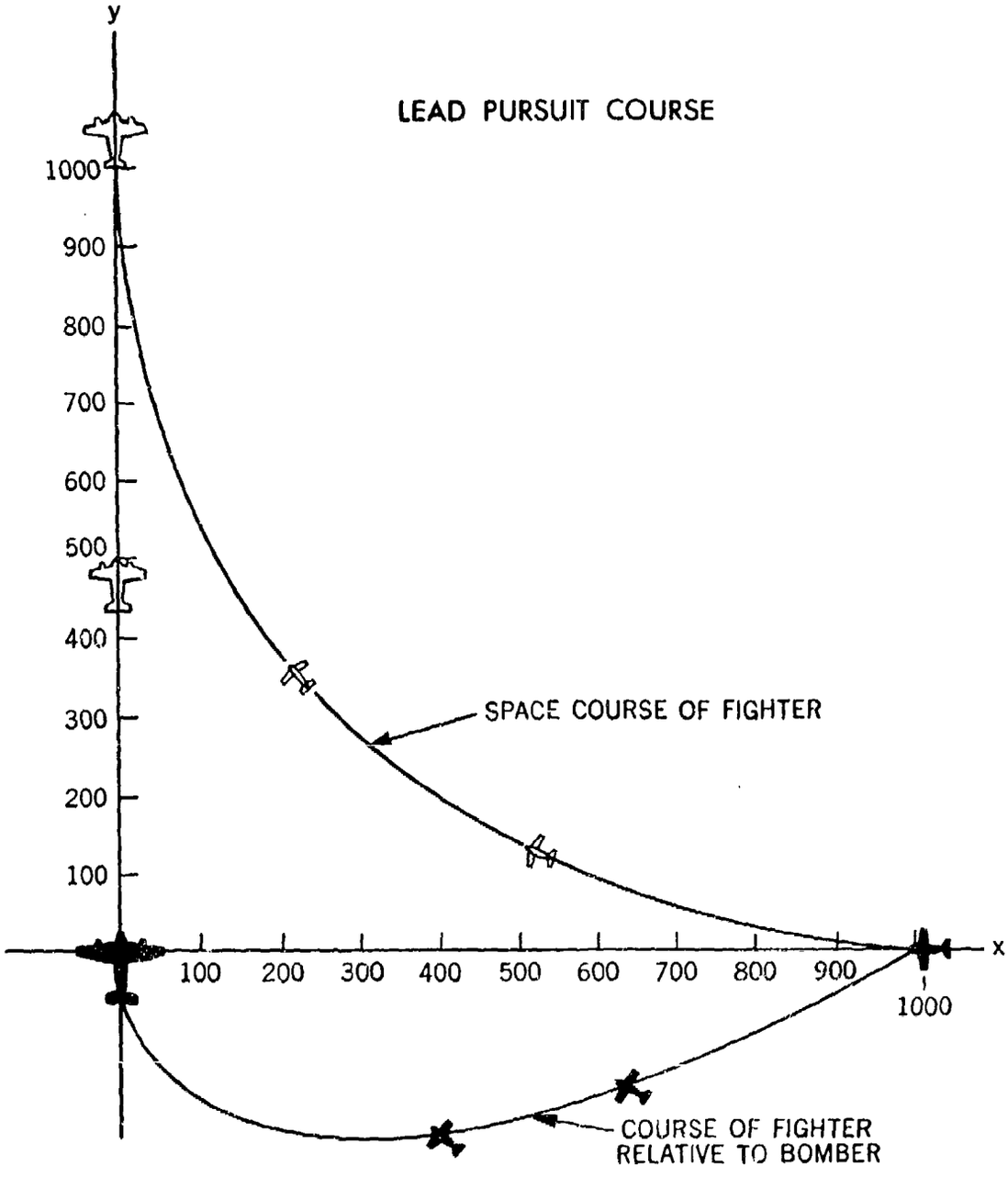

Figure 49. — Lead Pursuit Course Example

3.5 Time as a Parameter

The method of solving the pursuit course problem given in the last section has the disadvantage that the solutions are not given explicitly as functions of time. It is necessary to have this dependence on time expressed explicitly for many problems in fire control work and also for computation of the space courses. For example, the space coordinates may be found from the relative coordinates by using the relation (3.27) where the bomber's coordinates are given as

functions of time and thus the fighter's relative coordinates also must be found as functions of time. In determining the lead to take against a fighter flying a pursuit course, one usually matches the time along the course, from a chosen present position to the required future position of impact, with the time of flight of the projectile over the range to this future position.

There are many ways for getting points on a pursuit course which are labeled with the appropriate time, but to find the range or angle-off as explicit functions of time is another matter. Thus t may be obtained as a function of θ but the inverse solution is not readily obtainable. The implicit solution is found by knowing r as a function of θ from (3.41), and upon substituting it into (3.29) the time t is then found as a function of θ by a simple integration. Consider, for example, the case of a pure pursuit course, $\delta = O$, where

$$r = r_o \frac{\tan^{1/c} \frac{1}{2}\theta}{\sin\theta}$$

Upon the substitution of this solution into equations (3.29) we have

$$(3.44) \qquad r_o \left[\frac{\tan^{1/c} \frac{1}{2}\theta}{\sin\theta} \right] \frac{d\theta}{dt} = -V_B \sin\theta$$

or

$$(3.45) \qquad r_o \left[\tan^{1/c} \tfrac{1}{2}\theta \sin^{-2}\theta \right] d\theta = -V_B dt .$$

Equation (3.45) may now be integrated by employing the substitution

$$\tan \tfrac{1}{2}\theta = Z, \ \sin\theta = \frac{2Z}{1+Z^2}, \ d\theta = \frac{2dZ}{1+Z^2}.$$

we obtain

$$t = k - \frac{r_o}{2V_B} \left[\frac{\tan^{1/c-1} \frac{1}{2}\theta}{\frac{1}{c} - 1} + \frac{\tan^{1/c+1} \frac{1}{2}\theta}{\frac{1}{c} + 1} \right]$$

where k is the constant of integration to be determined by the initial conditions. Thus we have t as a function of θ, from which θ could best be obtained for a given t by graphical means.

Another method is to expand r and θ in power series valid in the neighborhood of any particular point about which the expansions are made. Thus expanding r and θ about $t = O$, we have the well known Maclaurin series.

$$r(t) = r(o) + \dot{r}(o)t + \ddot{r}(o)\frac{t^2}{2!} + \dddot{r}(o)\frac{t^3}{3!} + \dots ;$$

$$\theta(t) = \theta(o) + \dot{\theta}(o)t + \ddot{\theta}(o)\frac{t^2}{2!} + \dddot{\theta}(o)\frac{t^3}{3!} + \dots .$$

To obtain these expansions we need to know the values of r and θ at $t = O$. The derivatives are then obtained by successive differentiation of equations (3.28) and (3.29). The resulting series converge so that r and θ may be found at any t to the accuracy desired.

Still a third and perhaps the best method is to solve the system of differential equations given by (3.28) and (3.29) by a numerical process. Such a solution will, of course, yield values of r and θ at chosen increments of t.

3.6 The Acceleration of the Fighter Caused by the Curvature of His Space Course

In analyzing pursuit courses it is important to determine the extent to which the course curvature is restricted by the physiological effects on the pilot in flight and the structural and aerodynamic limitations of the aircraft. We

begin in this section by considering the normal acceleration and the centrifugal force acting on the plane and pilot.

It is well known that the normal acceleration may be expressed in terms of the radius of curvature,

$$(3.46)\qquad \frac{V_F^2}{R} = \text{normal acceleration}$$

where R is the radius of curvature of the space curve. The radius of curvature may be expressed in either rectangular or polar coordinates. For rectangular coordinates we have

$$(3.47)\qquad R = -\frac{(1+y'^2)^{\frac{3}{2}}}{|y''|},$$

and for pure pursuit we have by equation (3.15) and (3.17a)

$$(3.48)\qquad R = \frac{(1+y'^2)^{\frac{3}{2}}}{\frac{c}{x}\sqrt{1+y'^2}} = \frac{x}{c}(1+y'^2)$$

$$= \frac{1}{4c} \times \left[kx^c + \frac{1}{kx^c}\right]^2.$$

For pure pursuit we also have

$$(3.49)\qquad R = -\frac{V_F}{\dot{\theta}}$$

since the tangent to the circle of curvature also is the terminal side of angle θ. Thus in polar coordinates the radius of curvature is, using (3.29) with $\delta = \theta$,

$$(3.50)\qquad R = \frac{V_F}{\frac{V_B}{r}\sin\theta} = \frac{V_F r}{V_B \sin\theta}.$$

For deviated pursuit courses (lead pursuit) with $\sin\delta = c_1 \sin\theta$ we have

$$(3.51)\qquad R = \frac{V_F}{\dot{\delta} - \dot{\theta}}$$

$$= \frac{V_F}{\frac{V_F}{r}[c - c_1]\sin\theta\left[1 - \frac{c_1\cos\theta}{\cos\delta}\right]}$$

$$= \frac{r}{[c - c_1]\sin\theta\left[1 - \frac{c_1\cos\theta}{\cos\delta}\right]}$$

The normal acceleration, a, is usually expressed in units of gravity called "gees", i.e., ratio of acceleration to the acceleration of gravity, g. This acceleration is due solely to the curvature of the course and does not include the ever present acceleration due to gravity, which, of course, is one "gee". Upon combining (3.46) and (3.49) with (3.29), we find, in the case of pure pursuit,

$$(3.52)\qquad a = \frac{V_F V_B \sin\theta}{gr}.$$

For lead pursuit,

$$(3.53)\qquad a = \frac{V_F^2[c - c_1]}{gr}\sin\theta\left(1 - \frac{c_1\cos\theta}{\cos\delta}\right).$$

It is, therefore, possible to calculate both the radius of curvature and the normal acceleration for these pursuit courses.

Equation (3.52) may be solved for r to give

$$(3.54)\qquad r = \frac{V_F V_B}{ga}\sin\theta,$$

an equation which represents a family of circles of radii $\frac{V_F V_B}{2ga}$, each circle being tangent to the straight line path of the pursued bomber. By varying the parameter, a, we may plot members of the family and then superimpose the pursuit courses upon this plot. From such a graph we can read off the normal acceleration (or load) at any point on the pursuit course. See figure 50.

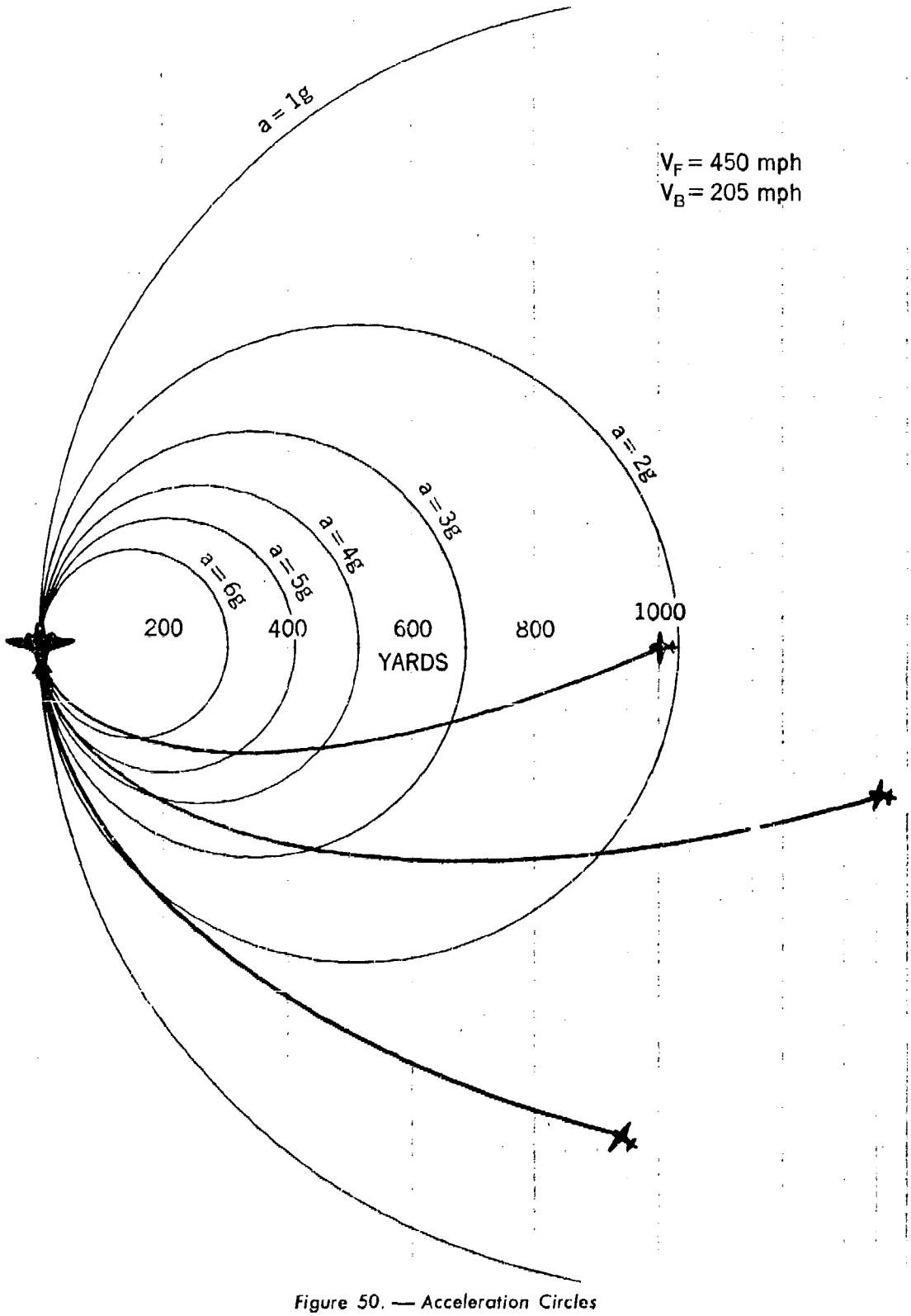

Figure 50. — Acceleration Circles

3.6.1 Maximum Acceleration

If we consider V_F, c, and c_1 as constants, the normal acceleration is given by equation (3.53) as a function of θ, r, and δ. Since both r and δ can be expressed as functions of θ, see equations (3.41) and (3.36), respectively, we have the normal acceleration as a function of θ alone. Thus, there may exist a value of θ for which the normal acceleration is a maximum. That this is actually the case can be verified by taking the derivative of equation (3.53) with respect to θ, setting it equal to zero and solve for θ; the usual calculus procedure for finding the maximum of a function. It is easily accomplished in the case of pure pursuit; in which case we find that the maximum acceleration is achieved at the value $\theta = \text{arc cos}\,\frac{1}{2c}$. Under the approximation that the $\cos\delta = 1$ we find that the maximum normal acceleration occurs at the value

$$\theta = \text{arc cos}\,\frac{c - \sqrt{c^2 - (2c_1^2 - 3cc_1)(cc_1 - c_1^2 - 1)}}{3cc_1 - 2c_1^2}.$$

The existence of a value θ, for which the normal acceleration is a maximum, enables one to find a limiting relative pursuit course on which, for a given normal acceleration a, the acceleration achieves the maximum value a. This course is limiting in the sense that it divides all pursuit courses into two groups, the one containing all courses on which the normal accelerations never build up greater than a, the other including only courses on which the accelerations eventually surpass a.

Let us consider pure pursuit courses. Since maximum gees must be achieved for points on the line $\theta_1 = \text{arc cos}\left(\frac{1}{2c}\right)$, the limiting pursuit course divides the plane into two separate regions, each containing curves of one and only one of the groups defined above. Geometrically, the limiting "$5g$" pursuit course is tangent to the "$5g$" circle at the point (r_1, θ_1), wherein r_1 is obtained from equation (3.52) for $\theta = \theta_1$. Thus, since $\theta_1 = \text{arc cos}\left(\frac{1}{2c}\right)$, we have

$$\sin\theta_1 = \sqrt{1 - \left(\frac{1}{2c}\right)^2} = \frac{\sqrt{4c^2 - 1}}{2c}$$

and,

$$a = \frac{V_F V_B}{g r_1} \sin\theta_1,$$

or,

$$r_1 = \left(\frac{V_F V_B}{5g}\right)\left(\frac{\sqrt{4c^2 - 1}}{2c}\right)$$

for $a = 5$.

Since

$$r_0 = r\,(\tan\tfrac{1}{2}\theta)^{-1/c} \sin\theta$$

we have

$$r_0 = r_1\,(\tan\tfrac{1}{2}\theta_1)^{-1/c} \sin\theta_1$$

$$= \left(\frac{V_F V_B}{5g}\right)\left(\frac{\sqrt{4c^2 - 1}}{2c}\right) \cdot \left(\frac{2c - 1}{2c + 1}\right)^{-\frac{1}{2c}} \left(\frac{\sqrt{4c^2 - 1}}{2c}\right)$$

$$= \frac{V_F V_B (4c^2 - 1)}{20\,g\,c^2}\left(\frac{2c + 1}{2c - 1}\right)^{\frac{1}{2c}}.$$

Thus, the equation of the limiting "*ng*" relative pure pursuit course is

$$r = \frac{V_F V_B (4c^2 - 1)}{4\,n\,g\,c^2}\left(\frac{2c + 1}{2c - 1}\right)^{\frac{1}{2c}} \frac{(\tan\frac{1}{2}\theta)^{\frac{1}{c}}}{\sin\theta}.$$

3.7 Aerodynamic Pursuit Course

In the pursuit courses considered thus far it has been assumed that the projectile leaves the fighter aircraft in the direction of the aircraft's motion. Thus it has been tacitly assumed that the aircraft moves in the direction in which it is pointing. However, it is well known from aerodynamic considerations that there exists an angle, the angle of attack, between the zero lift line of the wing and the direction of motion. The zero lift line is a hypothetical line through the wings in the general direction of the longitudinal axis; in steady flight, the airplane would move along this line if there were no gravity acting. Since the guns are fixed in the aircraft, there exists, then, an angle of attack, α, between the gun bore axis and the direction of motion of the aircraft, and the deviation function, δ, discussed in the preceding sections, should have a component due to this angle of attack. If the gun bore axis is parallel to the zero lift line of the wing, then α is the usual angle of attack for the aircraft. However, the gun bore axis is usually offset from the zero lift line to allow for gravity drop or other considerations so that the angle of attack of the gun bore is not necessarily the angle of attack of the aircraft wing.

The treatment of the problem of aerodynamic pursuit courses may be divided into two parts: (1) the equations of motion of the aircraft and (2) the conditions of pursuit. In order to find the equations of motion of the aircraft, it is necessary to consider the usual force system acting upon the aircraft; i.e., the forces of lift, thrust, drag, and weight. The conditions of pursuit then constrain this motion and we have a typical dynamic problem with constraints. If it is possible to obtain a sufficient number of equations to determine the variables under consideration, the problem is solvable. If not, it may still be possible to solve the problem if from experimental data a sufficient number of logical assumptions can be made which lead to consistent equations.

3.8 Attack in a Vertical Plane

The general problem is indeed a complicated one and for this reason it is advantageous to begin with a restricted case. Let us, therefore, consider an attack made in a vertical plane by a fighter on a bomber which moves in a straight and level flight path at a constant speed.

Let us assume that the gun bore axis coincides with the thrust axis of the fighter aircraft. This is no real restriction since if the two did not coincide, the equations would be changed merely by inserting a constant angle. We shall now use the following notation: (See figure 51.)

$\mathbf{L}$ = the fighter's lift vector, directed normal to $\mathbf{V}_F$;

$\mathbf{D}$ = the fighter's drag vector, directed along $-\mathbf{V}_F$;

$\mathbf{W}$ = weight of the fighter, directed vertically down;

$\mathbf{T}$ = fighter's thrust vector, directed along the thrust axis;

$\mathbf{V}_F$ = fighter's velocity vector, directed along its flight line;

$\mathbf{V}_B$ = bomber's velocity vector, directed along its flight line;

γ = angle from the horizontal reference line to the flight line;

θ = angle from the horizontal reference line to the sight line;

α = angle of attack of the gun bore line;

= angle from the thrust line (gun bore axis) to the flight line;

α_o = angle from the zero lift line to the thrust axis of the fighter;

$\alpha + \alpha_o$ = angle of attack of the fighter measured from the zero lift line;

R = radius of curvature of the fighter's path;

$\overline{u}$ = average speed of the projectile over its path;

ρ = relative air density.

From the force system shown in figure 51, we can write by Newton's second law the equations of motion, for motion along and normal to the flight line. Thus,

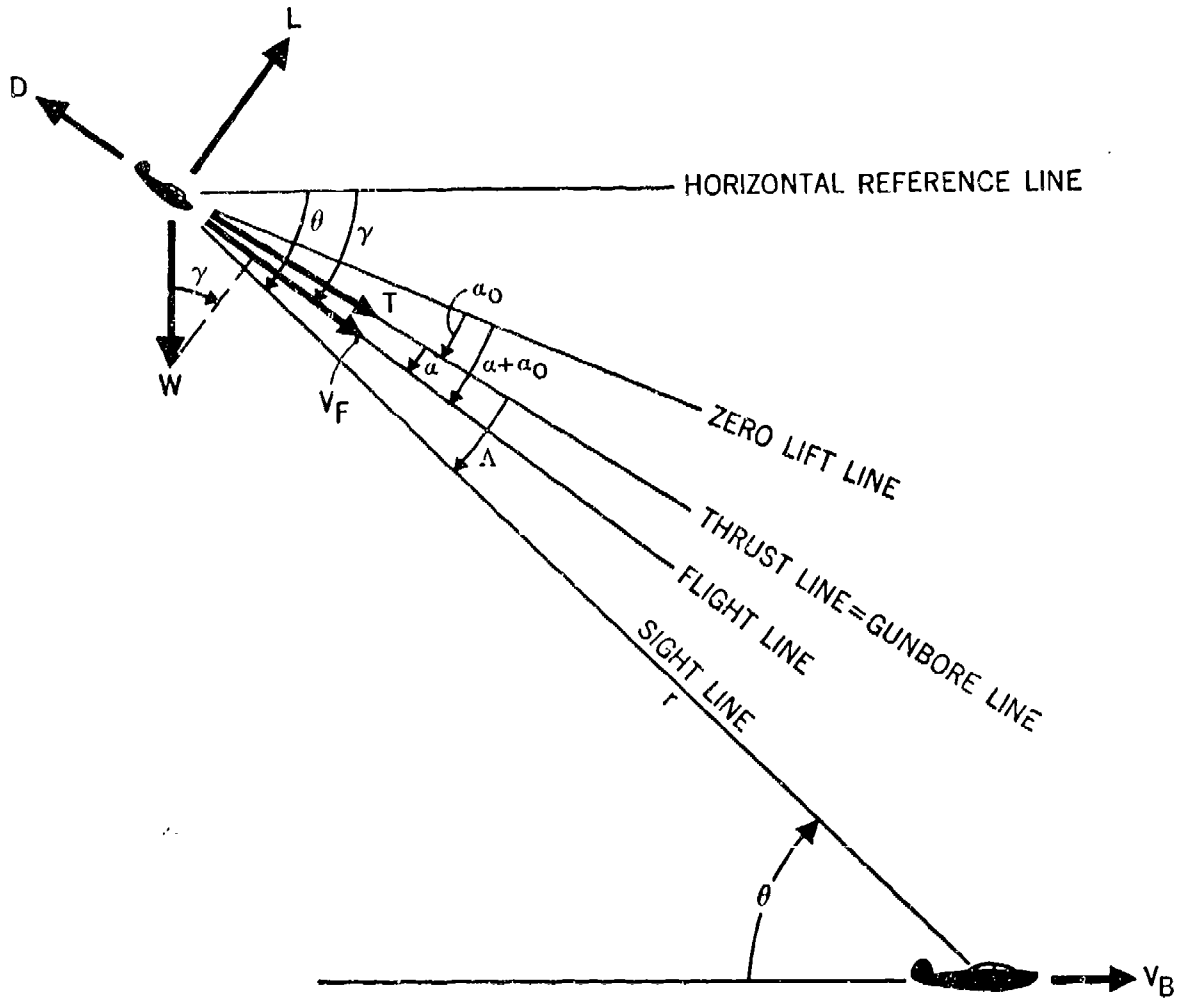

Figure 51. — Force Diagram

$$(3.55)\qquad \frac{W}{g}\dot{V}_F = W\sin\gamma + T\cos\alpha - D$$

and

$$(3.56)\qquad \frac{W}{g}\frac{V_F^2}{R} = L + T\sin\alpha - W\cos\gamma\,.$$

Now the radius of curvature can be written in terms of V_F and γ; in fact,

$$\frac{1}{R} = -\frac{1}{V_F}\frac{d\gamma}{dt}\,.$$

Hence, equation (3.56) may be written in the form

$$(3.57)\qquad \frac{W}{g}V_F\dot{\gamma} = W\cos\gamma - L - T\sin\alpha\,.$$

There also are two kinematic equations of pursuit which are obtained by considering the motion along and perpendicular to the sight line, r, and which are expressible in terms of the polar coordinates r and θ. Thus, we have

$$(3.58)\qquad \dot{r} = V_B\cos\theta - V_F\cos(\theta-\gamma)$$

and

$$(3.59)\qquad \dot{\theta} = -\frac{1}{r}\left[V_F\sin(\gamma-\theta) + V_B\sin\theta\right].$$

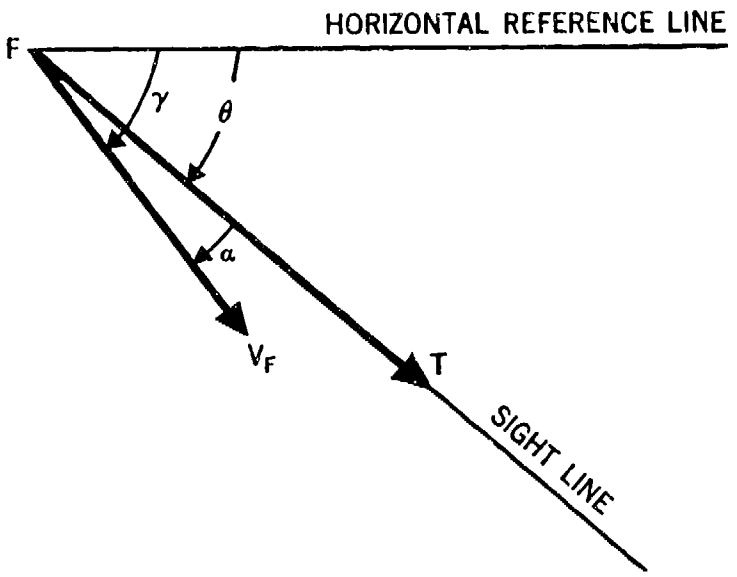

Figure 52. — Angles for Pure Pursuit

In pure pursuit, where we do not consider any lead or ballistics, the gun bore axis (thrust line) coincides with the line of sight so that

(3.60) $\gamma - \theta = \alpha$ or $\theta = \gamma - \alpha$. See figure 52.

We may then eliminate θ from equations (3.58) and (3.59) and together with (3.55) and (3.57) we have four non-linear differential equations to determine the four variables V, γ, α, r, as functions of time. Before proceeding, we must first determine the aerodynamic constants for the fighter airplane in question at a fixed throttle setting. This is accomplished from the weight and geometry of the airplane and its performance values of propeller efficiency, maximum engine brake power, and the corresponding maximum level flight speed at a certain altitude. With this knowledge, we have formulas which enable us to obtain expressions for L, D, T, and W.

The four differential equations must be integrated numerically, and, consequently, we need to know the initial values of V_F, γ, α, and r. The quantities V_F, γ, and r, may be assigned at will to give a family of cases. The initial value of α, however, has a "natural" value for a given value of γ. This natural value can be found by plotting γ against time for the first second for a few arbitrary choices of α, usually between 2° and 12°. The family thus obtained will funnel into one curve which then is extrapolated back linearly to give the natural value of α.

For a lead pursuit course we need to account for the ballistic effects. In this case, the gun bore axis is pointed so that the projectile leaving the gun at a muzzle velocity of V_o will travel the vector diagonal to the point of impact as shown in figure 53. In order to score a hit, the projectile's motion normal to the sight line should be equal to the bomber's motion normal to the sight line during the time of flight. If we let $\mathbf{n}$ be a unit vector perpendicular to the sight line, then this condition states

(3.61) $t_f(\bar{\mathbf{u}}) \cdot \mathbf{n} = t_f(\mathbf{V}_B) \cdot \mathbf{n}$,

where $\bar{\mathbf{u}}$ is the average velocity of the projectile over its impact range. If we let $\bar{\mathbf{u}} = \mathbf{V}_s + \mathbf{V}_F$, where $\mathbf{V}_s$ is a calculated average speed vector of the projectile which can be assumed to be in the direction of $\mathbf{V}_o$, then we may write equation (3.61) in the form

(3.62) $-V_F \sin(\alpha - \Lambda) + V_s \sin \Lambda = V_B \sin \theta$.

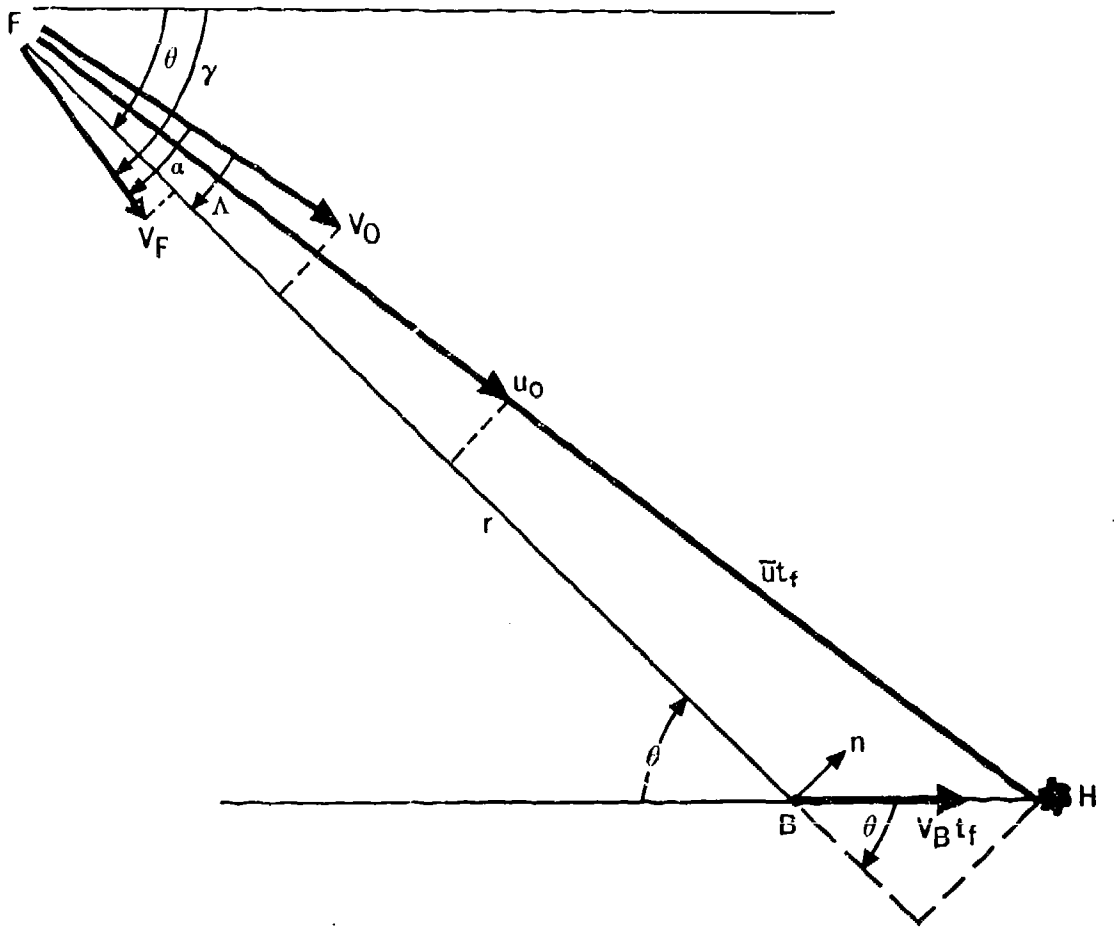

Figure 53. — Velocity Diagram

From figure 51 it also is clear that

$$\gamma - \theta = \alpha - \Lambda \tag{3.63}$$

or

$$\Lambda = \alpha + \theta - \gamma$$

so that Λ may be eliminated from (3.62) and, if V_x is known, equation (3.62) may be used to solve for α.

3.9 The Determination of the Aircraft Constants

In order to solve the system of equations given by (3.55), (3.57), (3.58), and (3.59), we need to determine the expressions for L, D, T and W. As was mentioned in the last section, the theory of aerodynamics furnishes us with formulas for these expressions if we know the geometry of the airplane and its performance characteristics. We shall not derive these expressions here but will adopt them without proof and refer the reader to a standard text on the theory of aerodynamics. It shall be our purpose here to exhibit the formulas and indicate their use.

The aerodynamic forces L, D, and T are expressed in the following form:

$$\begin{cases} L = \frac{1}{2}\rho_a V_F^2 S C_L; \\ D = \frac{1}{2}\rho_a V_F^2 S C_D; \\ T = 550\, P\eta / V_F; \end{cases} \tag{3.64}$$

where

$$(3.65)\quad \begin{cases} C_L = \text{lift coefficient} \\ \quad = K \sin(\alpha + \alpha_o)\,; \\ C_D = A + \dfrac{C_L^2}{B}\,; \\ K = \dfrac{2\pi}{1 + 2/\mathcal{AR}}\,; \end{cases}$$

and

A, B = constants for given airplane,

$$B = \frac{\pi b^2}{S}\,;$$

S = wing area;

P = brake horsepower of engine: 1 h.p. = 550 ft.-lb./sec.;

ρ_a = air density;

η = propeller efficiency;

b = wing span;

$\mathcal{AR} = \dfrac{b^2}{S}$, aspect ratio.

In the computation, new constants are usually introduced into equations (3.64) which are defined by

$$(3.66)\quad \begin{cases} c_1 = \rho_a K S/2W\,; \\ c_2 = \rho_a A S/2W\,; \\ c_3 = \rho_a K^2 S/2BW\,; \\ c_4 = 550\, P\eta/W\,; \end{cases}$$

so that equations (3.64) take the form

$$(3.67)\quad \begin{cases} L = c_1 V_F^2 W \sin(\alpha + \alpha_o)\,; \\ D = [c_2 + c_3 \sin^2(\alpha + \alpha_o)]\, V_F^2 W\,; \\ T = c_4 W/V_F. \end{cases}$$

The constants c_i ($i = 1, 2, 3, 4$) may be determined from the fundamental performance equation

$$(3.68)\quad \frac{\sqrt{\rho}}{\lambda_t} = \frac{V_i^3}{\lambda_P} + \frac{\lambda_s}{V_i},$$

where

$\rho = \rho_a/\rho_o$ = relative air density;

$V_i = \sqrt{\rho}\, V_F$ = indicated airspeed;

$$\lambda_t = \frac{W}{550\,\eta P}\,;$$

$$\lambda_P = \frac{2W}{\rho_o A S}\,;$$

$$\lambda_s = \frac{2W}{\rho_o B S} = \frac{2W}{\rho_o \pi b^2}\,;$$

so that

$$(3.69)\quad \begin{cases} c_4 = 1/\lambda_t\,; \\ c_2 = \rho/\lambda_P\,; \\ c_1 = \rho_a K S/2W\,; \\ c_3 = c_1^2\, \lambda_s/\rho. \end{cases}$$

The description of the aircraft should supply the geometry of the airplane, its gross weight (W), the propeller efficiency (η), maximum engine brake power ($P_{max.}$) and the corresponding maximum level flight speed ($V_{F\,max.}$) for a certain altitude or density ratio ρ'. With this information, we compute

$$(3.70)\quad \lambda_{t\,min.} = \frac{W}{550\,\eta P_{max.}}\,;\ \lambda_s = \frac{2W}{\rho_o \pi b^2}\,;$$

$$V_{i\,max.} = \sqrt{\rho'}\, V_{F\,max.}\,.$$

The values obtained from (3.70) may now be inserted into equation (3.68) and this equation solved for λ_P which depends only upon the

geometry of the airplane and is therefore not affected by changes in ρ and V_F. With λ_P and λ_s determined, it is possible to consider λ_t for any speed at any altitude. Thus, if we choose a V_F and ρ, we can solve for λ_t (or $\frac{1}{\lambda_t}$) from equation (3.68).

The computation of the aircraft constants may be summarized into the following steps:

(1) Given: W, b, S, $\mathcal{AR}$, η, $P_{max.}$, $V_{Fmax.}$, and ρ'.

(2) Compute: λ_s, $V_{i\ max.}$, $\lambda_{t\ min.}$, λ_P, and K.

(3) Choose: V_F and ρ.

(4) Compute: V_i, $1/\lambda_t$, c_4, c_2, c_1, c_3; (use equations (3.69)).

3.10 Dimensionless Form

In any numerical computation dealing with a physical system it is convenient to express the equations in dimensionless form. This is usually accomplished by dividing each variable by a reference value of that variable. The system expressed by equations (3.55), (3.57), (3.58), and (3.59) may be reduced to a dimensionless form by the following transformations. Let

$$t^* = gt/V_{F_o};\ v = V_F/V_{F_o};\ u_B = V_B V_{F_o};\quad s = gr/V_{F_o}^2; \tag{3.71}$$

where

V_{F_o} = reference velocity (usually taken to be initial value of V_F)

and

g = acceleration of gravity

involve the same distance units.

If we further let

$$K_1 = c_1 V_{F_o}^2;\ K_2 = c_2 V_{F_o}^2;\ K_3 = c_3 V_{F_o}^2;\quad K_4 = c_4/V_{F_o}, \tag{3.72}$$

the system of equations takes on the following form:

$$\left\{\begin{aligned} \frac{dv}{dt^*} &= \sin\gamma + \frac{K_4}{v}\cos\alpha - K_2 v^2 - K_3 v^2 \sin^2(\alpha+\alpha_o)\ ; \\ \nu\frac{d\gamma}{dt^*} &= \cos\gamma - K_1 v^2 \sin(\alpha+\alpha_o) + \frac{K_4}{v}\sin\alpha\ ; \\ \frac{ds}{dt^*} &= -v\cos(\gamma-\theta) + u_B\cos\theta\ ; \\ \frac{d\theta}{dt^*} &= -\frac{1}{s}\left[v\sin(\gamma-\theta) + u_B\sin\theta\right]. \end{aligned}\right. \tag{3.73}$$

3.11 Examples

In order to illustrate the computation of an aerodynamic lead pursuit course in a vertical plane let us consider two specific examples:

Example 1. We begin with the following data; units in feet, pounds, seconds.

(1) Aircraft data:

W = 14655 lbs.

b = 42.833333 ft.

S = 334 square feet.

$\mathcal{AR}$ = 5.5.

α_o = .033743 radians.

g = 32.174 ft/sec^2.

η = .85

$V_{F\ max.}$ = 493 ft./sec.

$P_{max.}$ = 1550 H.P.

$V_{i\ max.}$ = 337.58668 ft./sec.

ρ' = .4689.

ρ_o = .002378

(2) Attack data:

$r_o = 6000$ ft.

$V_B = 300$ ft./sec.

$V_s = 2500$ ft./sec.

$\theta_o = 30° = .5236$ radians.

$\rho = .81$

$V_{T_o} = 500$ ft./sec.

The aircraft constants are computed from the formulas of section 3.9. In their evaluation it will be assumed that the change in ρ during the attack may be neglected. The computation yields

$\lambda_s = 2138.406710$

$\lambda_{t\ min.} = 2.022425 \times 10^{-2}$

$1/\lambda_P = 7.154248 \times 10^{-7}$

$K = 4.607670$

$\frac{KS}{2W} = .052506373$

$c_1 = 1.011367 \times 10^{-4}$

$c_2 = .579494 \times 10^{-6}$

$c_3 = 27.003672 \times 10^{-6}$

$K_1 = 25.284175$

$K_2 = .1448735$

$K_3 = 6.750918$

It is to be noted here that $c_4 = 1/\lambda_t$, which is computed from equation (3.68), is a function of V_i which in turn is a function of V_T. Thus, strictly, c_4 is not a constant as V_T changes according to equations (3.73). The variation of c_4, or more precisely K_4, may be computed by tabulating or graphing K_4 versus v for each initial condition. In the present example we have table 3.6.

Table 3.6

K_4/v for Example I

v	K_4/v	v	K_4/v	v	K_4/v	v	K_4/v
1.00	.155434	1.10	.184025	1.20	.215951	1.30	.251085
1.01	.158138	1.11	.187069	1.21	.219322	1.31	.254771
1.02	.160876	1.12	.190147	1.22	.222725	1.32	.258488
1.03	.163650	1.13	.193259	1.23	.226159	1.33	.262237
1.04	.166459	1.14	.196404	1.24	.229625	1.34	.266016
1.05	.169301	1.15	.199580	1.25	.233123	1.35	.269826
1.06	.172178	1.16	.202790	1.26	.236652	1.36	.273668
1.07	.175089	1.17	.206032	1.27	.240213	1.37	.277539
1.08	.178034	1.18	.209306	1.28	.243806	1.38	.281442
1.09	.181013	1.19	.212613	1.29	.247429	1.39	.285376

To determine the "natural" initial value of the angle of attack, we first determine the "natural" initial value of γ and obtain α from equation (3.62). Thus in the example we choose $\gamma_o = .56$, $\gamma_o = .48$, and $\gamma_o = .42$ and solve the system (3.73) for $0 \leq t^* \leq .10$. The values for γ are then plotted over this range of values for t^* and extrapolated back linearly to give the natural initial value $\gamma_o = .4850$. See figure 54.

988995 O - 52 - 7

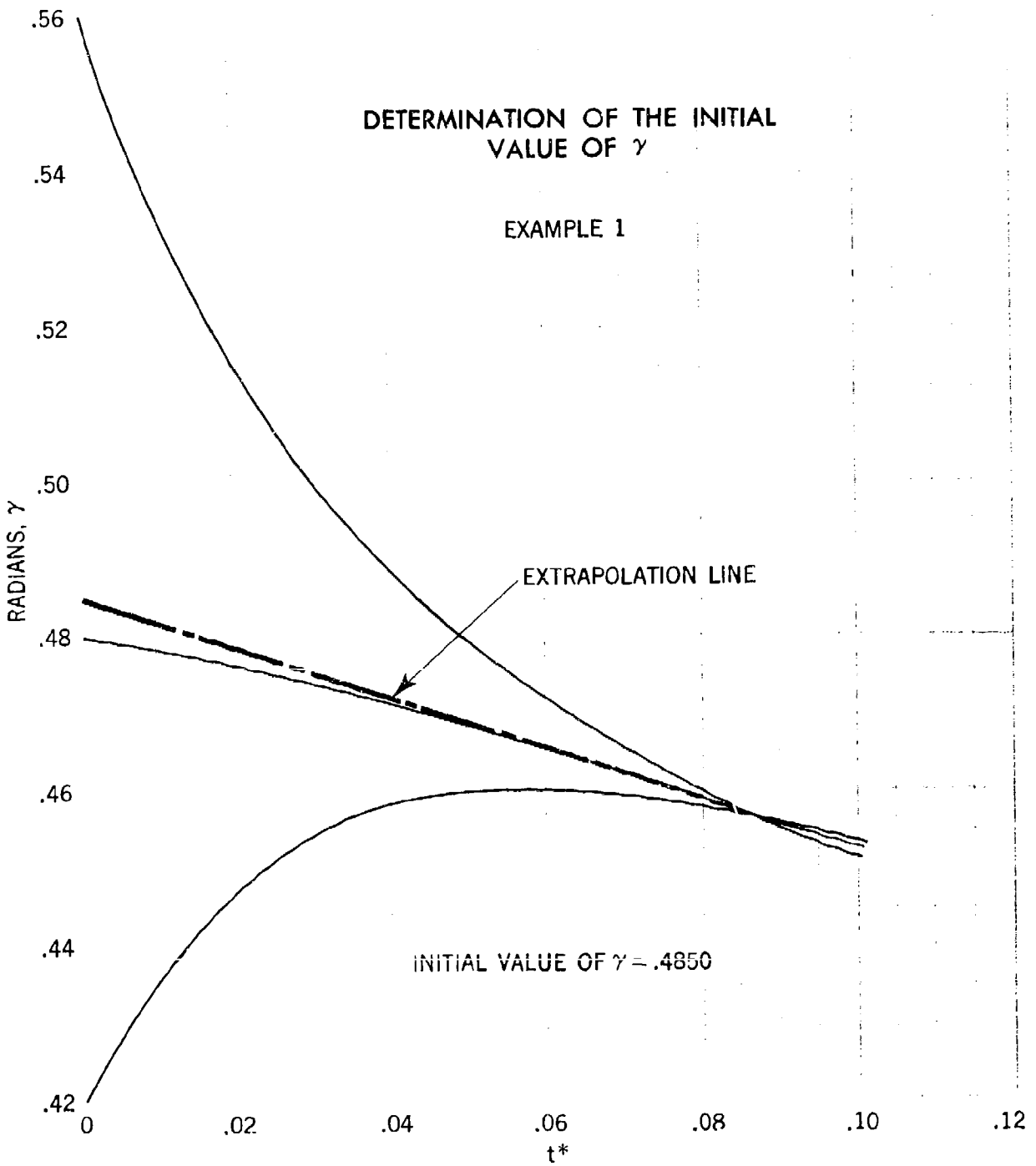

Figure 54. — Initial Value of γ — Example 1

The numerical solution of (3.73) can then be performed by the Runge-Kutta Method. The final values, obtained by this method, are tabulated in table 3.7.

Table 3.7

Example I

t^*	γ	θ	r	s	α	τ	x_F	z_F	x_B
0	.4850	.5236	1.	.772176	.0137	6000	−5196	3000	0
.1	.4525	.4898	1.044671	.722450	.0114	5613.6	−4489	2641	465.0
.2	.4199	.4563	1.086383	.699354	.0086	5201	−3736	2292	933.0
.3	.3879	.4228	1.125138	.613119	.0065	4764.1	−2947	1955	1398.0
.4	.3558	.3888	1.160913	.553983	.0048	4304.6	−2117	1632	1866
.5	.3235	.3544	1.193656	.492140	.0034	3824.1	−1255	1327	2331
.6	.2907	.3190	1.223297	.427945	.0024	3325.2	−361	1043	2796
.7	.2569	.2823	1.249721	.261641	.0017	2810	565	782.8	3264
.8	.2218	.2438	1.272776	.293454	.0014	2280.2	1516	540.4	3729
.9	.1843	.2023	1.292240	.223703	.0015	1738.2	2494	349.2	4197
1.0	.1431	.1559	1.307755	.152713	.0025	1186.6	3490	184.2	4662
1.1	.0944	.0995	1.318674	.082301	.0055	628.2	4502	62.4	5127

A coordinate system x, z was chosen such that $x_{B_0} = O$, $z_B = O$ and $x_B = V_B t$, $z_F = r \sin \theta$, $x_F = -r \cos \theta + x_B$. The space courses were then plotted and are shown in figure 55.

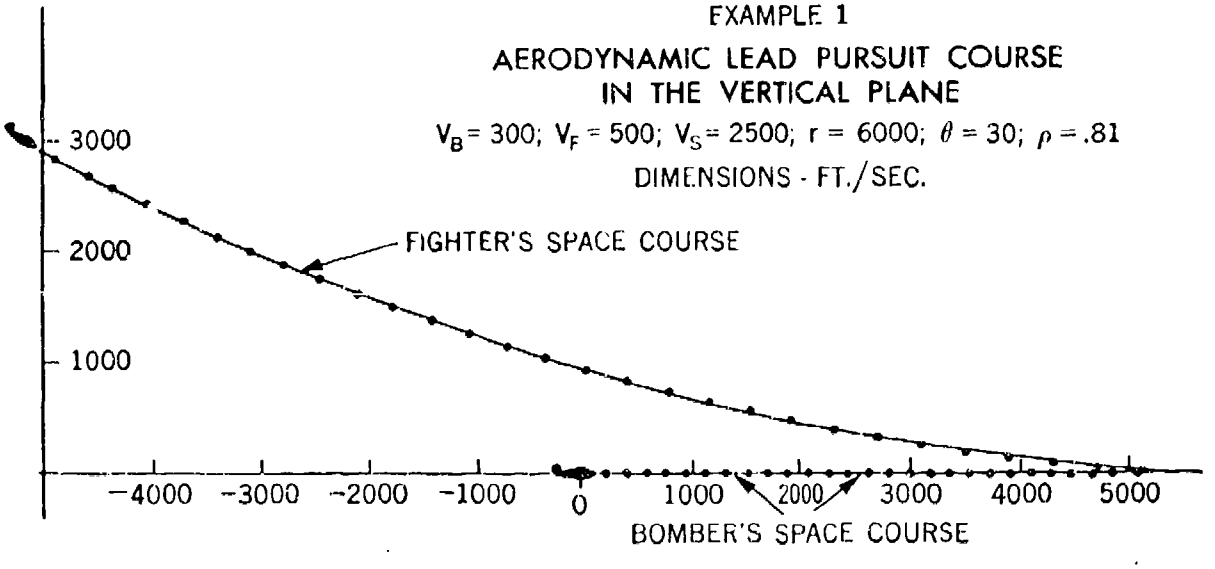

Figure 55. — Aerodynamic Lead Pursuit Course Example

Example 2. (Units in feet, pounds, seconds, radians.)

(1) Aircraft data:

W = 14,000 lbs.

b = 42

S = 315

$\mathcal{AR}$ = 5.6

η = .86

α_0 = .05

$P_{max.}$ = 1800 H.P.

$V_{T\,max}$ = 600 ft./sec.

ρ' = .347

ρ_0 = .002378

$V_{i\,max.}$ = 353.4402

ρ_a = .000825166

(2) Attack data:

r_0 = 4000 ft.

V_B = 360 ft./sec.

V_s = 2500 ft. sec.

ρ = .49

θ_0 = .8727 radians

V_{F_0} = 600 ft./sec.

(3) Computed constants:

λ_s = 2124.700332

$1/\lambda_{t\,min.}$ = 60.814286

K = 4.629716

$1/\lambda_P$ = 6.752215×10^{-7}

$\frac{KS}{2W}$ = .052084305

c_1 = 60.689674×10^{-6}

c_2 = 3.308585×10^{-7}

c_3 = 15.970967×10^{-6}

K_1 = 21.848283

K_2 = .119109

K_3 = 5.749548

The same calculations which were performed in Example 1 were carried out and are shown in tables 3.8 and 3.9. The values were plotted and are shown in figure 56 and figure 57.

Table 3.8

K_4/v for Example 2

v	K_4/v	v	K_4/v	v	K_4/v	v	K_4/v
1.00	.131154	1.10	.154076	1.20	.179882	1.30	.208422
1.01	.133311	1.11	.156530	1.21	.182614	1.31	.211422
1.02	.135198	1.12	.159012	1.22	.185374	1.32	.214448
1.03	.137716	1.13	.161523	1.23	.188162	1.33	.217502
1.04	.139964	1.14	.164062	1.24	.190976	1.34	.220580
1.05	.142243	1.15	.166630	1.25	.193817	1.35	.223685
1.06	.144551	1.16	.169224	1.26	.196684	1.36	.226816
1.07	.146888	1.17	.171847	1.27	.199579	1.37	.229973
1.08	.149256	1.18	.174497	1.28	.202500	1.38	.233156
1.09	.151651	1.19	.177176	1.29	.205447	1.39	.236365

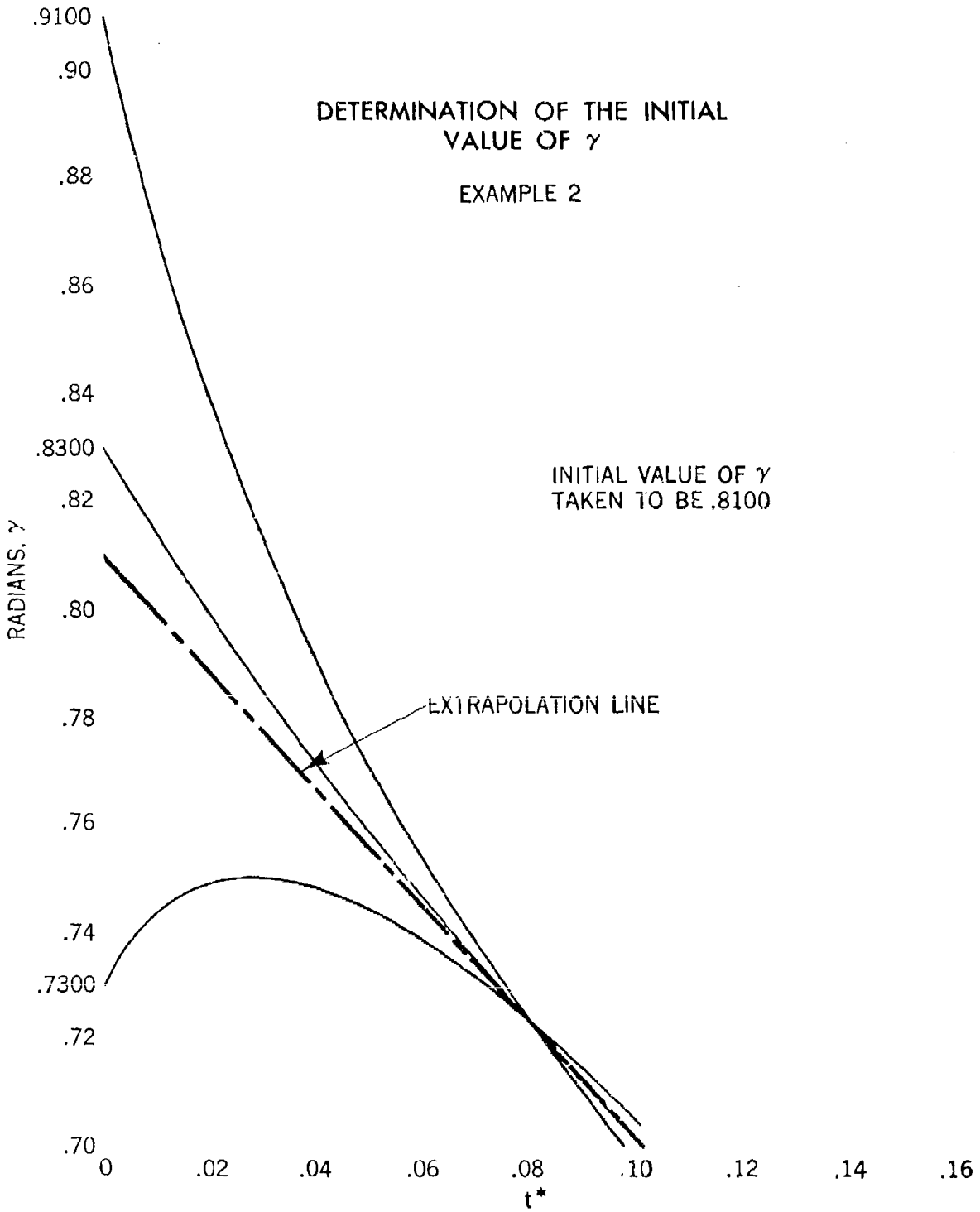

Figure 56. — Initial Value of γ — Example 2

Table 3.9

Example 2

t^*	γ	θ	v	s	α	r	x_F	z_F	x_B
0	.8100	.8727	1.	.357489	.0327	4000.	−2571.0	3064.3	0
.02	.7880	.8504	1.013790	.345182	.0308	3862.3	−2414.7	2902.7	133.2
.04	.7664	.8278	1.027280	.332827	.0296	3724.1	−2249.3	2742.6	270.
.06	.7448	.8049	1.040448	.320406	.0288	3585.1	−2081.9	2584.0	403.2
.08	.7232	.7816	1.053288	.307923	.0284	3445.4	−1909.1	2427.0	536.4
.10	.7014	.7580	1.065785	.295383	.0280	3305.1	−1730.6	2272.2	669.6
.12	.6794	.7339	1.077930	.282791	.0279	3164.2	−1543.2	2119.3	806.4
.14	.6571	.7094	1.089709	.270153	.0279	3022.8	−1354.0	1969.0	939.6
.16	.6345	.6844	1.101108	.257474	.0280	2880.9	−1159.3	1821.3	1072.8
.18	.6115	.6589	1.112116	.244760	.0282	2738.7	− 955.8	1676.8	1209.6
.20	.5882	.6329	1.122719	.232017	.0285	2596.1	− 750.5	1535.6	1342.8
.22	.5644	.6063	1.132903	.219250	.0288	2453.2	− 539.9	1397.9	1476.
.24	.5402	.5791	1.142653	.206465	.0293	2310.2	− 320.7	1264.3	1612.8
.26	.5155	.5513	1.151953	.193667	.0298	2167.2	− 99.9	1135.1	1746.
.28	.4903	.5227	1.160787	.180862	.0305	2023.7	125.7	1010.3	1879.2
.30	.4645	.4933	1.169134	.168057	.0313	1880.4	356.2	890.4	2012.4
.32	.4381	.4630	1.176974	.155257	.0324	1737.2	594.9	775.9	2149.2
.34	.4108	.4317	1.184281	.142468	.0334	1594.1	834.5	667.0	2282.4
.36	.3829	.3994	1.191037	.129696	.0348	1451.2	1078.6	564.3	2415.6
.38	.3540	.3658	1.197209	.116946	.0363	1308.5	1330.5	468.0	2552.4
.40	.3241	.3308	1.202764	.104225	.0382	1166.2	1582.6	378.8	2685.6
.42	.2931	.2940	1.207675	.091538	.0406	1024.2	1838.5	296.8	2818.8
.44	.2606	.2551	1.211887	.078890	.0434	882.7	2101.5	222.7	2955.6
.46	.2264	.2136	1.215344	.066288	.0471	741.7	2364.0	157.2	3088.8
.48	.1899	.1686	1.217966	.053728	.0517	601.2	2629.3	100.9	3222.
.50	.1506	.1186	1.219648	.041233	.0584	461.4	2897.0	54.6	3355.2

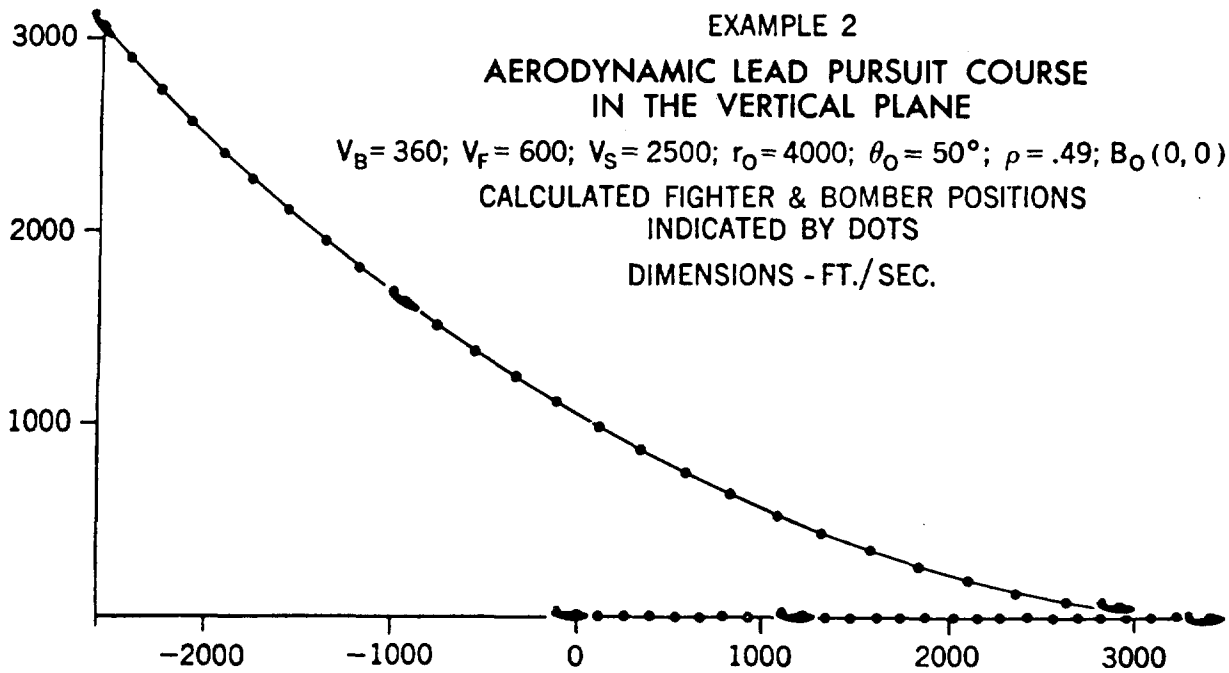

Figure 57. — Aerodynamic Lead Pursuit Course Example

3.12 The Three-Dimensional Equations

The complete derivation of the equations in the case of the three-dimensional aerodynamic lead pursuit course is rather complicated and will not be presented in this book. The form of the equations, of course, depends upon the coordinate system which is chosen. The most convenient set of equations is that which refers to the rectilinear trajectory traversed in space by the projectile from the fighter to the impact point. Let us adopt the following notation:

R = projectile air range.

A = azimuth angle of the projectile's rectilinear trajectory.

E = elevation angle of the projectile's rectilinear trajectory measured from the horizontal plane through the bomber's position.

α = angle of attack of the trajectory.
= angle between the direction of motion of the fighter and the trajectory at the time of departure.

β = the bank angle of the fighter about the projectile path.

= the angle from that perpendicular to the trajectory that lies in the vertical plane to the perpendicular to the trajectory that lies in the fighter's plane of symmetry.

τ = angle-off of the sight line from the bomber's direction of motion.

τ_B = angle-off of the projectile from the bomber's direction of motion.

A typical situation is shown in figure 58.

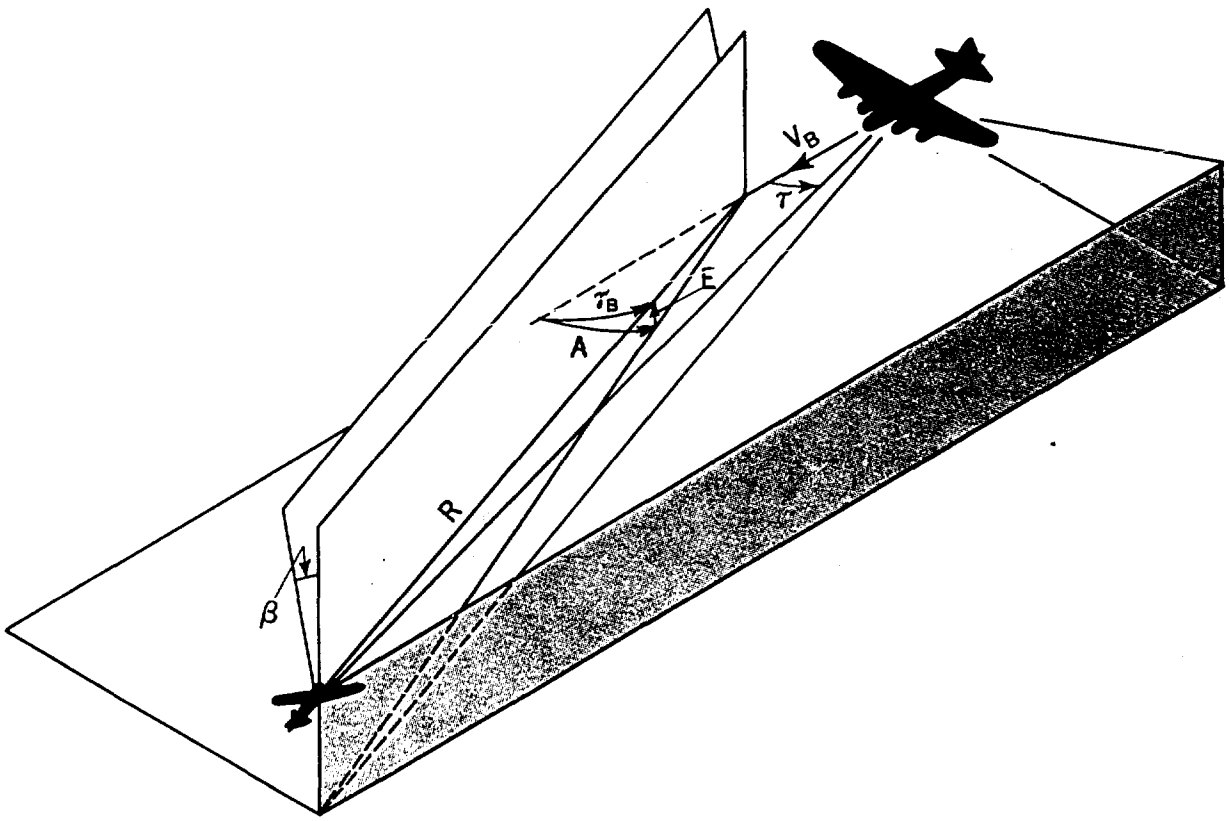

Figure 58. — A Three-dimensional Situation

The tangential equation is obtained by summing the forces along the direction of flight

$$(3.74)\quad \frac{W}{g}\frac{dV_F}{dt} = W\,(\cos\alpha \sin E + \sin\alpha \cos E \cos\beta) + T\cos\alpha_1 - D$$

where α_1 is the angle from the thrust axis to the aircraft's direction of flight. This angle, α_1, is a function of α and any constant offset of the gun bore axis from the thrust axis. There are two equations obtained by taking components in appropriate directions, normal to the direction of flight, which express the rate of change of the angles A and E. Thus,

$$(3.75)\quad -\frac{W}{g}V_F\left(\sin\beta\cos E\frac{dA}{dt} + \frac{d\alpha}{dt} + \cos\beta\frac{dE}{dt}\right) = L + T\sin\alpha_1 - W\,(\cos\alpha\cos E\cos\beta - \sin\alpha\sin E)$$

and

$$(3.76)\quad -\frac{W}{g}V_F\left[(\sin E - \cos\alpha\cos E\cos\beta)\frac{dA}{dt} + \cos\alpha\sin\beta\frac{dE}{dt} - \sin\alpha\frac{d\beta}{dt}\right] = W\sin\beta\cos E\,.$$

There exist also three kinematic equations. The impact point is the point which is being pursued. Since the distance from the bomber to this impact point is $V_B t_f$, where t_f is the projectile's time of flight over R, it follows that the velocity of the impact point is $V_B + V_B\dot{t}_f$. Thus, the range rate equation is given by

$$(3.77)\quad \frac{dR}{dt} = -V_F\cos\alpha - V_B\,(1+\dot{t}_f)\cos A\cos E\,.$$

The rate of change of azimuth and elevation are obtained by making projections normal to R. The equations are

$$(3.78)\quad \frac{dA}{dt} = -\frac{1}{R\cos\theta}\left[V_F\sin\alpha\sin\beta - V_B\,(1+\dot{t}_f)\sin A\right]$$

and

$$(3.79)\quad \frac{dE}{dt} = -\frac{1}{R}\left[V_F\sin\alpha\cos\beta - V_B\,(1+\dot{t}_f)\cos A\sin E\right]$$

Equations (3.74) to (3.79) comprise a system of non-linear differential equations which may be solved for the variables V_F, R, A, E, β, α. Ballistic considerations must, of course, furnish t_f and $\dot{t}_f$.

In this discussion it has been assumed that the fighter pilot flies with no sideslip. If sideslip is introduced, we have more unknowns than equations and a family of solutions results rather than a unique curve. It also has been assumed that the projectile's gravity drop may be superimposed upon the problem, that the bomber is flying straight and level at a constant speed and that the fighter's throttle setting is left unchanged. Variation in these assumptions must be introduced externally.

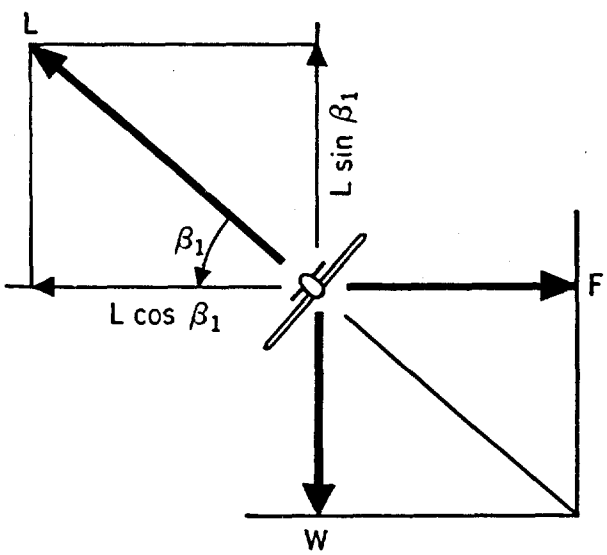

Figure 59. — Force System

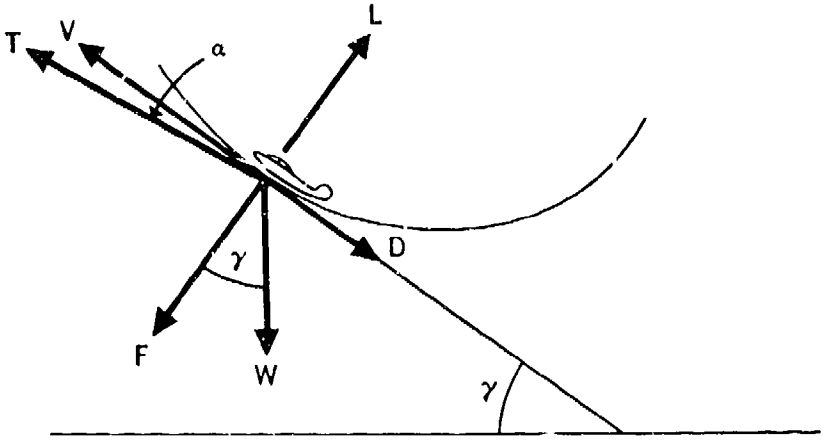

Figure 60. — Force System

3.13 Minimum Radius of Turn

The aerodynamic restrictions on an aircraft may be such that the aircraft cannot fly a pursuit course. In order to determine a criterion for this we may derive a formula for the minimum radius of turn. Let us consider the horizontal and vertical planes separately.

Let us consider the airplane to be a body of weight W which is kept in motion in a horizontal circle by a force of L pounds whose vertical component, $L \sin \beta_1$, is equal and opposite to W and whose horizontal component, $L \cos \beta_1$ is equal and opposite to the centrifugal force, F, exerted by this motion; where β_1 is the inclination of F to the horizontal. See figure 59. The airplane is then turning in a horizontal plane without any loss in altitude. Thus,

$$(L \sin \beta_1)^2 + (L \cos \beta_1)^2 = W^2 + F^2$$

or,

$$(3.80) \quad L^2 = W^2 + F^2$$

The centrifugal force may be expressed in terms of the radius of curvature R by the following formula:

$$(3.81) \quad F = \frac{WV^2}{gR}.$$

Let us further define the load factor, η,* to be

$$(3.82) \quad \eta = \frac{L}{W} \quad .$$

If we substitute the last two equations into equation (3.80) we may solve for the radius of turn

$$(3.83) \quad R = \frac{V^2}{g\sqrt{\eta^2 - 1}} \quad .$$

In the vertical plane, it is necessary to include the angle of climb, γ. From figure 60 we have, by summing the forces parallel to the lift,

$$(3.84) \quad L = F + W \cos \gamma + T \sin \alpha.$$

If we neglect the angle of attack, α, the radius is then given by

$$(3.85) \quad R = \frac{V^2}{g(\eta - \cos \gamma)} \quad .$$

For equations (3.83) and (3.85) it is clear that the radius of turn capable by the aircraft is a function of speed and the load factor, which in turn is a function of speed. The maximum load factor (given in "gees") is obtained from

*Do not confuse with propeller efficiency.

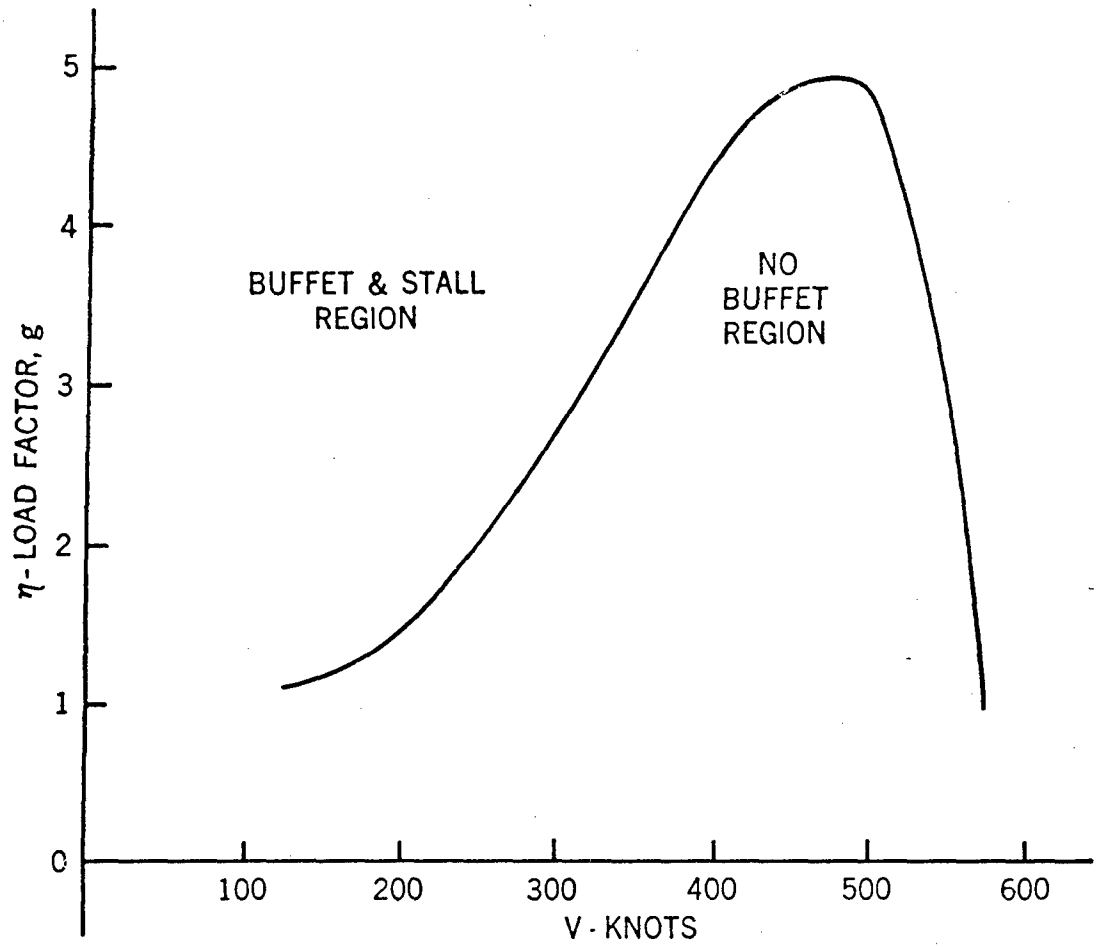

Figure 61. — Buffet Region

maximum lift and when plotted against an increasing speed will define a buffet and stall region in which the airplane cannot fly. A typical curve for modern aircraft is shown in figure 61.

The minimum radius of turn occurs at the maximum value of the load factor and a curve corresponding to figure 61 may be plotted for the minimum radius in either the vertical or horizontal plane. Figure 62 pictures the situation in the horizontal plane.

The following conclusions may be drawn:

(1) The load factor falls off rapidly as the speed increases beyond the peak for the maximum value of the load factor.

(2) As the speed increases, the minimum radius of turn increases.

Consequently, at very high speeds it becomes increasingly difficult to fly anything but a tail pursuit; that is, a pursuit course initiated well toward the stern of the pursued aircraft.

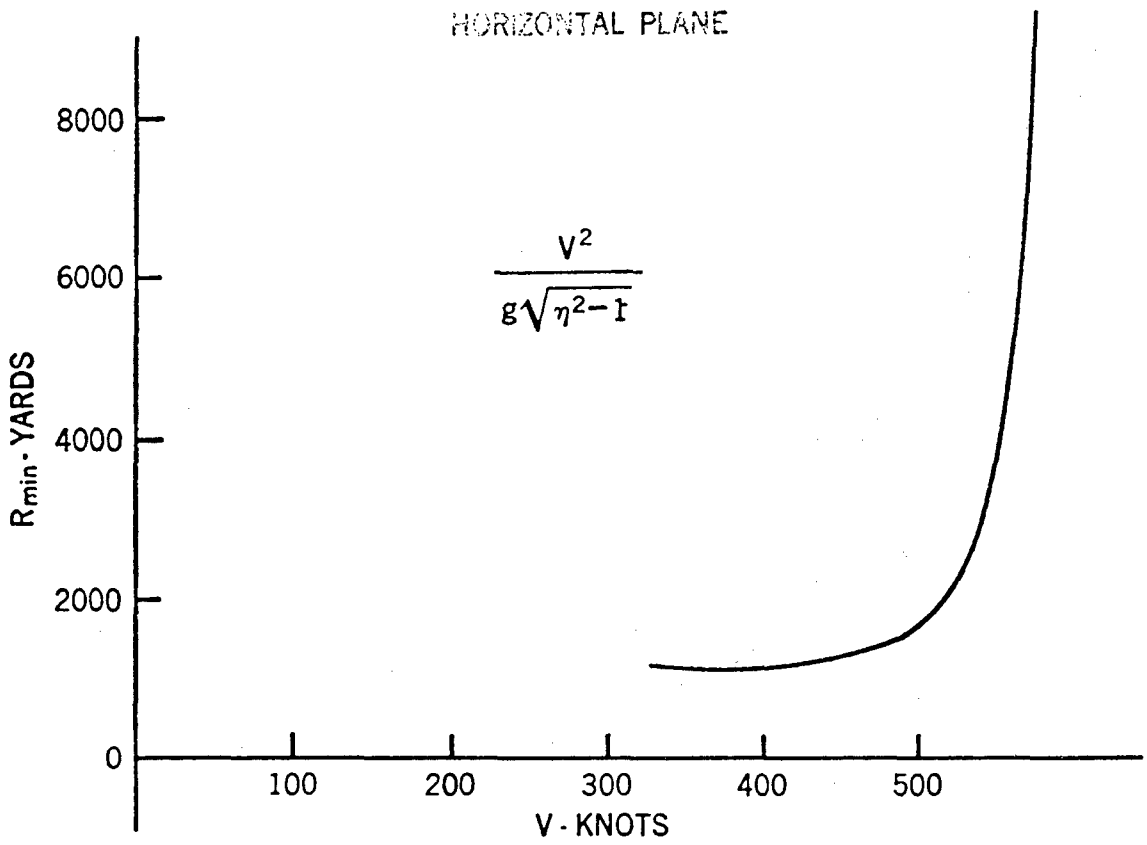

Figure 62. — Minimum Radius of Turn

3.14 Collision or Interception Courses

In order to avoid the high gees which arise in some pursuit courses, other types of attack must be adopted. We shall discuss one type which may be employed by a fighter with fixed guns. The principle of the attack is to fly in a straight line toward a point well in advance of the target. This point may be a collision point; that is, the point where the attacker would intercept the target. The course is, therefore, called a collision or interception course. Actually the point of aim should not be the point of collision between the two aircraft unless it is desired to destroy both aircraft. The point should be the collision point between the target and the projectile that the attacker is firing. This, of course, means that the attacker can fire only one salvo and, consequently, the projectile must be a large shell or a salvo of rockets.

The general problem may be visualized by referring to figure 63. The bomber is the target and flies a straight line path BH at constant speed V_B. The fighter is the attacker and flies the straight line path FH at constant speed V_F.

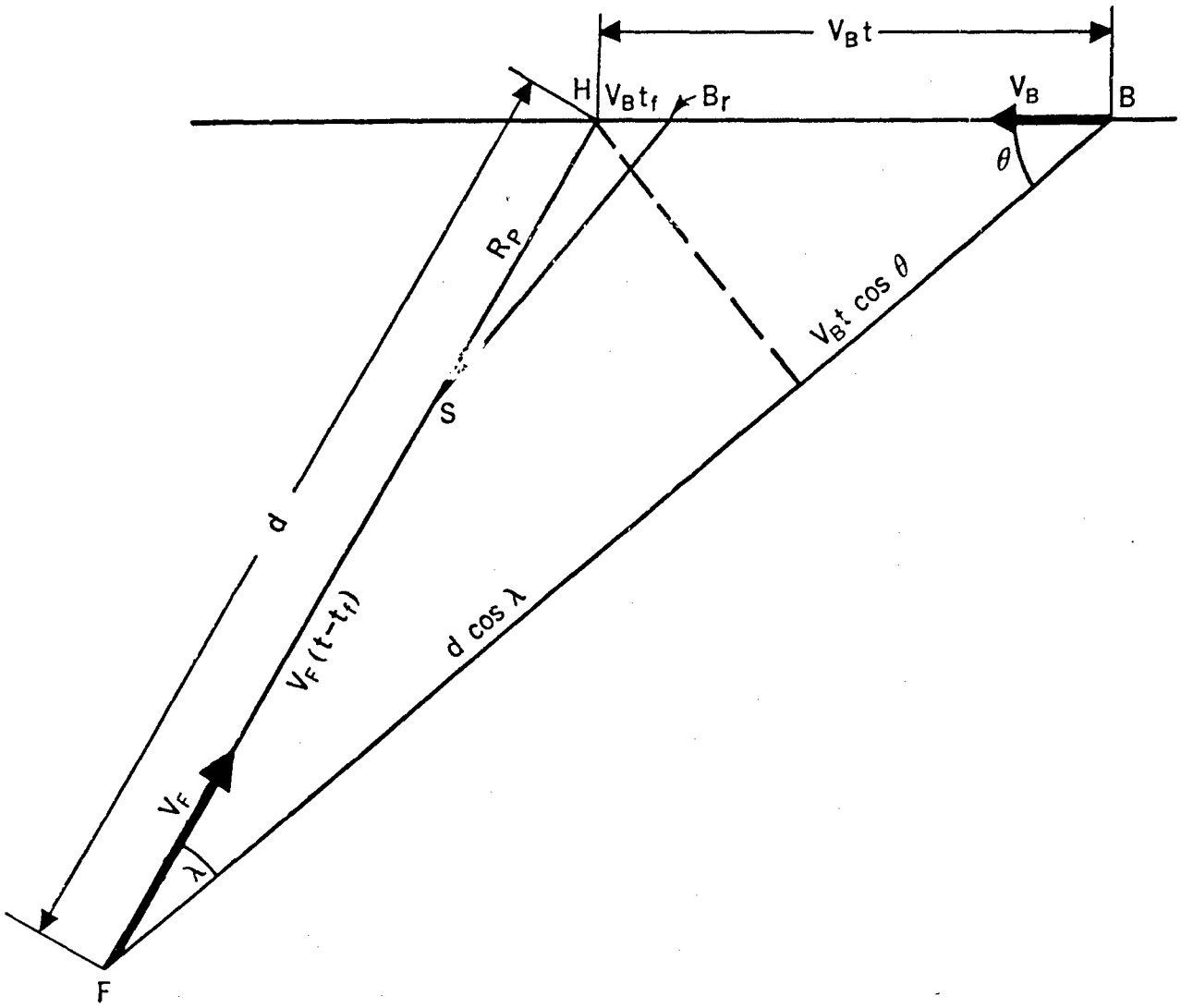

Figure 63. — Collision Course

Let S be the point of release of the salvo and let us define additional symbols as follows:

R_P = projectile range; distance from release point to impact point H.

t_f = time of flight of projectile from S to H.

t = time of flight of bomber from B to H.

r = present range, BF.

d = distance from F to H.

τ = angle-off of bomber from fighter; angle from V_F to r.

θ = angle from V_B to r.

λ = correct angle τ to insure a hit for a predetermined projectile range R.

From figure 63, it is easy to see that the following relations hold:

(3.86) $d \sin\lambda = V_B t \sin\theta$;

(3.87) $(V_B t)^2 = d^2 + r^2 - 2\,rd \cos\lambda$;

(3.88) $r = d\cos\lambda + V_B t \cos\theta$;

(3.89) $d = V_F\,(t - t_f) + R_P$;

(3.90) $-\dot{r} = V_F \cos\lambda + V_B \cos\theta$;

(3.91) $r\omega = V_B \sin\theta - V_F \sin\lambda$.

If the projectile range, R_P, has been predetermined, the type of ammunition determines t_f

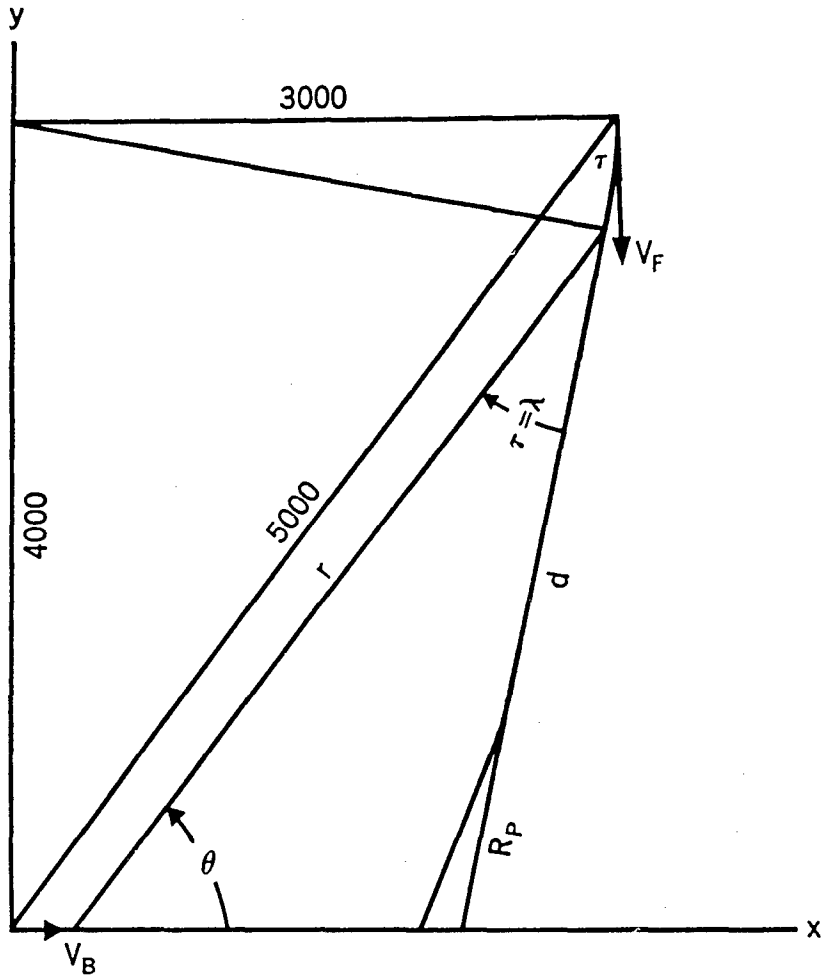

Figure 64. — Collision Course Example

and the problem is to get on the straight line course FH for which equations (3.86) to (3.91) hold. The fighter thus flies a variable course which has τ as the angle-off of the bomber and continues to vary his course until $\tau = \lambda$, after which he flies a straight line FH. It is then a mere matter of computing the release time for the projectile.

The fighter's inputs to his sighting system are τ, r, ω, V_F, $\dot{r}$, R_P, and t_f. The unknown quantities are θ, t, V_B, and d. The correct angle λ is computed from the inputs by means of

$$(3.92) \qquad \sin\lambda = \frac{r\omega}{\dot{r}}\left[\cos\lambda - \frac{r}{R_P - V_F t_f}\right].$$

Equation (3.92) is obtained by eliminating d, t, V_B and θ from equations (3.86) to (3.91).

The computed angle λ is then continuously compared with the measured angle τ until they are identical. The time t is then computed by means of

$$(3.93) \qquad t = \frac{1}{\dot{r}}\left[(R_P - V_F t_f)\cos\lambda - r\right]$$

and the release time is $t - t_f$.

Figure 64 shows a calculated example for the conditions

$V_B = 200$ yds./sec.
$V_F = 300$ yds./sec.
$r_o = 5000$ yds.
$R_P = 1000$ yds.
$t_f = 1$ sec.
$\tau = \arcsin 3/5$

The maneuvering path of the fighter is a circle of radius 3,000 yds. with center at (0,4000).

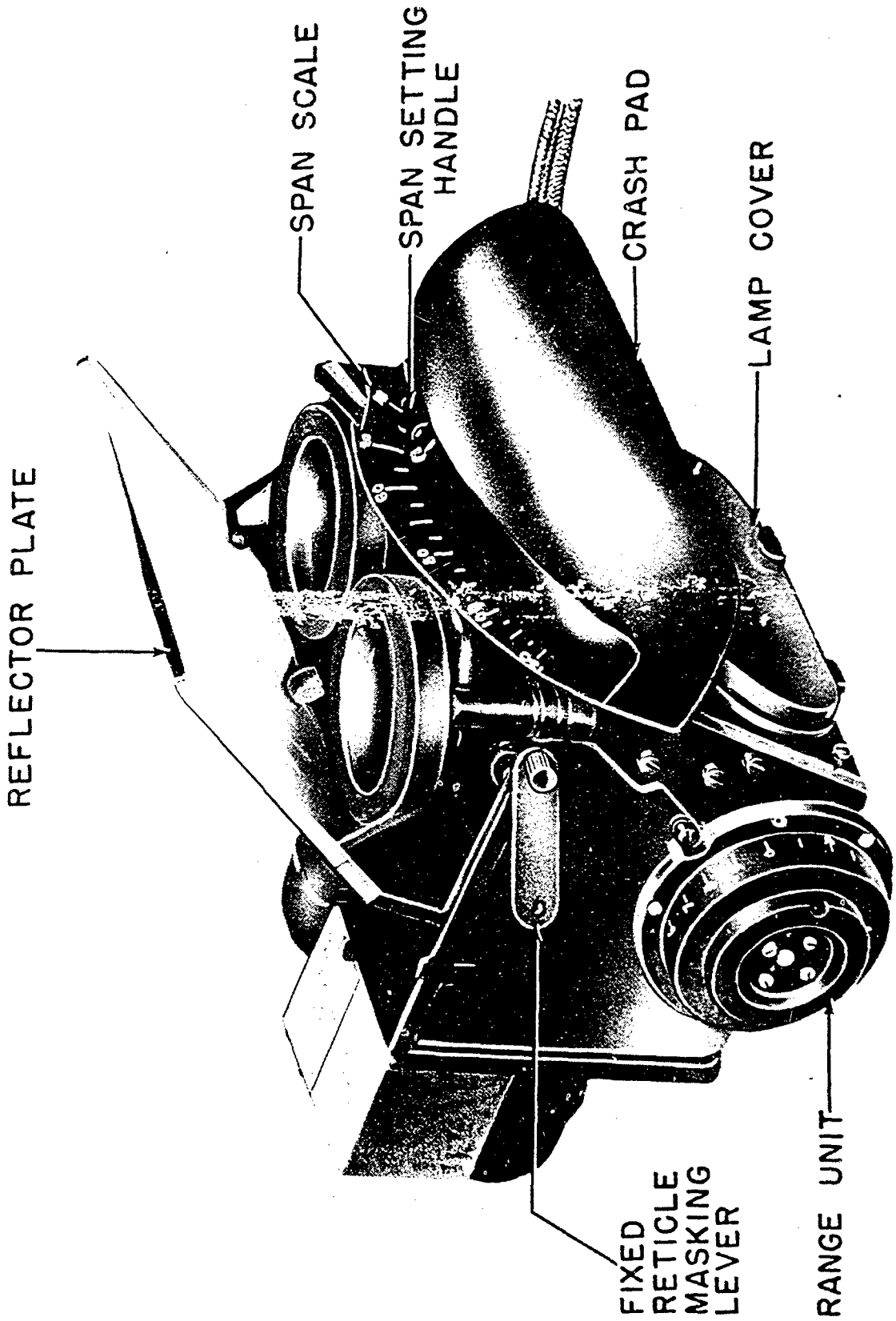

Figure 65. — Lead Computing Sight

Chapter 4

THEORY OF LEAD COMPUTING SIGHTS

4.1 Introduction

Reference to chapter 2, equations (2.9) and (2.15) in particular, indicates two distinct methods of calculating leads. One method, as exemplified by equation (2.9), expresses total lead in terms of: (1) bomber speed (V_G); (2) target speed (V_T); (3) angle-off of the target (τ); (4) approach angle of the target (α); (5) muzzle velocity (V_o); and, (6) the bullet slow-down factor (q). Essentially, this method, as has already been pointed out, breaks up the total lead into a correction for ownspeed and a correction for target motion. A sight which computes leads in this manner is spoken of as a vector-rate sight. Equation (2.15), on the other hand, furnishes total lead by decomposing it into a lead arising from the relative motion of the aircrafts, the so-called kinematic lead, and a ballistic lead. The purpose of this chapter is to consider the theory — not the mechanics — underlying devices which work on the basis of this second method. Hence, throughout this chapter, by a lead computing sight we shall mean one which computes kinematic lead from the angular velocity with which the gunner tracks the target and from the range which the gunner determines, and then combines the result with an appropriate ballistic deflection.

4.2 Essential Elements of a Fire Control System

Since a lead computing sight is but one type of fire control mechanism, it would be well to list the essential features of a fire control system. In general, a fire control system provides:

(1) A line of sight by means of a radar antenna or a telescope or other optical gear, mounted so that it can move as the target is tracked;

(2) A computing unit which determines the lead to be used;

(3) A gun;

(4) A system of control which keeps the appropriate angular distance between gun and line of sight.

A fire control system is classified as local or remote according to whether the means of controlling the gun is actually located at the gun or is physically separated from it. In the remote case, suitable electrical or mechanical interconnections must be provided to link the location of the sighting system, the gun, and the computing unit; any or all of which may be in separate locations, depending on each specific installation.

4.3 Disturbed and Director Systems

Fire control systems may be further classified according to the controls by which the gunner constrains the line of sight to track the target. This classification amounts essentially to describing sights as belonging either to director systems or disturbed systems. In a director system, the gunner has immediate control over the angular position of the line of sight by directly positioning the appropriate optical gear. The information gained from this positioning then goes, via electrical or mechanical means, to the computer which uses it to determine the proper lead and transmits this lead to the control system which in turn positions the gun. In modern fire control systems employing servomechanisms (automatic control devices), the director system is often of the remote control type wherein the gunner is replaced by a radar tracking mechanism which positions the line of sight automatically. The chain of events outlined here is indicated by figure 66 which characterizes a director system.

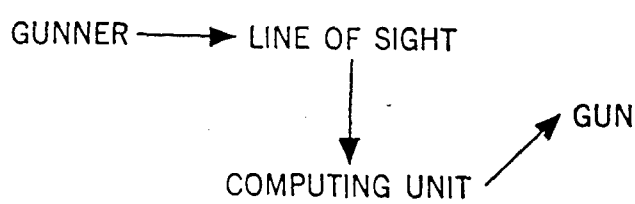

Figure 66. — Director System

In a disturbed system, the gunner, either manually or with the aid of a power mechanism, exercises immediate control over the position of the gun. Information giving the instantaneous angular position and angular rate of the gun is then fed into the computer which uses it to compute the proper lead. This computer output then actuates a control mechanism which drives the line of sight into tracking position to effect the required lead angle. The corresponding diagram for this is shown in figure 67.

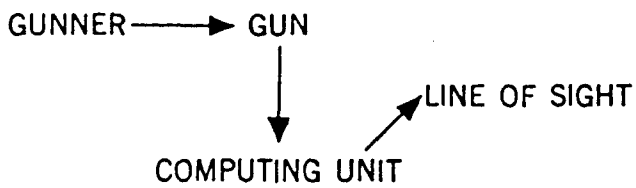

Figure 67. — Disturbed System

The important thing to notice here is that the gunner has only an indirect control over the line of sight. The name "disturbed sight" arises from the fact that a given motion of the gun will in general produce a different motion of the line of sight, a situation that is often confusing to the gunner.

For illustrative purposes we shall consider a particular version of a disturbed sight known as a disturbed reticle sight. This sight, the basic physics of which will be taken up in the next chapter, provides a line of sight by means of an illuminated reticle which is reflected, by a movable mirror system within the sight head, onto a viewing glass fixed on the gun. The gunner moves the gun so as to keep the reticle image centered on the target and in so doing automatically displaces the line of sight from the direction of the gun bore by the proper lead. The range to the target, a continuously varying quantity, is obtained by varying the diameter of the reticle image to agree with the wing span of the target, which in effect makes range a function of reticle image diameter. Range computed in this fashion is referred to as stadiametric ranging.

Whereas sights based on the director principle make the problem of tracking easier for the gunner, disturbed sights are, on the other hand, smaller, lighter, and simpler mechanically. This last follows from the fact that a low-powered mechanism can position an optical line of sight with respect to a gun, while a much higher power level is needed for positioning the gun with respect to the line of sight.

In this chapter, we shall be concerned primarily with lead computing sights which are disturbed reticle; local control systems although many of the concepts involved in the analysis, such as operational stability, transient behavior, smoothing of rates, etc., are applicable to more general situations.

4.4 Types of Tracking Controls and Their Peculiarities

To control the angular position of a telescope (or gun or turret) the gunner turns a handwheel (or a "pistolgrip"). If we denote the angular coordinate of the telescope by θ and the angle through which the handwheel has been turned by η, then we may classify the tracking controls by the manner in which the control mechanism relates the variables θ and η. This classification yields essentially three types of tracking controls:

(a) Direct Tracking. Here the angle through which the telescope moves is directly proportional to the angle through which the handwheel has been turned. The corresponding relation between θ and η is $\theta = A\,\eta$, (A = const.).

(b) Velocity Tracking. The velocity with which the telescope is moving at any time is proportional to the angle through which the handwheel has been moved. In symbols, $\dot{\theta} = B\,\eta$, (B = const.). Tracking of this type can be effected by having the telescope driven by a variable speed motor, the speed of the latter being regulated by positioning the handwheel. Velocity tracking enables the gunner to slew the telescope quickly through a large angle onto a new target merely by giving the handwheel a larger displacement.

(c) Aided Tracking. This combines (a) and (b) in that any displacement of the handwheel not only positions the telescope but also gives it a velocity. The equation of control may be written as

$$\dot{\theta} = A\dot{\eta} + B\eta. \tag{4.1}$$

From (a) and (b) it follows that for unit displacement of the handwheel, equation (4.1) effects a displacement of θ by A units and also changes its velocity by B units.

The ratio A/B, measured in units of time, is the ratio of direct to velocity control. By varying this ratio, the velocity control can be made more or less important relative to the direct control of the telescope.

Investigation has shown that aided tracking gives, in general, more satisfactory results than either direct or velocity tracking. Why this should be so may be seen from the following facts:

(1) A gunner can track a target whose angular velocity is constant merely by keeping his handwheel fixed, while with direct tracking the handwheel must be moved continually.

(2) For slowly changing target velocity, the gunner can correct for any angular distance he has fallen behind by putting in an additional displacement of the handwheel. This has the effect of simultaneously changing the position of the telescope and increasing its angular rate. By the time he has fallen behind again, all that is needed is another slight increment in the position of the handwheel.

(3) Aided tracking helps the gunner to continue tracking through a region in which the target is temporarily not visible.

(4) Experience shows that aided tracking is, in general, more "stable" than velocity tracking in that there is less tendency for the gunner to "hunt" with the controls.

4.5 Smoothing of Input Data

In order to predict the future position of a target, the computing unit of a sight must have as inputs coordinates of the target's present position, say the present range r and the present angle-off τ. In addition the present target rates, $\dot{r}$ and $\dot{\tau}$ also must be known in order to have information concerning past target behavior. The quantities τ, $\dot{\tau}$ and r, $\dot{r}$ are obtained by the gunner's tracking and ranging of the target. The values of r obtained by stadiametric ranging are generally poor and jumpy so that no usuable values of $\dot{r}$ can be obtained in this manner. Present day radar tracking is much more reliable.

The process of tracking furnishes the sight with continuous values of the telescope's angle-off, given say, by the function $\sigma(t)$. If the tracking is perfect, then at all times t we have $\sigma(t) \equiv \tau(t)$. Needless to say, tracking is never perfect and is always attended by an irregularly oscillating tracking error, $\sigma - \tau$. Thus, if $\sigma(t)$ is mechanically or electrically differentiated to give $\dot{\sigma}(t)$, the resulting rate will differ from the desired target rate by the derivative of $\sigma - \tau$. Since this may be a marked difference, it is advisable, before using the raw data $\dot{\sigma}(t)$, to subject it to a suitable smoothing or averaging process.

We shall show that the solution $x = x(t)$ of the first order linear differential equation

$$k\dot{x} + x = f(t), \ (x = x_o, t = t_o) \tag{4.2}$$

where k is a positive constant, is, in a certain sense, an averaged value of the input function $f(t)$. A computing unit whose input is $f(t)$ and which operates mechanically or electrically to produce an output $x(t)$ according to (4.2), automatically yields, then, smoothed values of the input. The equation (4.2) may be achieved in practice by a simple resistance-capacity or a resistance-inductance network with circuit time-constant equal to k.

Solving (4.2) by the appropriate formal procedure*, we find

*See "Elementary Differential Equations" by L. M. Kells, (McGraw-Hill), pp. 49-50.

988995 O - 52 - 8

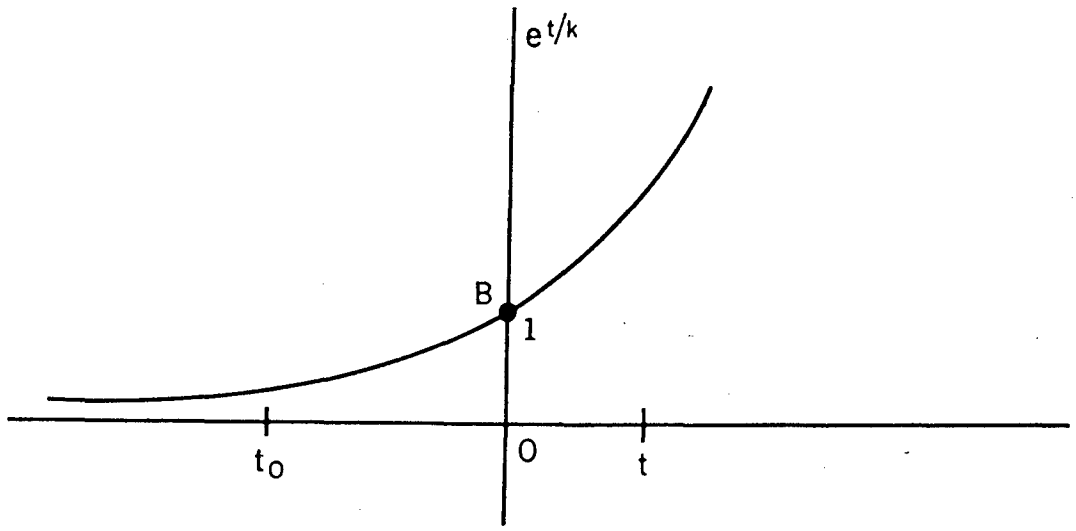

Figure 68. — Graph of the Weight Function $e^{t/k}$

$$(4.3) \quad x = x_o e^{-\left(\frac{t-t_o}{k}\right)} + \frac{1}{ke^{t/k}} \int_{t_o}^{t} e^{t/k} f(t)\,dt\,.$$

If we think of the term $e^{t/k}$ as a weight function, then the weighted average of $f(t)$ is

$$(4.4) \quad \frac{1}{k\left(e^{t/k} - e^{t_o/k}\right)} \int_{t_o}^{t} e^{t/k} f(t)\,dt = \bar{f}(t)$$

all of which suggests that we rewrite (4.3) in the equivalent form

$$(4.5) \quad x = x_o e^{-\left(\frac{t-t_o}{k}\right)} + \frac{1 - e^{-\left(\frac{t-t_o}{k}\right)}}{k\left(e^{t/k} - e^{t_o/k}\right)} \int_{t_o}^{t} e^{t/k} f(t)\,dt\,,$$

or what amounts to the same thing,

$$(4.6) \quad x = \bar{f}(t) + e^{-\left(\frac{t-t_o}{k}\right)} [x_o - \bar{f}(t)]\,.$$

The second term in the right member of (4.6) usually diminishes rapidly with increasing time and for this reason is spoken of as a transient. The time interval required for this transient to diminish to $\frac{1}{e}$ times its initial value is called the time constant of the circuit and is evidently equal to k. From (4.6) we see that, for a time interval $t - t_o$ which is large compared to k, the solution $x(t)$ is approximately the weighted average $\bar{f}(t)$ of the input $f(t)$. It is in this sense that the output $x(t)$ is a "smoothed" value of the input $f(t)$.

The time t being the present, (4.4) shows that $\bar{f}(t)$ is an averaged value obtained by averaging $f(t)$ over past values beginning with $f(t_o)$. The graph of the weight function $e^{t/k}$ has the form shown in figure 68. As k is varied,

there is obtained a family of curves all passing through the point $B(O, 1)$. Passing from left to right along these curves we see that for small k the curves rise more steeply through B than for large k, the measure of this steepness at B being in fact $1/k$. Hence, if we wish to weight recent values of $f(t)$ more heavily than earlier values, it suffices to choose a weighting curve that rises rapidly; this means choosing a small value for the time constant k. But if it is desired to make $\bar{f}(t)$ depend appreciably on early values of $f(t)$, k should be chosen larger. In general, we see then that the smoothing effect varies inversely as the time constant k.

The effect of a smoothing operation is to make the output value $x(t)$ equal to the input value at some past time, thus, in effect delaying the input. This may be shown analytically as follows. If $\dot{x}$ is eliminated between (4.2) and the equation obtained by differentiating (4.2), namely,

$$k\ddot{x} + \dot{x} = \dot{f}(t),$$

there is obtained

$$(4.7) \qquad x = f(t) - k\dot{f}(t) + k^2\ddot{x}.$$

If $\dot{x}$ is changing slowly, $\ddot{x}$ will be negligibly small; hence if, in addition, we choose k quite small, the $k^2\ddot{x}$ may be dropped. There is then obtained the approximate solution for $x(t)$ in the form

$$(4.8) \qquad x \doteq f(t) - k\dot{f}(t),$$

which is often sufficiently accurate to be useful in the typical applications of this equation to lead computing sights. The terms in the right member of (4.8) are the leading terms in the Taylor expansion of $f(t-k)$ about the point t. Thus the output $x(t)$ of the smoothing process is approximately

$$(4.9) \qquad x(t) \doteq f(t-k),$$

a form which shows that the output behaves roughly like the input delayed by k seconds. From (4.8) we have

$$(4.10) \qquad f(t) - x(t) = k\dot{f}(t),$$

which interpreted, says that the difference between input and output is, to a first approximation, proportional both to the time constant k and the rate of change of input. These conclusions which we have underlined are, as was stated subsequent to equation (4.7), valid only if k is small and x is changing slowly.

It is worth noticing that if we regard the input $f(t)$ as the sum of two terms, $f_1(t)$ and $f_2(t)$, the first a "signal", the second an "error" or "noise" term, then the solution of (4.2) can be regarded, by the Principle of Superposition, as the sum of the solutions $x_1(t)$ and $x_2(t)$, corresponding to $f_1(t)$ and $f_2(t)$, respectively, as inputs. In other words then, the output $x(t) = x_1(t) + x_2(t)$ will consist of "delayed signal" and "smoothed noise."

In conclusion, we summarize the role of the time constant k by noting that an increase in the value of this constant will

(a) Increase the time required for the transient term to die down by a specified percentage of its initial value;

(b) Increase the smoothing effect on input error, i.e., the averaging process will extend over an effectively longer interval;

(c) Increase the amount by which the signal or input will be out of date.

4.6 A Generic Lead Formula for the Coplanar Case

Equation (2.24) of chapter 2 gives an approximate formula for Λ_k, the kinematic lead, for the coplanar case of rectilinear gun and curvilinear target motion. This equation may be rewritten in the form

$$(4.11) \qquad \sin \Lambda_k = \frac{hM}{rV_f}$$

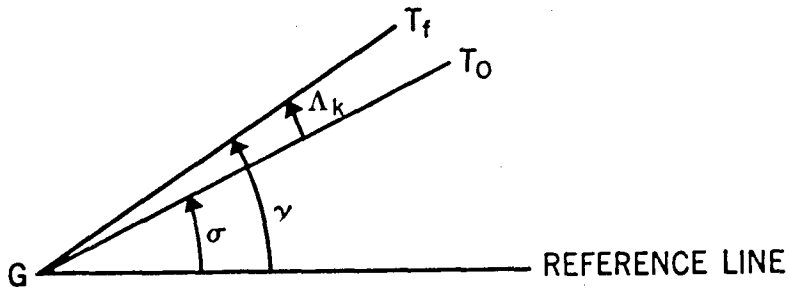

Figure 69. — The Kinematic Lead

where, it may be recalled,

$$V_f = \frac{r_f}{t_f} = \text{average projectile velocity over the future range,}$$

and

$$(4.12) \quad h = 1 + \frac{t_f}{2}\left(\frac{\dot{M}}{M}\right).$$

Replacing M by $r^2\dot{\tau}$ and r by $V_r t$, where V_r is the average projectile velocity over the present range and t is the present time of flight of the projectile over the present range, we find

$$\sin \Lambda_k = h\left(\frac{V_r}{V_f}\right) t\,\dot{\tau}.$$

If perfect tracking is not assumed, the angular rate actually used in the latter equation will be $\dot{\sigma}$ and not $\dot{\tau}$. Since the true lead is measured in radians and is a relatively small angle, $\sin \Lambda_k$ will be approximately equal to Λ_k. Thus,

$$(4.13) \quad \Lambda_k \doteq h\left(\frac{V_r}{V_f}\right) t\,\dot{\sigma}.$$

The average shell velocity Vr does not, for moderate ranges, change very rapidly. Hence, the fraction V_r/V_f does not deviate appreciably from 1.

The quantity h, given by (4.12), is worth further study. From equation (2.24) et seq., we note that, for straight line target motion, $\dot{M} = O$ and $h \equiv 1$. Also, if the target path relative to the gun is a circle traversed with constant speed, it is easily seen that $\dot{M} = O$, $h = 1$ and $V_r/V_f = 1$. In these cases, then, it may be said that the kinematic lead Λ_k is equal to the "angular travel lead" $t\,\sigma$. For the target traversing a pursuit course, numerical computations, supported by the theory of such curves as developed in chapter 3, show that $h \doteq 0.9$. All these facts suggest our writing the kinematic lead formula as

$$(4.14) \quad \Lambda_k = u\,\dot{\sigma}$$

where u is a quantity to be calibrated to fit certain classes of target paths. It has the dimensions of time and represents, in a sense, an averaged ideal time of flight. We shall refer to u henceforth as the "time of flight multiplier" or the sight "sensitivity".

4.7 The Basic Differential Equation of a Typical Gyro Sight

We shall now examine the tracking problem for a specific type of lead computing sight in which the kinematic lead is computed from (4.14) by solving a certain differential equation. Although other mechanizations are possible, a usual procedure is to employ a gyroscope to measure the target's angular velocity.

Referring to figure 69, if we ignore for the present the ballistic lead Λ_b, then GT_o and GT_f

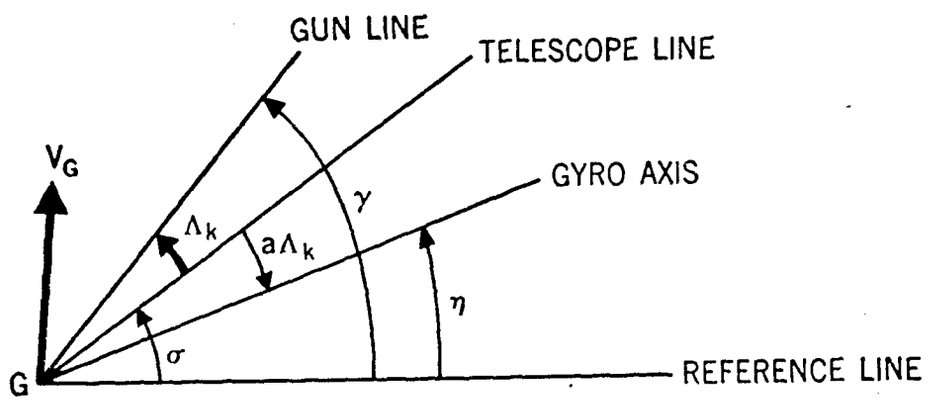

Figure 70. — The Gyro Axis as a Computing Line

give the telescope direction and the direction of the gun-bore axis, respectively. It should be noted that GT_f is along r_f. Letting the reference angles of the gun and telescope be γ and σ, we have then,

$$(4.15) \quad \Lambda_k = \gamma - \sigma$$

and

$$(4.16) \quad \dot{\Lambda}_k = \dot{\gamma} - \dot{\sigma}.$$

From (4.14) and (4.16), $\Lambda_k = u(\dot{\gamma} - \dot{\Lambda}_k)$, so that

$$(4.17) \quad u\dot{\Lambda}_k + \Lambda_k = u\,\dot{\gamma}.$$

This could well be the differential equation we are seeking except for the fact that tracking would be difficult with such a sight. Why this is so, may be seen as follows. From (4.14) and (4.15) we have as the equation connecting sight line and gun line,

$$(4.18) \quad \dot{\sigma} = \frac{\gamma - \sigma}{u}.$$

We notice here that $\dot{\sigma}$ is independent of $\dot{\gamma}$, the gun's rate of turn, and is a function of the magnitude of the angle between gun and telescope. This means, for example, that if the gun and telescope are originally aligned and the gun is given a sudden jerk away, the telescope, being independent of gun velocity, does not respond at once but begins to move only after the difference $\gamma - \sigma$ has made itself felt. This situation, known as neutral tracking, is characterized by a sluggishness in the telescope's rate of turn.

The situation can be remedied by modifying our basic equation (4.17). As things now stand, the gyro spin axis is along the telescope direction. Let us instead envision the situation depicted in figure 70, in which the gun, telescope, and gyro axes move in such fashion that the ratio of angles, gun line to telescope line and telescope line to gyro axis is constant.

If angles are measured positively in the clockwise sense, this implies that

$$(4.19) \quad \frac{\sigma - \eta}{\gamma - \sigma} = \frac{-a\,\Lambda_k}{\Lambda_k} = -a$$

where a is called the coupling constant or sight parameter. The ratio in (4.19) is kept constant in the sight by means of an optical or mechanical linkage. How this is actually done in a typical disturbed reticle sight will be clarified in the next chapter.

From (4.19) we also find

$$(4.20)\qquad \frac{-a}{1-a} = \frac{\sigma-\eta}{\gamma-\eta},$$

from which we see that, for a typical a-value, say $-.5$, the telescope line will be, at all times, one-third of the way from the gyro axis to the gun-bore axis.

One immediately obvious advantage of the linkage arrangement is that, when the gun is moved, the telescope will respond at once with at least a fraction of the motion, even though the gyro momentarily remains still. Thus, coupling the three axes removes the undesirable feature of neutral tracking mentioned earlier. Other advantages will appear in the discussions to follow.

Returning now to figure 70, we see, by way of the linkage arrangement, that Λ_k will be a function of the rate of turn of the gyro axis. In fact, equation (4.14) will be replaced by

$$(4.21)\qquad \Lambda_k = u\dot{\eta}$$

or, since $\eta = \sigma + a\Lambda_k$, by

$$(4.22)\qquad \Lambda_k = u(\dot{\sigma} + a\dot{\Lambda}_k).$$

From this it appears that we have introduced an appreciable error in substituting $\dot{\sigma} + a\dot{\Lambda}_k$ for $\dot{\sigma}$, but it will be shown later that for properly chosen values of a the error is a rapidly diminishing transient.

4.8 Solving the Basic Equation—Interpretation

Let us rewrite (4.22) in the form

$$(4.23)\qquad -au\dot{\Lambda}_k + \Lambda_k = u\dot{\sigma}.$$

This equation is a particular instance of (4.2) if we regard $-au$ as constant or, for our purposes, as being relatively constant. The quantity u depends essentially upon the range so that the assumption of the relative constancy of u implies that the range does not vary greatly during the projectile's time in flight. Using the solution to (4.2) we find, with the initial condition $t = t_o$, $\Lambda_k = \Lambda_k(t_o)$,

$$(4.24)\qquad \Lambda_k(t) = e^{\frac{-(t-t_o)}{-au}}\left[\Lambda_k(t_o) - \overline{u\dot{\sigma}}\right] + \overline{u\dot{\sigma}}$$

where $\overline{u\dot{\sigma}}$ is the weighted average of $u\sigma$ given by

$$(4.25)\qquad \overline{u\dot{\sigma}} = \frac{1}{-au\left(e^{t/-au} - e^{t_o/-au}\right)} \int_{t_o}^{t} e^{t/k}\, u\dot{\sigma}\, dt,$$

$$k = -au.$$

In the light of our previous discussion in 4.5, on smoothing data, we see that (4.24) furnishes a smoothed output $\overline{u\dot{\sigma}}$ of the input function $u\dot{\sigma}$, the exponential term being a transient for negative values of the sight parameter a. The rapidity of decay of this transient depends on the variable "time constant" $-au$, which, as mentioned before, is essentially a function of range. For short range, the target angular velocity $\dot{\sigma}$ and hence the input function $u\dot{\sigma}$ changes rapidly. But from (4.10),

$$(4.26)\qquad u\dot{\sigma} - \overline{u\dot{\sigma}} \doteq -au\frac{d}{dt}(u\dot{\sigma}).$$

In words, this says that lag in lead due to smoothing is proportional not only to the rate of change of $u\dot{\sigma}$ but also to $-au$. It is interesting to note that, depending on the target range, each of these factors helps in turn to keep the smoothed lead lag small. Thus for short ranges, larger values of $\frac{d}{dt}(u\dot{\sigma})$ are compensated for by small values of $-au$, while for longer ranges, $u\dot{\sigma}$ changes less rapidly, thereby making up for

larger values of $-au$. In addition, since the sight parameter is yet at our disposal, we note that for a numerically small value of a, the smoothing effect on input error will be less. In fact, we have already seen that the output behaves roughly like the input delayed by $k = -au$ seconds. The smaller k is, the more the output behaves like the input and the less, then, is the smoothing effect.

4.9 Transient Behavior

Upon locating a target in the sky, the gunner will probably find the gun pointing in some quite different direction, thereby necessitating his slewing the gun rapidly into the approximate target direction. So far as the sight is concerned, rapid slewing of the gun is interpreted in terms of very fast target motion, whereupon the computing unit puts out a correspondingly large lead. In fact, for so large a gun rate, the reticle may move far from the gun-bore axis and might even disappear from the gunner's field of view. When the gun has arrived in just about the right position, the reticle leisurely comes drifting back into the center of the field. It is of interest, therefore, to see what can be done to hasten the decay of the large transient lead set up. For this purpose we rewrite (4.22), recalling that $\sigma = \gamma - \Lambda_k$, in the form

$$(4.27) \qquad (1 - a)\ u\dot{\Lambda}_k + \Lambda_k = u\dot{\gamma}.$$

This equation shows how the computed kinematic lead depends on given motions of the gun. The equation corresponding to (4.24) is

$$(4.28) \qquad \Lambda_k(t) = e^{-(t-t_o)/(1-a)u}\,[\Lambda_k(t_o) - \overline{u\dot{\gamma}}] + \overline{u\dot{\gamma}},$$

the transient lead being the first term on the right.

In section 4.10, we shall show that for "operational stability" of a sight a negative a-value is necessary. With this in mind we see from (4.28) that for more rapid decay of the transient term a SMALL negative a-value is desirable. To employ this fact, some experimental sights have been constructed using two different a-values. The numerically smaller of these values is applied during the initial interval of tracking and transient decay, the numerically larger being switched on later.

As far as operation of the sight is concerned, we note the following:

(1) The transient term diminishes more rapidly when the range setting, and hence the sensitivity, is small.

(2) In order that the false lead introduced by slewing be as small as possible, the gunner should use minimum range setting (sensitivity) while slewing. Thus, the range should be set at a value appropriate to the target only after the gun has gotten on target.

(3) When possible to do so, the gunner should pick up the intended target well before it gets in range so that the transients can settle properly.

4.10 Operational Stability

We shall say that a sight is operationally stable if a small but sudden displacement of the gun in a given direction gives rise to a sudden displacement (not necessarily of the same size) of the reticle in the same direction. If the reticle is displaced opposite to that of the gun, we shall speak of the sight as being operationally unstable.

In conformance with the above definition, we now show that unless a sight has a negative a-value it will be operationally unstable. If in (4.27) we replace Λ_k by $\gamma - \sigma$, there results the equation

$$(4.29) \qquad (1 - a)\,u\dot{\sigma} + \sigma = -au\dot{\gamma} + \gamma,$$

which relates the telescope and gun-bore axis directions. One may easily show that, in carry-

ing through the discussion, there is no loss in generality in assuming the gun and telescope directions initially aligned. Then $\sigma = \gamma = O$, and $\dot{\sigma}$ and $\dot{\gamma}$ will represent the initial reticle and gun velocities. Hence, we have initially

$$(4.30) \quad \dot{\sigma} = \left(\frac{-a}{1-a}\right)\dot{\gamma},$$

which shows that the rate of reticle displacement is proportional to the rate of gun displacement and will be in the same or opposite direction according to whether a is negative or positive. (For all cases $|a| < 1$).

Thus when $O < a < 1$, the reticle will move in the direction opposite to that in which the gun moves and, by our definition, we have operational instability. This type of situation is very confusing to the gunner and leads to poor tracking. The tendency in trying to get on target would be to jerk the gun still farther in the same direction, an act which would result in sending the reticle farther in the opposite direction. To continue this divergent process for a few seconds may well put the gunner off course entirely.

The case $a = O$ is that of neutral tracking, discussed subsequent to equation (4.18). When $a < O$, the reticle and gun will move in the same direction, the velocity of the former being a proper fraction of the latter. In particular, if $a = -\frac{1}{2}$, the reticle will follow the gun with 1/3 of the gun's initial velocity. The particular a-value to be used in a given sight is a problem in design that can generally be determined only by trial and error. The different factors involved are summarized in section 4.12.

4.11 Amplification of Gun Motion with Respect to Sight Motion

As was pointed out in section 4.5, the process of tracking is never perfect but is always attended by an irregularly oscillating tracking error or "noise". Since the tracking is reflected in the motion of the reticle with respect to the correct target position as origin, we might inquire, since this is a disturbed-reticle system, what must be the gun motion to produce a particular reticle motion? In particular, if the gunner sees his line of sight oscillating with amplitude $A\sigma$, with what amplitude is the gun itself oscillating? If we denote the latter by $A\gamma$ and let C be the ratio $A\sigma/A\gamma$, hereafter referred to as the amplification ratio, then C is the factor by which the gun motion amplitude is multiplied when it is transmitted to the line of sight.

To initiate the study of the reaction of the sight to oscillations of the gun, we begin, quite naturally, with equation (4.29), relating sight position to gun position. Let us suppose that the actual gun motion $\gamma(t)$ consists of a steady motion $\gamma_o(t)$ upon which is superimposed an oscillatory motion $\gamma_1(t)$. Replacing γ in (4.29) by $\gamma_o + \gamma_1$, we can write solution $\sigma(t)$ in the form $\sigma_o + \sigma_1$, with σ_i, $(i = 0,1)$, being the solution of (4.29) with γ replaced by γ_i $(i = 0,1)$. The function $\sigma_o(t)$ does not concern us here. Hence, it is sufficient to assume a "reasonable" oscillatory motion of the gun, described by $\gamma_1(t)$, and study the corresponding function $\sigma_1(t)$. Thus, let us assume the sinusoidal oscillation

$$\gamma_1 = A\gamma \sin \omega t$$

of amplitude $A\gamma$ radians and frequency $f = \frac{\omega}{2\pi}$ oscillations per second. This assumption is not unreasonable in view of the theoretical possibility of decomposing more general oscillations into sinusoidal ones, using a Fourier analysis. Also in equation (4.29) we assume that u is constant. We may do this since, relative to high frequency oscillations of the gun, u would change slowly. Hence (4.29) becomes

$$(4.31) \quad (1-a)\, u\dot{\sigma} + \sigma = A\gamma \sin \omega t - au\,\omega A\gamma \cos \omega t,$$

whose "steady-state" solution is

$$(4.32) \quad \sigma_1(t) = \frac{-k_1 A\gamma\,\omega}{(\omega^2 + k_1^2)(1-a)} \cos \omega t + \frac{k_1 A\gamma\,[k_1 - au\,\omega^2]}{\omega^2 + k_1^2} \sin \omega t$$

where $k_1 = \dfrac{1}{(1-a)u}$.

The amplitude $A\sigma$ is obtained from (4.32) by taking the square root of the sum of the squares of the coefficients of the trigonometric functions in the right member. After much simplification we find that

$$(4.33) \quad C = A\sigma/A\gamma = \sqrt{\frac{1+4\pi^2(-a)^2u^2f^2}{1+4\pi^2(1-a)^2u^2f^2}},$$

In words, then, we may say:

Amplitude of Sight Oscillations = C (Amplitude of Gun Oscillations). The oscillatory motion of the gun may be due to a variety of causes such as gunner's jitters in handling the controls, recoil of the shot, etc. Since a is usually negative, the factor $C < 1$. As f varies from O to $+\infty$, C decreases monotonically from 1 and approaches as a limit the quantity $(-a/1-a)$. In particular, if C is much smaller than 1, the gunner will note only a small oscillatory motion of the sight, even when the gun has large oscillations. Thus, the gunner may think he is tracking well when in fact the gun is wobbling badly. This also shows that for high frequency gun oscillations, C tends to zero with a. Hence, in order to make the amplification of gun motion, with respect to sight motion less, a should be chosen larger in magnitude.

In the above discussion, the gun and sight motions are both of a sinusoidal nature. However, these motions differ not only in amplitude but also in phase. Thus, in reaching peaks, the sight will lag the gun by ε seconds, where ε is found from (4.32) to be

$$(4.34) \quad \varepsilon = \frac{1}{2\pi f}\tan^{-1}\left[\frac{2\pi f u}{1-4\pi^2 a(1-a)f^2u^2}\right].$$

4.12 Choice of the Sight Parameter a

We have seen throughout the preceding discussions in this chapter the significant part played by the sight parameter a in the behavior of the sight. In summary, we may say that the a-value of a lead computing sight must be chosen with due regard for the following somewhat contradictory requirements:

(1) For operational stability we need, first and foremost, a negative value of a.

(2) To make the amplification of gun motion with respect to sight motion less requires an a-value larger in magnitude. Specifically, this increase improves the operational stability by making the sight respond more emphatically to gun motion and hence makes for ease in tracking.

(3) For faster decay of transient leads, an a-value must be negative and smaller in magnitude.

(4) Smoothing of input data is greater for larger values of a.

(5) The delay in lead output is greater for larger values of a.

Thus, in designing a sight, the engineer or physicist must resolve to the best advantage these contradictory requirements. A compromise value somewhere in the neighborhood of $a = -\frac{1}{2}$ is often quite satisfactory. It should be mentioned that a sight with a positive a-value could be designed and used, but, not being operationally stable, it would take considerable practice on the part of the gunner to master its peculiarities. Such a sight, as mentioned earlier, would have initial reticle motion to the right for initial gun motion to the left, after which the reticle would again move left after a certain lapse of time.

4.13 The Basic Differential Equation Including Trail

The differential equation derived in section 4.7 and the associated diagram of figure 70 are inaccurate to the extent that the ballistic lead or bullet trail has been omitted from the considerations. Let us now see how the basic

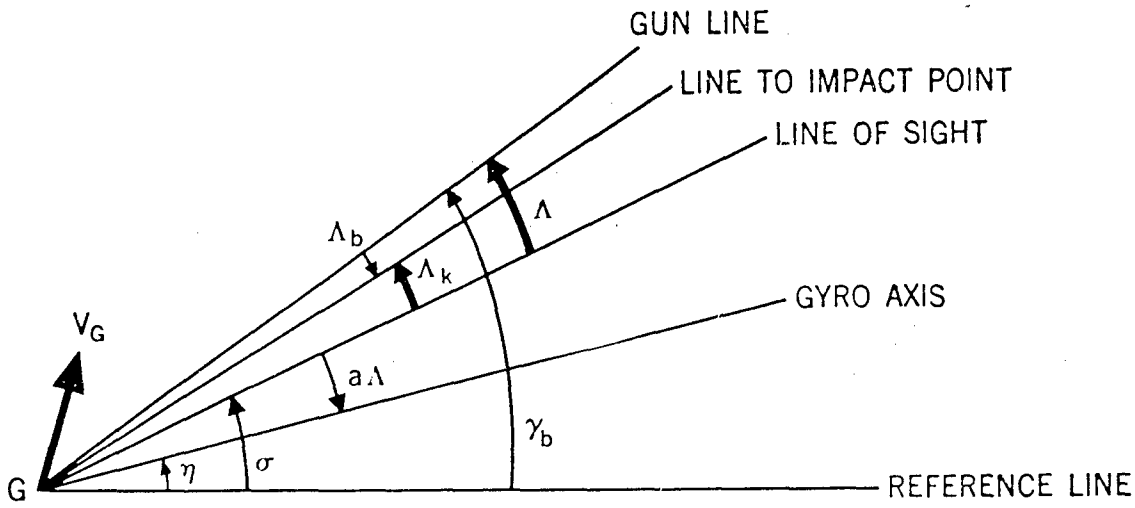

Figure 71. — Ballistic, Kinematic, and Total Lead Angles

equation (4.23) should be modified to include the effect of trail.

It was shown in chapter 2 that in firing against a relative target course from a bomber, the gun must be moved from a line pointing at the impact point, forward; the reason being that in relative motion the bullet curves to the rear. Considering a coplanar attack only and neglecting gravity drop, this bullet-trail angle, which we shall denote by Λ_b, will then lie, along with the kinematic lead Λ_k, in the plane determined by the gun position and the relative target path. The diagram appropriate to this situation is shown in figure 71.

For the total lead Λ there is the relation, evident from figure 71,

$$(4.35) \qquad \Lambda = \Lambda_k + \Lambda_b.$$

As was done in section 4.7, we calibrate a sensitivity function u such that

$$(4.36) \qquad \Lambda_k = u\,\dot{\eta}\,,$$

it being assumed here that the trail offset Λ_b is included in the angular deflection of the gyro spin axis from the gun-bore axis. Since

$$\eta = \sigma + a\,\Lambda = \sigma + a(\Lambda_k - \Lambda_b)\,,$$

we may write the basic equation (4.36) in the forms

$$(4.37) \qquad \Lambda_k = u(\dot{\sigma} + a\,\dot{\Lambda})\ ;$$

$$(4.38) \qquad -au\,\dot{\Lambda} + \Lambda = u\,\dot{\sigma} - \Lambda_b\ ;$$

$$(4.39) \qquad -au\,\dot{\Lambda}_k + \Lambda_k = u\,\dot{\sigma} - au\,\dot{\Lambda}_b\,.$$

In general, only a fractional mil error will be committed when $\dot{\Lambda}_b$ is neglected. If this be done, then equations (4.38) and (4.39) show that to obtain the total lead Λ it is sufficient to find Λ_k from equation (4.23) and combine it with Λ_b via (4.35). This fact will be looked into with greater detail in the next chapter when a particular mechanization of (4.38) will be considered.

It should be pointed out, in conclusion, that from the viewpoint adopted in this chapter the lead is obtained as a "steady state" solution of a first order linear differential equation whereas the formulas in chapter 2 are actual expressions for the leads derived independently of any defining differential equation. The basic mathematical formulation for the lead is dependent of course upon the specific manner of mech-

anization of inputs in the computer. Here also we made things simple by neglecting gravity drop of the projectile and by assuming a single plane of action. When the air courses of gun and target are not coplanar, it is best to break up the total lead into components as was done in section 2.8 of chapter 2. The manner in which these components are defined geometrically will depend upon the mounting of gun and line of sight. Thus, in section 2.8 an azimuth-elevation system of coordinates was used and the total lead was decomposed in that system. If in figure 34 the gun was constrained to move in a plane passing through i_G and this plane in turn was free to revolve about i_G we would have the so-called "roll-and-traverse" system of coordinates. The formulas expressing the lead components in one system can always be changed to the formulas appropriate to any other system, by a suitable transformation of coordinates.

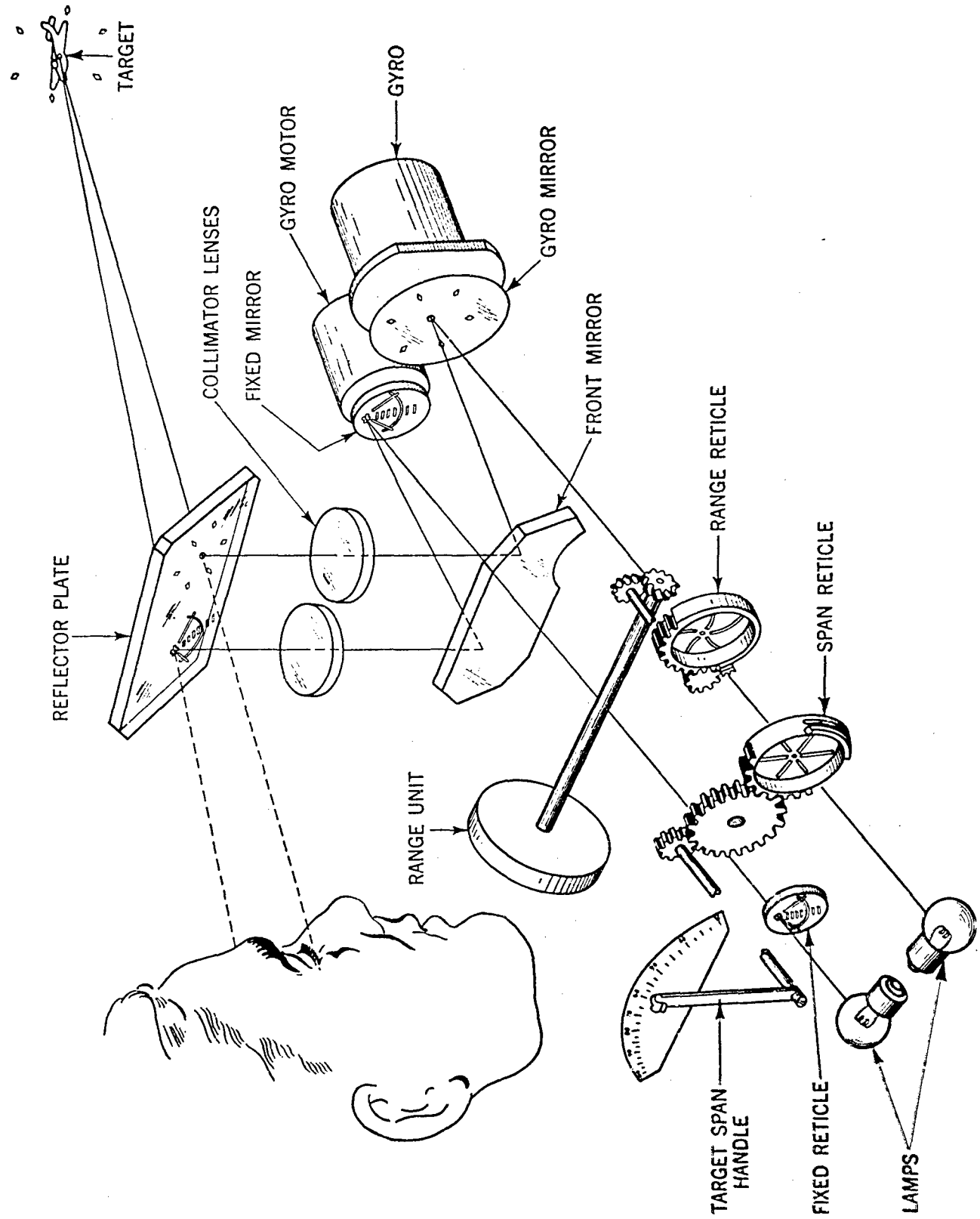

Figure 72. — Gyroscopic Lead Computing Sight

Chapter 5

GYROSCOPIC LEAD COMPUTING SIGHTS

5.1 Some Preliminary Ideas from Dynamics

To aid in understanding the gyroscope, its properties, and its many functions in fire-control instruments, we need to review briefly some fundamental ideas from dynamics and to understand how they apply in explaining gyroscopic behavior. We begin by considering the notion of the moment of a force about a point.

In figure 73, let P be a particle of mass m, acted on by the force $\mathbf{F}$, and moving with velocity $\dot{\mathbf{r}} = \mathbf{V}$ referred to the fixed point O. Then the moment of the force $\mathbf{F}$ about O is defined as*,

$$(5.1) \quad \mathbf{M}_o = \mathbf{r} \times \mathbf{F}.$$

The scalar value M_o, also called the torque, is easily seen to be

$$(5.2) \quad M_o = F_p$$

since

$$M_o = rF \sin(\pi - \alpha) = rF \sin \alpha = F_p$$

Thus the magnitude of the moment is equal to the product of the force magnitude and the perpendicular distance from O to the line of action of the force.

The momentum of the particle P is defined as the vector quantity $m\mathbf{V}$. The moment of momentum or angular momentum of P is then $\mathbf{r} \times m\mathbf{V} = \mathbf{H}$. Since

$$\dot{\mathbf{H}} = \mathbf{V} \times m\mathbf{V} + \mathbf{r} \times m\mathbf{a} = \mathbf{r} \times \mathbf{F}$$

where $\mathbf{a}$ is the acceleration of the particle and $\mathbf{F} = m\mathbf{a}$, we see that the time rate of change of the angular momentum about the fixed point O is equal to the moment of the force about O. In the case of a system of particles P_i of masses m_i acted upon by a set of external forces $\mathbf{F}_i$, the time rate of change of angular momentum of the system becomes equal to the sum of the moments of the external forces $\mathbf{F}_i$ about O. We shall refer to this as the Theorem of Angular Momentum. It should be noted that the internal forces, that is those forces consisting of the mutual actions between particles of the system, do not enter into the statement of this theorem. This follows, since these forces occur in pairs, each pair representing the interaction of two particles of the system. The two forces of each pair, since they represent action and reaction, respectively, are equal in magnitude and opposite in direction and possess the same line of action. Hence, the vector sum of the forces in each pair is zero. From this it follows easily that the vector sum of all the internal forces, and of their moments about the point O, is zero.

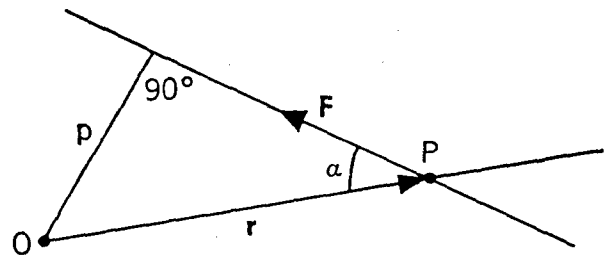

Figure 73. — Moment of Force About a Point

The Theorem of Angular Momentum, as stated here, assumed that the point O is fixed in space. However, the theorem can be shown to hold for the case where point O is in motion, providing that one of the following conditions is satisfied:

(a) The center of mass of the system of particles is at rest.

(b) The center of mass of the system of particles is in motion but coincides with the origin O.

Since application in this chapter is to be made to cases in which O is a point in an airplane, we

*See the Appendix for a review of vector definitions and operations.

shall assume hereafter that the point O is taken at the center of mass of the system of particles.

For a continuous body and not a discrete system of particles, the angular momentum $\mathbf{H}$ is obtained by the usual process of subdividing, summing and passing to the limit, and is expressed by

$$(5.3) \quad \mathbf{H} = \int \mathbf{r} \times \mathbf{V}\, dm$$

where the integration is taken throughout the body.

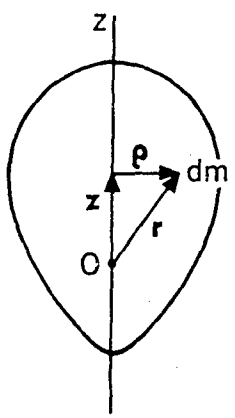

Figure 74. — Rotating Solid of Revolution

Since the present discussion is preliminary to a discussion of gyroscopic behavior, let us consider (5.3) for the case of a homogeneous solid of revolution rotating about its axis of symmetry with the fixed point O on this axis. We assume first that the axis of symmetry is fixed in space.

Let the angular velocity of rotation be $\mathbf{\Omega} = \Omega\mathbf{k}$, where $\mathbf{k}$ is a unit vector on the axis of rotation z and let $\boldsymbol{\rho}$, $\mathbf{r}$ and $\mathbf{z}$ be as shown in figure 74. Then since $\boldsymbol{\rho} \cdot \mathbf{k} = O$, we have

$$\mathbf{r} \times \mathbf{V} = (z\mathbf{k} + \boldsymbol{\rho}) \times \{\mathbf{\Omega} \times (z\mathbf{k} + \boldsymbol{\rho})\}$$
$$= \rho^2 \mathbf{\Omega} - z\,\Omega\,\boldsymbol{\rho}$$

and

$$\mathbf{H}_o = \mathbf{\Omega} \int \rho^2\, dm - \Omega \int \boldsymbol{\rho}\, z\, \mathrm{dm} \quad .$$

But because of symmetry,

$$\int \boldsymbol{\rho}\, z\, \mathrm{dm} = O$$

and hence

$$(5.4) \quad \mathbf{H}_o = I_z \mathbf{\Omega}$$

where

$$I_z = \int \rho^2\, dm$$

is the moment of inertia of the body about the z-axis. From (5.4) we obtain

$$(5.5) \quad \dot{\mathbf{H}}_o = I_z \boldsymbol{\alpha}$$

where $\boldsymbol{\alpha} = \dot{\mathbf{\Omega}}$ is the angular acceleration of the body.

On obvious generalization of the above situation is to consider the body of figure 74 as having a motion consisting of a rotation about a variable axis through O. Thus, in general, all points of the body except O will be in motion. The angular velocity vector $\mathbf{\Omega}$ can then be decomposed into components along the axes of symmetry z and along any two axes x, y perpendicular to z and to each other. Thus,

$$(5.6) \quad \mathbf{\Omega} = \mathbf{\Omega}_x + \mathbf{\Omega}_y + \mathbf{\Omega}_z \, .$$

The moment of momentum of the body about O is then, by an immediate extension of (5.4),

$$(5.7) \quad \mathbf{H}_o = A\, \mathbf{\Omega}_x + B\, \mathbf{\Omega}_y + C\, \mathbf{\Omega}_z$$

where A, B, C are the moments of inertia of the body about the x, y, z axes, respectively.

5.2 Theory of the Gyroscope

We shall define a gyroscope as any rigid body rotating around an axis through its center of mass. This axis will be referred to as the spin axis or gyro axis. The body is generally considered to be heavy, symmetric, and to have high angular speed about its spin axis. Two

separate mountings for a circular disk gyro are shown in figures 75 and 76. Either mounting permits the spin axis to be placed in any position. In figure 75, however, the center of mass of the system is always directly above the pedestal support. Rotation of gimbal 1 about AB moves the spin axis in elevation, while rotation of gimbal 2 about CD moves it in azimuth. This is known as Cardan suspension.

Let us analyze the situation shown in figure 76, where the spin axis is perpendicular to the vertical y-axis. The weight of the gyro rotor is **W** and its spin angular velocity is $\mathbf{\Omega}$. **R** is the reaction at the suport O. If the rotor were not spinning, the torque $T = W\,l$ would cause the gyro to fall; but, with the rotor spinning rapidly, the spin axis OA begins to rotate about the y-axis. We speak of this motion as precession. Assuming no bearing friction at O, we shall show that for precession in a horizontal plane the precessional velocity $\boldsymbol{\omega}'$ is given in magnitude by

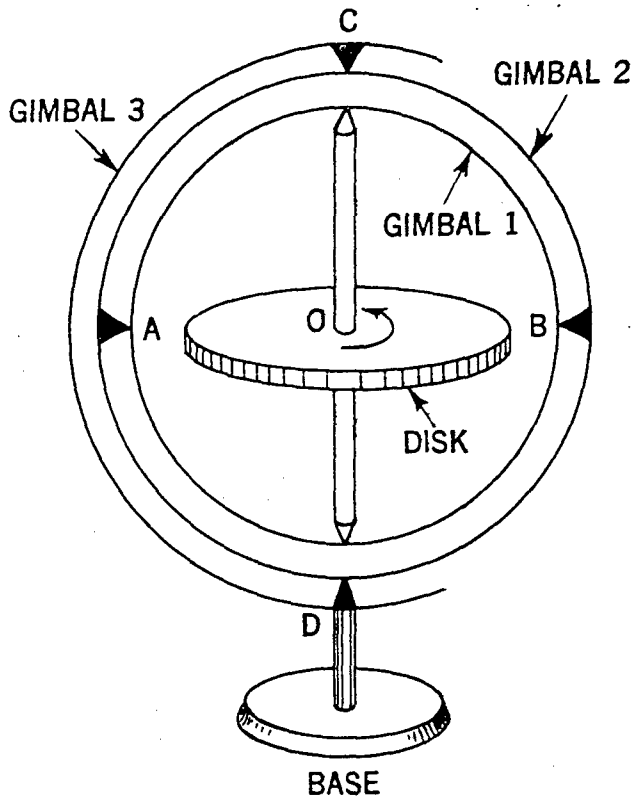

Figure 75. — Circular Disk Gyroscope

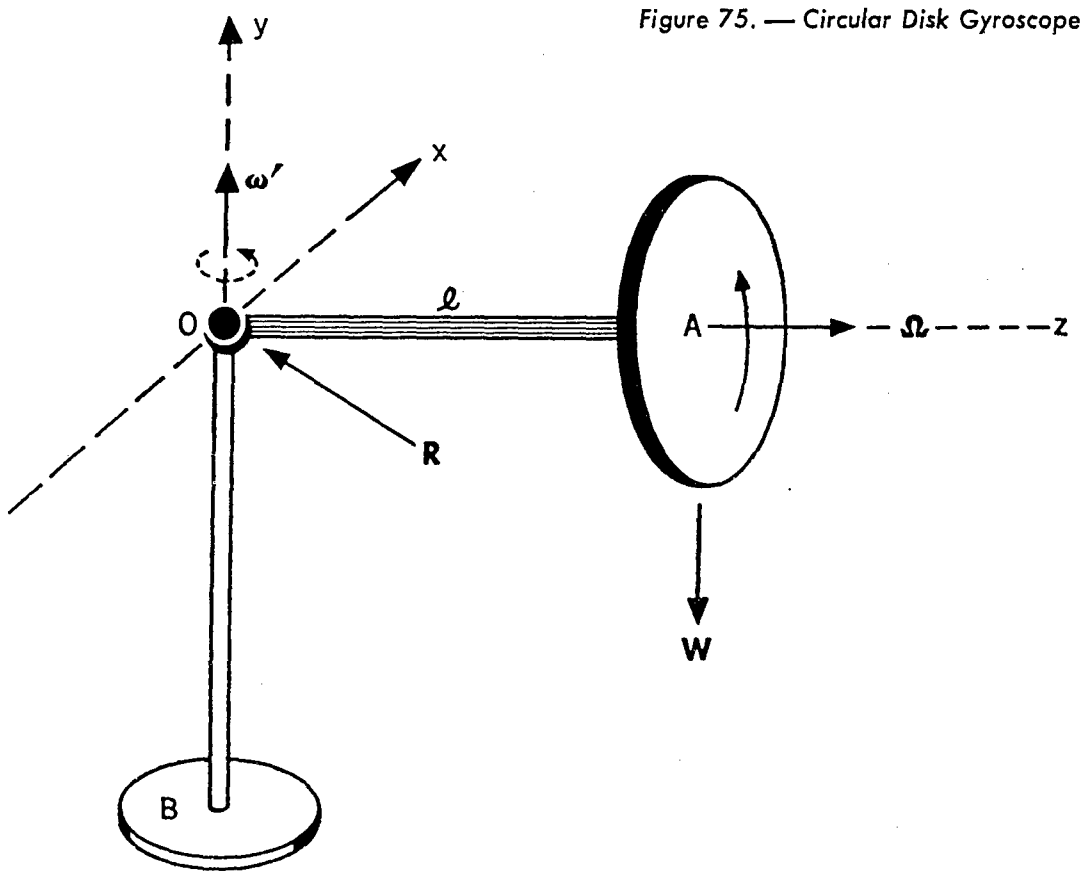

Figure 76. — Gyroscopic Precession

$$(5.8) \quad \omega' = \frac{W l}{C\Omega}$$

where C is the moment of inertia of the disk about the spin axis z.

If the total angular velocity of the system be denoted by $\boldsymbol{\omega}$ with components $\boldsymbol{\omega}_x$, $\boldsymbol{\omega}_y$, $\boldsymbol{\omega}_z$, we see immediately that, for the case of precession in a horizontal plane,

$$(5.9) \quad \boldsymbol{\omega}_x = 0, \quad \boldsymbol{\omega}_y = \boldsymbol{\omega}', \quad \boldsymbol{\omega}_z = \boldsymbol{\Omega},$$

and

$$(5.10) \quad \boldsymbol{\omega} = \boldsymbol{\Omega} + \boldsymbol{\omega}'.$$

The angular momentum of the system is then, using (5.7),

$$(5.11) \quad \mathbf{H}_o = B\boldsymbol{\omega}' + C\boldsymbol{\Omega}.$$

Relative to the moving set of axes $O - x\,y\,z$, the vector $\mathbf{H}_o$ is constant. Its angular velocity with respect to space is $\boldsymbol{\omega}'$. Hence,

$$(5.12) \quad \dot{\mathbf{H}}_o = \boldsymbol{\omega}' \times \mathbf{H}_o \qquad \text{(see appendix)}$$
$$= \boldsymbol{\omega}' \times C\boldsymbol{\Omega} = C\boldsymbol{\omega}' \times \boldsymbol{\Omega}.$$

By the Theorem of Angular Momentum, $\dot{\mathbf{H}}_o$ is equal to the sum of the moments of the forces $\mathbf{W}$ and $\mathbf{R}$ about O. Since the moment of $\mathbf{R}$ about O is zero,

$$(5.13) \quad \dot{\mathbf{H}}_o = \overrightarrow{OA} \times \mathbf{W}$$

and hence,

$$(5.14) \quad C\boldsymbol{\omega}' \times \boldsymbol{\Omega} = \overrightarrow{OA} \times \mathbf{W} = \mathbf{T}.$$

Taking scalars in (5.14) we find the desired relationship

$$(5.15) \quad C\,\omega'\,\Omega = W\,l.$$

The torque vector $\mathbf{T}$ in (5.14) is directed here along the positive x-axis. Since this is the same direction as that of $\boldsymbol{\omega}' \times \boldsymbol{\Omega}$, we see that the spin axis will always precess toward the torque axis.

When the spin axis makes an angle other than 90° with the vertical, say α, it is only slightly more difficult to show that the equation corresponding to equation (5.14) is

$$(5.16) \quad \left[C + (C - B)\frac{\omega'}{\Omega}\cos\alpha\right] \boldsymbol{\omega}' \times \boldsymbol{\Omega} = \overrightarrow{OA} \times \mathbf{W} = \mathbf{T}.$$

Equations (5.14) and (5.16) remain valid when $\mathbf{W}$ is replaced by a resultant force $\mathbf{F}$ other than the weight. In practice, the spin axis is not of negligible weight as compared with the weight of the gyro rotor and the point O is then best located at the center of mass of the system. Indeed, as was stated in connection with the Theorem on Angular Momentum, the point O must be so located in order that the theorem be applicable to cases where the center of mass is in motion as would be the case for a gyro mounted in an airplane in flight. From (5.16) we also note that when the precessional speed ω' is considerably less than the spin speed Ω (in symbols $\Omega >> \omega'$) the term containing $\cos\alpha$ may be dropped and (5.14) is then obtained as an approximation to (5.16).

To illustrate (5.8) numerically, let us suppose that for the system of figure 76

$W = 1$ lb., $l = 1$ ft., radius of disk $= 6$ in., and $\Omega = 400$ rps.

Then,

$$\omega' = \frac{1}{(400)\,2\pi \cdot C}$$

where

$$C = \frac{1}{2}\frac{W}{g}(\text{radius})^2 = \frac{1}{2}\left(\frac{1}{32.2}\right)\left(\frac{1}{2}\right)^2$$
$$= \frac{1}{257.6},$$

and ω' in radians/sec. is $\dfrac{257.6}{800\pi}$ or $\dfrac{257.6}{800\pi} \cdot \dfrac{180}{\pi}$ $= 5.87°$ per second.

When the gyro is mounted as in figure 75 and the disk is spun rapidly about the spin axis, no precession will occur since the center of mass of the system is at the point O and the torque $W\,l$ is then zero. However, if an external torque $\mathbf{L}$ be applied to the system, the gyro will behave in precisely the same manner as that in figure 76.

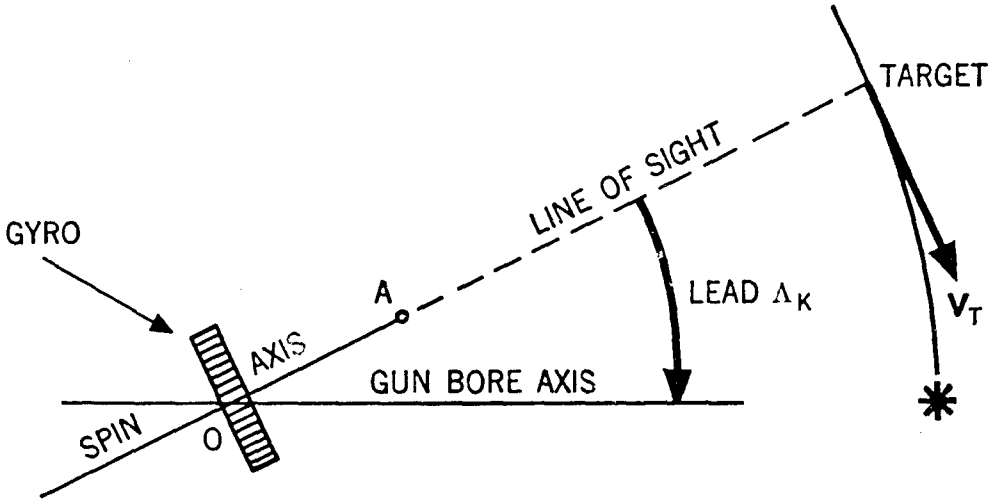

Figure 77. — Use of a Rate Gyro to Determine Lead

Thus, to sum up, we have the following two important facts of gyroscopic behavior:

(1) With no external torques present, the gyro spin axis will maintain a constant direction in space regardless of the motion of the system in which it is mounted.

(2) Under the influence of an external torque, the spin velocity vector will always precess toward the torque vector. More precisely, the spin velocity vector $\mathbf{\Omega}$, the torque vector $\mathbf{T}$, and the precessional velocity vector $\boldsymbol{\omega}'$, will always form a right-handed orthogonal set.

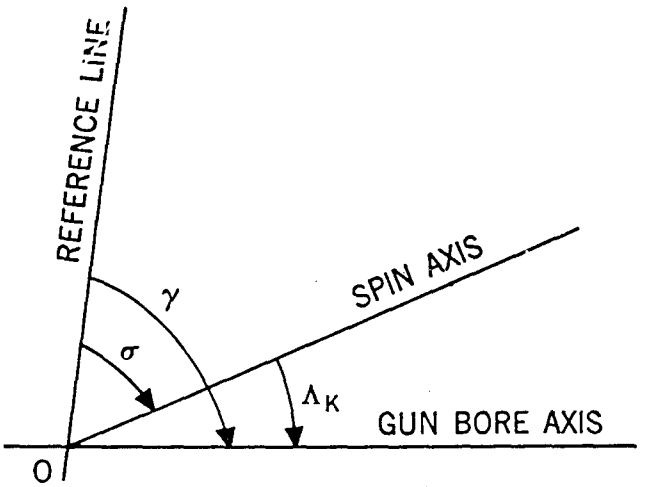

Figure 78. — Using Fixed Reference Line

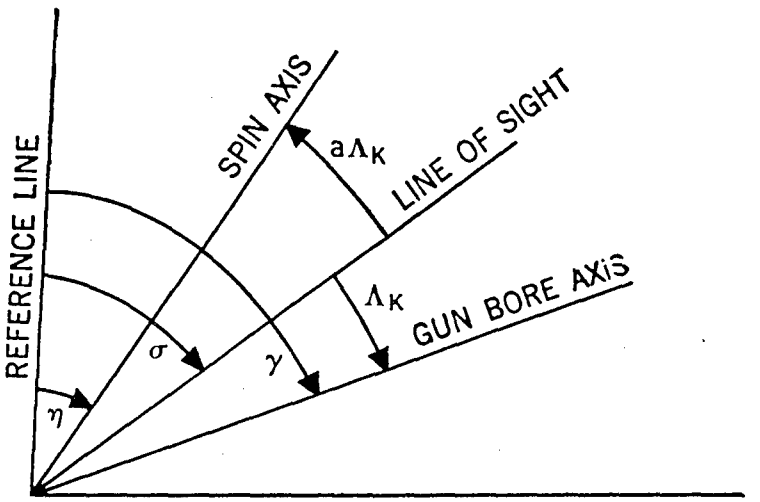

Figure 79. — The Gyro Axis as a Computing Line

988995 O - 52 - 9

5.3 Use of a Gyro to Produce Kinematic Lead

The preceding section will now serve as the basis for explaining how a gyroscope is actually used in a fire control system. Referring to figure 77, let us suppose that the gyroscope is mounted on a gun so that its spin axis is parallel initially to the bore axis of the gun, and so that the universal joint mounting at O is the center of mass of the gyro system and also is the point about which the gun rotates. Then as the gun is turned about O, the gyro axis will, according to the first property of gyroscopic behavior stated in 5.2, remain pointing in its original direction in space. If we now consider the spin axis to be directed along the line of sight to the target, then as the target is tracked the gyro must lag the gun by an angle equal to the required lead. In other words, the gyro will have to precess at the proper rate in the plane of rotation of the gun. Suppose that, as viewed from A, the gyro is spinning counterclockwise. Then to achieve precession in the direction required by the figure, a force **F** will have to be applied, at a point such as A, directed outward (perpendicular to the plane of the figure). The precession rate $\boldsymbol{\omega}$ is related to the force **F** according to equation (5.8), (with W replaced by F and $l = OA$). Thus,

$$(5.17) \qquad F = \frac{C\Omega}{l} \cdot \omega .$$

If a fixed reference line be chosen as in figure 78, so that

$$(5.18) \qquad \omega = \dot{\sigma} \text{ and } \Lambda_k = \gamma - \sigma ,$$

then (5.17) will be the equivalent of (4.14), providing that we can make the force **F** always proportional to the angle between the gun bore and spin axes, i.e., $F = K_1 \Lambda_k$, with the proportionality factor K_1 varying inversely with the time of flight multiplier u,

$$(5.19) \qquad K_1 = \frac{C\Omega}{l\,u} .$$

The quantity $\frac{C\Omega}{l}$ is a physical constant associated with the gyroscope.

To realize the relationship $F = K_1 \Lambda_k$, one might consider attaching a spring of variable stiffness from A to a point on the gun bore, in which case Hooke's Law would apply to give the desired ratio of F to Λ_k. However, this would give a force F in the plane of the gun's motion whereas we require, for precession in the right direction, a force perpendicular to this plane. Even if this difficulty were not present we would still have the disagreeable feature of having a sight with zero a-value, which, as we have seen in the preceding chapter, would make tracking impossible. One scheme for overcoming the first of these stumbling blocks is the use of electrical eddy currents. This is taken up in section 5.4. The theoretical remedy for the second was taken up in chapter 4 and consisted in keeping the line of sight at a fixed proportionate distance between the gyro spin axis and the gun-bore axis. With this in mind, we see from figure 79 that K_1 of (5.19) should be chosen so that

$$(5.20) \qquad K_1 = \frac{C\Omega}{lu} \cdot \frac{1}{1-a} .$$

This follows from the chain of equations

$$(5.21) \qquad \Lambda_k = u\dot{\eta}$$

$$(5.22) \qquad F = K_1 (\gamma - \eta) = \frac{C\Omega}{l} \dot{\eta}$$

$$(5.23) \qquad \gamma - \eta = (1-a)\Lambda_k .$$

5.4 The Eddy-Current Constrained Gyro

In the particular method of constraining a gyro to precess by use of eddy currents, the gyro rotor is not a cylindrical disk as in figures 75, 76, but consists instead of a spin axle with a flat circular mirror at one end and a spherical aluminum dome or cap at the other end (figure 80). It is mounted on a type of universal joint known as a Hooke's joint and through a pulley arrangement it is kept rotating about the axle at about 3000 rpm by a constant speed motor. This unit, together with accessories to be described later, is mounted in a sight head, which is rigidly attached to the gun mount. The gun rotates about the same fixed point O as does the gyro system (figure 81).

Suppose now, to the apparatus of figure 81 we add a pair of electromagnets, rigidly attached

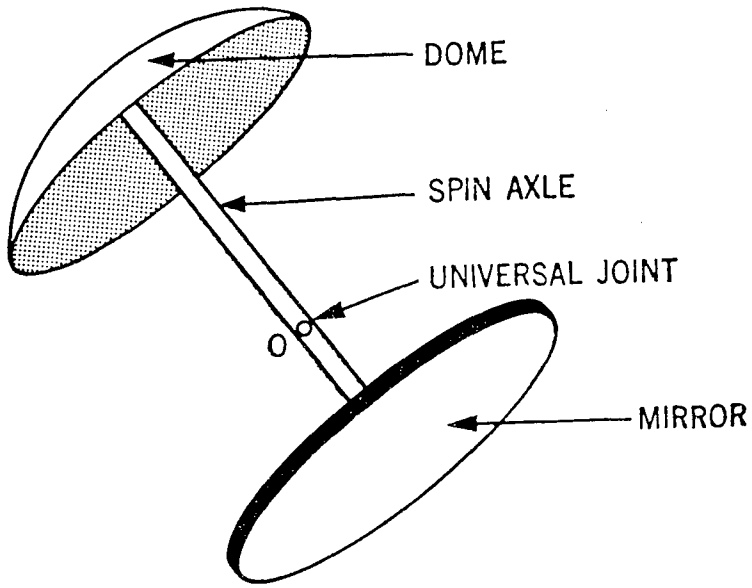

Figure 80. — Gyro Dome, Axle, and Mirror

to the sight head and aligned with the gun (figure 82).

The iron cores of the electromagnets are wound with coils of wire through which a current i flows under a constant EMF of voltage E. The current i may be varied through use of a variable resistance R. As the gyro precesses, the spinning dome moves through the narrow air gap between the magnet poles. With the situation as shown in figure 82, the gyro would be physically unable to take up its undeflected position. To avoid this difficulty, eight poles are used instead of two — four above and four below. The dome may then move freely through the narrow air gaps between them. The four magnets on each side of the dome together

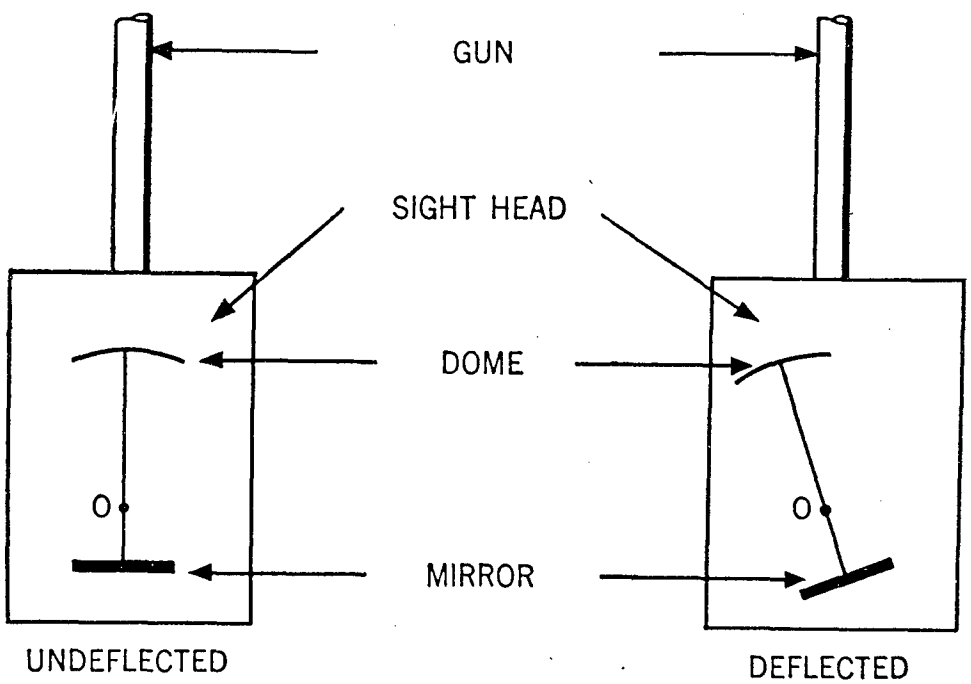

Figure 81. — Motion of Gun with Respect to Gyro Spin Axis

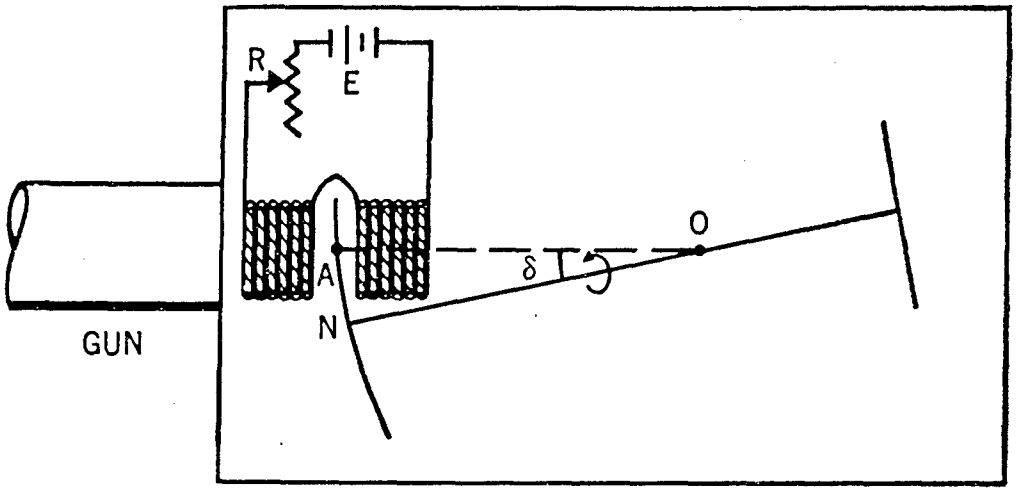

Figure 82. — Precessing Forces Introduced Electromagnetically

have the effect of single magnets, so that the result is equivalent to figure 82. Hence, in the ensuing discussion we shall speak of only two poles, each being the equivalent of the four poles actually used.

When current flows in the coils, a magnetic field of strength proportional to this current is set up between the two poles. Thus,

(5.24) $H = c_1 i$.

The lines of magnetic force pass through a circular area of the dome with center at A. Since the dome is spinning, this area is being continuously replaced by another. As a result of this motion across the lines of magnetic force, electric "eddy currents" are induced in the part of the dome between the poles. With the poles wound as indicated in figure 82 and with the dome spinning clockwise as seen from O (down into the paper at A) these currents will be directed from A toward the periphery of the dome in the plane of the paper. If the linear velocity of the dome at A is v and if the eddy current strength be denoted by i_e, then it is known from electromagnetic theory that

(5.25) $i_e = c_2 H v$.

The eddy currents, in their turn, react with the magnetic field to create a mechanical force on the dome. This force is directed opposite to the motion of the dome at A and hence vertically upward as desired. The magnitude of this force F is proportional to H and i_e. Hence,

(5.26) $F = c_3 H i_e$.

Combining (5.24) through (5.26) we find

(5.27) $F = c_1^2 c_2 c_3 i^2 v$.

From figure 82,

$$\widehat{AN} = l\delta,$$

and since δ is a small angle, we have, to a good approximation,

$$v = \widehat{AN} \cdot \Omega = l\delta\Omega.$$

The force F may then be written

(5.28) $F = (c_1^2 c_2 c_3 i^2 l \Omega)\delta$;

or, since

$$\delta = \gamma - \eta = (1 - a) \Lambda_k,$$

(5.29) $F = K_1 (1 - a) \Lambda_k$

with

(5.30) $K_1 = c_1^2 c_2 c_3 i^2 l \Omega$.

We now have a force proportional to Λ_k and in the right direction. It will have the right magnitude if (5.30) is now identified with (5.20). This becomes, if we replace i by E/R (Ohm's Law), and simplify,

(5.31) $$R^2 = \frac{(1 - a) c_2 c_3 (c_1 \cdot E \cdot l)^2}{C} \cdot u.$$

Hence, by varying R in accordance with (5.31), condition (5.20) will be satisfied, i.e., K_1 will then be inversely proportional to the time of

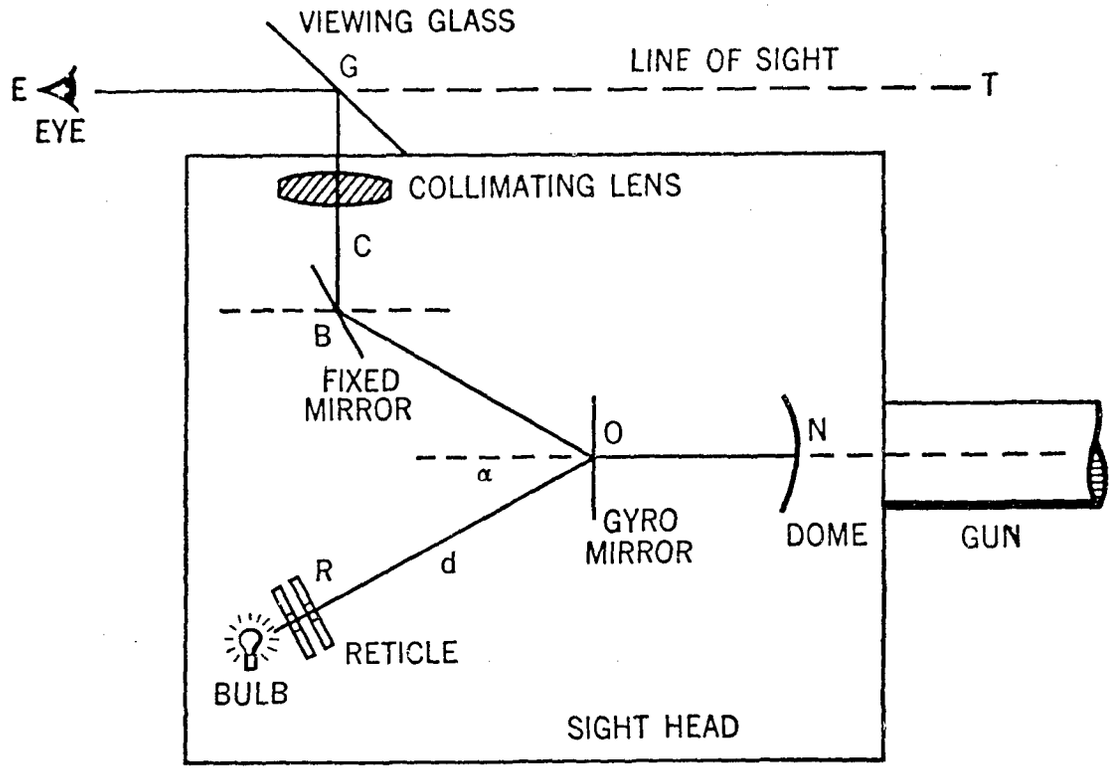

Figure 83. — Optical System of the Sight Head

flight multiplier u. It remains now to investigate by what means the sight line can be made to stay a fixed proportionate distance between the gyro and the gun-bore axis.

5.5 An Optical Linkage

An optical method of achieving the fixed ratio of angular separations of the gun-bore axis, line of sight and spin axis as desired in figure 79 will now be considered. A vertical cross-section of the sight head, with component parts of the optical system labeled, is shown in figure 83, with the gyro in undeflected position. In practice, the point O is taken so close to the gyro mirror that rotations can be thought of as being taken about a point in the plane of the mirror.

Referring now to figure 83 we note the following: the bulb sends a beam of light through a central hole in the two reticle disks. This beam hits the gyro mirror at O (when the gyro is undeflected) and is reflected along OB to a fixed mirror at B. From here it is reflected straight up through a lens C to a piece of plate glass at G. Part of the beam passes upward and is lost, but part is reflected to the operator's eye at E. He sees the image of the round circle of light at R as appearing on his line of vision ET. A primary function of the lens C is to focus this image at infinity, thus enabling the operator to move his eye without occasioning any change in the direction of line ET. When the gyro is undeflected, this image (or pip as it is called) will determine with E a line of sight parallel to the gun bore axis. The main function of the optical system then is to see that the line EG lies constantly between the gyro spin axis direction and the gun bore axis, and at the desired angular distance, for all deflections of the gyro.

Let the distance RO, which makes the constant angle α with the gun bore axis, be denoted by d and the point R so chosen that the optical distance $ROBC$ is equal to the focal length f of the collimating lens C. A detailed analysis reveals the following facts. If the gyro axis ON is deflected in elevation through an angle φ (this means a rotation about O in the plane of the paper) the line of sight ET is turned through an angle Λ_E given by

$$(5.32)\quad \tan \Lambda_E = \frac{\sin \varphi \cos \varphi}{\dfrac{f}{2d} - \sin^2 \varphi}.$$

Since the angles involved will not exceed, say 15°, first order approximations give

$$(5.33)\quad \Lambda_E = \frac{2d}{f}\varphi, \ (2d < f).$$

The angle φ corresponds in figure 79 to

$$\gamma - \eta = (1 - a)\,\Lambda_k,$$

which leads us to define the sight parameter, a, as

$$(5.34)\quad a = 1 - \frac{f}{2d}.$$

An azimuth deflection of the gyro axis through an angle θ (a rotation about O in a plane through ON perpendicular to the plane of the paper), on the other hand, occasions an azimuth deflection of ET through an angle Λ_A, where

$$(5.35)\quad \tan \Lambda_A = \frac{\sin \theta \cos \theta \cos \alpha}{\dfrac{f}{2d} - \sin^2 \theta \cos^2 \alpha}.$$

This expression, were it not for the factor $\cos \alpha$, would be identical in form with that of (5.32). First order approximations give

$$(5.36)\quad \Lambda_A = \cos \alpha \left(\frac{2d}{f} \theta \right)$$

which would correspond to a sight parameter of

$$(5.37)\quad a = 1 - \frac{f}{2d \cos \alpha}.$$

This dilemma of having two separate a-values may be resolved in practice by taking a weighted average of the two expressions in (5.34) and (5.37). The interested reader will find upon investigating that, for simultaneous azimuth and elevation deflections θ, φ of the gyro axis, the corresponding line of sight deflections are

$$(5.38)\quad \tan \Lambda_A = \frac{\sin \theta \cos \varphi\,(\cos \alpha \cos \theta \cos \varphi + \sin \alpha \sin \varphi)}{\dfrac{f}{2d} - (\sin^2 \varphi + \cos^2 \alpha \sin^2 \theta \cos^2 \varphi)}$$

and

$$(5.39)\quad \tan \Lambda_E = \frac{\cos \varphi\,(\cos \theta \sin \varphi - \sin \alpha \cos \alpha \sin^2 \theta \cos \varphi)}{\dfrac{f}{2d} - (\sin^2 \varphi + \cos^2 \alpha \sin^2 \theta \cos^2 \varphi)};$$

the first order approximations being the same as before. The errors made in accepting the approximations (5.33) and (5.36), known as "optical dips", are to second order terms only,

$$(5.40)\quad \Delta \Lambda_A = \left(\frac{2d}{f} \sin \alpha \right) \theta \varphi,$$

$$\Delta \Lambda_E = \left(\frac{2d}{f} \sin \alpha \cos \alpha \right) \theta^2.$$

Hence, we conclude that by proper choice of f, d, α, an average sight parameter, a, may be chosen. The theoretical implications and attendant advantages upon introducing a sight parameter have already been discussed in the preceding chapter.

The function of the reticle disks is the determination of present range, r, to the target and, mechanically, since the time of flight multiplier u is dependent upon r, they serve to effect the relationship (5.31). One of these disks is fixed, and is perforated with a central hole (whose image at G on the viewing glass is the pip) and six radial slits (figure 84). The second disk, rotatable with respect to the first by operating a pair of foot pedals or a throttle hand grip, has a central hole and six spiral slits (figure 85).

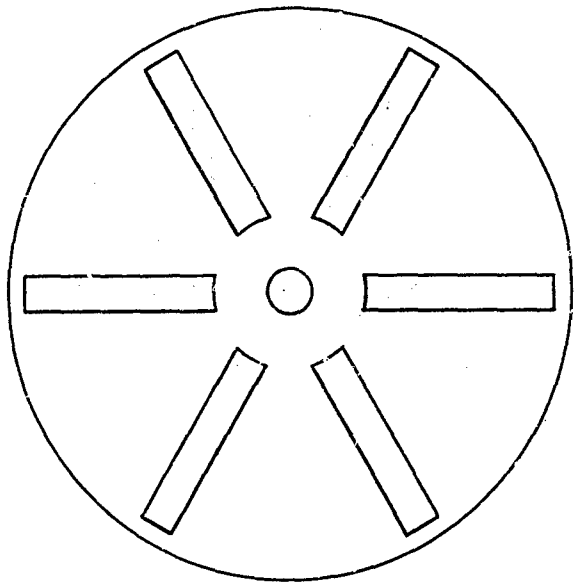

Figure 84. — Reticle and Stadiametric Ranging Disk — Radial Slits

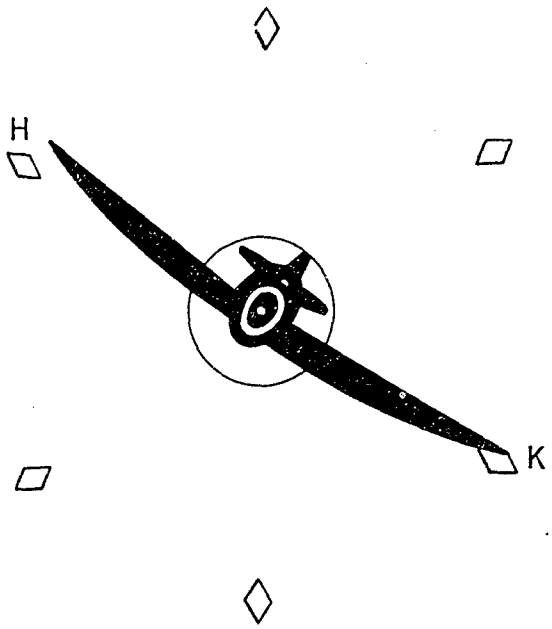

Figure 86. — Stadiametric Ranging

The only light passing through the reticle (and hence imaged on the viewing glass) will be that through the hole and the six diamond-shaped openings where the radial and spiral slits overlap. The resulting projection on the viewing glass is shown in figure 86. As the one disk rotates, the six diamonds approach or recede from the pip. Initially, the gunner presets the correct target span for the enemy plane by twisting the spiral disk to agree with the known wingspan of his target, thereby giving him a reference size around which he can expand and contract the ranging diamonds. Range is then determined automatically as the unknown part of a simple proportion arising from two similar triangles. Thus, in figure 87, if E represents the operator's eye which is essentially distant f units from the actual reticle, then if MP is the known wingspan, the range r out to the target is determined from the proportion

(5.41) $\dfrac{r}{f} = \dfrac{MP}{HK}$, where HK is the diameter of the reticle diamond image.

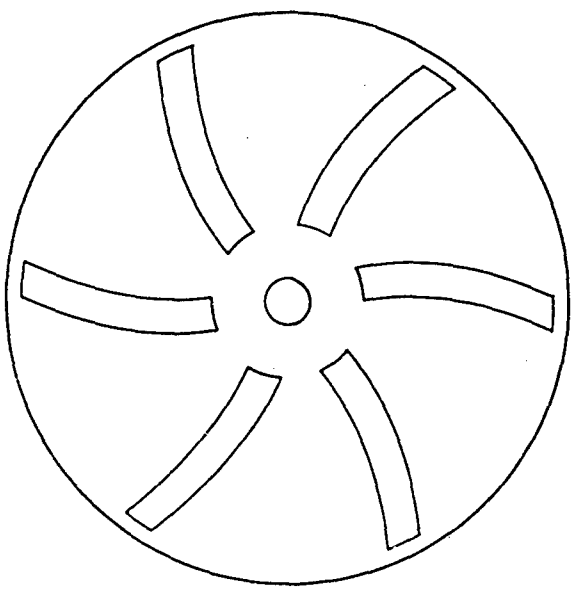

Figure 85. — Reticle and Stadiametric Ranging Disk — Spiral Slits

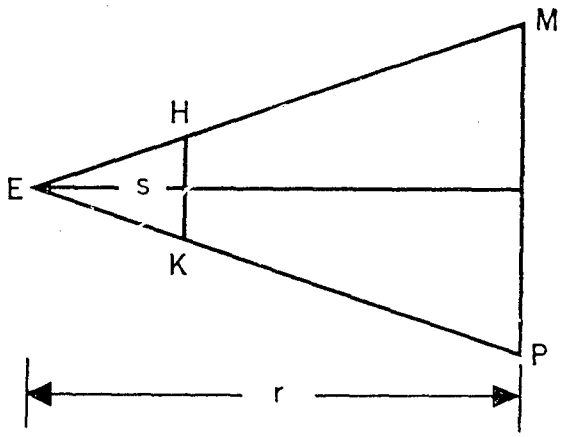

Figure 87. — Geometry of Stadiametric Ranging

It should be noted that in this proportion the distance f is actually independent of the distance of the operator's eye from the viewing glass since, as has been mentioned previously, the reticle image has been focused at infinity.

Range, determined by the method above, is said to be obtained stadiametrically.

5.6 Free, Constrained, and Captured Gyros and Their Uses

A gyroscope mounted as in figure 75 and subject to no external torques is said to be free. The spin axis is free to assume any direction in space and, once set spinning, will maintain that direction regardless of any motion of the system in which it is mounted. Besides serving as the basis of the navigational gyro-compass, free gyroscopes find ready application, in aircraft fire control systems, as attitude indicators. Thus in high level bombing, the free gyro with its axis set spinning in the vertical, is used by the bombsight as a physical reference line from which to measure the dropping angle. The bombsight also may employ a gyro with axis horizontal in order to provide a direction from which to measure the drift angle. The dive or glide angle of an unbanked aircraft can be measured with a free gyro, using the gimbal arrangement of figure 75, as the angle between the spin axis (set into the true vertical) and the plane of the two outer gimbal rings, assuming the bearings locked at C and D. A rearrangement of the Cardan suspension can be employed similarly to determine the angle of bank.

Theoretically, at least, a free gyro may be used in a lead computing sight instead of a precessing gyro, with the gyro, gun, and sight lines coupled as in figure 79, providing that the coupling parameter "a" be varied properly with the time. Thus in figure 79 we have, upon differentiating the coupling equation

$$\eta - \sigma = a(\gamma - \sigma)$$

with respect to the time,

$$(5.42) \qquad \dot{\eta} - \dot{\sigma} = \dot{a}(\gamma - \sigma) + a(\dot{\gamma} - \dot{\sigma}) .$$

Now if the gyro is free, $\dot{\eta} = O$ and (5.42) may be simpified to the form

$$(5.43) \qquad a\dot{\Lambda}_K + \dot{a}\Lambda_K = -\dot{\sigma} .$$

If now $\dot{a}$ be varied so as to yield values equal to $-\frac{1}{u}$, where u is the time of flight multiplier, there is obtained the familiar lead computing sight equation

$$-a\,u\dot{\Lambda}_k + \Lambda_k = u\,\dot{\sigma} .$$

Perhaps the most popular application of gyroscopes in aircraft fire control instruments is that of measuring the angular rate of a continuously varying direction in space. The direction may be a physical line like the gun-bore axis, telescope axis, or longitudinal axis of the aircraft, or it may be an artificial "computing line" related analytically to these by some sort of linkage. Rate gyros currently in use are of two main types:

(A) The constrained or "deflecting" type wherein the torque due to the imposed angular rate is opposed or constrained by a spring-like force so that the deflection of the gyro is proportional to the rate being measured and is used as a measure thereof.

(B) The captured type of rate gyro wherein the deflection of the gyro is opposed by a torque which always keeps the gyro from deflecting more than a small amount and where the torque required to thus "capture" the gyro is used as a measure of the angular rate.

An example of type A was taken up in section 5.4, wherein the spring-like force arose out of the interaction of the eddy currents in the dome with the magnetic field between the pole faces.

Chapter 6

BOMBING

6.1 Introduction

The methods of bombing from airplanes considered in this chapter may be listed as follows:

(A) Horizontal high-level bombing

(B) Horizontal low-level bombing

(C) Dive bombing

(D) Toss bombing.

In level bombing, the aircraft flies, during its bombing run, a horizontal straight line. Low-level bombing is restricted in general to altitudes below 5000 feet, a region in which the air resistance operating on the bomb during its fall is negligible by comparison with that obtaining at much higher altitudes. High-level bombing then refers to an altitude range extending from 5000 feet up to the ceiling of the aircraft.

The methods of dive and toss bombing are most simply explained by referring to figures 88 and 89. In dive bombing, figure 88, the aircraft is directed at a point A beyond the target T, so that when the bomb is released at point R it will not fall short due to gravity. Hence, at release, the sight line to the target and the line of flight are at an angle to each other. In toss bombing, on the other hand, the aircraft dives directly at the target along the "collision course" DT, pulls out of the dive at point B and releases the bomb at a suitable point R along the pull-out curve BRE.

It will be the aim of this chapter to investigate mathematically the determination of the correct release points in terms of suitable input variables for each of the four bombing methods.

A. HIGH-LEVEL BOMBING

6.2 Vacuum Trajectory

To initiate the study of the action of a bomb in the air, we start from a situation with which we are all familiar: the motion of a freely falling body in a vacuum. Referring to figure 90, suppose that the bomber traverses the line from O to O' with constant speed V knots during an interval of t_f seconds, releasing a bomb at O which is H feet above the target at T. Since no air resistance is presumed to be acting, the horizontal component of the bomb's velocity also will be V at all points of its trajectory, and hence, during its fall the bomb will remain ver-

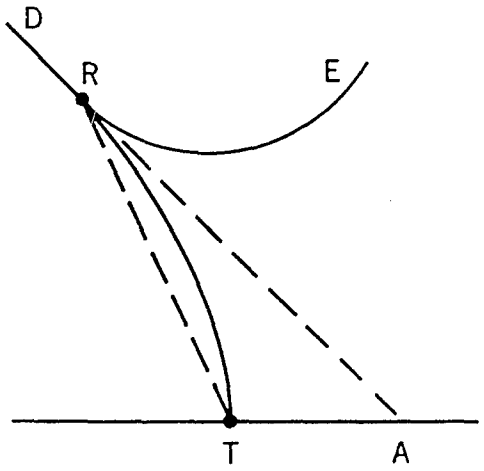

Figure 88. — Dive Bombing

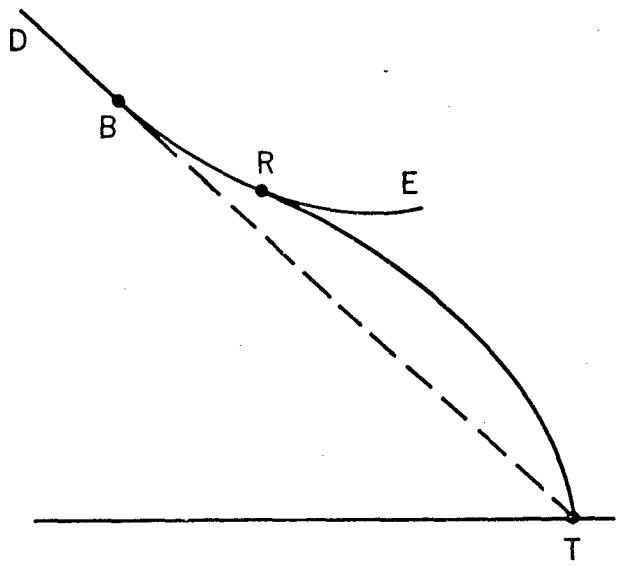

Figure 89. — Glide Bombing

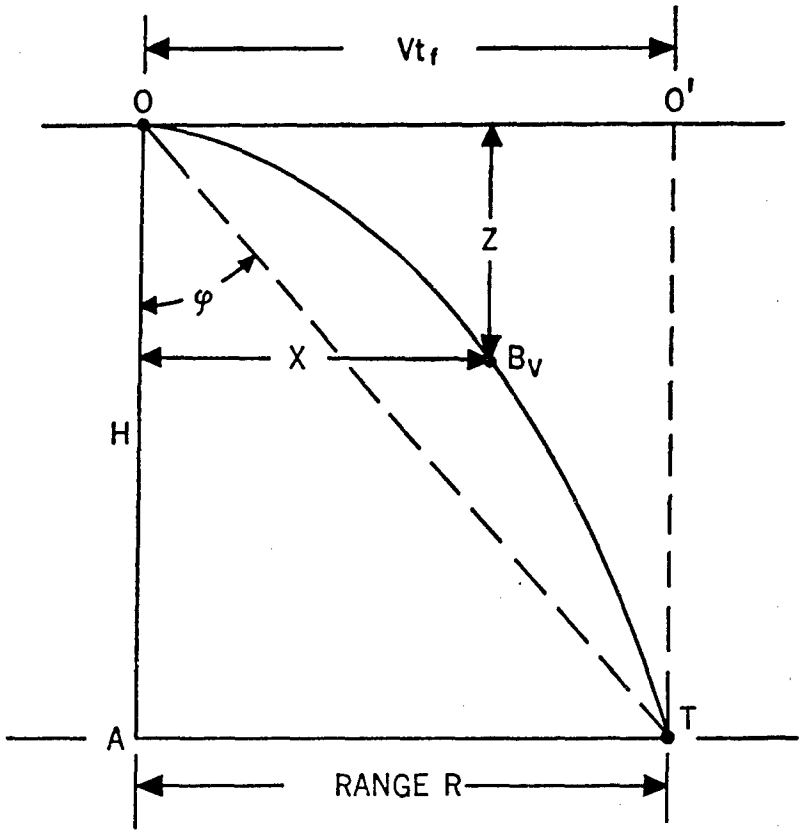

Figure 90. — Vacuum Trajectory — Bomb

tically below the aircraft. The space path of the bomb is the parabolic arc OBT while its path relative to the bombardier is simply a vertical straight line.

If at any instant t, the space coordinates of the bomb B_V are X and Z (see figure 90), then the differential equations defining the bomb trajectory are

$$(6.1) \quad \dot{X} = V, \quad \ddot{Z} = g = 32.2 \text{ ft/sec}^2.$$

Integrating (6.1) with the initial conditions $t = O$, $X = Z = O$, $\dot{Z} = O$, we find

$$(6.2) \quad X = Vt, \quad Z = \tfrac{1}{2} gt^2 .$$

The rectangular equation of the parabolic path is then

$$Z = \frac{gX^2}{2V^2} .$$

At time $t = t_f$, if the point O is correctly placed, the bomber is directly above the target at O' and a hit has been scored at T. The vacuum range R is then equal to Vt_f and the range angle φ, which is the angle at the time of release between the true vertical and the line of sight to the target, is given by

$$(6.3) \quad \varphi = \tan^{-1}\left(\frac{Vt_f}{H}\right) .$$

From (6.2),

$$H = \frac{g}{2} t_f^2 ,$$

so that (6.3) may be written free of t_f as

$$(6.4) \quad \varphi = \tan^{-1}\left(V \sqrt{\frac{2}{gH}}\right) .$$

To hit a target, then, when flying straight and level at a predetermined altitude and speed, it is only necessary, assuming air resistance on the bomb during its fall to be negligible, to fly in the invariant vertical plane containing the target and to drop the bomb as soon as the target appears at an angle φ from the vertical, given by (6.4). For an aircraft flying at 10,000 feet above the target and at a speed of 350 knots, the time of fall t_f would be 25 sec., the range 14,625 feet, and the range angle φ would amount to 55°38′.

6.3 Air Trajectory Under No Wind

Let us now remove the vacuum restriction, which is a poor first approximation at any but the lowest altitudes, and see what the effects of air resistance are upon the bomb. We shall assume in this section that there is no motion of the air with respect to the ground, i.e., no wind conditions prevailing.

Put qualitatively, air resistance has the following important effects:

(a) It decreases the vertical velocity of the bomb at any instant, thereby increasing the time of fall, t_f.

(b) It diminishes the horizontal velocity of the bomb at any instant, thus causing the bomb to trail behind the vertical line from the bomber.

These effects vary with

(a) The shape, weight, and size of the bomb,

(b) The altitude (and hence the air density)

(c) The airspeed of the bomber.

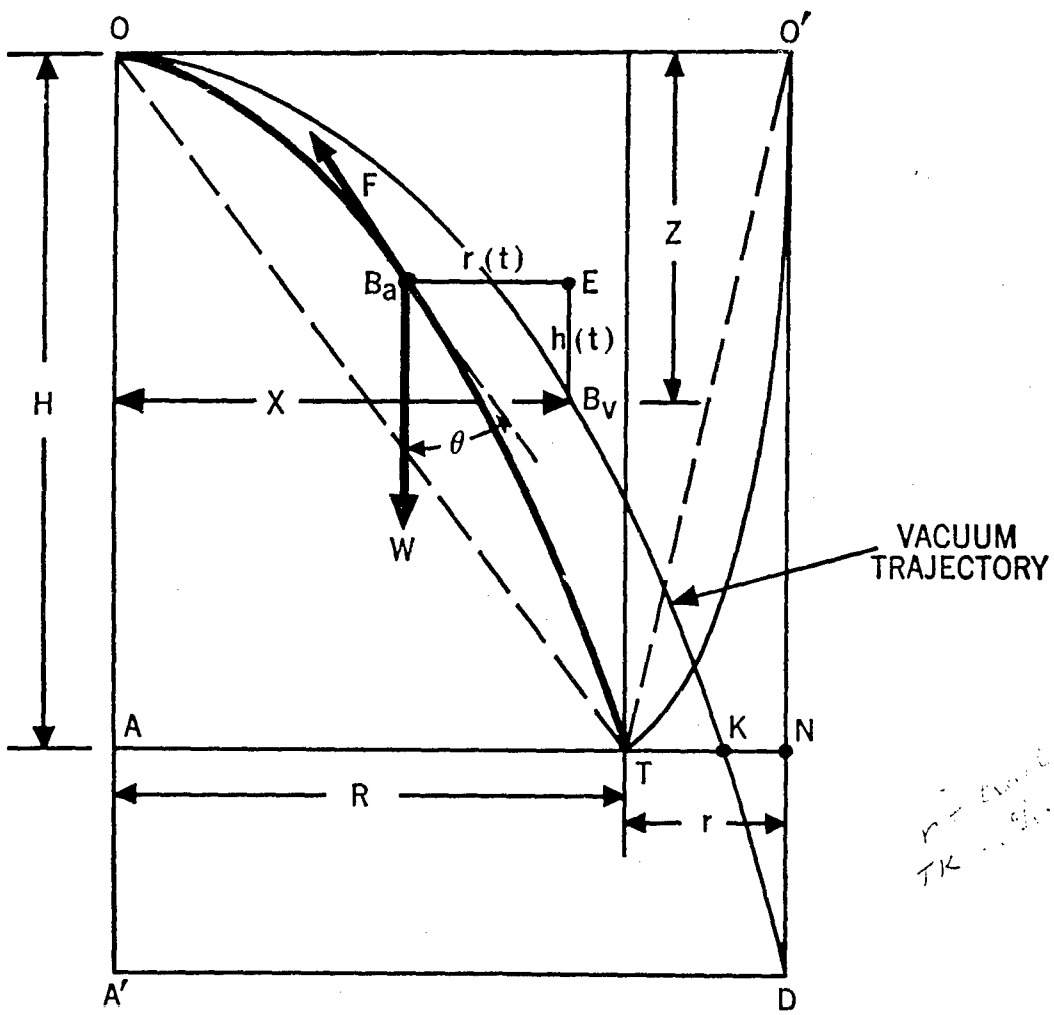

Figure 91. — Vacuum and Air Trajectories — Bomb

Figure 91 illustrates the change of the position of a bomb which is dropped in still air from that of a bomb dropped in a vacuum, if the bombs were observed at the same instant of time. Thus, two bombs released at the same instant at point O, the one falling in still air, the other in a vacuum, will describe the trajectories OB_aT and OB_vD, respectively, in the same time t_f. When the "air bomb" is at B_a, the "vacuum bomb" will be at B_v; when the "air bomb" strikes the target at T, the "vacuum bomb" will be at D. The bomb falling in air will describe, relative to the aircraft, the curved path $O'T$ while that falling in vacuo is describing the straight line $O'D$. At time t, then, B_a will lag B_v by $B_aE = r(t)$ horizontally and by $EB_v = h(t)$ vertically, the functional notations being used to indicate dependence on time. The quantity $r(t)$ is called the TRAIL and is denoted at the target by the letter r. Thus,

$$r(t_f) \equiv r.$$

It should be noted that the trail r is not equal to TK. The quantity TK is known as the ground lag. Actually, $r = TK + KN$, which says that trail r is equal to the ground lag plus the distance that the aircraft travels during the time lag. The time lag here is the fractional part of t_f which it takes the bomb on the vacuum trajectory to traverse the arc KD.

In figure 91 there is indicated the set of forces acting on the bomb B_a: the weight of the bomb W and the air resistance F, assumed tangent to the trajectory and directed opposite to the motion of the bomb. In the absence of yaw and other secondary effects, these then will be the only forces acting. The resistance function F depends upon the weight of the bomb, its shape and size, the air density ρ_a, and the velocity v of the bomb with respect to the air mass. As explained in chapter 1 the first two of these are incorporated into a single quantity C, called the ballistic coefficient. The force F can then be written

$$(6.5) \qquad F = \frac{\rho_a}{C} f(v)$$

where $f(v)$ is a function of velocity only. The air density ρ_a, in terms of the coordinate system of figure 91, is

$$(6.6) \qquad \rho_a = \rho_o e^{-K(H-Z)}.$$

The quantity ρ_o then represents the density at the point of fall T. For the standard air structure considered here, see section 1.7, assuming the target to be at sea level,

$$\rho_o = .07513 \text{ lb./ft}^3, \quad K = .0000316 \text{ ft.}^{-1}.$$

It will be noticed from (6.5) that F diminishes as C increases and hence, that the larger the ballistic coefficient the more efficient will be the bomb.

With θ defined as in figure 91, we find, upon taking components of the forces F and W upon the horizontal and vertical, that the equations of motion for the bomb are,

$$(6.7) \qquad m\ddot{X} = -\frac{\rho_a}{C} f(v) \sin\theta$$

$$(6.8) \qquad m\ddot{Z} = mg - \frac{\rho_a}{C} f(v) \cos\theta$$

$$(6.9) \qquad \dot{X} = \dot{Z} \tan\theta$$

$$(6.10) \qquad v = \dot{X} \csc\theta = \dot{Z} \sec\theta,$$

with the initial conditions

$$(6.11) \qquad t = O, \quad X = O, \quad Z = O, \quad \theta = \frac{\pi}{2},$$
$$v = V, \quad \dot{Z} = O$$

wherein V is the true airspeed of the bombing plane. Equations (6.7) and (6.8) reduce to (6.1) when $C = \infty$, that is, for a vacuum trajectory.

An interesting interpretation of the ballistic coefficient C, in terms of the terminal velocity v_t of a bomb falling vertically, can be made using (6.7) and (6.8). Here we should have $\theta \equiv O$, and, at the instant the bomb strikes the ground, $v = v_t$, $\rho_a = \rho_o$, $\ddot{Z} = O$; hence

$$(6.12) \qquad C = \frac{\rho_o}{g} f(v_t).$$

Thus, from a knowledge of the terminal velocity v_t, the ballistic coefficient can be computed as soon as the form of the function $f(v)$ has been assigned.

Integration of equations (6.7) thru (6.10) also will depend upon the retardation function $f(v)$. Considerable experimental research has gone into the determination of suitable forms for this function, the choice of form being guided by the accuracy with which experimentally determined trail values can be approximated. In particular, the form

$$(6.13) \quad f(v) = kv^2$$

where k is an empirical constant, leads not only to trail values of the proper order but also, as the interested reader may verify, renders the equations (6.7) to (6.10) solvable by quadrature when ρ_a is held constant.

The amount of trail is a function of the indicated airspeed of the bomb, or plane, at the time of release. It is, in addition, dependent upon the altitude of release and, of course, the ballistic coefficient C of the bomb. Trail and time of fall (t_f) values for each type of bomb are determined during the calibration of the bomb at the Proving Ground and are set forth in tabular form, trail being given in angular measure (mils). The latter measure, sometimes referred to as the bombing mil, is an angular measure that should not be confused with the Navy mil, the Army mil, or the mathematical mil. A Navy mil is a definite angle and is equal to the tan^{-1} .001; or 3.438 minutes of arc. An Army mil is 1/6400 of a circle; or 3.375 minutes of arc (tan^{-1} .000982). A mathematical mil is 1/1000 of a radian, which is the angle subtended by an arc whose length is equal to the radius of the circle.

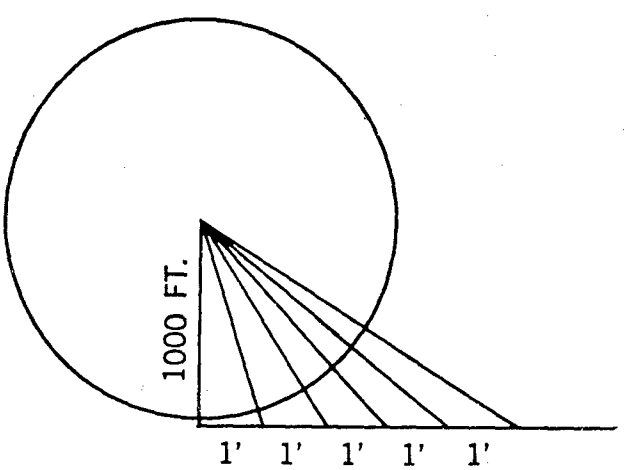

Figure 92. — The Bombing Mil

Angles with equal bombing mil values subtend the same distance on the base line, but are not equal in angular measure, growing smaller as they depart from the vertical as indicated in figure 92. The value of an angle in bombing mils may be found by dividing the distance on the ground by 1/1000 of the altitude; and this is its interpretation in bombing practice.

In comparing bombing scores, an air bomber whose average error from 10,000 feet is 100 feet should be considered as good a bomber as one whose average error from 5,000 feet is 50 feet because in each case the average error is 10 mils. The bombing mil system expresses distances on the ground in terms of altitude, therefore, statements concerning distances on the ground must be qualified by a statement of the bombing altitude.

From figure 91, it is evident that the range R of the bomb dropped in air is obtained by subtracting the linear trail value TN from the vacuum range AN. Since $AN = Vt_f$ (target assumed stationary), we have

$$(6.14) \quad R = Vt_f - r$$

and the range angle is then given by

$$(6.15) \quad \varphi = \tan^{-1} \frac{Vt_f - r}{H} .$$

For a bomber flying at $H = 10{,}000$ feet at an indicated airspeed of 300 knots ($V = 350$ knots true airspeed), the bomb ballistic tables show, for a bomb of ballistic coefficient $C = 2$, that $t_f = 26.01$ secs. (an increase of 1.01 secs. over the vacuum value), trail $r = 189$ mils ($= 1890$ feet in linear units), so that equations (6.14) and (6.15) yield $R = 12{,}735$ feet, $\varphi = 51°52'$. These figures show quite plainly that air resistance can by no means be neglected for precision bombing.

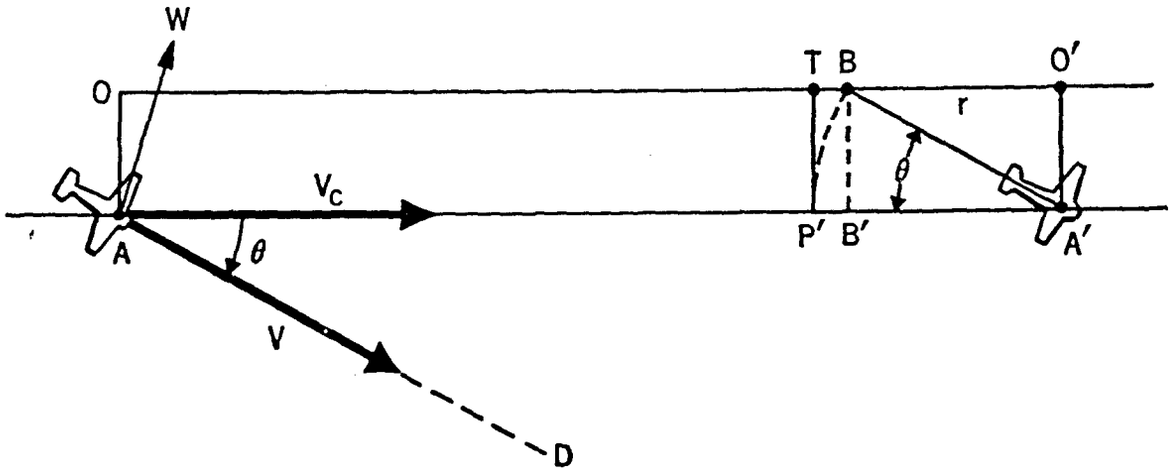

Figure 93. — Drift Angle and Trail

6.4 Drift and Target Motion

The discussion up to this point has been based strictly on the conditions of still air and a stationary target. Let us for the present remove the first of these restrictions and consider the problem of hitting a stationary target. Later in this section we shall see how target motion can be accounted for. Since we are here assuming a standard air structure, the wind will be considered as moving horizontally only, with constant speed and direction at all points of the bomb trajectory. Thus, we shall have no vertical component of wind to contend with.

In the plan view of figure 93, the horizontal plane through the bomber A is projected upon the horizontal plane through the target T. Line AD gives the direction in which the aircraft is being steered, namely the plane's heading. The vector $\mathbf{V}$ is then the velocity of the bomber with respect to the air. The wind vector $\mathbf{W}$, representing the velocity of the air with respect to the ground, combines with $\mathbf{V}$ to give $\mathbf{V}_c$, the velocity of the bomber with respect to the ground. Thus,

$$\mathbf{V} + \mathbf{W} = \mathbf{V}_c \ ,$$

wherein the line of action of the vector $\mathbf{V}_c$ is called the bomber's track, represented by line AA'. The angle $\angle\ A'AD = \theta$, formed by the heading and the track, is called the drift angle. We use the notation V_c here to denote the ground speed of the bomber rather than the notation V_g because the former, which we shall call the closing speed, includes the case of a moving target, even though, in the present instance, the target is considered to be stationary. The closing velocity, $\mathbf{V}_c$, is defined in general by

$$\mathbf{V}_c = \mathbf{V} + \mathbf{W} - \mathbf{V}_T, \tag{6.16}$$

where $\mathbf{V}_T$ is the velocity of the target. From this we see that if there is no wind or target motion, then $\mathbf{V}_c = \mathbf{V}$ and the closing speed is then the same as the true airspeed of the bomber. If there is a tail wind, V_c becomes true airspeed plus wind velocity; while in a head wind, V_c becomes true airspeed minus wind velocity. When the target is moving, that part or component of the motion which is in the same direction as the airplane's heading gives the same effect as if there were a head wind of the same force as the range component of the target's speed. A target moving toward the plane gives the same effect as a tail wind since it increases V_c.

There are three important points to be noted in figure 93. First of all, the direction of the trail r: the trail always lies in the vertical plane through the longitudinal axis of the aircraft, is measured from the vertical to the rear of the aircraft's heading, and is independent of the wind. Secondly, it will be noted that because of this fact the bomber, to secure a hit, must fly so that its track will pass to one side of the target by the amount $P'T = r \sin \theta$. This quan-

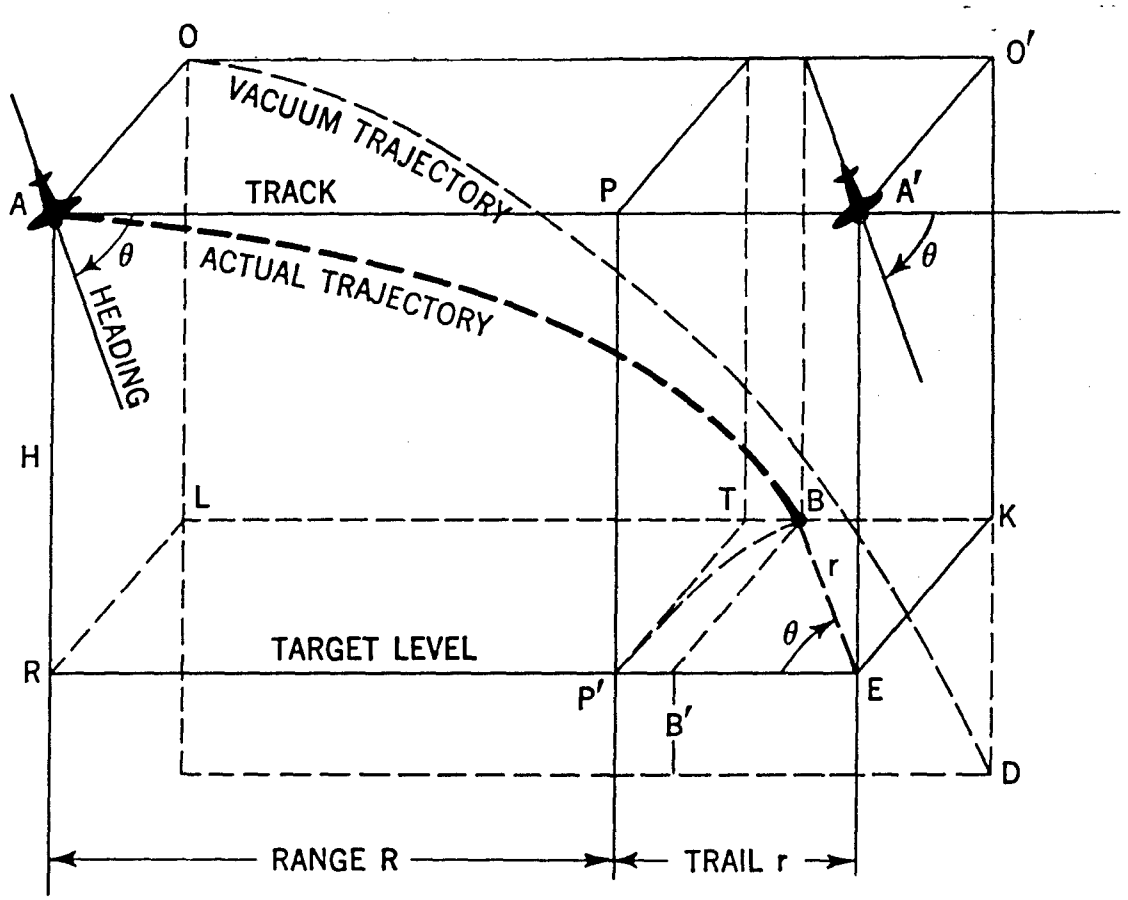

Figure 94. — The Bombing Problem — Three-dimensional View

tity, $r \sin \theta$, is called the cross trail. Thirdly, as figure 93 shows, the bomb will strike, unless a special correction is made, not at the target T but at a slight distance forward at B. To account for this, it must be remembered that r depends on C (ballistic coefficient), V_i (indicated airspeed of bomber at release), and H (altitude above target) but is independent of W and hence of θ. Thus, only when θ is zero, namely for flight in still air, upwind or downwind along OO' will the bomb strike at T. Hence, to secure a hit at T, the bomb should be released when the aircraft is a distance $TB = r\ (1 - \cos \theta)$ back from A along the track. The expression $r\ (1 - \cos \theta)$ is called the range component of cross trail. It is usually very small, being obscured by other bombing errors, and for this reason is sometimes omitted from consideration in constructing bomb sights.

So far, we have considered the target to be stationary. In order to take target motion into account we may resolve the target velocity $\mathbf{V}_T$ into components along and perpendicular to the plane's heading. Then, that component of the target's motion along the plane's heading gives the same effect as a head wind or a tail wind depending upon whether its direction is the same as that of $\mathbf{V}$ or $-\mathbf{V}$. Similarly, the component of the target's motion across the plane's heading may be considered as a cross wind and absorbed in the solution for the drift angle θ by combining it with the wind vector $\mathbf{W}$. Hence, the effect of target motion is merely to change the values of $\mathbf{V}$ and $\mathbf{W}$ and then to regard the target stationary as before. The range angle φ, whose accurate determination is the crux of the whole bombing problem, is thus obtained from

$$(6.17) \qquad \varphi = \tan^{-1} \frac{V_c t_f - r}{H} .$$

The final diagram for high-level bombing, depicting the situation in three dimensions, is shown in figure 94. The actual trajectory of

the bomb is shown with impact point at B, so that, as in figure 93, the range component of cross-trail is the distance TB. In still air, the track of the plane would be the line OO' but under wind conditions the track becomes AA'. A bomb dropped in a vacuum at point O would strike at D at the same instant that the actual bomb strikes at B. It should be noted finally that in the figure the actual trail is the distance EB and that this distance also is equal to EP'.

6.5 Mechanization

As formula (6.17) indicates, the correct range or dropping angle φ is a function of the trail, altitude above the target, time of flight of the bomb, and the closing speed, V_c. Preliminary to this, there is the problem of establishing the proper track, parallel to a collision course with the target and distant from it an amount equal to the cross-trail, $r \sin \theta$. A bombsight computer for determining φ will then have as inputs: r, H, t_f, and V_c. The trail, r, is obtained from trail tables, wherein it is given as a function of altitude, airspeed, and bomb ballistic coefficient, and can thus be set in by the bombardier. The altitude input is available from an altimeter while time of flight is tabulated as a function of altitude. Closing speed V_c is obtained by tracking the target with a telescope, keeping the horizontal (range) cross wire continuously on the target. Modern bombsights have the telescope mechanically stabilized with vertical and horizontal gyros so that physical reference lines are available from which to measure the range and drift angles. The drift angle θ can be obtained by having the bombsight always point directly at the target. Then the angle between the longitudinal axis of the aircraft and the direction in which the sight is pointing will be the drift angle providing that the heading of the plane is correct for the wind conditions prevailing. The bombardier establishes the angle of drift by positioning the telescope cross wires so that the target moves along the vertical cross wire. If the plane's heading is slightly off, the target will drift off the wire. By means of an instrument called the Pilot Direction Indicator, the pilot of the aircraft is afforded a continuous indication of the direction in which the target drifts off the vertical wire and can then direct his plane accordingly. Finally, the matter of cross trail is settled easily by tilting the telescope transversely through a small angle sufficient to intercept the correct amount of cross trail on the ground.

B. LOW-LEVEL BOMBING

6.6 Impracticability in Range Angle Aiming at Low Altitudes

A bombsight, designed to operate at altitudes below 5000 feet, requires extreme accuracy in measurement of the input variables when the range angle method, outlined in Part A of this chapter, is used as a criterion for bomb release. This is especially pronounced when the altitude falls below 1000 feet, as it does in the case of depth-charging of submarines from low-flying aircraft. At such low altitudes the trail term, r, of equation (6.17) is negligible by comparison and the range angle, φ, is given quite accurately by the "vacuum expression"

$$(6.18) \qquad \varphi = \tan^{-1}\left(\frac{V_c t_f}{H}\right) = \tan^{-1}\left(V_c\sqrt{\frac{2}{gH}}\right).$$

The very form of (6.18) shows the close dependence of the range angle upon altitude and closing speed. Hence, unless the altitude and closing speed can be held very closely to preassigned values, errors in these quantities will produce large range errors on the ground. Thus, a 1% error in altitude measurement at $H = 400$ feet will result in a range error of approximately 9 feet, V_c being assumed equal to 350 feet per second and without error. Similarly, a 1% error in closing speed at $V_c = 350$ feet per second and $H = 400$ feet gives a range error of 18 feet.

To overcome the above difficulties, recourse is had to measurement of the angular rate, $\dot{\varphi}$, instead of φ, as a criterion for bomb release. The mathematical expression for $\dot{\varphi}$, derived in the next section, shows it to be relatively independent of the altitude for small values of the altitude, a quality which serves as a sound basis for a low-altitude bombsight.

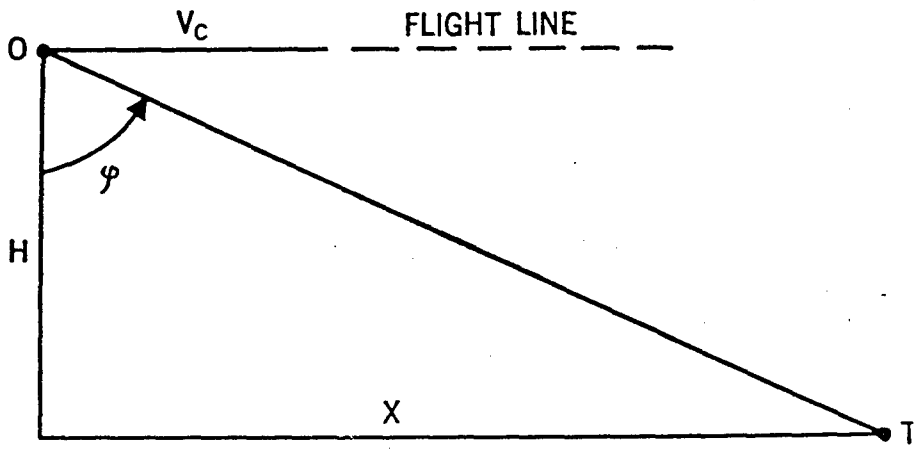

Figure 95. — Low-level Bombing

6.7 The Angular Rate Principle

During the early stages of a low-level approach, when the target is at a considerable distance from the aircraft, the angle of depression of the target $(90° - \varphi)$ changes very slowly so that the angular velocity of the target at the observer's eye is low. As the aircraft nears the target, the angular velocity increases, finally becoming a maximum as the aircraft passes vertically over the target. At some stage the target was in an appropriate position for a bomb to be released, and at that point it had an angular velocity that could be calculated in terms of the height and ground speed of the aircraft. If this calculated angular velocity is set up on an appropriate bombsight in such a manner that we can detect when the target has an equal angular velocity, then we have an indication as to the instant, during the tracking run, when a bomb should be released to strike the target. We now derive an expression for the calculated angular rate, $\dot{\varphi}$.

From figure 95 we note that

$$\tan \varphi = \frac{X}{H} . \tag{6.19}$$

Differentiating with respect to the time, we find, since $\dot{H} = O$,

$$\dot{\varphi} \sec^2 \varphi = \frac{H\dot{X}}{H^2} = \frac{HV_c}{H^2} .$$

Therefore,

$$\dot{\varphi} = \frac{HV_c}{(H \sec \varphi)^2} = \frac{HV_c}{H^2 + X^2} .$$

At the proper release time,

$$X = V_c\, t_f = V_c \sqrt{\frac{2H}{g}} ,$$

whence,

$$\dot{\varphi} = \frac{HV_c}{H^2 + \dfrac{2HV_c^{\,2}}{g}} .$$

With a little manipulating, this may be written finally as

$$\dot{\varphi} = \frac{g/2}{V_c \left(1 + \dfrac{gH}{2V_c^{\,2}}\right)} . \tag{6.20}$$

Thus, (6.20) furnishes, at the correct moment of bomb release, the angular velocity of the target in terms of the height and closing speed. It will be noted that for small values of H the term $\dfrac{gH}{2V_c^{\,2}}$ is small, thereby accounting for the relative insensitivity of $\dot{\varphi}$ to changes in altitude.

988995 O - 52 - 10

In actual practice, the time of free fall t_f used above must be corrected for bomb trail, lag of the bomb rack in making its release, and also for horizontal and vertical parallax introduced by the physical separation of bombsight and bomb.

6.8 Mechanization

An early mechanization of the angular rate principle involved a rotating, internally illuminated drum upon which was cut a fine pitch spiral. A portion of the drum, when viewed through an optical system, revealed to the bombardier a set of horizontal illuminated lines moving downwards at a uniform velocity. The drum was driven about a vertical axis by a constant speed motor through a variable speed gear which allowed for variation in the rate of rotation of the drum. The variable speed gear in turn was connected by a flexible drive to a computer whose inputs were ground speed and altitude. Proper functioning of the computer then produced a drum rotation rate such that the illuminated horizontal lines moved at an angular rate equal to that of the target at the correct moment of bomb release.

When the target first appeared to the bombardier, on the upper end of the illuminated "ladder", it was moving downward more slowly than the horizontal lines which appeared to be overtaking the target. The difference in rates of the target and the lines became less and less, until at one instant the target and lines appeared stationary together. This was the correct moment of bomb release. After this instant, the target had a greater angular velocity than the lines, and appeared to overtake them.

More modern mechanizations of the angular rate principle employ a gyroscope to measure the angular rate of the target. Such sights are rotatable about horizontal and vertical axes so that the bombardier, after first aligning the sight properly in azimuth, tracks the target by rotating the sight vertically at such a rate as to keep an illuminated reticle on the target. Rotation of the sight precesses the gyroscope whose precession in turn is opposed by a spring. The tension of the spring is preadjusted for the bombing course to be run. It is set so that it will balance the torque of the gyroscope when the gyroscope is precessed at the angular rate that is critical for that course. One of the principal advantages of the modern angular rate bombsight is that it removes the undesirable feature in the early mechanizations of having the pilot judge when zero relative rate between the moving lines and the target is achieved. Indeed, any successful mechanization which removes the personal element is bound to improve the accuracy of the sight in question.

C. DIVE OR GLIDE BOMBING

6.9 Introduction

The situation obtaining in dive or glide bombing under conditions of no wind is represented pictorially in figure 96. At the point of bomb release, the flight line OA is offset from the sight line to the target OT by the angle $AOT = \lambda$.

This angle intercepts on the ground a distance L, called the linear aiming allowance. In terms of the sighting angle φ and the dive or glide angle θ we have, where X is the range DT,

$$(6.21) \quad \lambda = 90° - \varphi - \theta = \arctan \frac{H}{X} - \theta .$$

The aiming allowance L is found from

$$(6.22) \quad L = H \cot \theta - X .$$

In the vacuum case, the range DS may be found by eliminating t_f, the vacuum time of flight, between the familiar relations

$$(6.23) \quad H = \tfrac{1}{2} g t_f^2 + V \sin \theta \, t_f, \; DS = t_f V \cos \theta ,$$

where V represents the true airspeed of the airplane. Thus it is found that

$$(6.24) \quad DS = \frac{V \cos \theta}{g} \cdot \left[\sqrt{(V \sin \theta)^2 + 2gH} - V \sin \theta \right]$$

and,

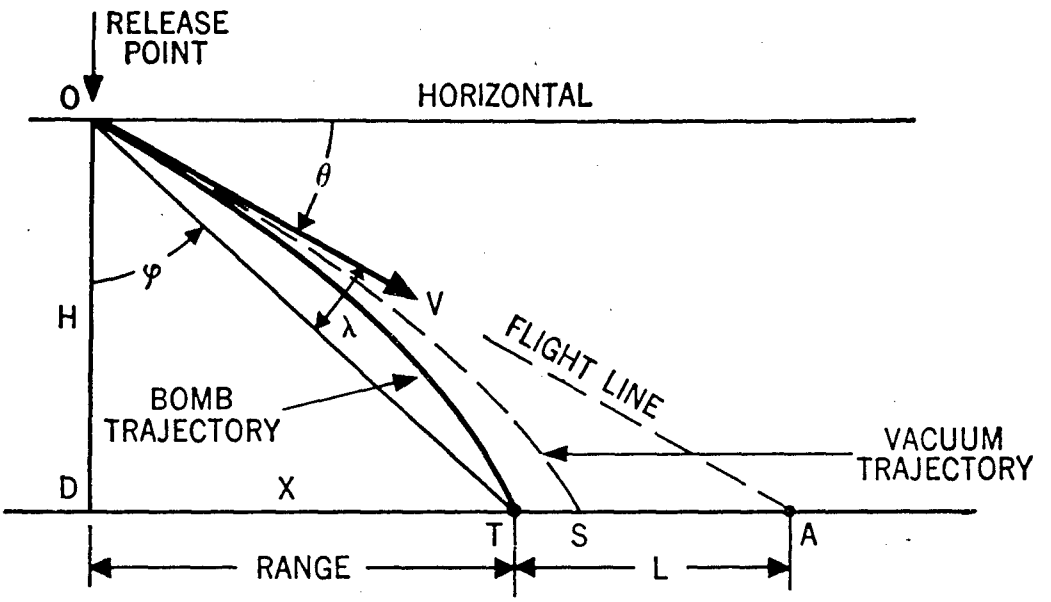

Figure 96. — Dive Bombing

(6.25) t_f (vacuum) =

$$\frac{\sqrt{(V \sin \theta)^2 + 2gH} - V \sin \theta}{g} .$$

Hence, neglecting air resistance, the angular aiming allowance λ is, from (6.21),

(6.26) λ (vacuum) =

$$\cot - {}^{1}\left[\frac{V \cos \theta}{gH}\left\{\sqrt{(V \sin \theta)^2 + 2gh} - V \sin\theta\right\}\right] - \theta .$$

By way of illustration we find that for $V = 300$ knots, $H = 4000$ feet, $\theta = 40°$:

$$DS = 3345 \text{ feet}, \quad t_f \text{ (vac.)} = 8.62 \text{ secs.},$$

$$\lambda \text{ (vac.)} = 10°6' .$$

Upon consulting a ballistics table for dive bombing, we find that when air resistance is taken into account, the range DT is 3299 feet, t_f becomes 8.91 secs., and λ is increased to 10°29′. The ground lag TS here is thus 46 feet.

6.10 Angular Rate of Sight Line (Vacuum Case)

From figure 96 and the relationship

(6.27) $$\tan \varphi = \frac{X}{H},$$

we find, upon differentiating with respect to the time,

$$\dot{\varphi} \sec^2 \varphi = \frac{H\dot{X} - X\dot{H}}{H^2} .$$

Solving for $\dot{\varphi}$ and using (6.27) we find

$$\dot{\varphi} = \cos^2 \varphi \left[\frac{H\dot{X} - X\dot{H}}{H^2}\right]$$

$$= \cos^2 \varphi \left[\frac{\dot{X} - \dot{H} \tan \varphi}{H}\right]$$

or

(6.28) $$\dot{\varphi} = \frac{\cos \varphi}{H}\left[\dot{X} \cos \varphi - \dot{H} \sin \varphi\right] .$$

If we consider the origin of coordinates to be at the target, then

$$\dot{X} = -V\cos\theta = -V_X$$

and

$$\dot{H} = -V\sin\theta = -V_H\,.$$

Equation (6.28) then becomes

$$(6.29)\qquad \dot{\varphi} = \frac{\cos\varphi}{H}\left[V_H\sin\varphi - V_X\cos\varphi\right].$$

Let us now rewrite (6.29) in the form

$$\dot{\varphi} = \frac{\sin\varphi\cos\varphi}{H}\left[V_H - V_X\cot\varphi\right]$$

and combine it with the "hitting criterion"

$$\cot\varphi = \frac{H}{V_X t_f} = \frac{H}{DS}$$

to get

$$(6.30)\qquad \dot{\varphi} = \frac{\sin 2\varphi}{2H}\left[V_H - \frac{H}{t_f}\right].$$

From (6.23) we find

$$\frac{H}{t_f} = V_H + \tfrac{1}{2}gt_f\,,$$

which, combined with (6.30), yields

$$(6.31)\qquad \dot{\varphi} = -\frac{g}{4H}\,t_f\sin 2\varphi\,.$$

Employing (6.25) we may write, finally,

$$(6.32)\qquad \dot{\varphi} = -\frac{\sin 2\varphi}{4H}\left[\sqrt{V_H^2 + 2gH} - V_H\right].$$

We note from (6.32) that the angular rate of the sight line, $\dot{\varphi}$, is a function of H, V_H, and φ only.

6.11 Mechanization, using Angular Rate

Formula (6.32) suggests a possible mechanization for a dive bombsight. If a mechanical computer, with inputs φ, H, V_H, and operating in accord with (6.32), is used to drive a telescope at the rate $\dot{\varphi}$ given by (6.32) then conceivably a pilot could so fly his plane that the target when viewed through the telescope would show no motion with respect to its cross-wires. At the instant of synchronization of target and cross-wires, the bomb would be released. The input φ would be obtained from the telescope's position in a vertical plane relative to the spin axis of a vertical gyro while H and V_H would be obtained from an altimeter and its differential output.

During the recent war, a sight was constructed to operate on the above principle but, after numerous flight tests, was finally rejected for several reasons. Firstly, it was found too difficult for the pilot to maneuver his plane in the diving attitude so as to achieve synchronization. Actually, the pilot had to fly a curved path through space and at the same time try to recognize a condition of no drift between the cross-wires and the target. Secondly, when once in a dive, the pilot found it almost impossible to make a deflection drift correction since there is no way to make an airplane move sideways in space. The fact that range and deflection drift change continuously creates a problem virtually impossible for the dive bombing pilot to solve.

The difficulties just cited could be made less prominent perhaps by a new mechanization procedure but could hardly be avoided altogether, since they are inherent in the dive bombing method. The method of toss bombing, considered in section (6.13), eliminates these difficulties for the pilot by permitting him to dive straight at the target.

6.12 Correction of Angular Rate for Trail

Since bombing does not take place in a vacuum, account must be taken of the effects of air resistance upon range. Referring to figure 96 we note that the actual range X is $DT = DS - TS$, where, because of the relatively low altitude for release H, the ground lag TS may

be replaced by the trail r, both being small. We have, then,

$$(6.33) \quad X = V_x t_f - r$$

$$(6.34) \quad \cot\varphi = \frac{H}{V_x t_f - r} .$$

Using (6.34) in

$$\dot{\varphi} = \frac{\sin 2\varphi}{2H}(V_H - V_x \cot\varphi) ,$$

we obtain at release time

$$\dot{\varphi} = \frac{\sin 2\varphi}{2H}\left[\frac{V_x(V_H t_f - H) - rV_H}{V_x t_f - r}\right] ,$$

or, upon rearrangement,

$$\dot{\varphi} = \frac{\sin 2\varphi}{2H}\left[\frac{V_H t_f - H}{t_f} - \frac{rV_H}{V_x t_f}\right] \cdot \left(1 - \frac{r}{V_x t_f}\right)^{-1} .$$

If now the last factor be expanded and non-linear terms in $\frac{r}{V_x t_f}$ be dropped, we find,

$$\dot{\varphi} = \frac{\sin 2\varphi}{2H}\left[\frac{V_H t_f - H}{t_f} \cdot \left(1 + \frac{r}{V_x t_f}\right) - \frac{rV_H}{V_x t_f}\right]$$

$$(6.35) \quad \dot{\varphi} = \frac{\sin 2\varphi}{2H}\left[\frac{V_H t_f - H}{t_f}\right] \cdot \left[1 + r\left(\frac{1}{V_x t_f} - \frac{V_H}{V_x(V_H t_f - H)}\right)\right] .$$

Recalling now the relation

$$V_H t_f - H = -\tfrac{1}{2} g t_f^2 ,$$

and using it in (6.35), we obtain

$$(6.36) \quad \dot{\varphi} = -\frac{g}{4H} \cdot t_f \sin 2\varphi \cdot \left[1 + \frac{H}{V_x t_f} \cdot \frac{r}{\frac{1}{2} g t_f^2}\right] .$$

Since $\cot\varphi \doteq \frac{H}{V_x t_f}$, we can put (6.36) in the form

$$(6.37) \quad \dot{\varphi} = -\frac{g}{4H} \cdot t_f \sin 2\varphi \left[1 + \frac{r\cot\varphi}{\frac{1}{2} g t_f^2}\right] .$$

Comparing (6.37) with (6.31) we note that the quantity in the brackets in (6.37) is the necessary correction factor to the vacuum rate given by (6.31). Thus,

$$(6.38) \quad \dot{\varphi}_{\text{air}} = \dot{\varphi}_{\text{vacuum}} \cdot \left[1 + \frac{r\cot\varphi}{\frac{1}{2} g t_f^2}\right] .$$

D. TOSS BOMBING

6.13 Basic Release Conditions for a Stationary Target

In toss bombing, the airplane is flown initially along a collision course, a straight line path containing the target. If the bomb were released enroute, gravity would cause it to fall short. To overcome the latter, the pilot pulls out of his straight-line dive and releases the bomb at a precalculated point along this pull-out curve. The essential geometric features of the problem are indicated in figure 97.

The straight-line dive at the target T, here considered to be stationary, is begun at a point above N, pull-out takes place at O along the curve OP. If the point P is calculated properly and release of the bomb occurs when this point is reached, the bomb trajectory will intersect the target. In the theoretical development to follow, we assume the final velocity of the aircraft in the dive to be reached at the point N and that this final velocity, which we shall denote by V, remains constant along the timing run NO and the pull-up arc OP. Knowledge of the time it takes the aircraft to cover the distance NO is used in determining the closing time, t_c, i.e., the time it would take the aircraft

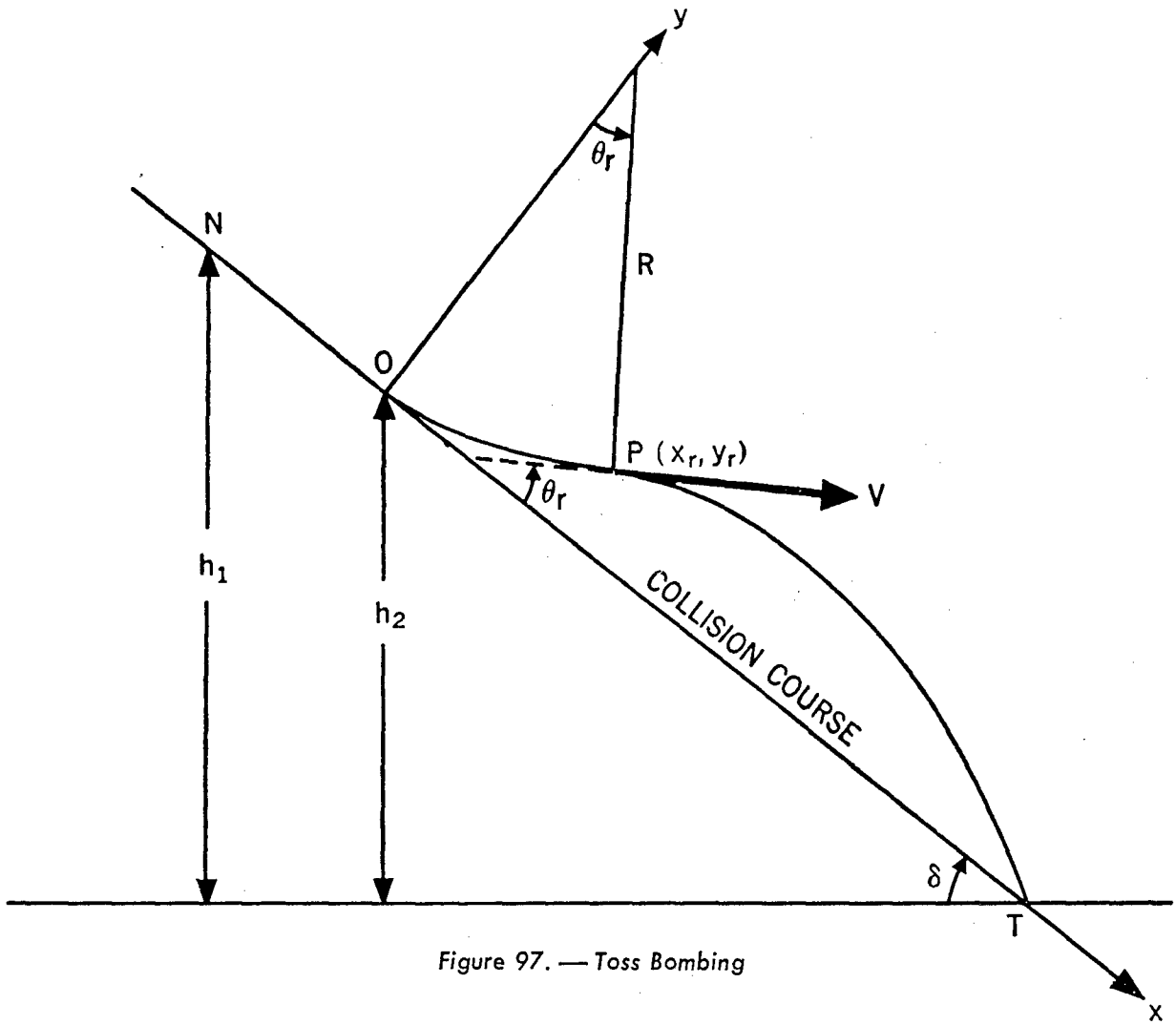

Figure 97. — Toss Bombing

to fly into the target along the collision course OT. The quantity t_c, in turn, is needed for computing the position of the release point P.

Since the speed V is constant, the point O can be determined by requiring the time for the aircraft to cover NO to be a fixed fraction f, $(f < 1)$, of the closing time, t_c. If we denote the altitudes of the points N and O by h_1 and h_2, then from similar triangles it is apparent that

$$\frac{h_1 - h_2}{h_2} = \frac{t_{NO}}{t_c} = f,$$

wherein t_{NO} is the time for the aircraft to cover the timing run distance, NO. From this it follows that the point O corresponds to an altitude h_2, where

$$(6.39) \quad h_2 = \frac{1}{1+f} h_1 .$$

The relationship (6.39) can be effected by use of a suitably arranged altimeter. The quantity t_c is then $1/f$ of the time taken for h_1 to drop to $1/(1+f)$ of its original value.

As a solution to the toss bombing problem, we seek a formula, in terms of basic inputs, for the pull-up time t_r, that is, the time to fly along the pull-up arc from the initial pull-up point O to the bomb release point P. We shall assume a stationary target and neglect air resistance.

We note first that the airplane has an acceleration arising from the curvature of the pull-up path and that this acceleration is normal to the direction of motion at any instant since the tangential component of the acceleration vanishes in accord with our assumption of constant speed along the pull-up path. If we denote this acceleration, measured in gees, by μ, and

the corresponding radius of curvature of the pull-up path by R, then $\mu g = V^2/R$. Let a set of coordinate axes xOy be chosen with origin at O and with the positive x-axis passing through the target. If now t is the time taken for the aircraft to fly a distance s along the arc OP, and θ is the angle through which the tangent to the path has turned during this time, then,

$$(6.40) \quad d\theta = \frac{ds}{R} = \frac{\mu g}{V^2}\, ds = \frac{\mu g}{V}\, dt\,.$$

Consequently, at any time during the pull-up period, the angle θ will be given by the integral

$$(6.41) \quad \theta = \frac{g}{V}\int_0^t \mu dt, \quad t \leq t_r\,,$$

where time is measured from the point O.

The total pull-up angle is then

$$(6.42) \quad \theta_r = \frac{g}{V}\int_0^{t_r} \mu dt\,.$$

If now we introduce the average normal acceleration $\bar{\mu}$ computed over the time interval $O \leq t \leq t_r$, that is,

$$\bar{\mu} = \frac{1}{t_r}\int_0^{t_r} \mu dt\,,$$

equation (6.42) can be rewritten

$$(6.43) \quad \theta_r = \frac{g\bar{\mu}}{V}\, t_r\,.$$

A standard aircraft accelerometer mounted in an airplane shows at each instant during pull-up the number K of gees present at that instant and acting normal to the direction of motion. If δ is the dive angle, then approximately,

$$(6.44) \quad \mu g \doteq (K - \cos\delta)\, g\,.$$

This relation is sufficiently accurate to be useful for small pull-up angles. It is exact at the beginning of pull-up since in the dive, $K = \cos\delta$ and $\mu = O$.

If x and y are the coordinates of the bomb at any time, t, always measured from the beginning of pull-up, then the components of velocity on the coordinate axes at any instant during pull-up are,

$$(6.45) \quad \dot{x} = V\cos\theta, \quad \dot{y} = V\sin\theta\,.$$

Hence,

$$(6.46) \quad x = V\int_0^t \cos\theta\, dt, \; y = V\int_0^t \sin\theta\, dt\,.$$

Eliminating dt from (6.46) by using (6.40), we obtain

$$(6.47) \quad x = \frac{V^2}{g}\int_0^\theta \frac{\cos\theta}{\mu}\, d\theta,$$

$$y = \frac{V^2}{g}\int_0^\theta \frac{\sin\theta}{\mu}\, d\theta\,.$$

By placing $t = t_r$ in these relations, expressions are obtained for x_r, y_r, $\dot{x}_r$, $\dot{y}_r$, where x_r and y_r are the coordinates of the release point P.

After the bomb has been released, the important force acting on it is gravity. Hence, for this phase of the motion, the components of velocity and the coordinates are

$$(6.48) \quad \begin{cases} \dot{x} = \dot{x}_r + g(t - t_r)\sin\delta\,, \\ \dot{y} = \dot{y}_r - g(t - t_r)\cos\delta\,, \\ x = x_r + \dot{x}_r(t - t_r) + \frac{1}{2}g(t - t_r)^2\sin\delta\,, \\ y = y_r + \dot{y}_r(t - t_r) - \frac{1}{2}g(t - t_r)^2\cos\delta\,. \end{cases}$$

In order to secure a hit, x must equal Vt_c when $y = O$, since the coordinates of the target are (Vt_c, O). Let this occur when $t = t_h$, so that, from equations (6.48),

$$(6.49) \quad \begin{cases} Vt_c = x_r + \dot{x}_r(t_h - t_r) \\ \qquad\qquad + \frac{1}{2}g(t_h - t_r)^2\sin\delta\,, \\ O = y_r + \dot{y}_r(t_h - t_r) \\ \qquad\qquad - \frac{1}{2}g(t_h - t_r)^2\cos\delta\,. \end{cases}$$

On replacing x_r, y_r, $\dot{x}_r$, $\dot{y}_r$ by their values from equations (6.46) and (6.47), the following basic equations are obtained.

$$(6.50)\quad \begin{cases} Vt_c = \dfrac{V^2}{g}\displaystyle\int_0^{\theta_r} \dfrac{\cos\theta}{\mu}\,d\theta \\ \qquad +V(t_h - t_r)\cos\theta_r + \tfrac{1}{2}g(t_h - t_r)^2 \sin\delta \\ O = \dfrac{V^2}{g}\displaystyle\int_0^{\theta_r} \dfrac{\sin\theta}{\mu}\,d\theta \\ \qquad +V(t_h - t_r)\sin\theta_r - \tfrac{1}{2}g(t_h - t_r)^2\cos\delta\,. \end{cases}$$

Equations (6.50) form the basis for a toss bomb computer since a formula for t_r may be obtained from them by eliminating the parameter t_h. The formula will be a function of the input parameters t_c, V, θ_r, and δ. The value for t_c is obtained during the timing run, δ is given by a dive angle indicator, and θ_r is determined in terms of pull-up acceleration. When values for these parameters are fed into the computer, the release time is automatically computed.

Instead of eliminating only t_h from equations (6.50), it is easier to eliminate $t_h - t_r$, to solve the resulting equation for θ_r, and to then find the release time t_r from (6.43). Solving the second of equations (6.50) for $t_h - t_r$ we find,

$$(6.51)\quad t_h - t_r = \frac{V}{g\cos\delta}\left[\sin\theta_r + \sqrt{\sin^2\theta_r + 2\cos\delta\int_0^{\theta_r}\frac{\sin\theta}{\mu}\,d\theta}\right]$$

Substituting the right member of (6.51) into the first of equations (6.50) gives,

$$(6.52)\quad \frac{gt_c}{V} = \frac{\cos\delta\cos\theta_r + \sin\delta\sin\theta_r}{\cos^2\delta}\cdot\left[\sin\theta_r + \sqrt{\sin^2\theta_r + 2\cos\delta\int_0^{\theta_r}\frac{\sin\theta}{\mu}\,d\theta}\right] + \int_0^{\theta_r}\frac{\cos\theta}{\mu}\,d\theta + \tan\delta\int_0^{\theta_r}\frac{\sin\theta}{\mu}\,d\theta\,.$$

In equation (6.51) the positive sign is used before the radical since a negative sign would make t_h less than t_r.

Equation (6.52) contains the desired quantity θ_r in a rather complicated way, one from which an exact explicit solution is not easily obtained. Nevertheless, this equation is basic to further discussion insofar as a practical solution of the toss bombing problem is concerned. We shall, in the next paragraph, solve equation (6.52) for θ_r by making suitable approximations.

6.14 An Approximate Solution for the Release Time

As a first step in obtaining an approximate solution of the basic equation (6.52) we replace μ in the integrals by the average normal acceleration, $\bar{\mu}$. Approximate values for the integrals can then be found. The resulting form of the relation is

$$(6.53)\quad \frac{gt_c}{V} = \frac{\cos\delta\cos\theta_r + \sin\delta\sin\theta_r}{\cos^2\delta}\cdot\left[\sin\theta_r + \sqrt{\sin^2\theta_r + 2\cos\delta\,\frac{1-\cos\theta_r}{\bar{\mu}}}\right] + \frac{1}{\bar{\mu}}\sin\theta_r + \frac{1-\cos\theta_r}{\bar{\mu}}\tan\delta\,.$$

On the assumption that pull-up angles will be small, we next replace the trigonometric functions $\sin\theta_r$ and $\cos\theta_r$ by θ_r and $1 - \frac{1}{2}\theta_r^2$, respectively. The resulting equation in θ_r then has the form

$$(6.54)\quad \frac{gt_c}{V} = \theta_r\left[\frac{(1-\frac{1}{2}\theta_r^2)\cos\delta + \theta_r\sin\delta}{\cos^2\delta}\right]\cdot\left[1 + \sqrt{1 + \frac{1}{\bar{\mu}}\cos\delta}\right] + \frac{1}{\bar{\mu}}\theta_r + \frac{1}{2\bar{\mu}}\theta_r^2\tan\delta\,.$$

Equation (6.54) is a cubic polynominal in θ_r. However, since the solution sought is expected to be valid only for small pull-up angles, we may

ignore the term of degree 3 in θ_r, at least if $\cos\delta$ is not too small. This then gives the following quadratic in θ_r.

$$(6.55)\quad (1+2\sigma)\,\theta_r^2 \tan\delta + 2(1+\sigma)\,\theta_r - \frac{2gt_c\bar{\mu}}{V} = O,$$

where

$$\bar{\sigma} = \frac{\bar{\mu} + \sqrt{\bar{\mu}(\bar{\mu} + \cos\delta)}}{\cos\delta}.$$

The corresponding equation for t_r, obtained by using relation (6.43), is

$$(6.56)\quad \frac{1+2\sigma}{2V}\, g\bar{\mu}t_r^2 \tan\delta + (1+\sigma)\,t_r - t_c = O.$$

Equation (6.56) has a positive and a negative solution. The positive solution, which applies here, is

$$(6.57)\quad t_r = 2t_c\left[1+\sigma+\sqrt{(1+\sigma)^2 + 2\frac{1+2\sigma}{V}g\bar{\mu}t_c\tan\delta}\,\right]^{-1}$$

This may be rewritten in the form

$$(6.58)\quad t_r = \frac{t_c\cos\delta}{\bar{\mu}+\cos\delta+\sqrt{\bar{\mu}(\bar{\mu}+\cos\delta)}}\cdot\frac{2}{1+\sqrt{1+2\beta}},$$

where

$$\beta = \left[\frac{1+2\sigma}{(1+\sigma)^2}\right]\cdot\frac{g\bar{\mu}t_c}{V}\tan\delta = \frac{gt_c\sin\delta}{V}\cdot\frac{\bar{\mu}}{\bar{\mu}+\cos\delta}.$$

Let $\bar{K}$ designate the time average of K from the beginning of pull-up until the release of the bomb. From equation (6.44) it follows that $\bar{K} = \bar{\mu} + \cos\delta$, so that equation (6.58) can be expressed in the form

$$(6.59)\quad t_r = \frac{t_c\cos\delta}{\bar{K}+\sqrt{\bar{K}(\bar{K}-\cos\delta)}}\cdot\frac{2}{1+\sqrt{1+2\beta}},$$

wherein β can be rewritten now as

$$(6.60)\quad \beta = \frac{gt_c\sin\delta}{V}\cdot\frac{\bar{K}-\cos\delta}{\bar{K}}.$$

As the final form for the expression for the release time t_r, we rewrite (6.59) as

$$(6.61)\quad t_r = \frac{t_c\,\psi}{\bar{K}+\sqrt{\bar{K}^2-\bar{K}}},$$

where the function ψ is given by

$$(6.62)\quad \psi = \frac{\bar{K}+\sqrt{\bar{K}^2-\bar{K}}}{\bar{K}+\sqrt{\bar{K}(\bar{K}-\cos\delta)}}\cdot\frac{2\cos\delta}{1+\sqrt{1+2\beta}}.$$

The particular property of the ψ function which makes it useful in this connection is that, although it is a function of the three variables $\bar{K}$, δ, and t_c/V, it is chiefly a function of δ, showing but little variation with $\bar{K}$ and t_c/V over the ranges of values of $\bar{K}$ and t_c/V which occur in toss bombing. Values of the ψ function are tabulated for appropriate ranges of these variables in table 6.1 (Units used in this table are feet and seconds, with g taken as 32.2).

Since ψ reduces to unity when $\delta = O$, and since ψ shows relatively little change when $\bar{K}$ and t_c/V are varied, equation (6.61) shows that ψ can be regarded as a factor whose purpose is to reduce the pull-up time from that for horizontal bombing to the correct value for bombing from a dive.

Table 6.1

Values of the ψ Function

δ	$t_c/V=.01$	.02	.03	.04	.05
			$K=2$		
0	1.000	1.000	1.000	1.000	1.000
10	0.968	0.955	0.943	0.932	0.920
20	0.903	0.880	0.859	0.840	0.822
30	0.808	0.778	0.752	0.728	0.708
40	0.691	0.657	0.629	0.605	0.584
50	0.558	0.525	0.498	0.476	0.457
60	0.418	0.388	0.366	0.347	0.332
70	0.275	0.253	0.237	0.224	0.213
80	0.134	0.123	0.114	0.107	0.102
90	0.000	0.000	0.000	0.000	0.000
			$K=3$		
0	1.000	1.000	1.000	1.000	1.000
10	0.965	0.949	0.933	0.919	0.905
20	0.901	0.872	0.846	0.824	0.802
30	0.809	0.773	0.742	0.716	0.692
40	0.697	0.658	0.626	0.599	0.576
50	0.568	0.531	0.501	0.477	0.456
60	0.430	0.397	0.373	0.353	0.336
70	0.286	0.262	0.245	0.231	0.219
80	0.141	0.129	0.120	0.113	0.107
90	0.000	0.000	0.000	0.000	0.000
			$K=4$		
0	1.000	1.000	1.000	1.000	1.000
10	0.964	0.945	0.928	0.912	0.898
20	0.899	0.868	0.840	0.816	0.794
30	0.809	0.770	0.737	0.709	0.685
40	0.698	0.657	0.623	0.595	0.571
50	0.572	0.532	0.501	0.476	0.455
60	0.434	0.401	0.375	0.355	0.338
70	0.290	0.266	0.248	0.234	0.222
80	0.144	0.132	0.122	0.115	0.109
90	0.000	0.000	0.000	0.000	0.000
			$K=5$		
0	1.000	1.000	1.000	1.000	1.000
10	0.963	0.943	0.925	0.909	0.893
20	0.898	0.865	0.836	0.811	0.788
30	0.809	0.768	0.734	0.705	0.680
40	0.699	0.656	0.621	0.593	0.568
50	0.574	0.533	0.501	0.475	0.454
60	0.437	0.402	0.376	0.356	0.338
70	0.293	0.268	0.250	0.235	0.223
80	0.146	0.133	0.124	0.116	0.110
90	0.000	0.000	0.000	0.000	0.000

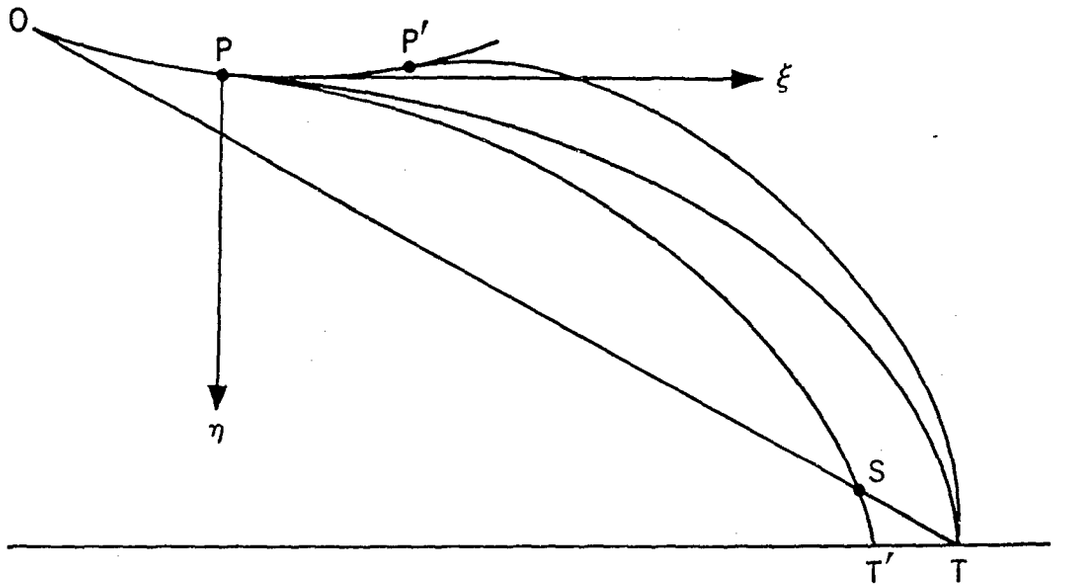

Figure 98. — Air and Vacuum Trajectories

6.15 Air Resistance in Toss Bombing

6.15.1 The Trajectory Equations in Air

In studying the effects of air resistance on the bomb trajectory it is best to employ a coordinate system consisting of horizontal and vertical axes ξ and η with origin at the point of release as indicated in figure 98. In this figure, the curve PT is a vacuum trajectory through the target at T, PST' an air trajectory with the same release conditions, and $P'T$ an air trajectory from a release point determined so that the bomb will hit the target. The percentage increase in t_c required to obtain the trajectory $P'T$ is

$$(6.63) \qquad \frac{\Delta t_c}{t_c} = \frac{V\Delta t_c}{Vt_c} = \frac{TS}{OT}.$$

The equations of the vacuum trajectory, using ξ, η coordinates, are

$$(6.64) \qquad \begin{cases} \xi = U_r(t - t_r) \\ \eta = W_r(t - t_r) + \frac{1}{2}g(t - t_r)^2, \end{cases}$$

where U_r and W_r are the horizontal and vertical components of velocity at release. If the coordinates of the target are ξ_h and η_h at time $t = t_h$, elimination of the quantity $t_h - t_r$ from equations (6.64) yields the relation

$$(6.65) \qquad \eta_h = \frac{W_r}{U_r}\xi_h + \frac{g}{2U_r^2}\xi_h^2.$$

The corresponding relation for the air trajectory PST' will now be obtained. If $u = \dot{\xi}$ and $w = \dot{\eta}$, then the velocity of the bomb in its path is $v = \sqrt{u^2 + v^2}$. The retarding acceleration, a, due to the air, is assumed to be representable in the form

$$(6.66) \qquad a = Bv^2,$$

where B is constant along the trajectory. The components of the acceleration in the ξ and η directions are then,

$$(6.67) \qquad a_\xi = Buv, \quad a_\eta = Bwv.$$

From equation (6.67) the equations of motion of the bomb are

$$(6.68) \qquad \dot{u} = -Buv, \quad \dot{w} = g - Bwv.$$

Let φ be the angle between a tangent at any point on the trajectory and the horizontal, so that

$$(6.69) \quad \tan \varphi = \frac{w}{u}.$$

Equations (6.68) can now be integrated approximately under the simplifying assumption that the total change in direction along the trajectory is small. Thus, if we denote the mean value of φ over the arc PT' by $\bar{\varphi}$, the constant B can be conveniently replaced by $B\dfrac{\cos\varphi}{\cos\bar{\varphi}}$, so that equations (6.68) then become

$$(6.70) \quad \dot{u} = -Bu^2 \sec\bar{\varphi}, \; \dot{w} = g - Buw \sec\bar{\varphi}.$$

Integrating the first of these equations and simplifying, we obtain

$$(6.71) \quad u = \frac{U_r}{1 + BU_r\,(t - t_r)\sec\bar{\varphi}}.$$

Using this result in the second of equations (6.70) gives

$$\dot{w} = g - \frac{BU_r w \sec\bar{\varphi}}{1 + BU_r\,(t - t_r)\sec\bar{\varphi}},$$

whose solution is

$$(6.72) \quad w = \frac{W_r + [g(t - t_r) + \frac{1}{2}BU_r(t - t_r)^2 g \sec\bar{\varphi}]}{1 + BU_r(t - t_r)\sec\bar{\varphi}}$$

Equations (6.71) and (6.72) give the components of velocity in terms of time measured from the beginning of pull-up and the conditions at release. Further integration gives the coordinates ξ and η of the bomb after release in the form

$$(6.73) \quad \begin{aligned} \xi &= \frac{\cos\bar{\varphi}}{B}\, ln \left[1 + \frac{BU_r(t - t_r)}{\cos\bar{\varphi}}\right] \\ \eta &= \tfrac{1}{4}g(t - t_r)^2 + \frac{g\,(t - t_r)}{2BU_r \sec\bar{\varphi}} \\ &\quad + \frac{W_r - g\cos\bar{\varphi}/(2BU_r)}{BU_r \sec\bar{\varphi}} \cdot \\ &\quad ln \left[1 + \frac{BU_r\,(t - t_r)}{\cos\bar{\varphi}}\right]. \end{aligned}$$

The elimination of the quantity $t - t_r$ between these equations yields the equation of the air trajectory PT' in the form

$$(6.74) \quad \eta = \frac{W_r}{U_r}\xi + \frac{g\xi^2}{2U_r^2}\,[1 + \varepsilon(\xi)],$$

where

$$(6.75) \quad \varepsilon(\xi) = -1 - \frac{\cos\bar{\varphi}}{B\xi} + \frac{\cos^2\bar{\varphi}}{2B^2\xi^2}(e^{2B\xi\sec\bar{\varphi}} - 1).$$

By taking the first four terms in the expansion of $e^{2B\xi\sec\bar{\varphi}}$ and dropping the rest, an approximate formula for $\varepsilon(\xi)$ is found to be

$$(6.76) \quad \varepsilon(\xi) = \tfrac{2}{3}B\xi\sec\bar{\varphi}.$$

Since equation (6.74) differs from equation (6.65) only in the term $\varepsilon(\xi)$, this term is then the desired term that accounts for air resistance.

6.15.2 The Ground Error

The distance $T'T$, which is the error on the ground due to air resistance acting on the bomb, can now be evaluated. We shall denote this error by $\Delta\xi_h$. (It will be recalled that the coordinates of the target T are (ξ_h, η_h) in the ξ, η system of

coordinates.) The coordinates of the point T' are then $(\xi_h - \Delta\xi_h, \eta_h)$. If these are substituted into equation (6.74) and use of relation (6.65) be then made, the result is

$$(6.77) \quad O = -\frac{W_r \Delta\xi_h}{U_r} + \frac{g}{2U_r^2}\left[-2\xi_h \Delta\xi_h + \Delta\xi_h^2 + (\xi_h - \Delta\xi_h)^2 \varepsilon(\xi_h - \Delta\xi_h)\right].$$

Since the unknown $\Delta\xi_h$ is obviously much smaller than ξ_h, the term $\Delta\xi_h^2$ can be neglected in comparison with the term $-2\xi_h \Delta\xi_h$. Similarly, upon employing relation (6.76) with

$$\xi = \xi_h - \Delta\xi_h$$

we can replace the term

$$(\xi_h - \Delta\xi_h)^2 \ \varepsilon\ (\xi_h - \Delta\xi_h)$$

by

$$\tfrac{2}{3}B(\xi_h^3 - 3\xi_h^2\Delta\xi_h) \sec\bar{\varphi}.$$

Thus equation (6.77) can be rewritten as

$$O = -\frac{W_r \Delta\xi_h}{U_r} + \frac{g}{2U_r^2}\left[-2\xi_h \Delta\xi_h + \tfrac{2}{3}B(\xi_h^3 - 3\xi_h^2 \Delta\xi_h) \sec\bar{\varphi}\right],$$

whose solution for $\Delta\xi_h$ is

$$(6.78) \quad \Delta\xi_h = \frac{Bg\xi_h^3 \sec\bar{\varphi}}{3(U_r W_r + g\xi_h + Bg\xi_h^2 \sec\bar{\varphi})}.$$

In using the formula (6.78) it is sufficiently accurate to replace $\bar{\varphi}$ by δ. The quantities U_r, W_r and ξ_h can be computed from the formulas

$$U_r = V\cos(\delta - \theta_r),$$

$$W_r = V\sin(\delta - \theta_r),$$

$$\xi_h = Vt_r\cos\delta - x_r\cos\delta - y_r\sin\delta.$$

Formula (6.78) can now be used in calculating the percentage correction $\Delta t_c/t_c$ of t_c necessary to secure a hit. Upon adjusting the toss bomb computer to account for this correction, the bomb will then be released at point P' (see figure 98) and its trajectory will pass through the target. Although we shall not justify the statement here, it can be shown that the percentage correction cited is given approximately by $k\dfrac{Vt_c}{C}$, where k is an empirically determined constant and C is the ballistic coefficient of the bomb.

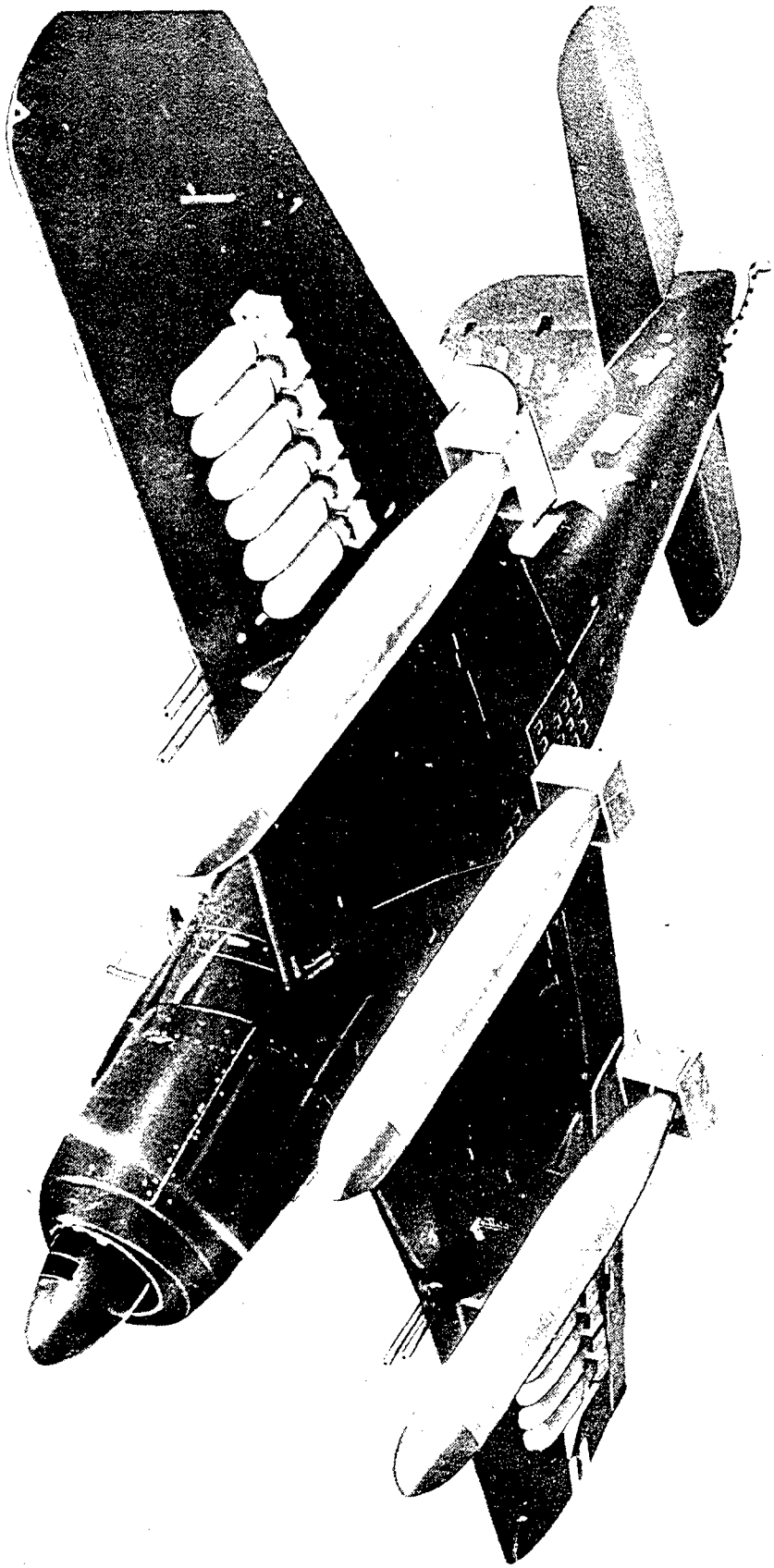

Figure 99.—Complex Armament Installation

Chapter 7

ROCKETRY

7.1 Introduction

The problem of how to aim and fire rockets from aircraft is considerably more complicated than that of aiming and firing bullets. The complications stem mainly from the ballistics of the rockets and the method of launching airborne rockets. The two are not mutually exclusive since the trajectory of the rocket depends upon the manner in which it is launched as well as upon other considerations. A complete discussion of the theory of motion of a rocket is beyond the scope of this book. For such a discussion the reader is referred to Reference 18 of the bibliography in the back of this book. We shall concern ourselves only with a qualitative discussion of how rocket trajectories are obtained and the corresponding sighting problem. Furthermore, we shall be mainly concerned with air-to-ground firing of rockets. Air-to-air combat using rockets will be briefly mentioned at the close of this chapter.

7.2 Methods of Launching Airborne Rockets

The motion of a rocket can be divided into three distinct periods: the launching period, the period of burning after launching, and the period of motion after burning is over. During the launching period, the rocket is under the influence of the aircraft which is carrying it. During the burning period, the rocket is subjected to the forces of gravity, jet forces, and aerodynamic forces. After the rocket fuel is consumed, the rocket moves under the gravity and aerodynamic forces only and its behavior is then similar to that of a bomb.

Most rockets are fin-stabilized in the same manner as bombs. The trajectory of such rockets differs from that of bullets in three respects: (1) rockets are slower; (2) rockets tend to follow the direction of flight of the aircraft while bullets travel in the direction of aim of the gun; and, (3) the rocket trajectory has an appreciable curvature. These three characteristics have considerable influence upon the aiming problem. Since we have a longer time of flight, greater allowance for target speed and wind must be made and, in addition, the greater curvature of the trajectory means larger gravity drop allowance.

Since the rocket tends to follow the direction of flight of the aircraft, its trajectory is highly dependent upon the manner in which it is launched. Thus the launching device, the method of stabilization (whether fin or spin-stabilized), and the attitude of the aircraft at the instant of launching, all contribute to the aiming problem. Since spin-stabilized rockets are still very much in the experimental stage we shall limit our discussion to fin-stabilized rockets.

There are four methods in common use for launching airborne rockets: (1) retro-launching, (2) fixed launching, (3) Dynamic controlled-displacement launching, and (4) drop launching. Let us consider each of these in order.

In retro-launching, the rocket is fired to the rear of the launching aircraft. This method of launching is very effective in anti-submarine warfare.

Fixed launching applies to rockets fired while held in fixed positions and in orientation relative to the launching aircraft. Thus the term includes: (a) post launching, in which the rocket is held in position by lugs and is free of the aircraft after moving a very short distance; (b) rail or tube launching, in which the rocket is guided for the first several feet of travel; and (c) fixed displacement launching, whereby the rocket is lowered into a fixed position below the aircraft before it is ignited.

Dynamic controlled-displacement launching is the term applied to the method of launching in which the rocket is dropped before ignition, but is guided by a yoke which holds the rocket in fixed orientation relative to the airplane until ignition occurs. This method of launching has been abandoned in favor of drop launching.

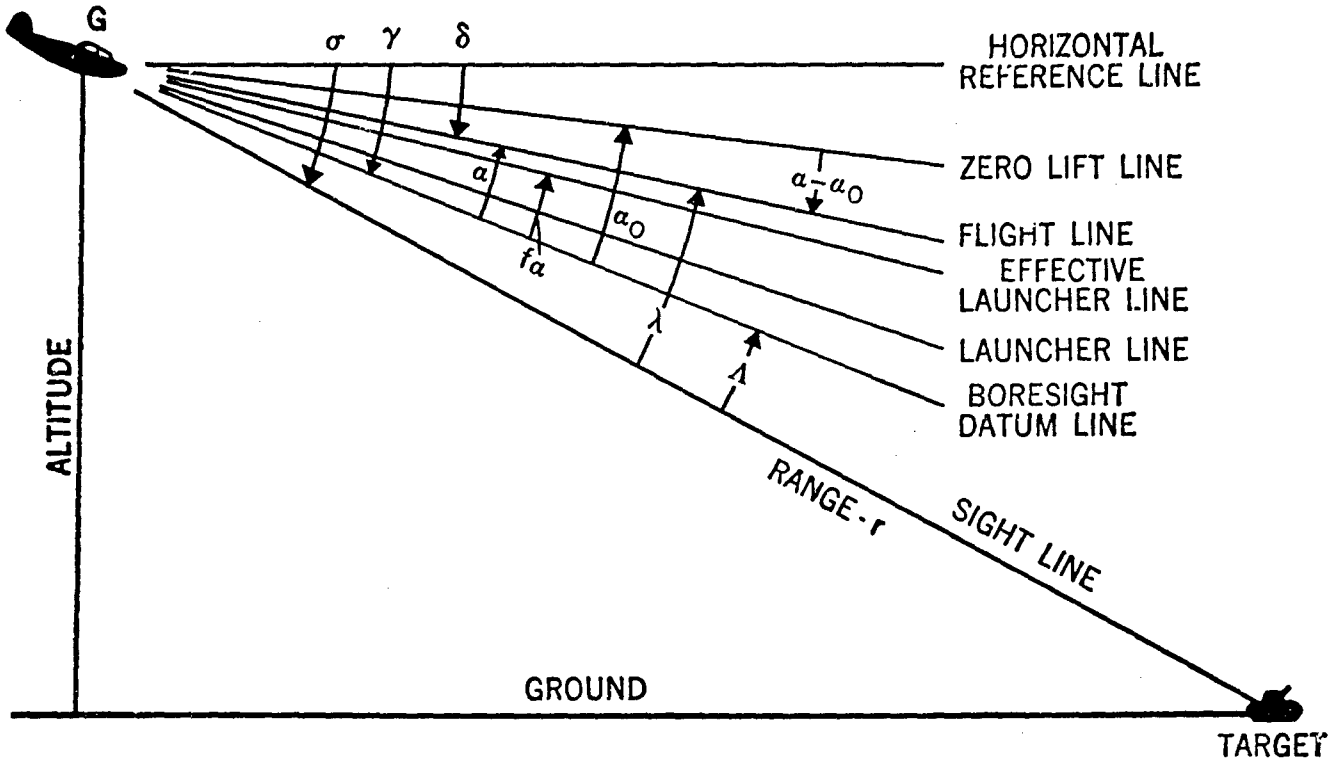

Figure 100. — Coordinate System

Drop launching is the term applied to the method of launching in which the rocket is dropped completely free of the aircraft and is ignited by a delay firing device after it reaches a safe distance below the airplane.

7.3 Coordinate System

Before we consider the trajectory of the rocket, let us focus our attention upon the coordinate system which will be used to describe the trajectory. The action will be considered to take place in the vertical plane and any horizontal corrections will be superimposed. Figure 100 shows the orientation of the lines and angles. Let us further define

(7.1) $F.L.$ = Flight line, the direction of motion of the aircraft;
$L.L.$ = Launcher line, attitude of launchers;
$E.L.L.$ = Effective launcher line, line of departure of rocket;
$S.L.$ = Sight line, line from ownship to target;
$B.S.D.L.$ = Boresight datum line — a reference line fixed in the airplane;
$Z.L.L.$ = Zero lift line; a reference lift line fixed in the airplane;
α = Angle of attack, angle from the B.S.D.L. to the F.L.;
α_0 = Angle from the B.S.D.L. to the Z.L.L.;
δ = Dive angle, angle from horizontal reference line to F.L.;
σ = Angle from the horizontal to the sight line;
λ = Angle from the sight line to the flight line;
Λ = Lead angle, angle from the sight line to the B.S.D.L.;
γ = Angle from the horizontal to the B.S.D.L.;
$f\alpha$ = Angle from boresight datum line to E.L.L.;
r = Present range.

The clockwise direction is taken to be positive.

Note that the launcher line may be offset from the boresight datum line by a fixed angle. Since both lines are fixed in the airplane, this angle is constant and is measurable. The angle $f\alpha$ is actually the angle that the rocket turns

in the direction of the flight line from the launcher line and thus it should actually be defined from the launcher line. However, to simplify the derivation which will appear later, we shall assume that the boresight datum line and launcher line coincide. In any airplane where this is not the case, the constant offset angle can easily be accounted for as is made amply clear in rocket sighting tables.

7.4 Qualitative Discussion of Trajectories

The motion of a rocket can be defined by Newton's laws and the differential equations involved can be derived. However, these equations are quite complex and their derivation would consume considerable space as can easily be seen by referring to Reference 18, in the Bibliography. For the purpose of this book, let it suffice to say that under justifiable assumption of the aerodynamic forces and with experimentally determined values of the necessary parameters, the equations of motion can be solved and the pertinent data of the trajectory can be tabulated. We shall, therefore, discuss only the qualitative characteristics of the trajectories and their application to the sighting problem.

We begin the discussion by considering the trajectories of fixed-launched rockets. Since the rocket is already moving through the air mass with the speed of the aircraft, the air acts on the fins, turning it into the wind as soon as it leaves the launcher. Angular momentum carries it beyond the direction of the wind and, consequently, its direction oscillates about the direction of its vector velocity. This oscillation dies out, leaving a well defined initial direction for the rocket trajectory which we shall refer to as the effective launcher line. Thus the initial direction of the path is along this imaginary line whose direction is a certain fraction f of the way from the launcher line to the flight direction. The quantity f is called the launching factor. It is possible to derive a formula for this launching factor and to compute its value which depends upon the rocket type, the length of the constrained motion on the launcher, the propellant temperature, and the indicated airspeed of the aircraft, but not on the dive angle. There is a launching factor both in the vertical plane and the traverse plane.

Since the rocket starts out in the general direction of the aircraft it is necessary to de-

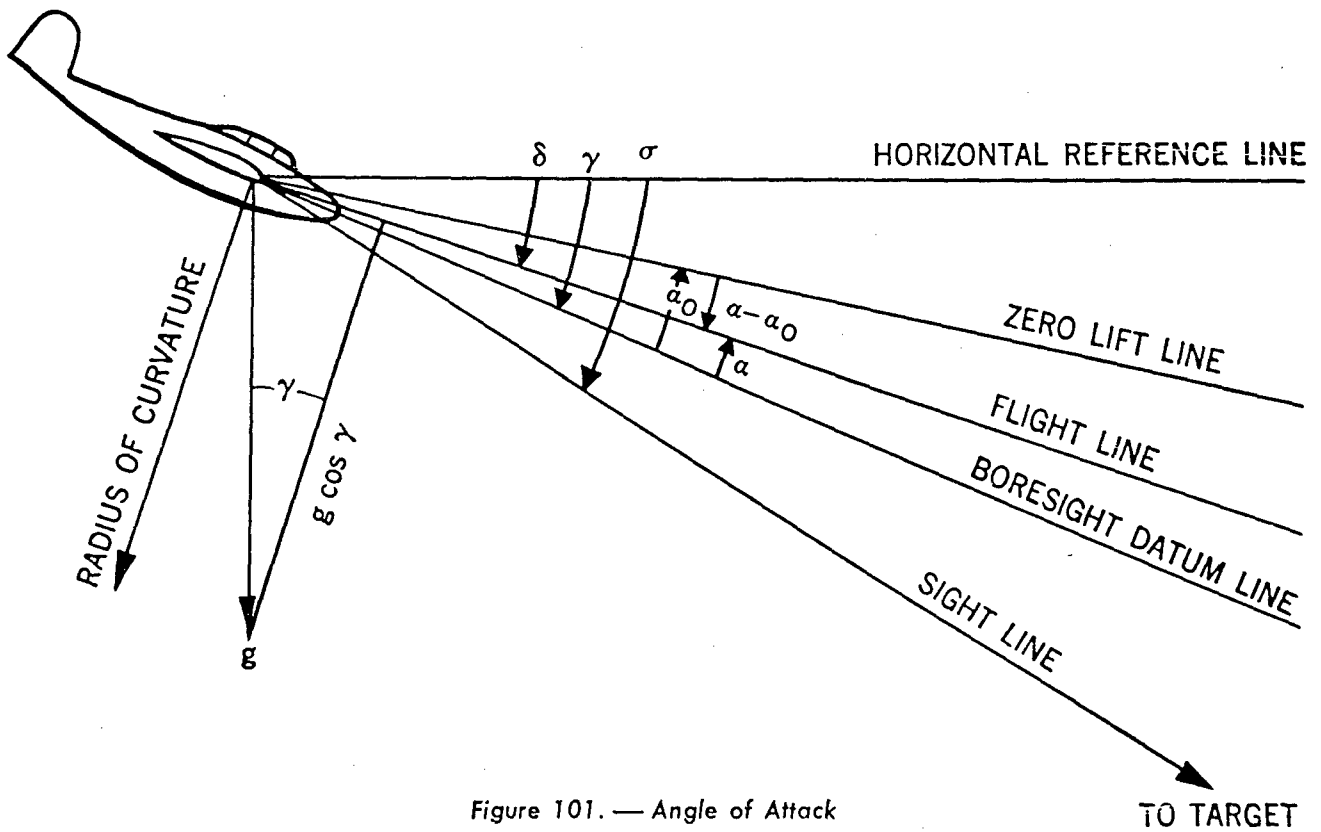

Figure 101. — Angle of Attack

termine the aircraft's direction in terms of the thrust direction. This is accomplished by considering the boresight datum line which is fixed in the airplane. Since the latter is at an angle α_o from the zero lift line of the aircraft, then, considering the influence of gravity, the flight direction will be at some angle $\alpha - \alpha_o$ below the zero lift line. This angle is inversely proportional to the square of the indicated airspeed, V_{G_i}. If the airplane is nosing up or down, there is a centripetal acceleration a_N in the direction normal to the flight path to be considered. This acceleration is given by

$$(7.2) \quad a_N = V_G \dot{\delta}.$$

The formula for the attack angle α can then be written as

$$(7.3) \quad \alpha = \alpha_o + \frac{b}{V_{G_i}^2} (g \cos \delta - V_G \dot{\delta})$$

where b is a constant of proportionality which depends upon the airplane. See figure 101.

The above discussion assumes that the rocket is launched into a uniform air stream. This assumption does not hold in regions close to an aircraft wing. It is, therefore, necessary to determine an "effective angle of attack" from sighting data. The method will be explained subsequently.

The gravity drop term of the rocket trajectory depends upon the rocket type, propellant temperature, the dive angle, the launching speed, and the slant range to the target. This gravity drop is computed from the simplified equations of motion and the values are tabulated together with other ballistic data for each standard rocket type. This data consists of tables of trajectory drops, launching factor, flight times, and projectile velocities. Numerical studies on the values of the trajectory drop for many rockets currently in use has revealed that there exists linear and quadratic functions of the range which can approximate the trajectory drop and angle of fall. The coefficients for these functions also are tabulated. A portion of a typical trajectory drop table for a 30° dive angle is illustrated in table 7.1.

Table 7.1

Trajectory Drop — 30° Dive Angle

Trajectory Drop (Mils) Normal to Effective Launching Line								
Range (yds)	0°F	40°F	70°F	100°F	0°F	40°F	70°F	100°F
	320 knots				380 knots			
$f \rightarrow$	.98	.97	.97	.95	.99	.99	.98	.97
500	27	24	21	19	23	20	18	16
600	30	26	23	21	25	22	20	18
800	34	30	27	25	29	26	23	22
1000	39	34	31	29	33	29	27	25
1200	43	38	35	32	37	33	30	28
1500	49	44	41	39	43	39	36	34
2000	61	55	51	50	53	49	46	44
2500	74	68	64	62	65	60	57	55
3000	88	82	78	76	78	73	69	68
4000	118	112	107	106	107	101	97	97

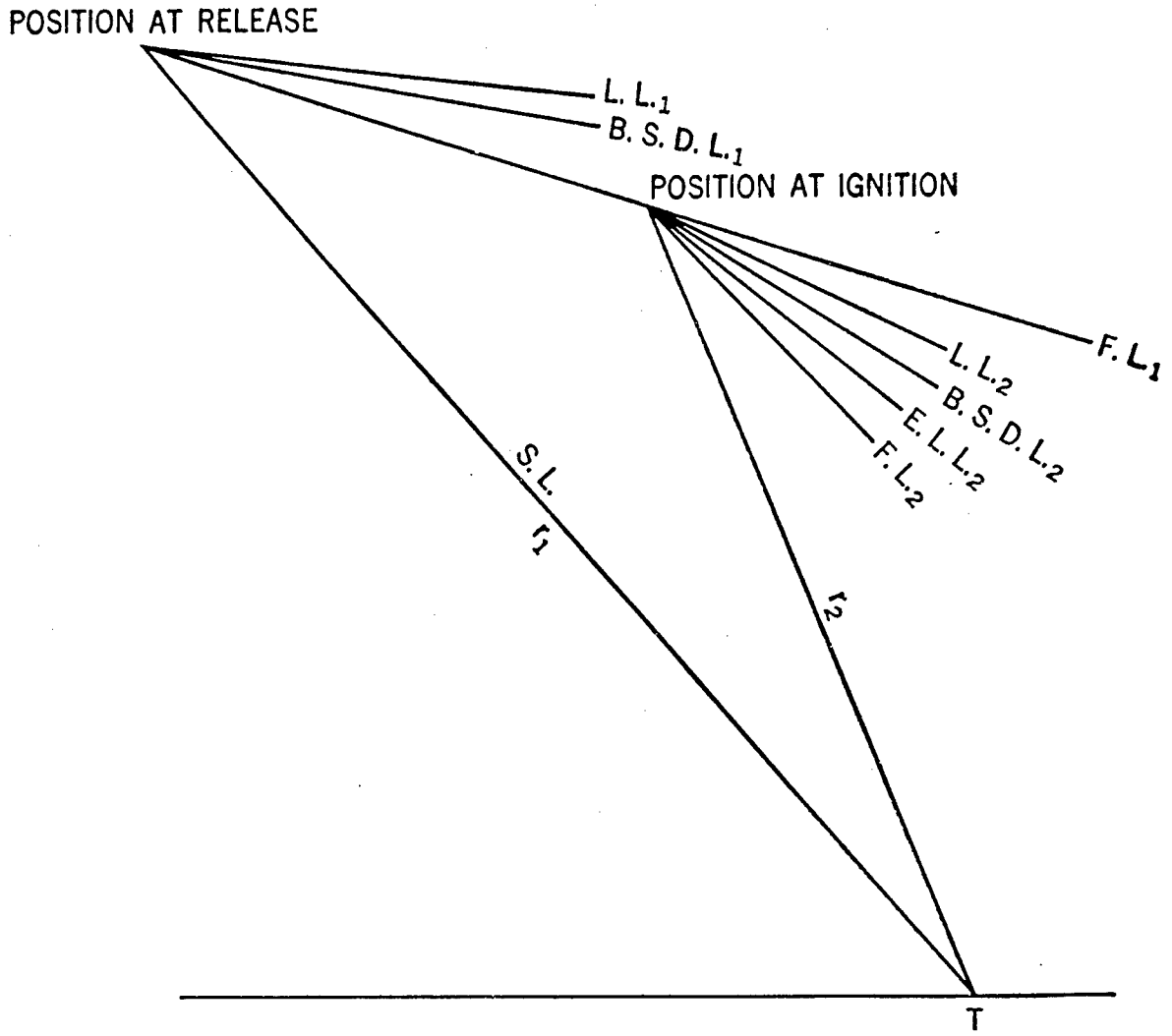

Figure 102. — Drop-launching Conditions

In drop launching, the rocket is dropped completely free of the airplane and the ignition of the rocket is delayed. Thus, there is a period of free fall. The effective launcher line becomes effective at the ignition point and a further correction would be necessary on the sighting equation. See figure 102. Experiments have been devised in order to obtain the necessary information on the free-fall part of the trajectory and the effective angle of attack.

Retro-launched rockets are fired backward relative to the aircraft in a vertical plane and at low altitudes. See figure 103. Under these conditions we may make the assumption that the only forces acting upon the rocket are the rocket jet which produces a constant acceleration equal to the velocity during burning divided by the burning time, and the force of gravity. The computation of the rocket's velocity relative to the aircraft becomes the major ballistic data. The trajectory is then combined with the sighting problem.

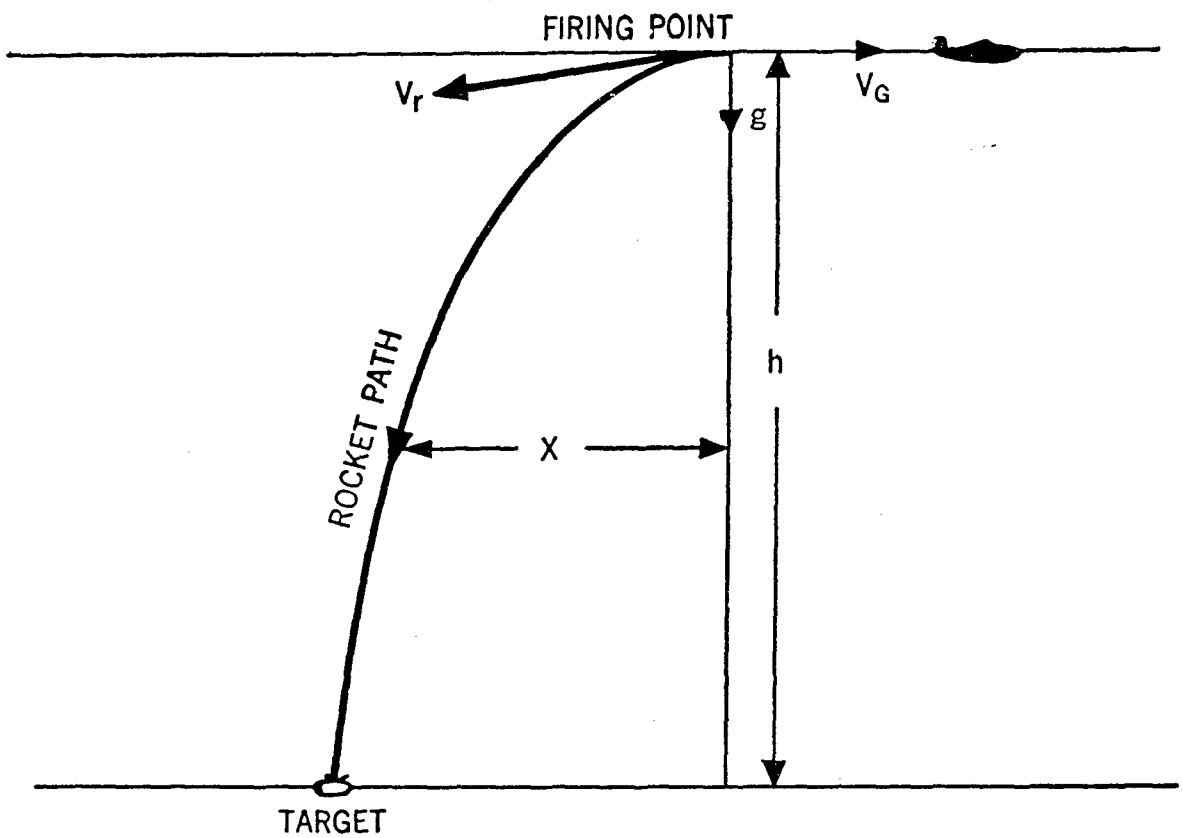

Figure 103. — Retro-launching Conditions

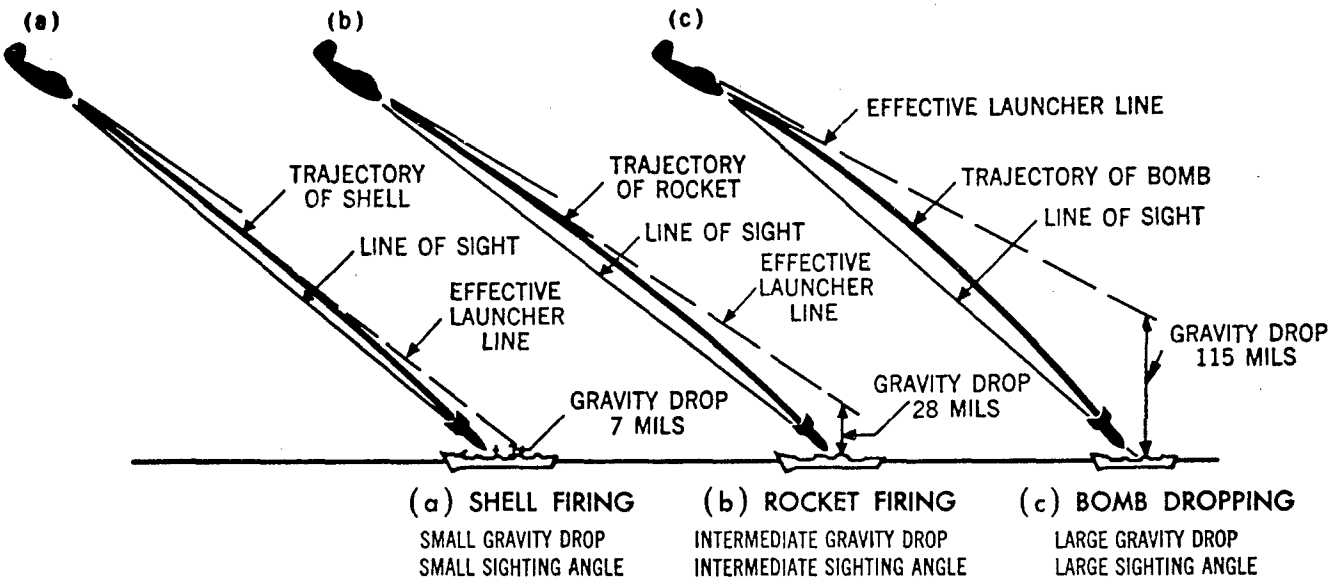

Figure 104. — Gravity Drop Comparison

7.5 Illustrations of the Effects on Rocket Trajectories

Many things enter into the determination of rocket trajectories. Some of these factors introduce errors in the firing of airborne rockets. These effects are best described by illustrations and the following figures are presented here for visual explanation.

Figure 104 shows the difference in magnitude of the gravity drop effect for shell fire, rocket fire, and bomb dropping, and clearly illustrates the intermediate role of the rocket.

Figure 105 shows the effect of the dive angle on the trajectory drop and illustrates the fact that the trajectory drop decreases as the dive angle increases.

Figure 106 shows the effect of Launching Speeds on the rocket trajectory and illustrates the well-known fact that the greater the speed the smaller the trajectory drop.

Figure 107 shows the effect of range misestimation on the trajectory.

Figure 108 shows the effect of temperature on the rocket trajectory. The burning time and distance of a rocket depends greatly upon the temperature of the rocket propellant at ignition. This in turn affects the trajectory as illustrated in the figure.

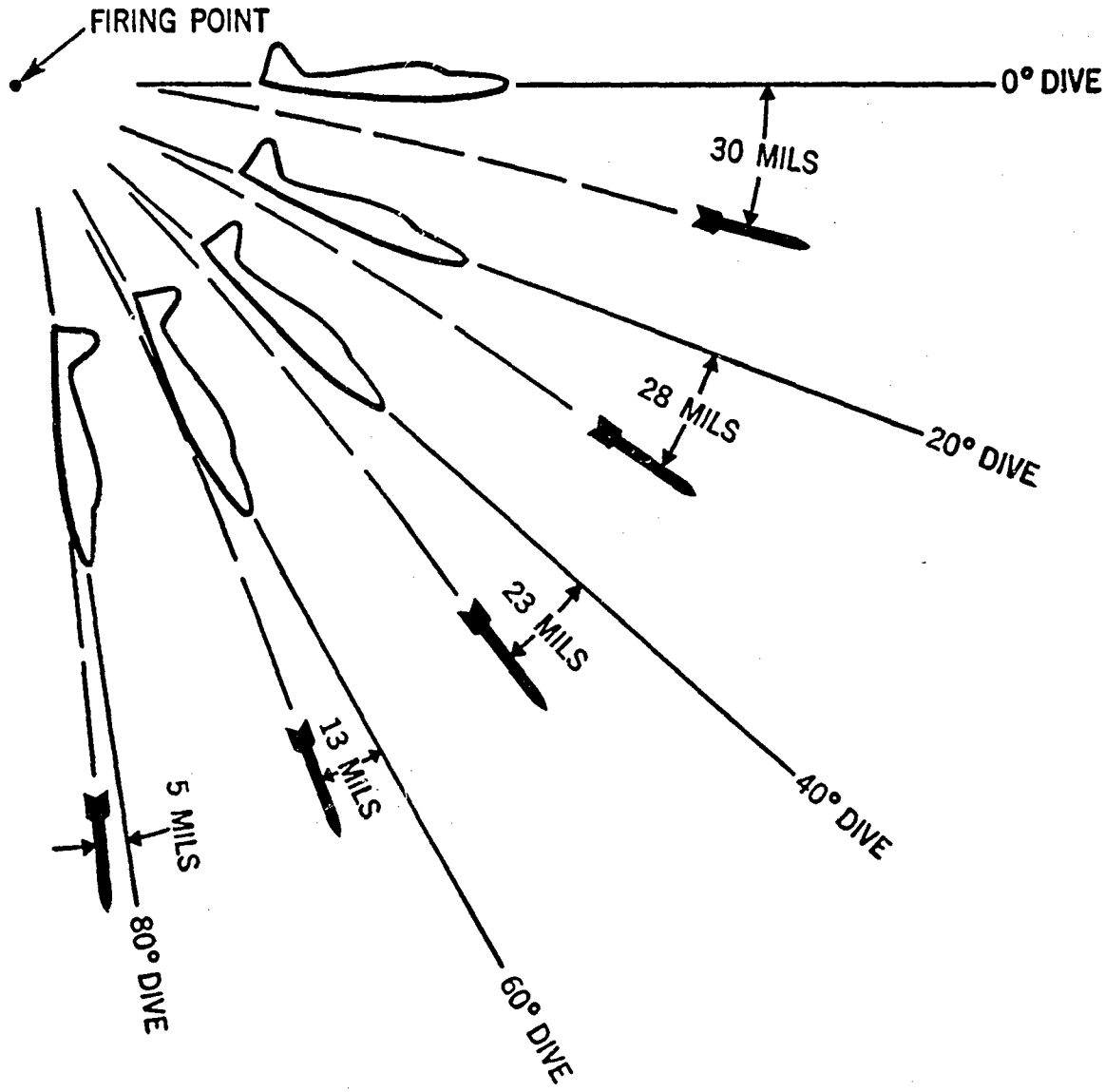

Figure 105. — Effect of Dive Angle

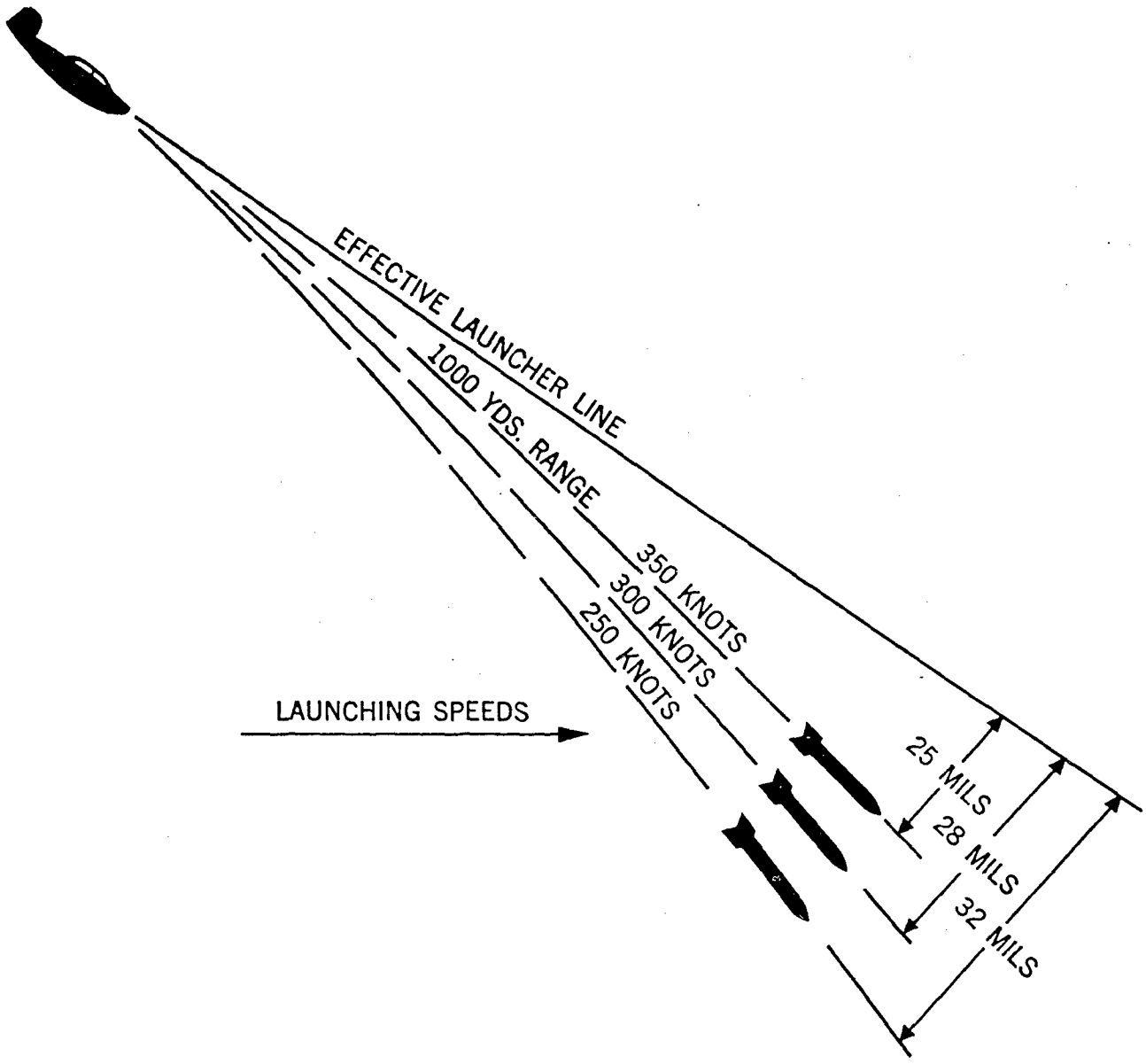

Figure 106. — Effect of Launching Speed

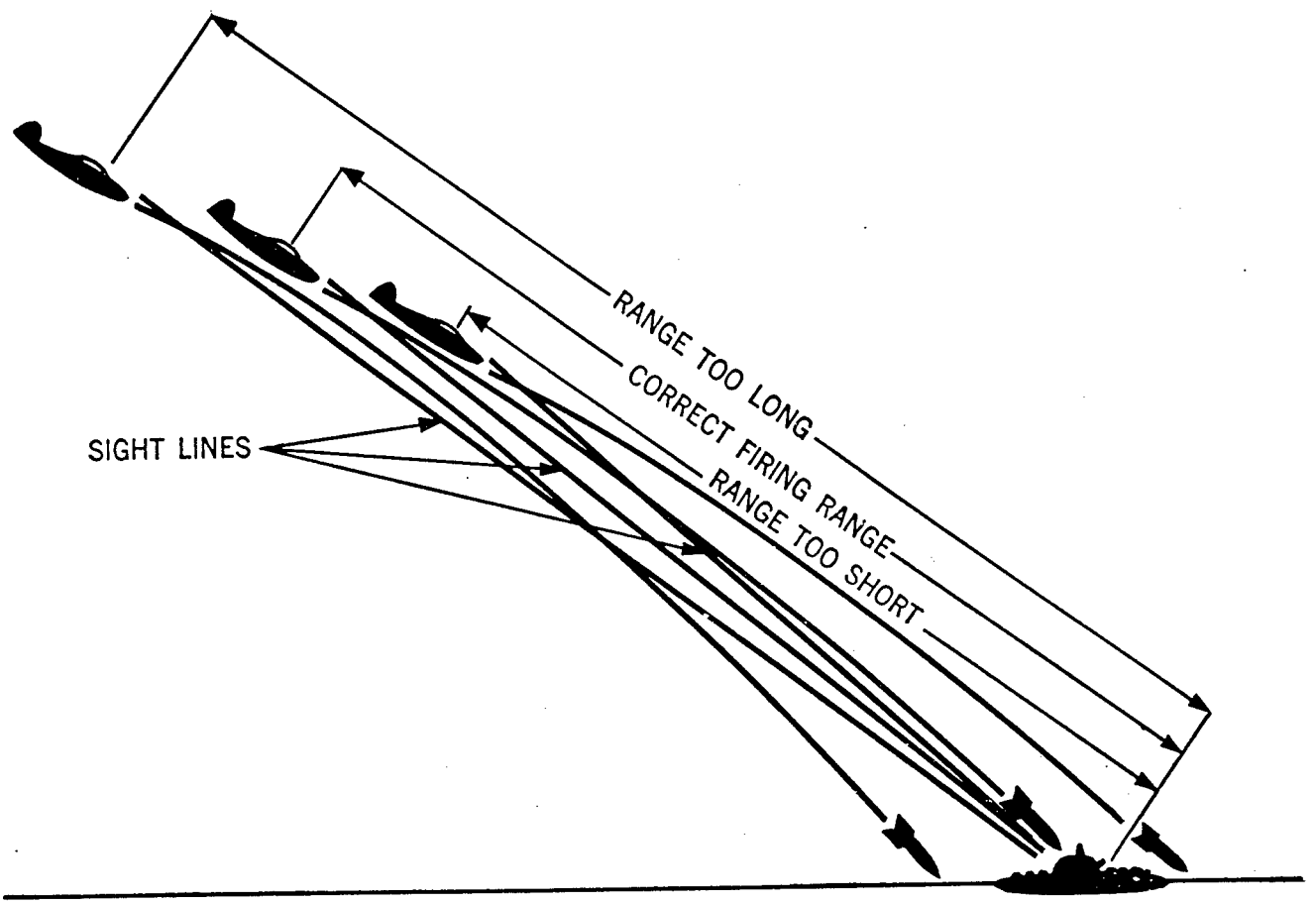

Figure 107. — Range Misestimation

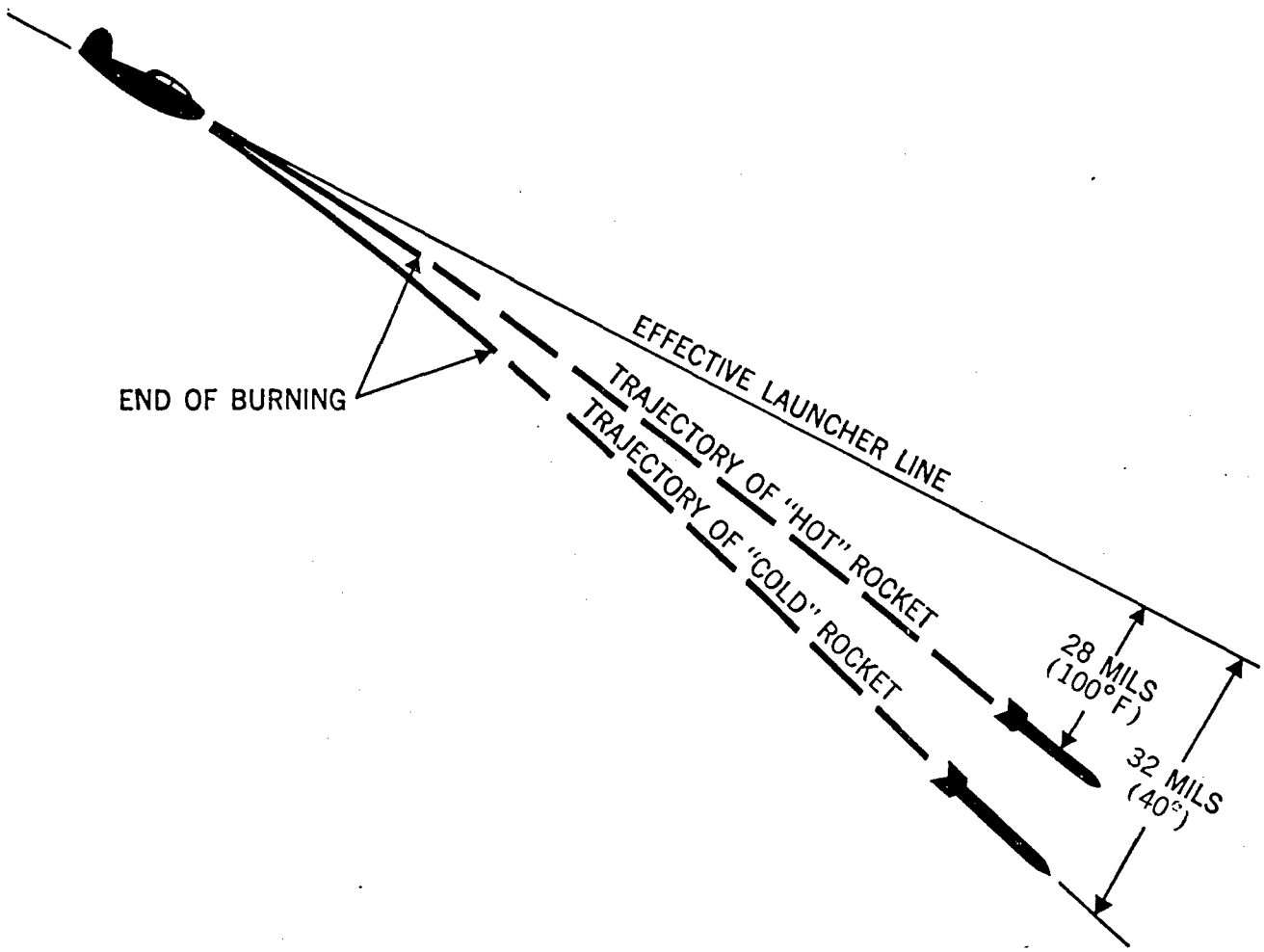

Figure 108. — Effect of Rocket Temperature

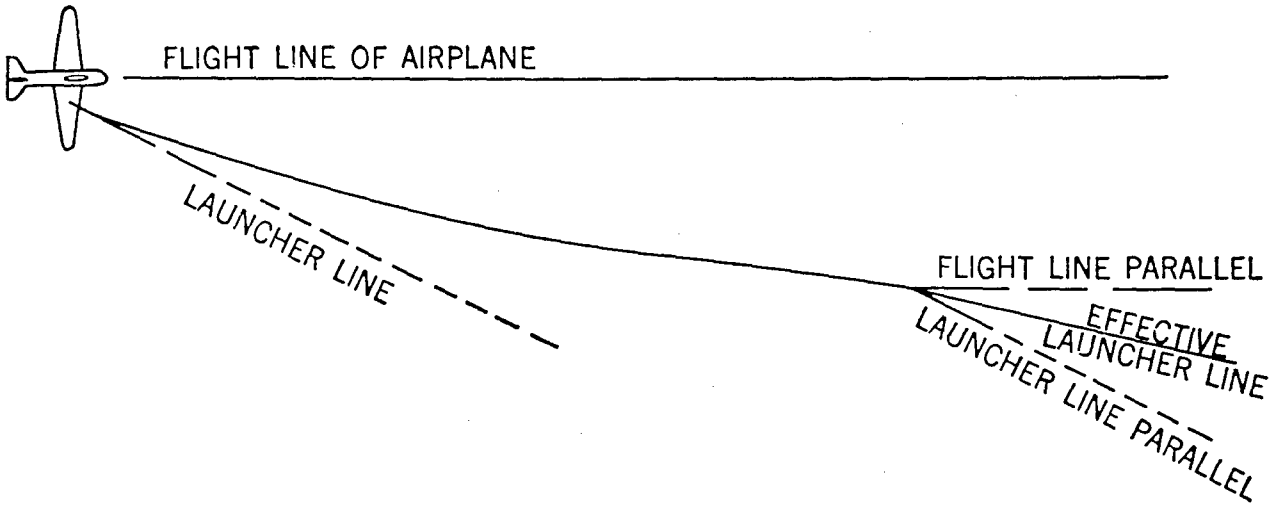

Figure 109. — Effective Launcher Line in Lateral Plane

Figure 109 illustrates how the rocket turns into the flight line of the aircraft in the lateral plane. Thus, there is an effective launcher line in both the vertical and lateral plane.

Figure 110 illustrates the effect of firing in a skid or side-slip. The rocket will again tend to follow the direction of motion of the aircraft.

Figure 111 shows the effect of the angle of attack on the aiming problem of rockets. If the B.S.D.L. rides higher with respect to the flight line, a large sighting angle is necessary. Conditions to increase the angle of attack are shallow dive, heavy airplane loading, or low indicated airspeed.

Figure 112 illustrates the effect of nosing over or pulling up at the time of fire. A pull-up will tend to undershoot the target while a nosing over will tend to overshoot the target. This kind of pull-up is not to be confused with the toss bombing technique where the projectile is released at a predetermined instance during a pull-up from a straight-line dive.

Figure 113 illustrates a typical curve of approach for a standard airplane tracking a ground target with a fixed sight setting.

Figure 114 illustrates the effect of wind and target motion on the aiming problem. It is seen that the effect of the wind is essentially the same as a target motion and therefore need not be considered as a separate problem. Conventional sighting systems measure the relative motion of the airplane and the target and this relative motion contains the wind effect as an inherent part.

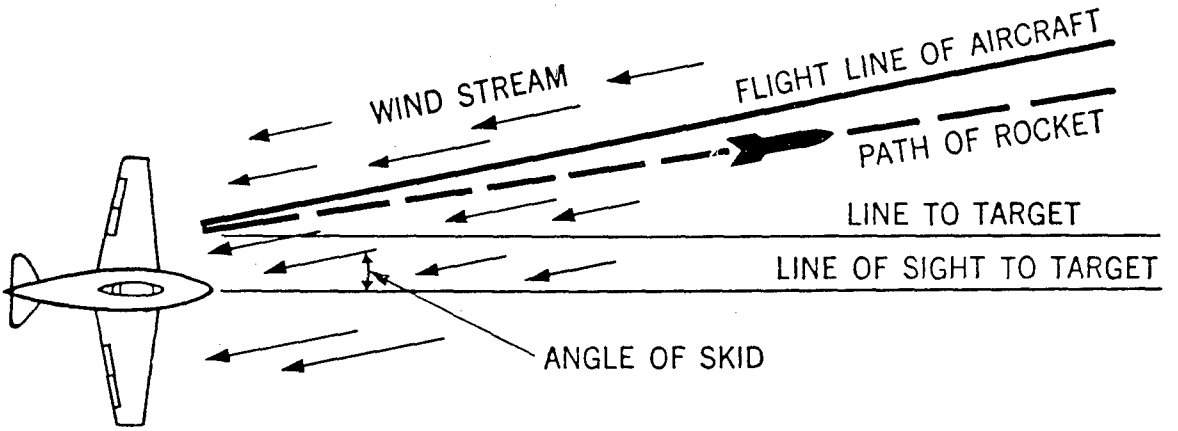

Figure 110. — Skid

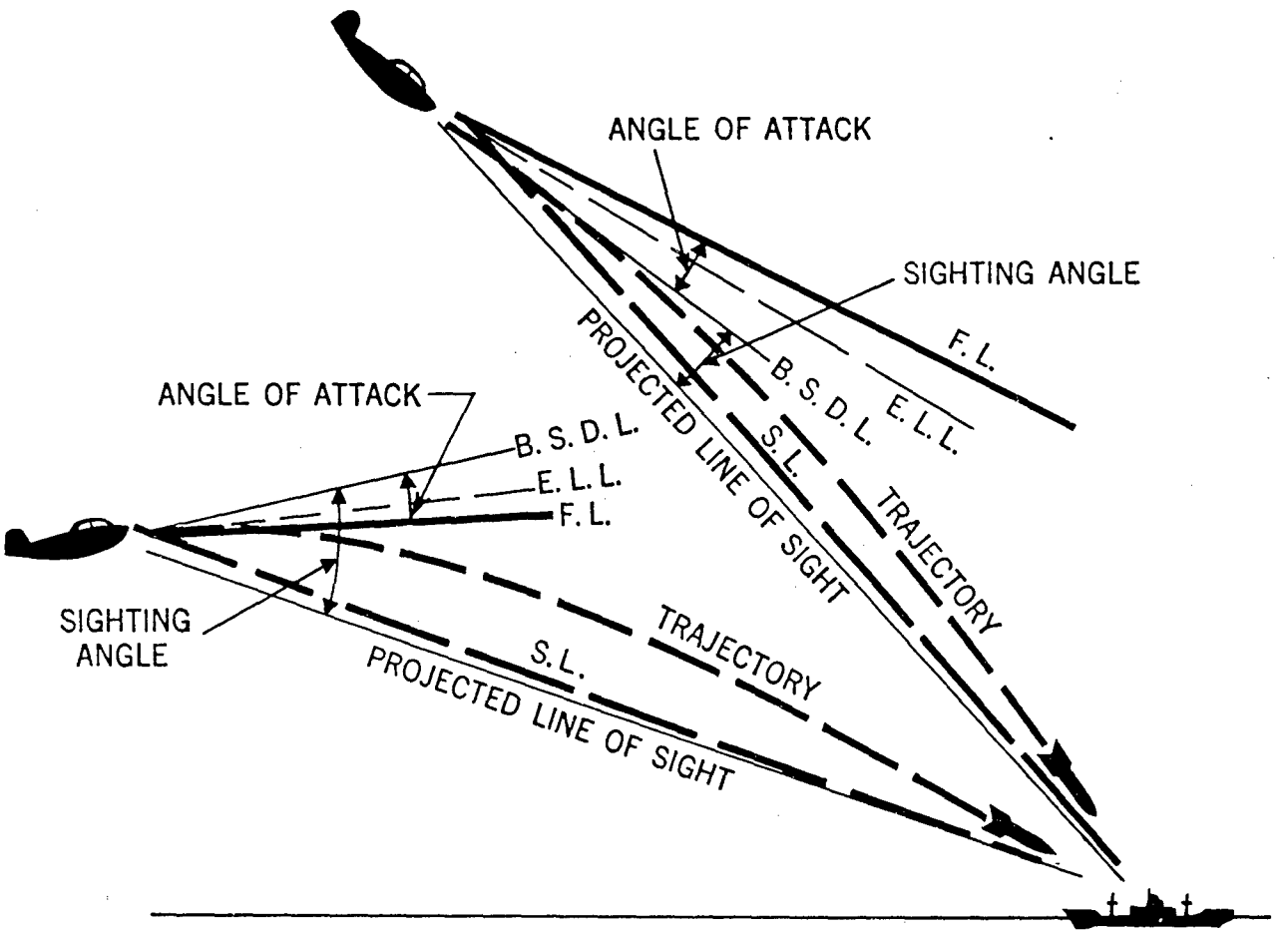

Figure 111. — Effect of Angle of Attack

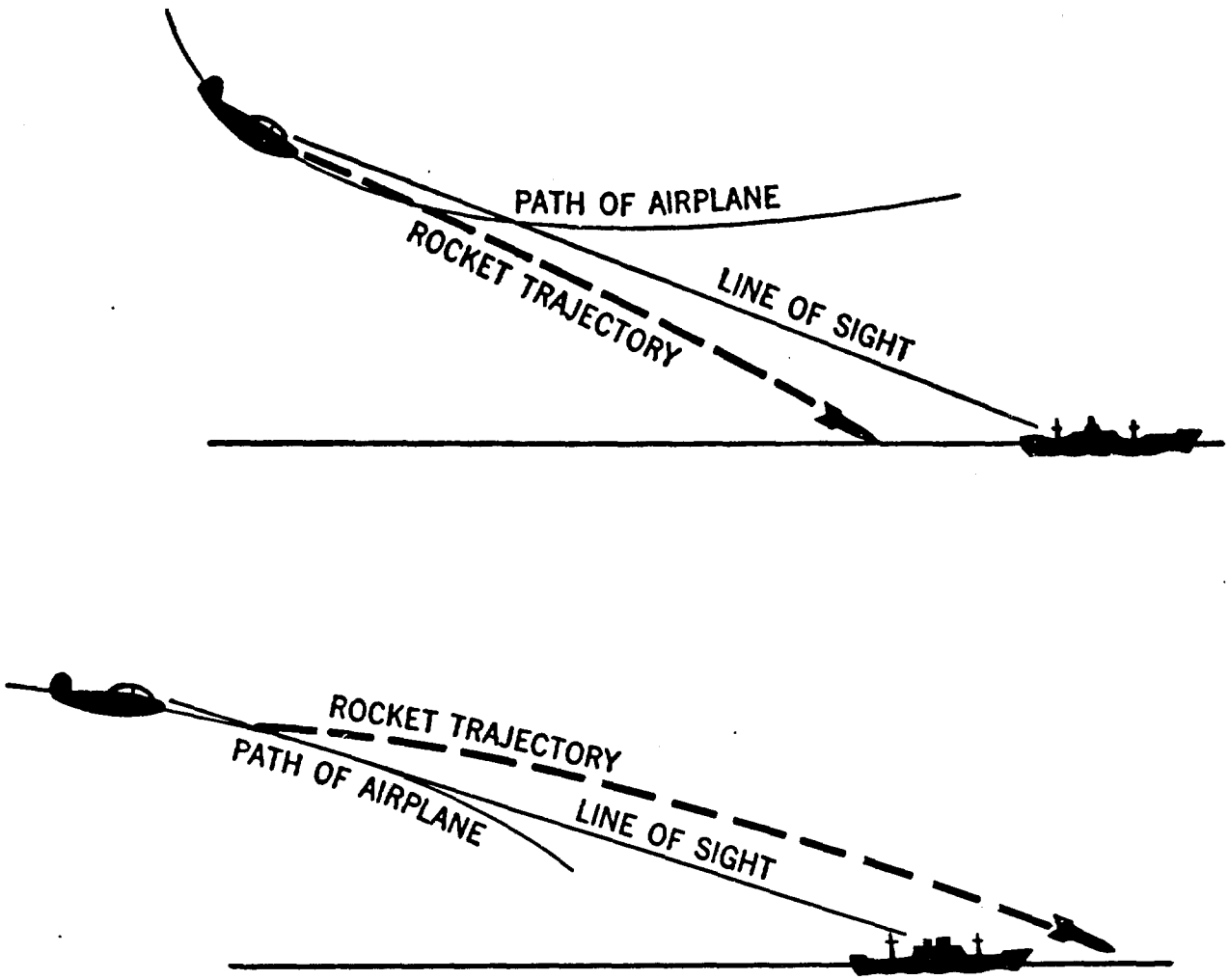

Figure 112. — Nosing Over or Pulling Up

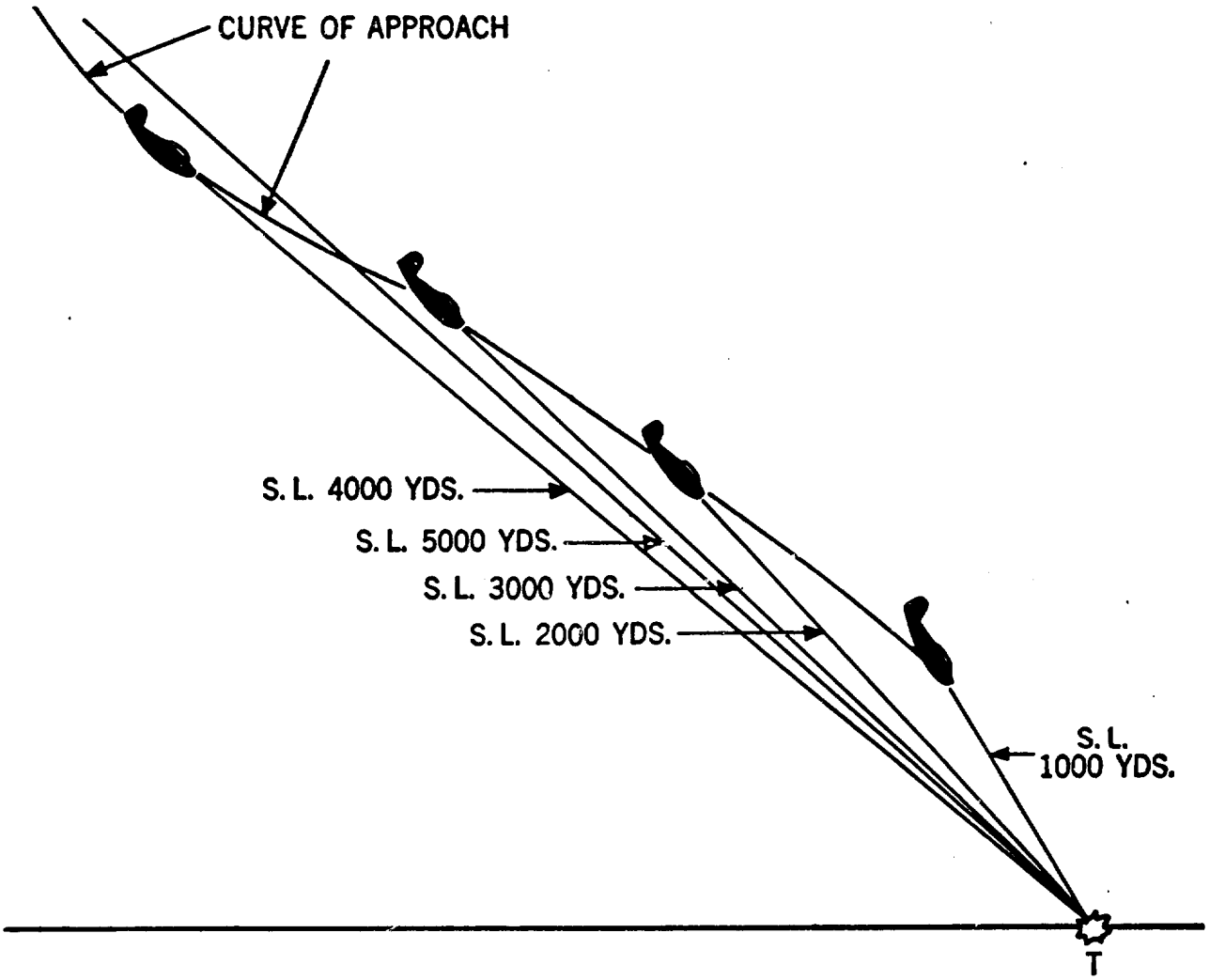

Figure 113. — Curve of Approach

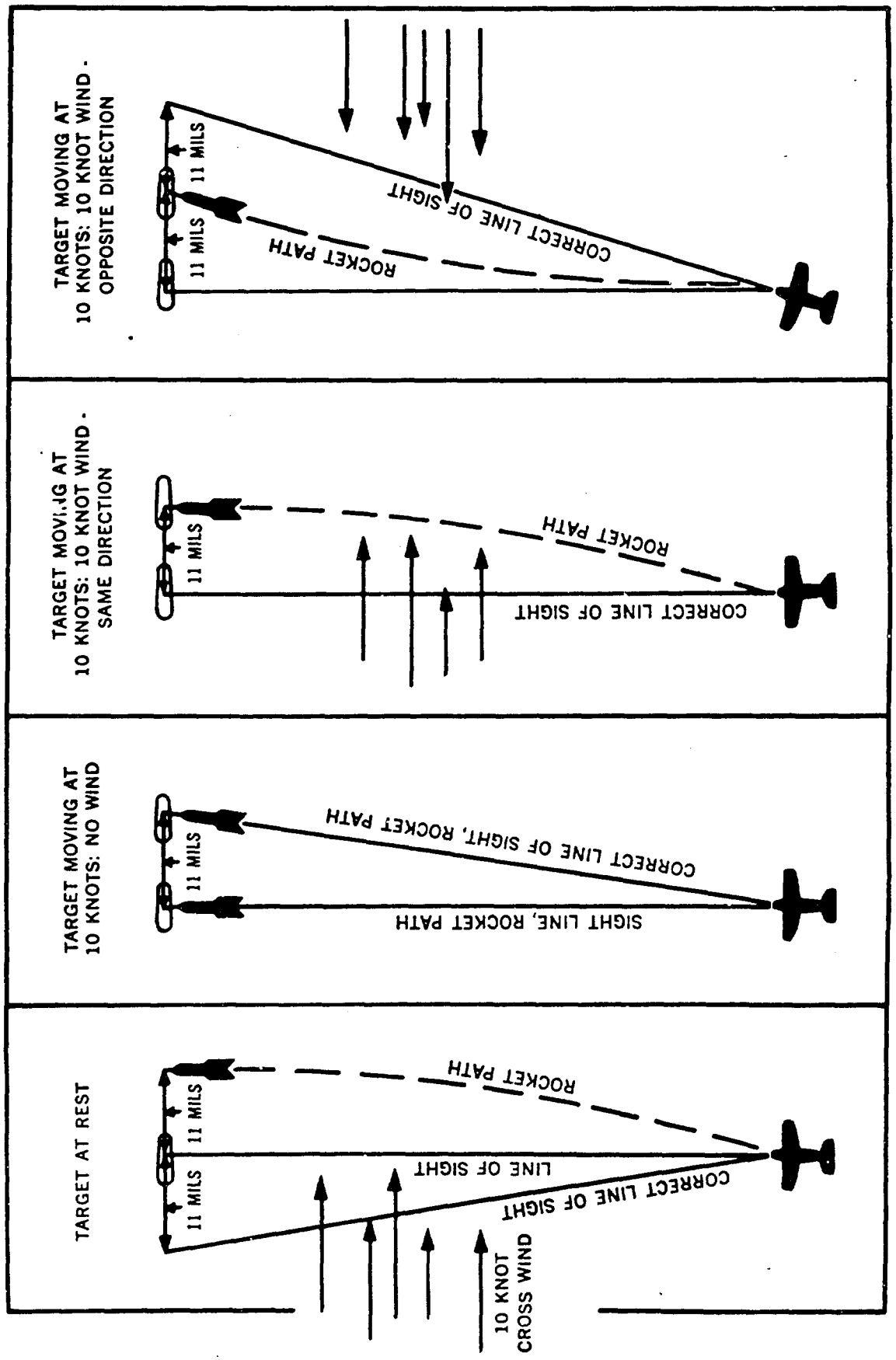

Figure 114. — Wind and Target Motion

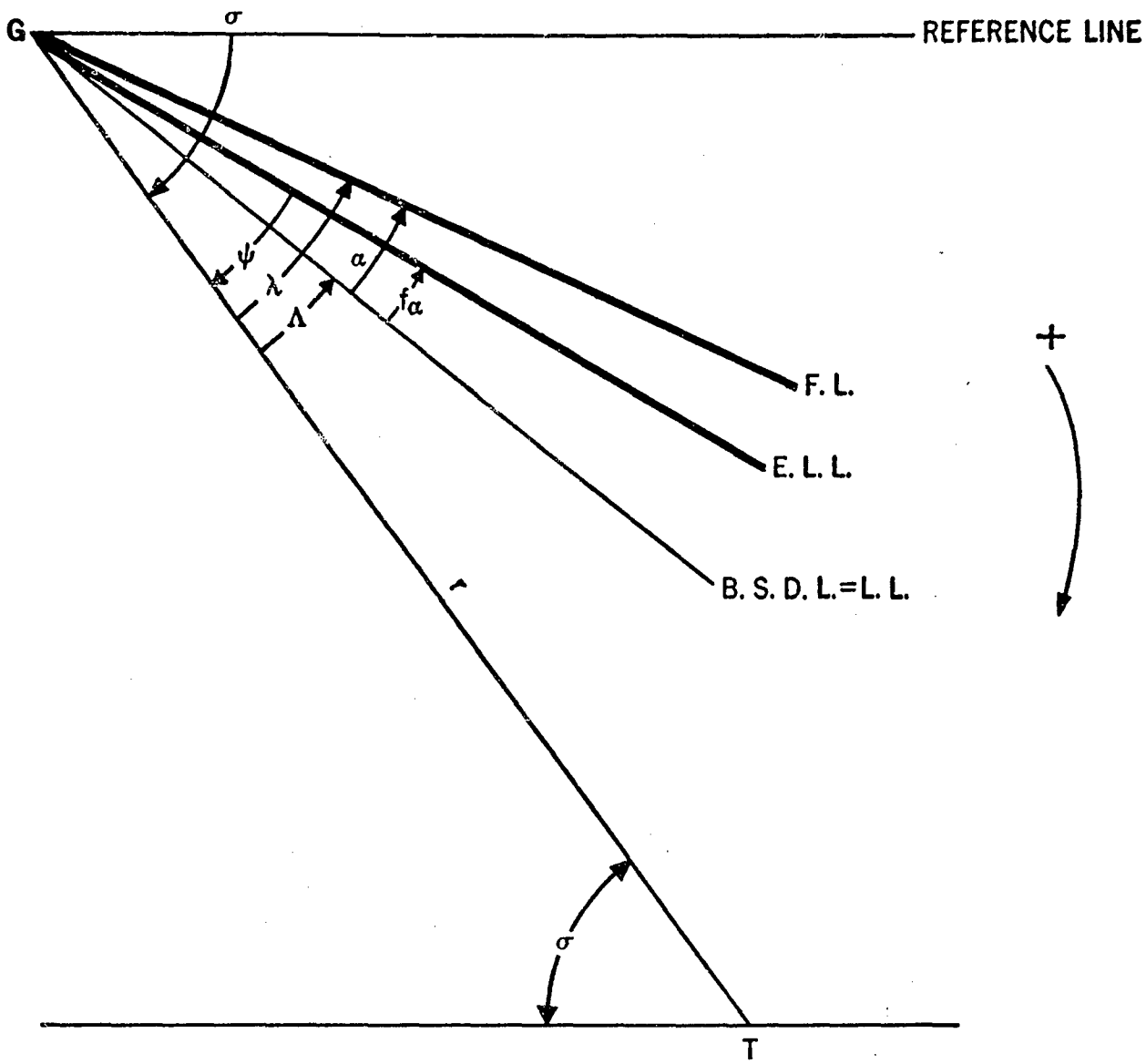

Figure 115. — Trajectory Drop, ψ

7.6 The Sighting Problem

It has been pointed out that in the forward firing of rockets the direction of motion of the rocket is essentially the direction of motion of the airplane at the instant of firing. Hence, in order to hit the target the airplane must have the proper direction of motion at the instant of firing. The airplane, therefore, is maneuvered into a correct attitude and held there for a period of time after which the direction of motion will have taken a calculable position with respect to the airplane. This direction of motion may be specified in terms of an angle between the flight line and the sight line. The behavior (ballistics) of the rocket itself may now be superimposed upon this problem and the correct lead angle may be determined. This, then, is the sighting problem, of which we consider the following three distinct cases:

(a) attacks against a stationary target;

(b) attacks against a target moving in range;

(c) attacks against a target moving in azimuth.

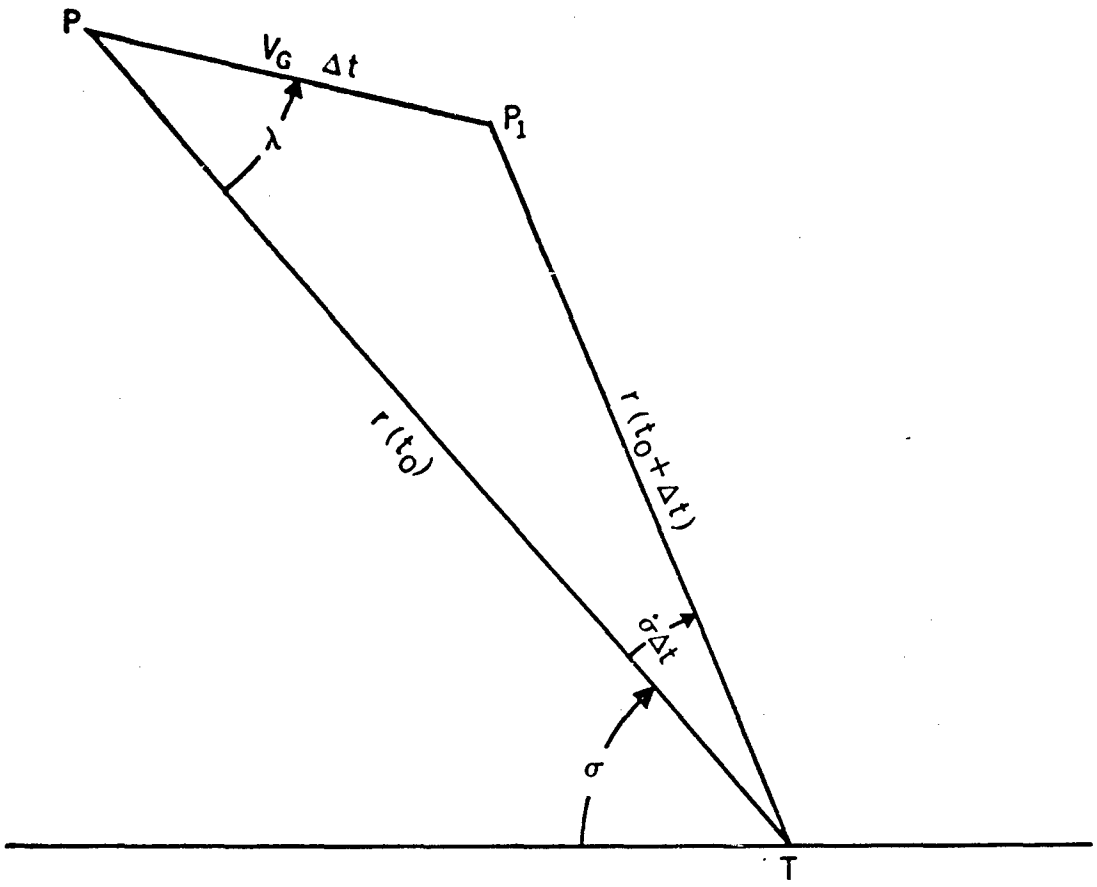

Figure 116. — Rate of Change of σ

These cases are treated separately and the complete picture is obtained by superposition.

A. Stationary Target

We shall first consider "the sighting angle" which is needed to compensate for the gravity drop of the rocket. This angle may be measured from the sight line to the boresight datum line (Λ) or to the flight line (λ). Since the rocket turns from the launcher line to the effective launcher line through the angle $f\alpha$, the trajectory drop to be considered is ψ, the angle between the effective launcher line and the sight line. See figure 115.

It is then clear that

$$(7.4) \quad \Lambda = -(\psi + f\alpha)$$

or, in terms of the lead of the flight line over the sight line,

$$(7.5) \quad \lambda = \Lambda + \alpha = -\psi + (1 - f)\,\alpha\,.$$

The above formulas are expressions for the sighting angle, except for the parallax correction which arises because the sighting system is invariably mounted in the airplane at some distance, d, above the launchers. This correction may be approximated by d/r and is added to the right-hand side of equations (7.4) and (7.5). Since this parallax correction can be superimposed it will not be carried along in future mathematical expressions.

Let us again emphasize that ψ and f depend upon the rocket type and the launching conditions only and, therefore, tables of their values may be used for all aircraft. On the other hand, α and d depend upon the aircraft type and the manner of installation of the launchers and, therefore, must be determined separately for each kind of aircraft and installation.

The existence of the sighting angle gives rise to an angular rate of the sight line during a

tracking period. This angular rate may be used to obtain the required lead which must be computed by any instrument which measures the angular rate. Consequently, we need a relationship between the angular rate of the sight line and the lead angle.

Let us refer to figure 116 and ignore any changes in the angle of attack, α, during the time under consideration. The airplane is considered at two positions $P(t_o)$ and $P_1(t_o + \Delta t)$. The law of sines applied to ΔPP_1T yields

$$(7.6) \quad \frac{|\sin(\dot{\sigma}\Delta t)|}{V_G \Delta t} = \frac{|\sin \lambda|}{r(t_o + \Delta t)}.$$

Since both $\dot{\sigma}\Delta t$ and λ are small, we may use the angle approximation to the sine of the angle so that

$$(7.7) \quad \frac{|\dot{\sigma}\Delta t|}{V_G \Delta t} = \frac{|\lambda|}{r(t_o + \Delta t)} \text{ or } \frac{|\dot{\sigma}|}{V_G} = \frac{|\lambda|}{r(t_o + \Delta t)}.$$

Since Δt is small, a further approximation may be used on the range, so that $r(t_o + \Delta t) \doteq r(t_o) = r$. Let us now consider the signs and directions of the angles as given in figure 116 so that we may remove the absolute value signs in equation (7.7). According to our convention, σ is positive and λ is negative. The motion described is such that σ increases as t increases, therefore $\dot{\sigma}$ is positive. Equation (7.7) may then be written in the following form

$$(7.8) \quad \dot{\sigma} = -\frac{V_G}{r}\lambda = -\frac{V_G}{r}(\Lambda + \alpha).$$

This equation gives the rate of rotation of the sight line that is required to keep it on the target and to provide the proper gravity drop.

B. Target Moving Along the Firing Range

This problem is solved by resolving it into two parts and superimposing their solutions. The first part is the problem of the stationary target discussed above from which we get all the necessary information as far as the gravity drop is concerned. In the second part, we assume the airplane to be stationary and the rocket path to be a straight line. We are then interested in expressions for the kinematic lead required by the motion of the target and for the rate of rotation of the sight line necessary to produce this lead. We introduce Λ_K to express the kinematic lead and give it direction as shown in figure 117, where we have pictured a situation with the target moving away from the airplane at a speed V_T. Let t_f be the time of flight of the rocket over the path $r(t_o + t_f)$. From the law of sines we have

$$(7.9) \quad \frac{|\sin \Lambda_K|}{V_T t_f} = \frac{\sin \sigma}{r_f}.$$

Since Λ_K is small, we use the approximation

$$(7.10) \quad |\Lambda_K| = |\sin \Lambda_K| = \frac{V_T t_f}{r_f} \sin \sigma.$$

Again we use the approximation $r_f \doteq r$ and the fact that the times of flight over the present and future ranges are very nearly equal. (Remember that the target is a ground target and is, therefore, moving relatively slowly.) If we let $\overline{V}$ be the average velocity of the rocket over the future range we have

$$(7.11) \quad \overline{V} = \frac{r_f}{t_f}$$

and the magnitude of the desired kinematic lead at any instant of firing is given by

$$(7.12) \quad |\Lambda_K| = \frac{V_T}{\overline{V}} \sin \sigma.$$

Since Λ_K and σ are oppositely directed angles as shown in figure 117, we have

$$(7.13) \quad \Lambda_K = -\frac{V_T}{\overline{V}} \sin \sigma.$$

988995 O - 52 - 12

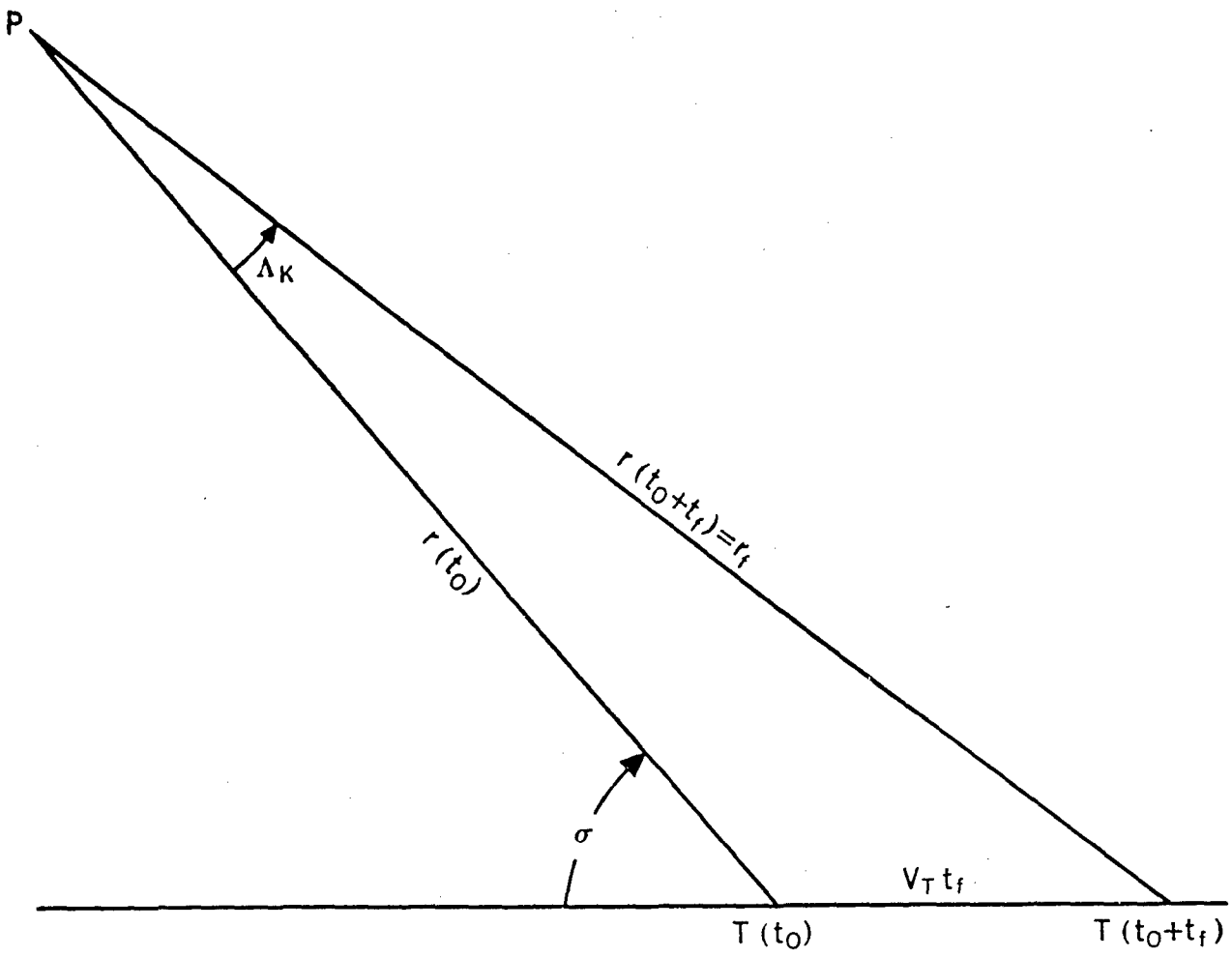

Figure 117. — Target Moving in Range

By superposition we can now express the total lead by

$$\Lambda = \Lambda_{S.T.} \pm \Lambda_K \tag{7.14}$$

or in terms of the flight line over the sight line

$$\lambda = \lambda_{S.T.} \pm \Lambda_K = -\psi + (1-f)\,\alpha \pm \Lambda_K \tag{7.15}$$

where $\Lambda_{S.T.}$ and $\lambda_{S.T.}$ are the leads for stationary targets; the plus sign holds when the target is moving away from the airplane and the minus sign holds when the target is moving toward the airplane.

The problem of proper tracking to give this lead requires an expression for $\dot{\sigma}$, the rate of rotation of the sight line. Consider the problem over a short increment of time, Δt, during which both the airplane and the target are in motion. Let us refer to figure 118.

Apply the law of sines to $\Delta T_0 T_2 T^*$ to give

$$\frac{\overline{T_0T_2}}{|\sin\lambda|} = \frac{V_G \Delta t}{\sin(180^\circ - \sigma)} \tag{7.16}$$

or,

$$\overline{T_0T_2} = \frac{V_G \Delta t\,|\sin\lambda|}{\sin\sigma}. \tag{7.17}$$

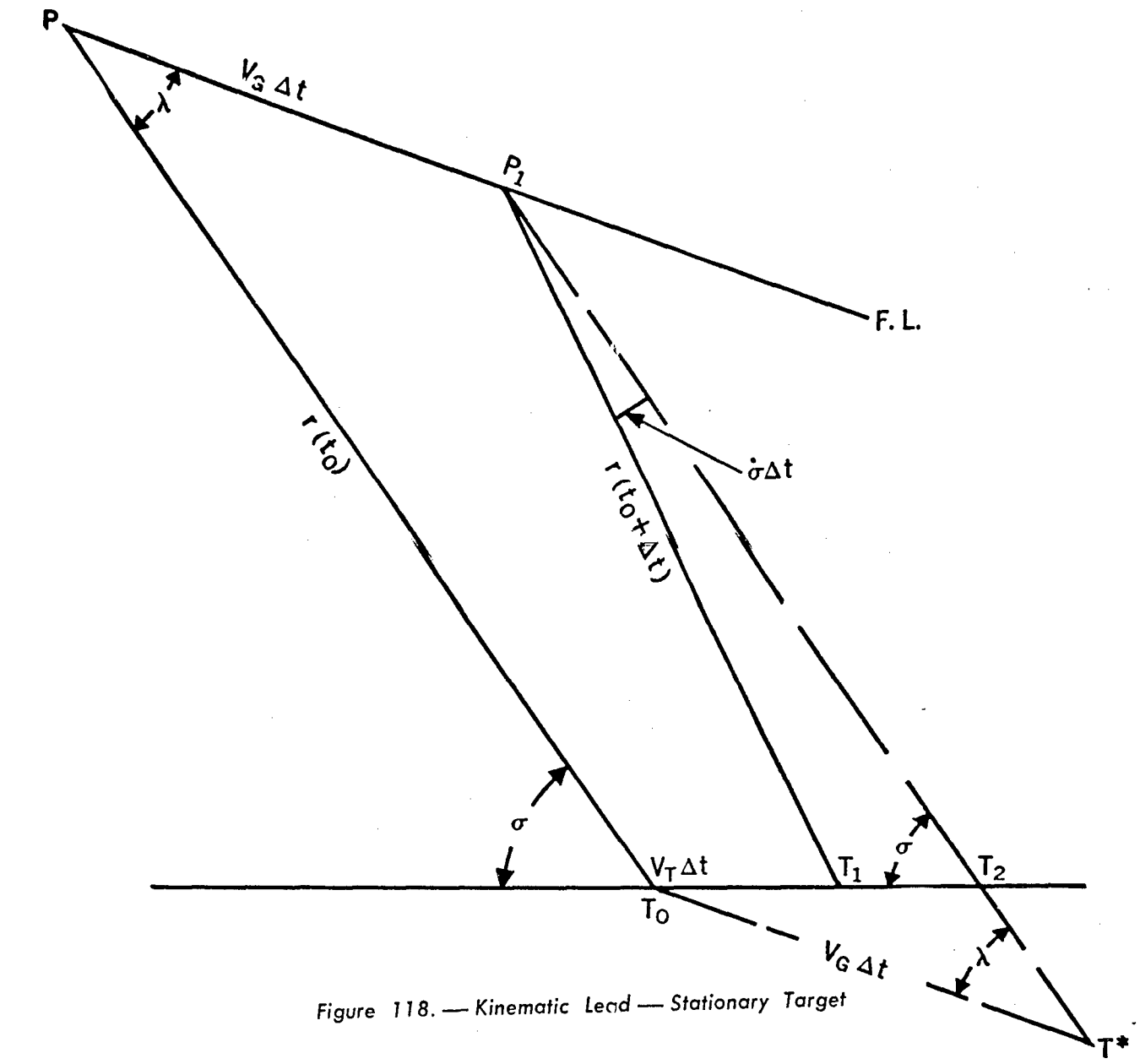

Figure 118. — Kinematic Lead — Stationary Target

Apply the law of sines to $\Delta P_1T_1T_2$ to give

$$(7.18) \qquad \frac{\overline{T_1T_2}}{\sin(\dot{\sigma}\Delta t)} = \frac{r(t_o+\Delta t)}{\sin\sigma}$$

or,

$$(7.19) \qquad \dot{\sigma}\Delta t = \overline{T_1T_2}\,\frac{\sin\sigma}{r},$$

since $r(t_o+\Delta t) \doteq r$ and $\sin\dot{\sigma}\Delta t \doteq \dot{\sigma}\Delta t$.

Now, $\overline{T_1T_2} = \overline{T_oT_2} - \overline{T_oT_1} = \overline{T_oT_2} - V_T\Delta t$, and using $\sin\lambda \doteq \lambda$, we may write

$$(7.20) \qquad \dot{\sigma}\Delta t = \frac{\sin\sigma}{r}\left(\overline{T_oT_2} - V_T\Delta t\right)$$

$$= \frac{\sin\sigma}{r}\left[\frac{V_G\Delta t|\lambda|}{\sin\sigma} - V_T\Delta t\right]$$

or,

$$(7.21) \qquad \dot{\sigma} = \frac{V_G}{r}|\lambda| - \frac{V_T}{r}\sin\sigma.$$

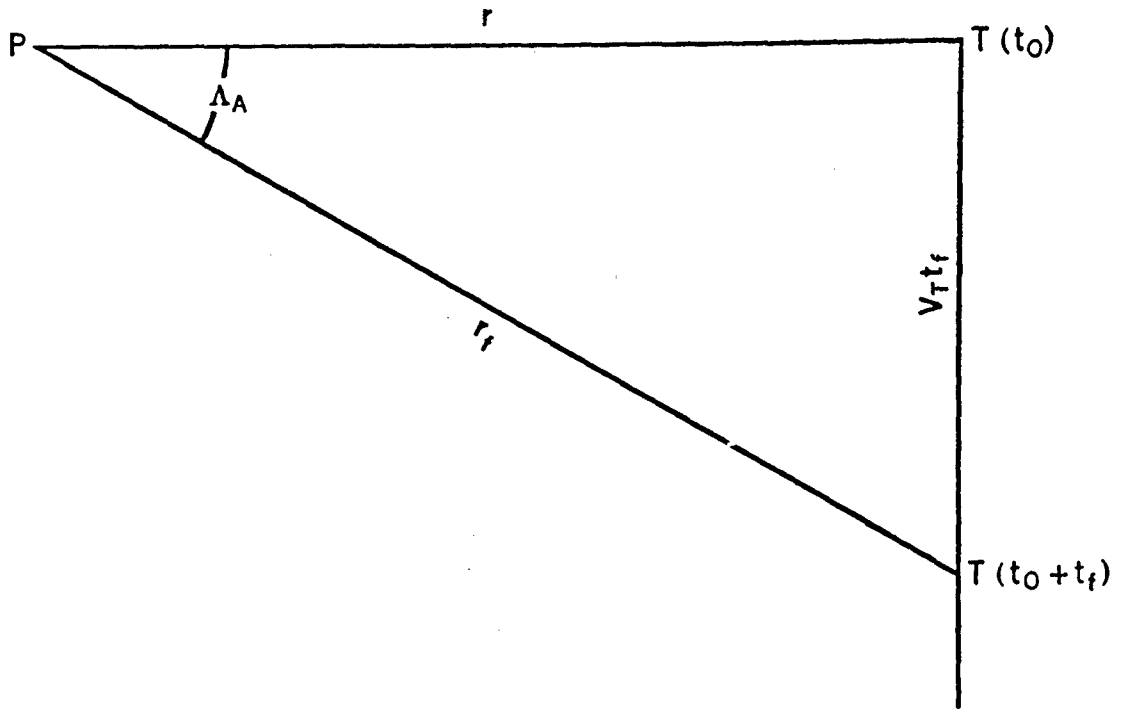

Figure 119. — Azimuth Target Motion

To remove the absolute value sign from λ we note that for the situation pictured $\dot{\sigma} > O$ and, since $\lambda < O$, it is necessary to have a negative sign for the first term. Further, making use of (7.13), we have $\dot{\sigma}$ in terms of λ and Λ_K. Thus,

$$(7.22) \quad \dot{\sigma} = -\frac{V_G}{r}\lambda - \frac{V_T}{r}\sin\sigma$$

$$= -\frac{V_G}{r}\lambda + \frac{\overline{V}}{r}\Lambda_K .$$

If the target is moving toward the airplane, then σ is increasing more rapidly and the component of $\dot{\sigma}$ due to target motion has the opposite sign from that given in equation (7.22).

C. Azimuth Target Motion

Azimuth target motion is a correction applied to the sighting problem. The amount of this correction is obtained from the formula

$$(7.23) \quad \tan\Lambda_A = \frac{V_T t_f}{r}$$

which is easily obtained by considering figure 119.

By using an approximation for the tangent, this expression usually takes the form

$$(7.24) \quad \Lambda_A = \frac{V_T}{\overline{V}} .$$

7.7 Determination of Sighting Tables

Sighting settings are determined for aircraft-launched rockets by firing enough rounds under a number of specified controlled conditions and from these data sight settings for all other desired firing conditions are extrapolated or interpolated by theoretical methods. The number of conditions needed for the computation of reliable sighting tables depends upon how completely the ballistics for the particular rocket, aircraft, and launcher are known. Usually, a large number of rounds have to be fired under many conditions.

The usual procedure is first to determine the launching factor and trajectory drop for the particular type of ammunition. The parallax

factor can be introduced by direct measurement in the aircraft. The problem then is to determine the "effective angle of attack" for the firing condition. This is accomplished by having an accurately boresighted airplane fire a given number of rounds of one type of ammunition at known initial release conditions, making successive passes in opposite directions to cancel out wind effects. An arbitrarily chosen sight setting is used. The range data are then reduced to a standard set of firing conditions and the corrected sight setting, which would bring the mean point of impact on the target, is established.

Thus, everything in equation (7.4) is known except the angle of attack α, and thus the effective angle of attack is determined. Having established the effective angle of attack, sighting tables of the lead angle can then be computed. It has been found that the effective angle of attack can be computed from the formula

$$\alpha = \frac{CW \cos \delta}{V_{G_i}^2} - K$$

where C and K are constants determined from firings. Thus, C and K are tabulated in sighting tables for the particular aircraft.

The above discussion conveniently pertained to post launchers. In the case of drop launchers, another variable, namely the time of drop, must be determined. This is again accomplished by firing enough rounds to establish the correct sight settings for a number of conditions.

A typical sight setting table is shown in table 7.2.

Table 7.2

Typical Sight Setting Table

Type of Rocket 30° Dive	Sight Setting (Degrees)							
Slant Range (yds)	Propellant Temperature (F)							
	0°	40°	70°	100°	0°	40°	70°	100°
	Speed→ 240 MPH				300 MPH			
400	2.9	2.5	2.3	2.2	1.5	1.3	1.2	1.1
500	3.0	2.6	2.4	2.2	1.6	1.4	1.3	1.1
600	3.1	2.7	2.5	2.3	1.7	1.5	1.3	1.2
800	3.3	2.9	2.6	2.5	1.9	1.7	1.5	1.4
1000	3.4	3.0	2.8	2.6	2.1	1.8	1.6	1.5
1200	3.7	3.3	3.0	2.8	2.2	2.0	1.8	1.7
1500	4.0	3.5	3.2	3.1	2.5	2.2	2.0	1.9
2000	4.4	4.0	3.7	3.6	2.9	2.6	2.5	2.3
2500	4.9	4.5	4.2	4.0	3.4	3.1	2.9	2.8
3000	5.4	5.0	4.7	4.5	3.8	3.6	3.3	3.3
4000	6.6	6.1	5.7	5.7	4.8	4.5	4.3	4.2

7.8 Basic Principles of a Rocket Sight

In the forward firing of any projectile, the aircraft must have the proper direction of motion at the instant of firing. A "sight" may be regarded as a device which insures this correct direction of motion. As has already been shown, this direction of motion may be specified in terms of the sighting angle or lead angle and hence is a function of a number of variables such as range, airspeed, dive angle, type of rocket, etc. The sight then must perform the following functions:

(1) It must measure or predict the values that the variables will assume at the instant of fire;

(2) From these data it must compute the correct lead angle;

(3) It must employ some aiming device so that the pilot can produce the required direction of motion.

Each of these functions may be performed in a number of ways and the goal is to arrive at a combination of these ways which not only will give the correct lead angle but also will be easy to mechanize. Although the correct direction of motion of the aircraft can be attained by using a fixed sight, it has been demonstrated that greater accuracy can be obtained by using a computing sight. We shall, therefore, limit our attention to computing sights.

A computing sight is a device which automatically computes the correct lead from input data which is continuously made available to it. Such a device can be designed to reproduce the tabular sight settings that have been arrived at by calculations discussed in the last section. Thus, a computer circuit of a sight may be designed to provide a continuous solution to a basic sighting equation and, by proper adjustment of the computer constants to match the equation, the computer can be made to reproduce the sight settings for any type of projectile. The tabular sight settings are then used to calibrate the sight.

The fundamental equation may take many forms depending upon the method of mechanization to be used. Thus the simple rocket sight may be based on the equation:

(7.25) Sight angle = trajectory drop + f times the angle of attack; i.e., equation (7.15); or it may utilize the angular rate of the sight line and be based upon equation (7.22).

7.9 A Rocket Sight Based on Equation (7.25)

A simple rocket sight suitable for use against stationary targets can be designed on the basis of equation (7.25). This equation for no target motion also is equation (7.4) or,

$$(7.26) \qquad -\Lambda = \psi + f\alpha .$$

Tests on rocket ballistics indicate that the trajectory drop, ψ, can be approximated by $(a + br) \cos \delta$ where a and b are the coefficients for a linear approximation. If, further, the sight is based upon the measurement of the altitude and not the range, we have

$$(7.27) \qquad r = \frac{h}{\sin \sigma} = \frac{h}{\sin (\delta - \Lambda - \alpha)} .$$

If we substitute these approximations into (7.26), we have,

$$(7.28) \qquad -\Lambda = \left(a + \frac{bh}{\sin \sigma} \right) \cos \delta + f\alpha .$$

The effective angle of attack is determined from the following formula

$$(7.29) \qquad \alpha = \frac{CW \cos \delta}{V_{G_i}^2} - K$$

where C and K are constants determined from firings and given for the particular aircraft in sighting tables. Equation (7.28) will then take the form

$$(7.30) \qquad -\Lambda = \left(f_1(v) + \frac{hf_2(v)}{\sin \sigma} \right) \cos \delta - fK$$

where

$$f_1(v) = a + \frac{fCW}{V_{G_i}^2} \text{ and } f_2(v) = b .$$

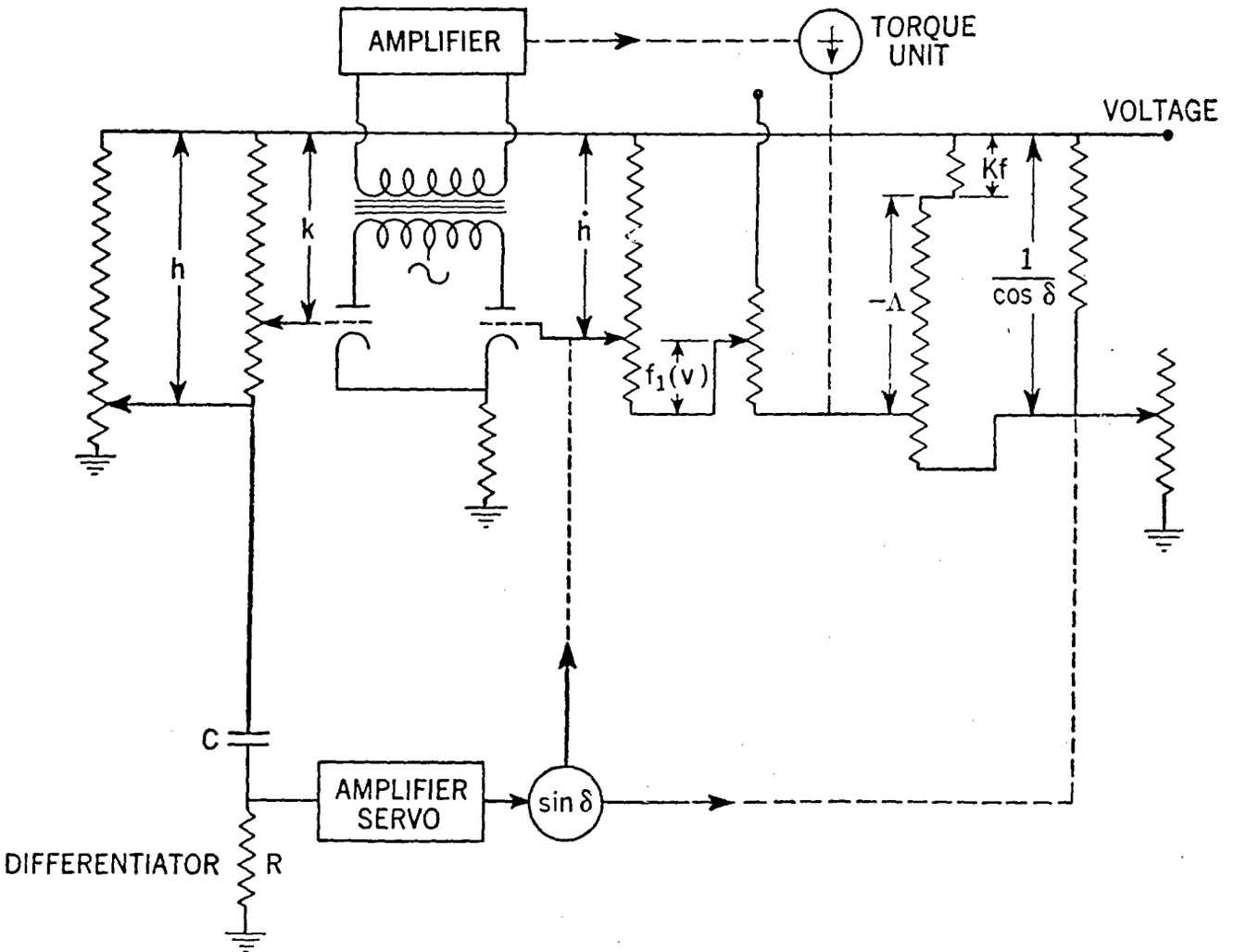

Figure 120. — Voltage Computer — Wiring Diagram

A further simplification is obtained from the fact that

$$\sin\sigma = \sin(\delta - [\Lambda + \alpha])$$
$$= \sin\delta\cos(\Lambda+\alpha) - \cos\delta\sin(\Lambda+\alpha)$$

and since $\Lambda + \alpha$ is small, we may approximate $\sin\sigma$ by

$$(7.31)\qquad \sin\sigma \doteq \sin\delta - (\Lambda+\alpha)\cos\delta$$
$$= \frac{\dot{h}}{V_G} - (\Lambda+\alpha)\cos\delta\,.$$

The function $f_2(v)$ is now assumed to be inversely proportional to V_G; i.e., $f_2(v) = \dfrac{k}{V_G}$, so that the final form of equation (7.26) is then

$$(7.32)\qquad -\Lambda = \left[f_1(v) + \frac{hk}{\dot{h} - V_G(\Lambda+\alpha)\cos\delta}\right]\cos\delta - Kf\,.$$

The mechanization of this equation is accomplished by a voltage computer in which the various parameters are represented by variable electrical potentials. The necessary operations of addition, subtraction, multiplication, and division are performed by suitably connected potentiometers. A simplified diagram showing the principle of this computing circuit is illustrated in figure 120.

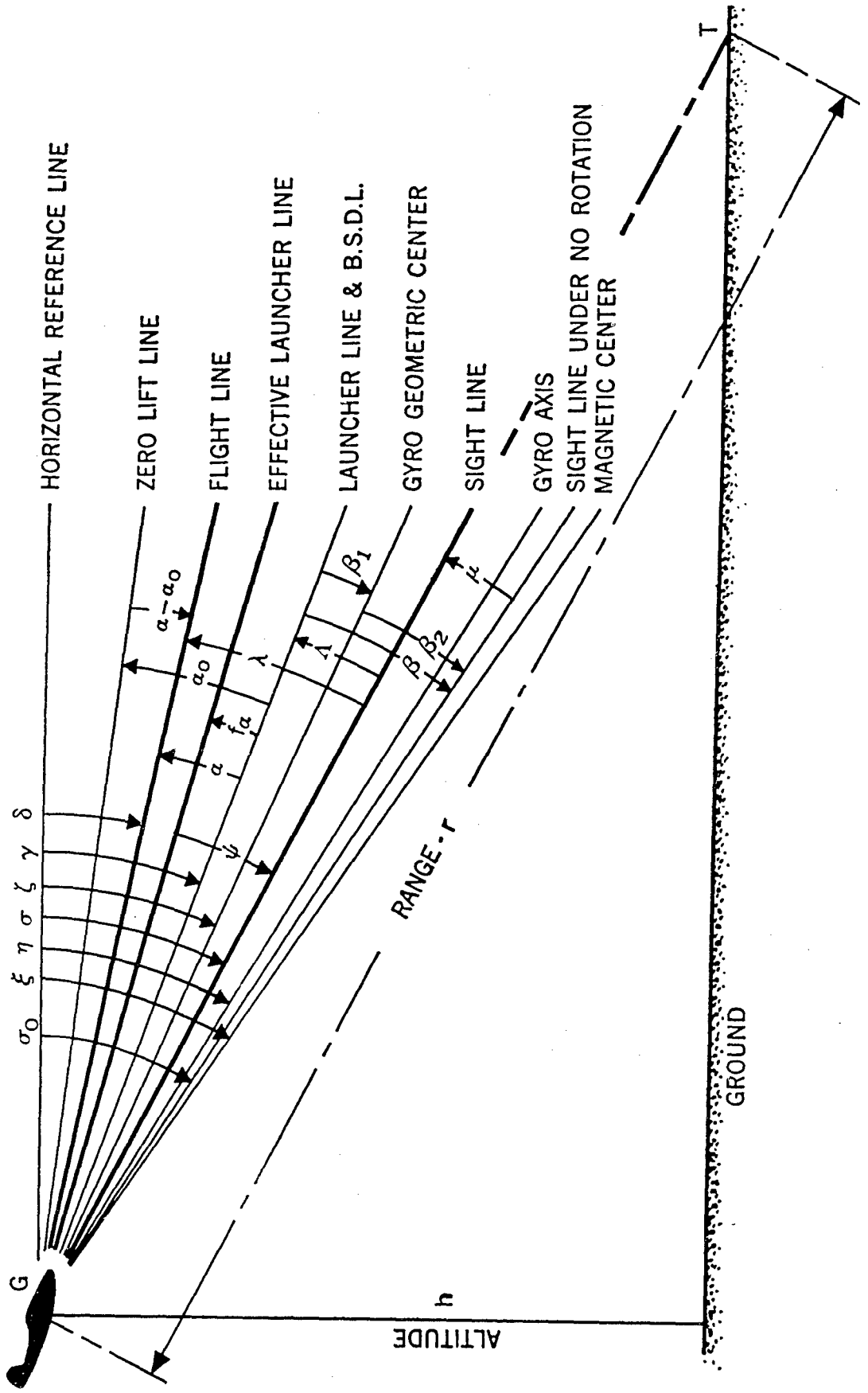

Figure 121. — Instantaneous Diagram for the Sighting Problem — Elevation Plane (Magnitude of Angles are Exaggerated)

7.10 A Rate Gyro Rocket Sight

Another type of rocket sight utilizes the rate of rotation of the sight line which may be measured by a gyroscope (gyro). If the basic mechanization of the gunsight described in chapter 5 is adopted for rocketry, then, as explained there, the precession rate of the gyro and the coupling factor or sight parameter, a, will be employed for solving physically a linear differential equation of the first order in the lead, similar to equation (4.23) for gunnery.

To initiate the discussion that will finally lead to a differential equation of the type just mentioned, let us assume that the rocket firing aircraft is tracking a ground target, all motion being in a vertical plane. Let us further assume that the rocket sight, basically similar to the gunsight of chapter 5, performs physically in its operation in accordance with the geometry of figure 121. With the launcher line and boresight datum line taken to be coincident for convenience, the essentially new feature to be noted here is the initial angle β_2 by which the gyro axis is offset from its geometric center or, since normally the latter direction and the B.S.D.L are separated by an angle β_1 the initial angle $\beta = \beta_1 + \beta_2$ between gyro axis and launcher line. Thus, if initially the line of sight and gyro axis coincide, the sight reticle will be depressed below the B.S.D.L. by the angle β. In order to fly with the depressed reticle on the target, the pilot must keep pushing the aircraft into a dive of increasing steepness. This downward curvature of the flight path, and consequent rotation of the sight unit with the gyro loosely constrained, causes the reticle to drift up from the offset position, thus reducing the lead.

Figure 121 shows the situation with gyro axis and sight line undergoing rotation and also shows where the sight line would be if there were no rotation to influence the gyro.

The new angles which enter the problem are defined as follows:

σ_0 = sight line angle under no rotation;

ξ = angle from the reference line to the magnetic center line of the gyro;

η = angle from the reference line to the gyro axis;

ζ = angle from the reference line to the gyro geometric centerline;

β_1 = angle from the B.S.D.L. to the gyro geometric centerline; a constant offset;

β_2 = angle from the gyro geometric centerline to the sight line under no rotation;

$\beta = \beta_1 + \beta_2$.

The precession rate of the gyro is proportional to the angle between the actual magnetic field center and the gyro axis so that we may write

$$\dot{\eta} = K\ (\xi - \eta) \tag{7.33}$$

where K is a positive constant.

A discussion similar to the one in section 4.7 shows that the coupling factor, a, achieved by an optical linkage satisfies the relationship.

$$|\sigma - \zeta| = \frac{|\eta - \zeta|}{1 - a}. \tag{7.34}$$

Furthermore, it is clear from figure 121 that

$$|\sigma - \zeta| = |\Lambda + \beta_1| = -\ (\Lambda + \beta_1) \tag{7.35}$$

so that the coupling equation (7.34) states

$$-\ (\Lambda + \beta_1) = \frac{\eta - \zeta}{1 - a}. \tag{7.36}$$

Differentiation of this equation yields

$$-\dot{\Lambda} = \frac{\dot{\eta} - \dot{\zeta}}{1 - a} \tag{7.37}$$

since β_1 is a constant.

If we now employ equation (7.33), we have

$$-(1 - a)\ \dot{\Lambda} = K(\xi - \eta) - \dot{\zeta}. \tag{7.38}$$

Figure 121 clearly shows that $\beta_2 = \sigma_o - \zeta$, so that in the zero position of the coupling equation

$$(7.39) \quad \xi - \zeta = (1-a)\ (\sigma_o - \zeta) = (1-a)\ \beta_2 .$$

From equation (7.36) we have

$$(7.40) \quad \eta = -(1-a)\ (\Lambda + \beta_1) + \zeta .$$

If we combine (7.39) and (7.40), we obtain

$$(7.41) \quad \begin{aligned} \xi - \eta &= (1-a)\ \beta_2 + (1-a)\ (\Lambda + \beta_1) \\ &= (1-a)\ (\Lambda + \beta_1 + \beta_2) \\ &= (1-a)\ (\Lambda + \beta) . \end{aligned}$$

Equation (7.38) then takes the form

$$(7.42) \quad -(1-a)\ \dot{\Lambda} = K(1-a)\ [\Lambda + \beta] - \dot{\zeta} .$$

We now define

$$(7.43) \quad K(1-a) = \frac{1}{u}$$

where u is the sensitivity of the gyro. Furthermore,

$$(7.44) \quad \zeta = \sigma + \Lambda + \beta_1$$

so that

$$(7.45) \quad \dot{\zeta} = \dot{\sigma} + \dot{\Lambda}$$

and equation (7.42) becomes

$$(7.46) \quad (1-a)\ \dot{\Lambda} + \frac{1}{u}\Lambda = -\frac{1}{u}\beta + \dot{\sigma} + \dot{\Lambda}$$

or

$$(7.47) \quad -a\ \dot{\Lambda} + \frac{1}{u}\Lambda = \dot{\sigma} - \frac{1}{u}\beta .$$

Equation (7.47) is the differential equation which a rate gyro rocket sight solves. The quantity $\dot{\sigma}$ is obtained from (7.21) in terms of the inputs to the system. The sighting system may be calibrated for a few constant values of β or a variable β may be introduced into the system.

7.11 General Theory of Rocket Tossing

The technique for rocket tossing is similar to that for bombs (see chapter 6). Rocket tossing differs from bomb tossing in that the rocket has a propellant which causes its trajectory to differ from that of bombs. The geometry of rocket tossing may be decomposed into three parts, see figure 122):

(1) The pull-up period, arc OP.

(2) The delay period, arc PD.

(3) The period after the ignition of the propellant, arc DT.

The forces acting on the aircraft during the pull-up period are the same as those which we discussed in the case of bomb tossing. During the delay period, the rocket is acted upon only by the force of gravity, and if we assume that the rocket is released so that its direction of motion is that of the line of flight of the airplane at release, its coordinates may be obtained in the same manner as those for the falling bomb. The deviation of rocket tossing from bomb tossing then is in the behavior of the rocket during the third period. Thus, the path of the rocket may be described completely by considering only two parts; namely, the part which is the same as the bomb (path from O to D) and the rocket trajectory from D to T. It also is assumed that the rocket does not yaw.

We shall consider the rocket tossing problem under the same conditions that we considered the tossing of bombs. That is, the rocket carrying airplane flies a straight line collision course at a constant velocity, V_a, against a stationary target. The pull-up from this collision course is begun at the point O; the rocket is released at the point $P(x_r, y_r)$ and is ignited at the point $D(x_d, y_d)$. The time delay between release and ignition is denoted by t_d and if there is no time delay, it is only necessary to set $t_d = O$ in the following equations.

The equations of motion of the rocket over the path from O to D are the same as those for the bomb. See equations (6.48), (6.45) and (6.46). Let us rewrite equations (6.48) at the end of the delay time, t_d,

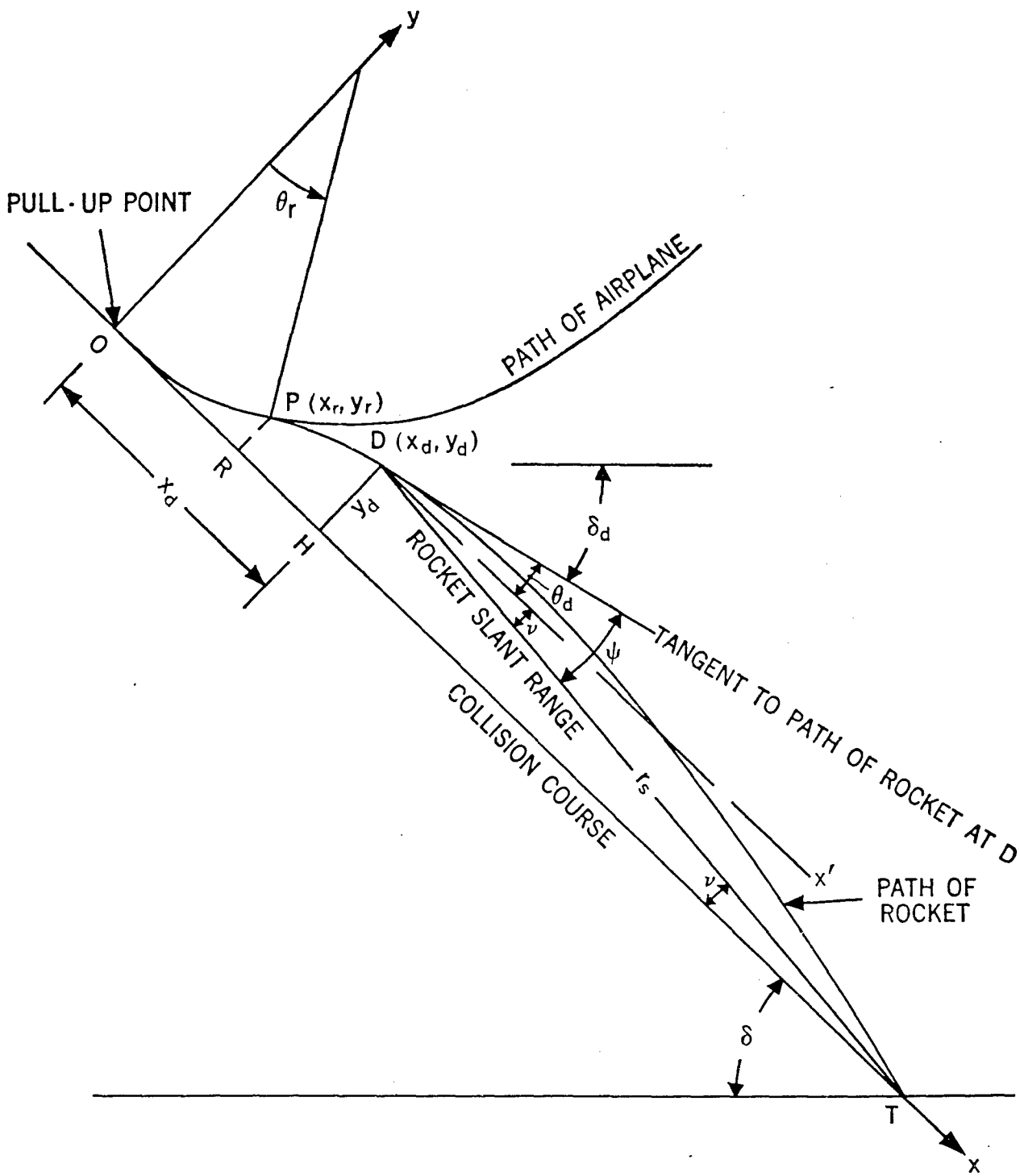

Figure 122. — Rocket Tossing (Greatly Exaggerated)

$$(7.48)\quad \begin{cases} \dot{x}_d = \dot{x}_r + gt_d \sin\delta \\ \dot{y}_d = \dot{y}_r - gt_d \cos\delta \\ x_d = x_r + \dot{x}_r t_d + \frac{1}{2}gt_d^2 \sin\delta \\ y_d = y_r + \dot{y}_r t_d - \frac{1}{2}gt_d^2 \cos\delta\,. \end{cases}$$

Let us recall a few definitions and clearly focus our notation. Refer again to figure 122.

(x, y) The coordinate system which has the x-axis along the collision course OT and the origin at the point of initiation of pull-up, O.

(x_r, y_r) Coordinates of the rocket at release time.

(x_d, y_d) Coordinates of the rocket at point of ignition.

t_r The release time.

t_c The closing time.

t_d The delay time.

r_s The slant range of the rocket from the ignition point to the target, DT.

δ The flight line dive angle before pull-up.

θ The pull-up angle at any instant, t.

θ_r The pull-up angle at release.

θ_d The angle the tangent to the path of the rocket at D makes with the x-axis.

ν The angle between the rocket slant range and the collision course.

ψ The trajectory drop of the rocket.

δ_d The dive angle of the tangent line to the path of the rocket at D. Since the tangent line is actually the effective launcher line at D, the angle $\delta_d = \gamma + f\alpha$; see figure 121. From figure 122 it also is easily seen that $\delta_d = \delta - \theta_d$.

The path of the rocket from D to T is defined by the trajectory ψ. A study of trajectory drop tables for rockets currently in use has shown that it can be fitted with an empirical formula of the type

$$(7.49)\quad \psi = \left[ar_s e^{-V_G/b} + \frac{c\Phi(T)}{V_G} \right] \psi_R\,(\delta_d)$$

where

a, b, and c are empirical constants for a particular type of rocket;

$\Phi(T)$ is an empirically determined quadratic function of the propellant temperature T;

$\psi_R\,(\delta_d)$ is an empirical function which depends essentially upon the dive angle δ_d and thus is the same for all rockets. This function was originally defined graphically; however, a table of values has been calculated and it also has been fitted by expressions involving trigonometric functions.

The rocket tossing problem can now be formulated by a close study of figure 122. This study reveals that a necessary and sufficient condition for the rocket to hit the target is that the following angular relation must be satisfied:

$$(7.50)\quad \psi = \nu + \theta_d\,.$$

The problem then reduces to one of finding expressions for these angles which when substituted into equation (7.50) will permit that equation to yield a solution for the correct pull-up time.

It is easily seen by referring to figure 122 that

$$(7.51)\quad \tan\nu = \frac{y_d}{\overline{OT} - x_d}$$

and upon the substitution of the values for x_d and y_d from equation (7.48) and $\overline{OT} = t_c V_G$ we obtain

$$(7.52)\quad \tan\nu = \frac{y_r + \dot{y}_r t_d - \frac{1}{2}gt_d^2 \cos\delta}{t_c V_G - x_r - \dot{x}_r t_d - \frac{1}{2}gt_d^2 \sin\delta}$$

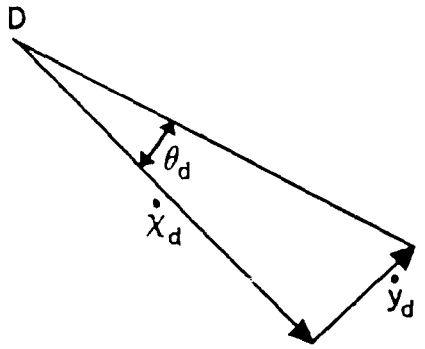

Figure 123. — Velocity Diagram at D

An expression for θ_d is obtained by considering the velocity diagram at D as shown in figure 123.

Thus,

$$(7.53) \qquad \tan\theta_d = \frac{\dot{y}_d}{\dot{x}_d} = \frac{\dot{y}_r - gt_d\cos\delta}{\dot{x}_r + gt_d\sin\delta}$$

If we now recall from chapter 6, equations (6.45) and (6.46), that

$$(7.54) \qquad \begin{cases} \dot{x}_r = V_G\cos\theta_r\,, \\ x_r = \dfrac{V_G^2}{g}\displaystyle\int_0^{\theta_r}\frac{\cos\theta}{\mu}\,d\theta\,, \\ \dot{y}_r = V_G\sin\theta_r\,, \\ y_r = \dfrac{V_G^2}{g}\displaystyle\int_0^{\theta_r}\frac{\sin\theta}{\mu}\,d\theta\,, \end{cases}$$

we could substitute these values into (7.52) and (7.53) and obtain expressions involving only the unknown θ_r. The subsequent substitution of (7.49), (7.52) and (7.53) into (7.50) would yield the general equation which should be solved for θ_r and finally the release time t_r. The complexity of this equation, however, renders it impractical from the point of view of mechanization. Consequently, further simplification is necessary and we shall turn our attention to the approximations which, although quite numerous, nevertheless, has resulted in an equation that, when mechanized, has given good results in field tests.

7.12 A Specialized Equation for Pull-up Time in Rocket Tossing

Due to the fact that the pull-up angle is small and the rocket trajectories which are considered in rocket tossing are rather flat, the following approximations are considered to be acceptable:

(1) During pull-up, the spacial acceleration of the airplane is in a direction perpendicular to the collision course.

(2) The slant range of the rocket is given by

$$(7.55) \qquad r_s \doteq \overline{HT} = (t_c - t_d - t_r)\,V_G\,.$$

(3) The angle θ_d is approximated by its tangent.

(4) The angle ν is approximated by its tangent.

It is necessary to make one further assumption which is to be placed on the spacial acceleration of the airplane during pull-up. There exists two possibilities for this choice. One of these assumes, as was done in toss bombing, that there exists a suitable mean value $\overline{K}$ of K during the pull-up. This assumption results in a quadratic equation for the pull-up time.* However, studies of rocket tossing have shown that the rocket is usually released while the spacial acceleration is increasing so that the second choice is to assume that the spacial acceleration is proportional to some power of t ; that is,

$$\ddot{y} = kgt^r \quad \text{or} \quad K = \cos\alpha + kt^r\,.$$

In particular, the acceleration can be approximated by a linear expression so that we shall develop the case for which $r = 1$ or

* The reader can easily verify this by following the procedure which we shall present for the second choice.

$$(7.56) \quad \ddot{y} = kgt\,,$$

where k is a constant of proportionality.

In view of these assumptions, the velocity components at release are given by

$$(7.57) \quad \begin{cases} \dot{x}_r = V_G\,, \\ \dot{y}_r = \displaystyle\int_0^{t_r} kgt\,dt = \tfrac{1}{2}kgt_r^2 \end{cases}$$

and the coordinates at release are given by

$$(7.58) \quad \begin{cases} x_r = V_G t_r\,, \\ y_r = \tfrac{1}{6}kgt_r^3\,. \end{cases}$$

If we substitute these values into equations (7.52) and (7.53) and use approximations (3) and (4) above, we obtain

$$(7.59) \quad \nu \doteq \tan \nu$$

$$= \frac{\tfrac{1}{6}kgt_r^3 + \tfrac{1}{2}kgt_r^2\,t_d - \tfrac{1}{2}gt_d^2 \cos\delta}{t_c V_G - V_G t_r - V_G t_d - \tfrac{1}{2}gt_d^2 \sin\delta}$$

and

$$(7.60) \quad \theta_d \doteq \tan\theta_d = \frac{\tfrac{1}{2}kgt_r^2 - gt_d \cos\delta}{V_G + gt_d \sin\delta}\,.$$

Let us rewrite equation (7.49) in the form

$$(7.61) \quad \psi = \frac{1}{V_G}\,[\tfrac{1}{2}g\,(t_c - t_d - t_r)\,A_2 + c\Phi]\;\psi_R$$

where

$$(7.62) \quad A_2 = \frac{2V_G^2}{g}\,ae^{-\nu_G/b}\,,$$

$$\Phi = \Phi(T) \text{ and } \psi_R = \psi_R(\delta_d)$$

and

r_s has been replaced by its approximation (2).

Upon substitution of (7.59), (7.60) and (7.61) into equation (7.50), we have

$$(7.63) \quad \frac{g}{2}\,\frac{1}{V_G}\left[A_2\,(t_c - t_d - t_r) + \frac{2c\Phi}{g}\right]\psi_R$$

$$= \frac{\tfrac{1}{2}g\,[\tfrac{1}{3}kt_r^3 + kt_d t_r^2 - t_d^2 \cos\delta]}{[V_G(t_c - t_r - t_d) - \tfrac{1}{2}gt_d^2 \sin\delta]}$$

$$+ \frac{\tfrac{1}{2}g\,[kt_r^2 - 2t_d \cos\delta]}{[V_G + gt_d \sin\delta]}\,.$$

To simplify this equation and ease the notation, first multiply by $\dfrac{2V_G}{g}$ and let

$$c_1 = gt_d \sin\delta / V_G \text{ and } \Phi_1 = \frac{2c}{g}\,\Phi$$

thus, we obtain

$$[\,(t_c - t_d - t_r)\,A_2 + \Phi_1]\;\psi_R$$

$$= \frac{\tfrac{1}{3}kt_r^3 + kt_d t_r^2 - t_d^2 \cos\delta}{t_c - t_r - (1 + \tfrac{1}{2}c_1)\,t_d}$$

$$+ \frac{kt_r^2 - 2t_d \cos\delta}{1 + c_1}\,.$$

After clearing the fractions and combining terms, we get a cubic equation in t_r

$$(7.64) \quad \tfrac{1}{3}(2 - c_1)\,k\,t_r^3 - B_2 t_r^2 - B_1 t_r + B_o = O$$

where

$$B_2 = k\,(t_c + \tfrac{1}{2}c_1 t_d) - (1 + c_1)\,A_2 \psi_R$$

$$B_1 = 2t_d \cos\delta + (1 + c_1)\,\psi_R \;.\; [\Phi_1 + 2A_2\,(t_c - t_d - \tfrac{1}{4}c_1 t_d)]$$

$$B_o = (1 + c_1)\,\psi_R\,[t_c - (1 + \tfrac{1}{2}c_1)\,t_d] \;.\; [\,(t_c - t_d)\,A_2 + \Phi_1] + 2t_d t_c \cos\delta - t_d \cos\delta$$

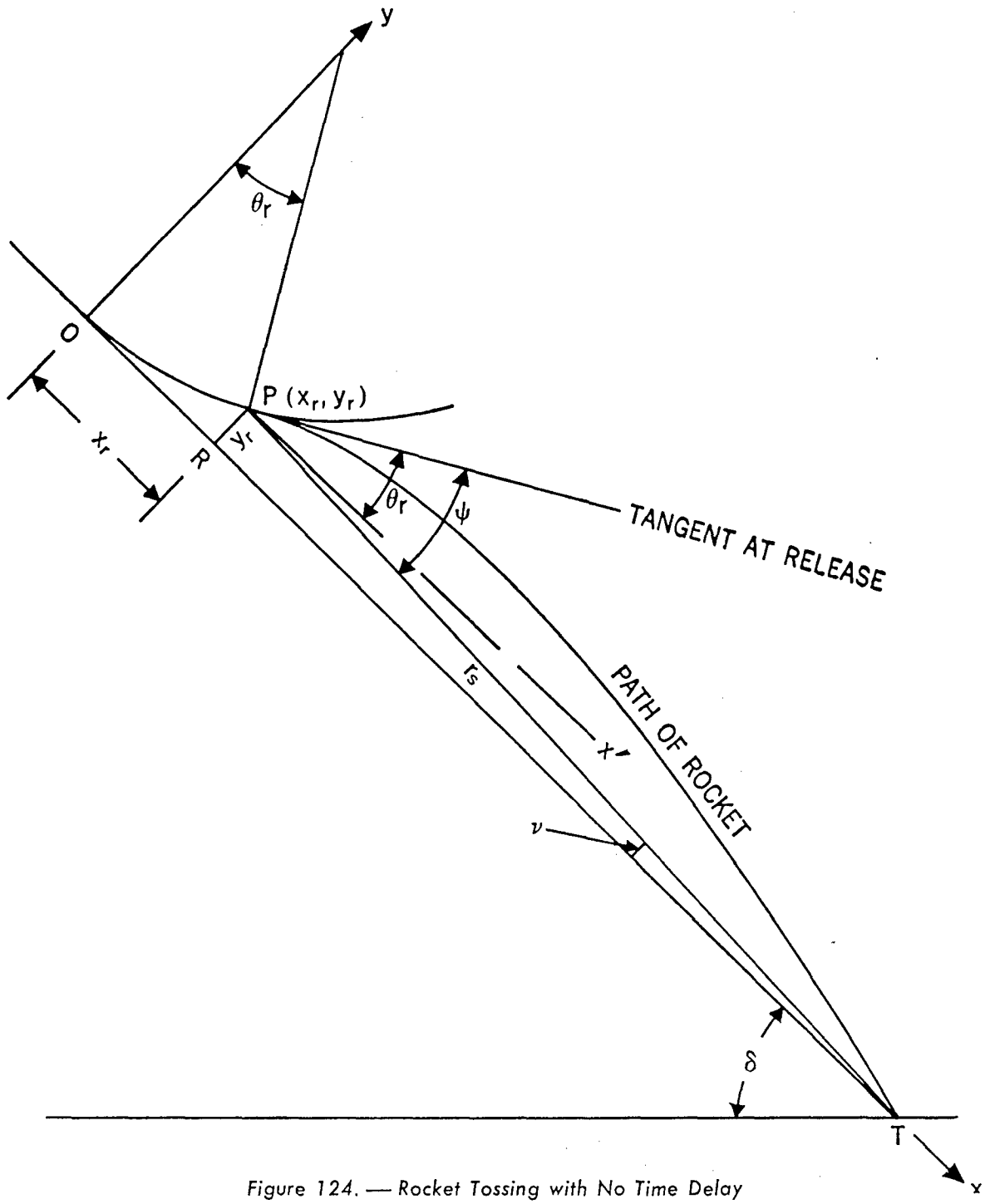

Figure 124. — Rocket Tossing with No Time Delay

The solution of this cubic equation will then yield the release time t_r.

The exact solution of this cubic equation is difficult to express and, more to the point for our consideration, is difficult to mechanize. Consequently, various approximate solutions have been derived. We shall not concern ourselves with these approximations since that would entail a study of the relative magnitudes of the constants involved. Suffice it to say that such approximations are arrived at by extensive study of experimental data obtained from firings.

7.13 Rocket Tossing with no Time Delay

The special case of rocket tossing where there is no time delay is of interest because one of the first rocket tossing directors was fashioned after the toss bombing director. Furthermore, it is possible to design a rocket tossing director by first ignoring the time delay and also the temperature variations of the propellant, and then to correct for these effects by proper changes in the mechanism. We shall, therefore, develop the equation which results when these two assumptions are applied. Thus, if we delete those terms in equation (7.64) which contain t_d and Φ_1, this equation reduces to

$$(7.65)\quad \tfrac{2}{3}kt_r^3 - (kt_c - \psi_R A_2)\,t_r^2 - 2\psi_R A_2 t_r + \psi_R A_2 t_c^2 = O\,.$$

The solution of this equation would then yield the release time t_r. We shall, however, obtain the equation in a different form. We note that θ_d now becomes the pull-up angle θ_r (see figure 124) which is given by

$$(7.66)\quad \theta_r = \frac{g}{V_G}\int_0^{t_r} (K - \cos\delta)\; dt\;;$$

[See equations (6.42) and (6.44)].

Thus, we now have

$$(7.67)\quad \begin{cases} \psi \doteq \dfrac{1}{V_G}\,[\tfrac{1}{2}g\,(t_c - t_r)\,A_2]\;\psi_R \\[2ex] \nu \doteq \dfrac{y_r}{V_G(t_c - t_r)} \\[2ex] \quad = \dfrac{g}{V_G(t_c - t_r)}\displaystyle\int_0^{t_r}\int_0^{t} (K - \cos\delta)\; dt'dt\,. \end{cases}$$

Equation (7.50) then takes the form

$$(7.68)\quad \frac{g\psi_R A_2}{2V_G}\,[t_c - t_r] = \frac{g}{V_G}\int_0^{t_r} (K - \cos\delta)\,dt + \frac{g}{V_G(t_c - t_r)}\int_0^{t_r}\int_0^{t} (K - \cos\delta)\; dt'dt\,.$$

which, after multiplying through by $V_G(t_c - t_r)/g$, may be written

$$(7.69)\quad \tfrac{1}{2}\psi_R A_2 (t_c - t_r)^2 = (t_c - t_r)\int_0^{t_r} (K - \cos\delta)\,dt + \int_0^{t_r}\int_0^{t} (K - \cos\delta)\,dt'dt\,.$$

If we now apply the assumption that $K - \cos\delta = kt$ we have

$$\int_0^{t_r} (K - \cos\delta)\,dt = \tfrac{1}{2}kt_r^2$$

and

$$\int_0^{t_r}\int_0^{t} (K - \cos\delta)\,dt'dt = \int_0^{t_r} \tfrac{1}{2}kt^2 dt = \tfrac{1}{6}kt_r^3$$

and (7.69) becomes

$$(7.70)\quad \tfrac{1}{2}\psi_R A_2 (t_c^2 - 2t_c t_r + t_r^2) = t_c\int_0^{t_r} (K - \cos\delta)\,dt - \tfrac{1}{2}kt_r^3 + \tfrac{1}{6}kt_r^3$$

or, dividing through by t_c,

$$(7.71)\quad \tfrac{1}{2}\psi_R A_2 t_c + \tfrac{1}{2}\psi_R A_2 t_c^{-1} t_r^2 = \psi_R A_2 t_r - \tfrac{1}{3}kt_c^{-1}t_r^3 + \int_0^{t_r} (K - \cos\delta)\; dt\,.$$

If we use

$$t_r^2 = \frac{1}{k}\,A_2\psi_R t_c$$

as a first order approximation to the solution of (7.65), equation (7.71) takes the form

$$(7.72)\quad \tfrac{1}{2}\psi_R A_2 t_c + \frac{1}{2k}\,\psi_R^2 A_2^2 = (\psi_R A_2 - \tfrac{1}{3}A_2\psi_R)\,t_r + \int_0^{t_r} (K - \cos\delta)\,dt\,.$$

Since $t_r = \int_0^{t_r} dt$, we rewrite to obtain

$$(7.73) \int_0^{t_r} (K - \cos\delta + \tfrac{2}{3}\psi_R A_2)\, dt = \tfrac{1}{2}\psi_R A_2 t_c + \frac{1}{2k}\psi_R^2 A_2^2 .$$

The term $\frac{1}{2}k\psi_R^2 A_2^2$ would not have occurred if we had replaced $\overline{RT}$ by $\overline{OT}$ in the formula for v. If such an approximation is acceptable, equation (7.73) reduces to

$$(7.74) \quad \frac{2}{A_2}\int_0^{t_r} (K - \cos\delta + \tfrac{2}{3}\psi_R A_2)\, dt = \psi_R t_c .$$

Equation (7.74) is easy to mechanize since the electrical circuit can be made to solve

$$(7.75) \quad \frac{2}{A_2}\int_0^{t_r} \frac{dt}{R(t)} = \psi_r t_c$$

where $R(t)$ is a resistor whose value is determined by the integrand of (7.74).

7.14 Spin-Stabilized Aircraft Rockets

Since fin-stabilized rockets are suitable only for forward firing from aircraft and because their direction of travel is so dependent upon the direction of motion of the aircraft and the effective angle of attack, much thought has been given to the problem of spin-stabilized rockets. Such rockets are often called spinners. The advantages of spinners are numerous. Theoretically, they may be fired in any direction and thus may be used in air-to-air combat as well as air-to-ground firings. They are less sensitive to changes in angle of attack. They are shorter and thus are adaptable to being released by automatic launchers installed in many parts of the aircraft. Their aeroballistics thus become similar to the ballistics of spinning shells. They differ from spinning shells in that they do not have their final spin nor their final velocity when released from the launcher since most spinners obtain their spin as the propellant burns.

The stability of spinning rockets is a major problem both in the design and the use of spinners. When a spinning rocket is fired from a moving aircraft, it is acted upon by large aerodynamic forces as soon as it is released. Any slight yaw which may be produced by static or dynamic unbalance, cross currents of air, or gravity tip-off, transforms these forces into an overturning moment as was explained in chapter 1. Now the gyroscopic action of the spin tends to turn the rocket about an axis at right angles to that about which the moment is acting, and if the spin is too weak the yaw will increase and, in turn, the overturning moment increases and the rocket may become unstable. The action of the overturning moment causes the rocket to travel in a spiral during its initial period of motion. The phase and amplitude of this spiral at the end of burning determine the subsequent direction of flight. This spiral motion tends to average out the cross thrust due to initial yaw; however, the amplitude and period must be made as small as possible.

It took much experimentation to develop spin-stabilized rockets, but successful ones have been designed and tested. The theoretical behavior and analysis follows that of spinning shells.

7.15 Air-to-Air Rocketry

The entire discussion of this chapter has been limited to air-to-ground rocketry. The air-to-air problem should probably be compared with gunnery rather than bombing. Since rockets are slower and have a larger trajectory drop than bullets, the problem of aiming is far more difficult. However, the innovation of the spin-stabilized rocket has led to considerable study in attempting air-to-air combat with rockets.

The mathematical theory is similar to that for gunnery. The only changes in the theory are those arising from the differing ballistics of rockets and bullets and the consequent redesign of sighting systems. The large gravity drop and the large target speed results in very large lead angles. This in turn limits the combat tactics of the attacking aircraft. An attack suitable for a rocket salvo in air-to-air combat is that of a collision or interceptor course which was considered briefly in chapter 3.

988995 O - 52 - 13

TERMS AND SYMBOLS

GREEK ALPHABET

Letters		Names	Letters		Names	Letters		Names
A	α	Alpha	I	ι	Iota	P	ρ	Rho
B	β	Beta	K	κ	Kappa	Σ	σ	Sigma
Γ	γ	Gamma	Λ	λ	Lambda	T	τ	Tau
Δ	δ	Delta	M	μ	Mu	Υ	υ	Upsilon
E	ε	Epsilon	N	ν	Nu	Φ	φ	Phi
Z	ζ	Zeta	Ξ	ξ	Xi	X	χ	Chi
H	η	Eta	O	o	Omicron	Ψ	ψ	Psi
θ	θ	Theta	Π	π	Pi	Ω	ω	Omega

SYMBOLS

$=$, is equal to;

$\neq$, is not equal to;

$\doteq$ is aproximately equal to;

$<$, is less than;

$>$, is greater than;

$\leq$, is less than or equal to;

$\geq$, is greater than or equal to;

$\dot{x}$, derivative of x with respect to t;

V_F , V sub F;

A' , A prime

$n \rightarrow \infty$, n approaching infinity;

$\sqrt{n}$, square root of n;

$\angle ABC$, angle with vertex at B;

$(\mathbf{V}, \mathbf{u})$, angle from $\mathbf{V}$ to $\mathbf{u}$;

ΔABC , triangle ABC;

Δx , increment of x;

. . . , and so on;

$\overrightarrow{OA}$, vector from O to A;

$\triangle$ triangles;

$f(u)$ function of u.

Chapter 8

GLOSSARY OF NOTATION

8.1 Introduction

The mathematical theory of airborne fire control is the work of many writers. Each of these writers has employed more or less his own notation, a circumstance which has often led to considerable confusion. The publication of this book affords an opportunity to attempt to standardize the notation.

The notation employed in this book conforms in general to the standard notation of mathematical writers and insofar as is possible agrees with that used by organizations such as NACA, Bureau of Standards, Aberdeen Proving Grounds, universities, and with textbooks on ballistics, vector analysis, and other mathematical subjects.

A situation which has been found to be unavoidable is that of employing the same letter to represent more than one concept. However, judicious care has been taken to keep the meaning of a letter or symbol the same throughout any one chapter and thus the meaning to be ascribed to a given symbol should be that corresponding to the chapter in which it is defined. Moreover, whenever it was possible to do so, a given concept was represented by the same symbol in all chapters. Thus, for example, the lead angle has been denoted by Λ throughout; the present range by r; future range by r_f.

Care has been exercised in the use of subscripts and the attempt has been made to attach a meaning to all the subscripts. Thus the practice of using the subscript "o" to denote initial values has been applied to the muzzle velocity, V_o. In order to eliminate cumbersome mathematical notation, subscripts are employed as sparingly as possible.

There are some general definitions and statements concerning notation which apply to the book as a whole. These are summarized in section 8.2. The individual symbols are defined chapter-by-chapter in sections 8.3 through 8.9, inclusive.

8.2 General Definitions

The following definitions are general and hold throughout the book.

Vectors are denoted by bold face letters and their respective magnitudes are indicated by ordinary print of the same letter.

Example: The vector **V** has magnitude V.

Unit vectors are denoted by small letters.

Example: **i, j, k, e, e**$_o$.

The derivative of any function with respect to time is indicated by placing a dot above the letter representing the function.

$$\text{Example: } \dot{x} = \frac{dx}{dt};\ \ddot{\theta} = \frac{d^2\theta}{dt^2};\ \dddot{y} = \frac{d^3y}{dt^3}$$

The resolution of forces, velocities, and accelerations into their components along coordinate axes is accomplished by attaching to the letters denoting the quantity subscripts employing the letters of the axes.

Example: The components of the velocity V along the axes x, y, and z are denoted by V_x, V_y, and V_z.

The position of any object in the figures and diagrams is represented by a letter which most nearly describes the object.

Example: The position of a gun station is denoted by G. The position of a bomber aircraft is denoted by B.

In the main, Greek letters are used to denote angles. For the complete Greek alphabet, see the list of Terms and Symbols at the beginning of this chapter.

It should be pointed out that the term mil has four definitions. The Army mil is defined to be an angle equal to $\frac{1}{6400}$ of one revolution. Thus,

$$\textbf{1 Army mil} = \frac{360}{6400}\ \textbf{degrees} = 0.05625^\circ = 0.0009817\ \textbf{radians.}$$

The Navy mil is defined to be an angle equal to $\tan^{-1}.001$. Thus,

$$\textbf{1 Navy mil} = \tan^{-1}.001 = 3.438\ \textbf{minutes of arc.}$$

The mathematical mil is defined to be an angle equal to $\frac{1}{1000}$ of a radian; i.e., it is a milliradian.

Thus, $\textbf{1 mil} = 0.001\ \textbf{radian} = 0^\circ 3' 26''.3$.

The bombing mil values subtend the same distance on a base line, but are not equal in angular measure. The value of an angle in bombing mils may be found by dividing the distance on the base line (the ground) by $\frac{1}{1000}$ of the altitude.

8.3 Definitions of Symbols for Chapter I

A axial moment of inertia.

A_o azimuth angle of the gun bore; that is, the angle from the V_G vector to the projection of the gun bore axis upon the horizontal plane.

A' azimuth angle of the Siacci coordinate P; i.e., the angle from the gun station direction of motion, V_G, to the projection of the Siacci coordinate P upon the horizontal plane, P'.

$A(u)$ Siacci altitude function.

a speed of sound.

B moment of inertia about the transverse axis.

$$b = \frac{AN}{md}\frac{K_L}{K_M} \text{ (Formula 1.86).}$$

C the ballistic coefficient $= \frac{mg}{id^2}$.

C_n dimensionless ballistic coefficient for type n projectile.

$$c = (c_1 + c_2)\ \rho_o \cdot \text{ (Formula 1.69).}$$

$$c_1 = \frac{d^4 K_H}{2B} + \frac{d^2 K_L}{2m} \text{ (Formula 1.46).}$$

$$c_2 = \frac{d^2}{2(s_o - 1)m} K_D \text{ (Formula 1.54).}$$

D drag force.

d diameter of the projectile.

E_o elevation angle of the gun bore.

e the exponential symbol.

F force acting on the projectile.

F_x, F_y, F_z components of the force F along the x, y, z axes.

f subscript denoting future situation.

G gun station position.

$G_n(u)$ drag function for type n projectile at zero yaw.

g acceleration of gravity.

H point vertically above projectile at any time t.

$I(u)$ Siacci inclination function.

i form factor for a projectile.

$[i, j, k]$ auxiliary coordinate system.

$$K = \frac{1}{2C_n c} K_{D\delta}\, \delta_o^2 \frac{s_o - \frac{1}{2}}{s_o - 1} \text{ (Formula 1.71).}$$

K_D drag coefficient.

$K_{D\delta}$ yaw drag coefficient.

K_H yawing moment coefficient.

K_L cross wind force coeffiient.

K_M moment coefficient.

L cross wind force.

M overturning moment.

m mass.

N spin of the projectile.

n number of calibers for one turn of the rifling.

O origin of coordinate system.

o subscript denoting initial values.

P Siacci range coordinate.

P' projection of P upon the horizontal plane.

$p = \sqrt{1 - (1\ s)}$ (Formula 1.43).

Q Siacci gravity drop coordinate.

R retardation force.

r_f future range of the projectile.

$S(u)$ Siacci space function.

$S_o(u) = S(u_o)$, initial value of Siacci space function for which $u = u_o$.

s stability factor.

$s_o = V_o^2 s_* / \rho\ u_o^2$.

s_* value of the stability factor near the muzzle of a stationary gun in air of standard density.

$T(u)$ Siacci time function.

t_f time of flight of the projectile.

u Siacci pseudo velocity.

u_o initial true airspeed of the projectile.

V projectile velocity relative to the air.

V_G gun station velocity.

V_o muzzle velocity of the projectile.

v velocity of the projectile.

v_x, v_y, v_z components of the projectile velocity in the direction of the coordinate axes x, y, z.

W weight of the projectile.

w wind velocity.

$[x, y, z]$ stationary coordinate system (See figure 2).

(x, y, z) coordinates of the center of gravity of the projectile at any time t.

$[X, Y, Z]$ moving coordinate system (See figure 1).

Z zenith angle of the gun bore.

δ angle of yaw.

δ_o initial angle of yaw.

ε windage jump.

(ξ, η, ζ) projectile coordinates in gun-line axes system.

$[\xi, \eta, \zeta]$ gun-line coordinate system.

θ angle of inclination of the tangent to the trajectory.

θ_o initial angle of inclination of the trajectory.

κ moment factor.

λ lateral deflection.

μ vertical deflection.

ν angle from V_G to u_o.

$\pi = 3.14159$

ρ relative air density, ρ_a/ρ_o.

ρ_a air density.

ρ_o reference density (.07513 lbs/-ft^3).

σ Viscosity of the air.

τ angle from V_G to V_o.

φ angle of orientation of the plane of yaw from the vertical.

ψ angle between the horizontal plane and the plane containing V_o and V_G.

8.4 Definitions of Symbols for Chapter 2

A_o azimuth angle of the gun bore axis.

A azimuth angle of the sight line.

$\mathbf{a}$ total acceleration of the ownship with components a_1, a_2, a_3 along $\mathbf{i}_G$, $\mathbf{j}_G$, $\mathbf{k}_G$.

B_1 $\mathbf{i}_G$ — component of $\boldsymbol{\xi}$.

B_2 $\mathbf{j}_G$ — component of $\boldsymbol{\xi}$.

B_3 $\mathbf{k}_G$ — component of $\boldsymbol{\xi}$.

b ballistic constant appearing in the formula for windage jump.

C air course of the gun-platform.

C_1 tangent line drawn to C' at point T.

C' air course of the target.

C_2 parabola tangent to C' at point T.

E elevation angle of the sight line.

E_o elevation angle of the gun bore axis.

$\mathbf{e}$ unit vector in the direction of the sight line to the target.

$\mathbf{e}_l$ unit vector along the line of intersection of the plane $\mathbf{e}$, $\mathbf{k}_G$ with the plane $\mathbf{e}_o$, $\mathbf{i}_E$.

$\mathbf{e}_o$ unit vector in the direction of the gun bore axis.

F decrease in the vertical acceleration of the bullet due to air resistance.

$\mathbf{g}$ acceleration due to gravity.

G present position of the gun-platform.

G_o position of gun-platform at start of combat.

G_f future position of the gun-platform.

$\mathbf{i}_A$ unit vector along the terminal side of angle A.

$\mathbf{i}_{A_o}$ unit vector along the terminal side of angle A_o.

$\mathbf{i}_E$ unit vector along the terminal side of angle $A + \frac{\pi}{2}$.

$\mathbf{i}_G$ unit vector directed forward along the longitudinal axis of the ownship.

$\mathbf{i}_L$ unit vector along the terminal side of the angle $E - \frac{\pi}{2}$.

$\mathbf{i}_s$ horizontal unit vector fixed in space.

$\mathbf{J}$ windage jump vector.

$\mathbf{j}_G$ unit vector directed outboard from ownship and parallel to the starboard wing.

$\mathbf{j}_s = \mathbf{n} \times \mathbf{i}_s$.

$\mathbf{k}_G$ unit vector directed downward along the ownship vertical.

$\mathbf{k}_s = \mathbf{n}$

$l = q - 1$.

$\mathbf{M} = r^2\boldsymbol{\omega}$ angular momentum of the sight line at the time of fire.

$\mathbf{M}(t)$ angular momentum of the sight line at the time t.

M_E component of $\mathbf{M}$ along $\mathbf{i}_E$.

M_L component of $\mathbf{M}$ along $\mathbf{i}_L$.

m slope of gun-target line (coplanar case) with respect to fixed axes in space.

$N = (1 - \sin^2 \alpha_2 \sin^2 \alpha_3)^{-1/2}$.

$\mathbf{n}$ unit vector directed vertically downward in space.

O origin of coordinate system fixed in space.

$\mathbf{P}$ Siacci range.

Q Gravity drop of bullet during its time of flight.

q bullet slowdown factor.

R bullet range $= \overrightarrow{GT_f}$.

r present range to target $= \overrightarrow{GT}$.

$\mathbf{r}_f$ future range to target $= \overrightarrow{G_fT_f}$.

T present position of target.

T_o position of target at start of combat.

T_f future position of target.

T_{f_1} position of target as predicted by a first order computer.

T_{f_2} position of target as predicted by a second order computer.

t variable time t, measured from instant of fire $t = O$.

t present time of flight, i.e. time of flight of the bullet over the present range r.

t_f time of flight of bullet from present position of the gun to the point of impact with the target.

t_i value of t at time of impact.

t_o time for bullet to traverse R in a vacuum.

u_o initial speed of bullet with respect to inertial space.

$\bar{u}$ average speed of bullet over the Siacci range.

V_f average speed of bullet over the future range.

$\mathbf{V}_G$ velocity of gun-platform.

$\mathbf{V}_o$ muzzle velocity of bullet.

$\mathbf{V}_r$ average projectile speed over the present range.

$\mathbf{V}_T$ velocity of target.

w rate of gravity drop.

(x_s, y_s) rectangular coordinates of the point labeled S.

α approach angle of the target $= (-\mathbf{r}, \mathbf{V}_T)$.

α_2 angle of attack $= (\mathbf{i}_G, \boldsymbol{\xi}')$

α_3 angle of skid $(\mathbf{i}_G, \boldsymbol{\xi}'')$.

β bank angle of ownship = angle through which aircraft has rolled.

γ gun angle-off $= (\mathbf{i}_G, \mathbf{V}_o)$.

δ_o initial yaw angle of the projectile.

δ dive angle of ownship $= 90° - (\mathbf{i}_G, \mathbf{n})$.

$\varepsilon_1, \varepsilon_2$ first and second order bias errors.

η angle from fixed reference line to V_G.

θ angle directed from reference line to sight line.

Λ total lead angle $= (\mathbf{e}, \mathbf{e}_o)$.

Λ_A azimuth component of Λ $= A_o - A$.

Λ_b ballistic lead $= (\mathbf{V}_o, \mathbf{r}_f)$.

Λ_E elevation component of Λ $= E_o - E$.

Λ_k kinematic lead angle $= (\mathbf{r}_f, \mathbf{r})$.

Λ_{SL} sight lateral component of Λ.

Λ_{SV} sight vertical component of Λ.

μ angle directed from a horizontal reference line to $\mathbf{u}_o$.

ν angle $(\mathbf{V}_G, \mathbf{u}_o)$.

$\boldsymbol{\xi}$ unit vector directed along $\mathbf{V}_G$.

$\boldsymbol{\xi}'$ unit vector directed along the projection of $\mathbf{V}_G$ upon the ownship vertical plane determined by $\mathbf{i}_G, \mathbf{k}_G$.

ξ'' unit vector directed along the projection of $\mathbf{V}_G$ upon the ownship azimuth plant determined by $\mathbf{i}_G$, $\mathbf{j}_G$.

ψ central angle subtended at the center of a circular path by an arc traversed by the gun platform at time of fire.

ψ_i value of ψ at time $t = t_i$.

ρ relative air density.

τ sight line angle-off $= (\mathbf{i}_G, \mathbf{r})$.

τ_o $(\mathbf{i}_G, \mathbf{e}_o)$.

τ_f future range line angle-off $= (\mathbf{i}_G, \mathbf{r}_f)$.

φ angle between bullet range and the sight line $= (\mathbf{R}, \mathbf{r})$.

$\mathbf{\Omega}_s$ angular velocity of the sight coordinate system with respect to space.

$\boldsymbol{\omega}$ angular velocity of the sight line with respect to space

ω_e component of $\mathbf{\Omega}_s$ along $\mathbf{e}$.

ω_E component of $\mathbf{\Omega}_s$ along $\mathbf{i}_E$.

ω_L component of $\mathbf{\Omega}_s$ along $\mathbf{i}_L$.

8.5 Definitions of Symbols for Chapter 3

A azimuth angle of projectile's rectilinear trajectory.

$\mathcal{AR}$ aspect ratio, b^2/S.

a_n normal acceleration.

B subscript pertaining to bomber aircraft.

b wing span of aircraft.

C_D drag coefficient.

C_L lift coefficient.

$c = V_B/V_F$.

$c_1 = V_B/\bar{u}$.

c_i aerodynamic constants (Formula 3.66).

D drag force.

E elevation angle of projectile's rectilinear trajectory.

F force notation; as a subscript it pertains to fighter aircraft.

$(\mathbf{i}, \mathbf{j}, \mathbf{k})$ unit vectors.

$$K = \frac{2\pi}{1 + 2/\mathcal{AR}} \quad \text{(Formula 3.65)}.$$

K_i dimensionless constants (Formula 3.72).

L lift force.

m slope of line.

R radius of curvature.

R_P projectile air range.

r present range.

r_f future range.

S wing area.

s length of arc; dimensionless range (Formula 3.71).

T thrust force.

t variable time.

t_f time of flight of projectile.

t^* dimensionless time (Formula 3.71).

u_B dimensionless bomber velocity (Formula 3.71).

$\mathbf{V}_B$ velocity of bomber aircraft.

$\mathbf{V}_F$ velocity of fighter aircraft.

$\bar{u}$ average speed of projectile over r_f.

V_i indicated air speed.

v dimensionless velocity (Formula 3.71).

W weight of aircraft.

(x_B, y_B, z_B) coordinates of bomber aircraft.

(x_F, y_F, z_F) coordinates of fighter aircraft.

α angle of attack of gun bore line.

α_o angle from zero lift line to thrust line.

β bank angle.

γ angle from reference line to flight line.

δ angle of deviation.

η propeller efficiency.

θ angle from reference line to sight line.

Λ angle from V_o to sight line.

$\lambda_P, \lambda_t, \lambda_s$ see Formula (3.68).

ρ relative air density.

τ angle-off of the sight line.

8.6 Definitions of Symbols for Chapter 4

a sight parameter.

A, B constants in the aided tracking formula.

C amplification ratio = amplitude of sight oscillation amplitude of gun oscillation.

d distance from reticle to gyro mirror.

e base of natural logarithms $= 2.71828\ldots$

f focal length of collimating lens.

$f(t)$ arbitrary input function of the time.

$f_1(t), f_2(t)$ "signal" and "noise" components of $f(t)$.

G present position of gun platform.

$h = 1 + \frac{1}{2} t_f \left(\frac{\dot{M}}{M}\right)$, a dimensionless quantity.

k coefficient in linear differential equation, $k\dot{x} + x = f(t)$.

$k_1 = 1/(1-a)u$.

$\mathbf{M}$ angular momentum of line of sight.

q bullet slowdown factor.

r present range to target.

r_f future range to target.

T_f future position of target.

T_o position of target at time of fire.

t time variable measured from an arbitrary origin.

t_f time of flight of projectile.

t_o arbitrary origin of time t.

V_G speed of gun-platform at time of fire.

V_T speed of target at time of fire.

V_r average projectile speed over present range.

V_f average projectile speed over future range.

V_o projectile muzzle speed.

x output functions of the time corresponding to the input $f(t)$.

x_o value of x at time t_o.

x_1 output function of the time corresponding to the input $f_1(t)$.

x_2 output function of the time corresponding to the input $f_2(t)$.

α approach angle of target.

γ gun angle-off $= (\mathbf{V}_G, \mathbf{V}_o)$.

γ_1 sinusoidal oscillatory motion of the gun.

γ steady state value of γ.

ε time lag corresponding to phase difference of gun and sight oscillations.

η angle between reference line and gyro axis.

η angle through which gunner's handgrips have turned from a neutral position.

θ angular coordinate of tracking device.

Λ total lead angle.

Λ_b ballistic lead angle.

Λ_k kinematic lead angle.

$\pi = 3.14159 \ldots$

σ angle between reference line and and sight line.

σ_0 steady state value of σ.

σ_1 value of σ corresponding to γ_1.

τ sight line angle-off.

ω angular rate of the line of sight.

8.7 Definitions of Symbols for Chapter 5

A, B, C moments of inertia of a solid of revolution with respect to the principal axes of inertia, x, y, z.

a sight parameter.

B fixed mirror in the sight head optical system.

c_1, c_2, c_3 proportionality constants.

d distance from reticle to gyro mirror.

E electro-motive force.

$\mathbf{F}$ an arbitrary force.

f focal length of collimating lens.

G viewing glass on the sight head.

H magnetic field strength.

$\mathbf{H}_o$ moment of momentum of a force system about the point O.

I_z moment of inertia about the z-axis.

i current strength.

i_e eddy current strength.

$\mathbf{k}$ unit vector along the z-axis.

K_1 constant of proportionality.

l length of torque axis.

$\mathbf{L}$ arbitrary torque vector.

m mass.

$\mathbf{M}_o$ moment of mass m about point O.

N center of spinning dome, located on its surface.

O any fixed point.

P a particle.

ρ perpendicular distance from point O to line of action of force $\mathbf{F}$.

$\mathbf{r}$ position vector of particle P relative to O.

R electrical resistance.

R reaction force at point of gyro support.

$\mathbf{T}$ torque vector, $\mathbf{W}l$.

u gyro sensitivity.

$\mathbf{V}$ velocity of particle P relative to O.

$\mathbf{V}_T$ target velocity.

v linear speed of a point on the spinning dome.

$\mathbf{W}$ weight of gyro rotor.

$[x, y, z]$ principal axes of inertia of a solid of revolution.

α angle by which the line from the reticle to the gyro mirror is offset from the gun bore axis. Also used elsewhere as a variable angle and as angular acceleration.

$\boldsymbol{\alpha} = \dot{\boldsymbol{\Omega}}$

γ gun angle-off.

δ angle between gryo spin axis and gun bore axis.

Δ error operator.

η angle between reference line and gyro axis.

θ angle of deflection of gyro spin axis in azimuth.

Λ_A azimuth component of Λ_k.

Λ_E elevation component of Λ_k.

Λ_k kinematic lead angle.

$\pi = 3.14159\ldots$

ρ distance of mass m from z-axis.

σ angle between reference line and line of sight.

φ angle of deflection of gyro spin axis in elevation.

ω angular rate of the line of sight.

$\boldsymbol{\omega} = \boldsymbol{\Omega} + \boldsymbol{\omega}'$.

$\omega_x, \omega_y, \omega_z$ components of angular velocity of $\boldsymbol{\omega}$ along x, y, z-axes.

ω' angular velocity of precession.

$\boldsymbol{\Omega}$ = spin angular velocity of gyro rotor.

8.8 Definitions of Symbols for Chapter 6

A. AND B. LEVEL BOMBING

B_a position of bomb in still air at an arbitrary time t since release.

B_v position of bomb in vacuo at an arbitrary time t since release.

d diameter of bomb.

$\mathbf{F}$ drag force due to air resistance acting on bomb.

$\mathbf{f}(v)$ drag force acting on bomb; function of bomb velocity only.

g acceleration due to gravity.

H altitude of plane above target level.

$h(t)$ difference in altitudes of points B_v and B_a at time t.

i ballistic form factor of bomb.

K empirical constant = .0000316 ft.$^{-1}$.

k constant of proportionality.

m mass of bomb.

OO' line of flight of bomber during time of flight of bomb in vacuo.

R range of target along the horizontal.

r bomb trail.

$r(t)$ difference in abscissas of points B_v and B_a at time t.

T target.

t arbitrary time since release of bomb.

t_f time of flight of bomb.

V_c closing speed between plane and target = ground speed of plane when target is stationary.

V true air speed of bomber.

V_i indicated air speed of bomber.

$\mathbf{V}_T$ target velocity.

$\mathbf{v}$ velocity of bomb with respect to the air mass.

$\mathbf{v}_t$ terminal velocity of bomb in air.

$\mathbf{W}$ weight of the bomb.

$\mathbf{W}$ wind velocity.

X horizontal coordinate of bomb.

Z vertical coordinate of bomb.

θ angle which tangent line to bomb trajectory makes with the vertical.

θ drift angle.

$\pi = 3.14159\ldots$

ρ_a density of air at a given altitude.

ρ_0 density of air at sea level.

φ range angle of target.

C. Dive or Glide Bombing

[Note: Letters not defined have same meaning as for Level Bombing.]

L linear aiming allowance.

V_y vertical component of V.

V_x horizontal component of V.

X horizontal range of target.

θ angle between flight line and the horizontal.

λ lead angle of flight line over the sight line to the target.

D. Toss Bombing

[Note: Letters not defined have the same meaning as for Level and Dive Bombing. Letters with zero subscript indicate values of letters at the time of pull-out from a straight dive.]

a retarding acceleration on bomb due to air resistance.

B proportionality constant.

$f = (h_N - h_O)\ f$.

h_N, h_O altitudes of points N and O, respectively.

K number of gees acting on aircraft due to both curvature and gravity at any point on the pull-up path.

$\bar{K}$ time average of K over the pull-up arc OP.

N point at which straight-line dive at target is begun.

O point of pull-out from a straight dive.

P point of bomb release.

R radius of curvature of pull-up path.

s variable distance measured along the pull-up path, beginning at O.

t time taken to fly the distance s, a variable time since initiation of pull-up.

t_c closing time = time for aircraft to cover distance OT.

t_{NO} time for aircraft to cover distance NO.

$t_h = t_r + t_f$ = time when bomb strikes the target measured from start of pull-up.

t_r pull-up time measured from point of pull-out to point of bomb release.

u, w horizontal and vertical components of bomb velocity since release.

$\overline{U}_r, \overline{W}_r$ horizontal and vertical components of V at P.

V true air speed of plane along the pull-up path.

x, y coordinate axes, along and perpendicular to the collision course, respectively, with origin at O.

x_r, y_r coordinates of point P.

β a particular function of input variables $t_c, \delta, \overline{\mu}, V$.

δ dive angle of the collision course OT.

$\epsilon(\xi)$ a term which accounts for change in trajectory due to air resistance.

θ angle between x-axis and the tangent line to pull-up path at time t.

θ_r angle between x-axis and the tangent line to the pull-up path at P.

$\mu \doteq K - \cos\delta$ = normal acceleration on aircraft along its pull-up path, in gees.

$\bar{\mu}$ average normal acceleration over the pull-up arc OP.

ξ, η horizontal and vertical axes with origin at P.

ξ_h, η_h coordinates of T at time t_h.

σ a function of $\bar{\mu}$ and δ.

φ angle between the horizontal and the tangent line to the bomb trajectory.

$\bar{\varphi}$ mean value of φ over arc PT.

ψ a function of K, δ and β.

8.9 Definitions of Symbols for Chapter 7

a_n normal acceleration.

B.S.D.L. boresight datum line; a reference line fixed in the airplane.

b constant of proportionality.

E.L.L. effective launcher line; the line of departure of rocket.

F.L. flight line; the direction of motion of the aircraft.

f launching factor.

H altitude of the airplane above the target.

L.L. launcher line; altitude of launchers.

r present range.

r_f future range.

S.L. sight line; line from own ship to target.

t_b burning time of rocket.

t_c closure time.

t_d the delay time.

t_f time of flight of rocket.

t_p the time the rocket stays in the launchers.

t_r release time of rocket.

V_f average velocity of the rocket over future range.

$\mathbf{V}_G$ gun station velocity.

V_{G_i} indicated airspeed of the gun station.

$\mathbf{V}_r$ final velocity of the rocket relative to the aircraft.

$\mathbf{V}_T$ velocity of the target.

x horizontal position of the rocket.

Z.L.L. zero lift line; a reference line fixed in the airplane.

α angle of attack of the *B.S.D.L.*

α_0 angle from *B.S.D.L* to *Z.L.L.*

$f\alpha$ angle from *B.S.D.L.* to *E.L.L.*

$\beta = \beta_1 + \beta_2$.

β_1 angle from *B.S.D.L.* to the gyro geometric centerline.

β_2 angle from the gyro geometric centerline to the sight line under no rotation.

δ angle from the horizontal to the *B.S.D.L.*

γ dive angle, angle from horizontal reference line to the *F.L.*

ζ angle from the reference line to the gyro geometric centerline.

η angle from the reference line to the gyro axis.

θ pull-up angle at any instant t.

θ_r pull-up angle at release.

θ_d the angle the tangent to the path of the rocket at D makes with the x-axis.

Λ lead angle, angle from sight line to *B.S.D.L.*

Λ_A lead angle in azimuth plane.

Λ_k kinematic lead angle.

$\Lambda_{S.T.}$ lead angle for stationary target.

λ angle from the flight line to the sight line.

$\lambda_{S.T.}$ angle λ for stationary target.

ν the angle between the rocket slant range and the collision course.

ξ angle from reference line to the magnetic centerline of the gyro.

σ angle from the horizontal to the sight line.

σ_o sight line angle under no rotation.

ψ trajectory drop; the angle from the effective launcher line to the sight line.

Appendix A

VECTOR OPERATIONS

A.1 Vector Algebra—Addition and Subtraction

By a vector is meant a straight line segment possessing a definite length and direction. Any physical magnitude which also involves the idea of direction may be represented vectorially. Thus we may cite as examples: velocity, acceleration, force, and torque.

Notationally, we shall distinguish between a vector quantity **A** and its corresponding scalar value A by employing bold face type for the former and ordinary type for the latter. Thus for vector A we have **A** while its scalar value is denoted by A. Alternately, we shall employ the notation $\overrightarrow{AB}$ for the vector directed from point A to point B.

Definition 1: Vectors possessing the same length and direction are said to be equal. Geometrically speaking, this means that the vectors in question are necessarily parallel or segments of the same straight line.

Definition 2: The sum of two vectors **A** and **B** is written **A** + **B** and is defined as the vector represented by the diagonal of a parallelogram of which **A** and **B** are adjacent sides. This is shown in figure 125.

Since from the figure we also have $\mathbf{B} = \overrightarrow{PQ}$, we see immediately that an alternate way of constructing **A** + **B** is to draw **B** from the terminus of **A** and recognize that **A** + **B** is then the vector directed from the initial point of **A** to the terminus of **B**.

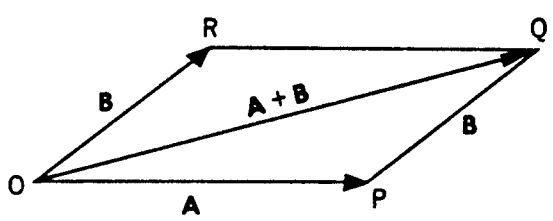

Figure 125. — Vector Parallelogram

Also, from the figure, we note that

$$\overrightarrow{OP} + \overrightarrow{PQ} = \overrightarrow{OR} + \overrightarrow{RQ},$$

which expresses the fact that vector addition is commutative. Thus,

$$\mathbf{A} + \mathbf{B} = \mathbf{B} + \mathbf{A}.$$

The reader may convince himself, by drawing an appropriate figure, that the associative law also holds for vector addition:

$$(\mathbf{A} + \mathbf{B}) + \mathbf{C} = \mathbf{A} + (\mathbf{B} + \mathbf{C}).$$

The sum of any number of vectors may now be obtained by constructing a broken line whose component segments are the vectors in question; the sum vector will then be directed from the beginning to the end of the broken line.

Definition 3: The negative of a vector is defined as a vector of the same length but of opposite direction. Thus $-\overrightarrow{AB} = \overrightarrow{BA}$ and $-(-\overrightarrow{AB}) = \overrightarrow{AB}$. To subtract the vector **B** from the vector **A**, amounts then to forming the sum **A** + (− **B**). In figure 125, **A** − **B** would be given by the vector $\overrightarrow{RP}$.

Definition 4: The product $a\mathbf{A}$ or $\mathbf{A}a$ of a vector **A** and a real number a is defined as a vector whose length is $|a|$ times that of **A** and whose direction is the same as that of **A** if $a > 0$, opposite to that of **A** if $a < 0$.

Multiplication of vectors by real numbers is commutative, associative, and distributive. This is reflected in order by the following equations:

$$a\,\mathbf{A} = \mathbf{A}\,a$$

$$(ab)\,\mathbf{A} = a\,(b\mathbf{A})$$

$$(a + b)\,\mathbf{A} = a\,\mathbf{A} + b\,\mathbf{A}.$$

The product of the sum of two vectors by a number also is distributive:

$$a\,(\mathbf{A} + \mathbf{B}) = a\,\mathbf{A} + a\,\mathbf{B}.$$

In summary, we may say that so far as addition, subtraction, and multiplication by real numbers is concerned, vectors may be operated upon formally, using the rules of ordinary algebra.

A.2 Vector Algebra—Scalar and Vector Products

The product of one vector by another may lead to a scalar or to a vector quantity depending upon what type of product is specified. Two types of product are defined: the scalar or "dot" product and the vector or "cross" product. For vectors **A** and **B**, these products are denoted by $\mathbf{A} \cdot \mathbf{B}$ and $\mathbf{A} \times \mathbf{B}$.

1. Scalar Product

Definition 5: The scalar product $\mathbf{A} \cdot \mathbf{B}$ is defined by

$$\mathbf{A} \cdot \mathbf{B} = AB \cos (\mathbf{A}, \mathbf{B}),$$

where $(\mathbf{A}, \mathbf{B})$ is the angle included between **A** and **B**, $(0^\circ \leq (\mathbf{A}, \mathbf{B}) \leq 180^\circ)$.

It will be noted that $\mathbf{A} \cdot \mathbf{A} = A^2$. Thus the scalar product of a vector by itself gives the square of its length. Also, if **A** is a unit vector, i.e., $A = 1$, then $\mathbf{A} \cdot \mathbf{B}$ will give the directed length of the projection of **B** upon the line of **A**. Since the defin expression for $\mathbf{A} \cdot \mathbf{B}$ is symmetric in **A** and **B**, it follows that scalar multiplication of vectors is commutative:

$$\mathbf{A} \cdot \mathbf{B} = \mathbf{B} \cdot \mathbf{A}$$

Using the definition for dot product, it also can be shown that scalar multiplication is distributive with respect to addition:

$$\mathbf{A} \cdot (\mathbf{B} + \mathbf{C}) = \mathbf{A} \cdot \mathbf{B} + \mathbf{A} \cdot \mathbf{C}.$$

A useful formula for evaluating $\mathbf{A} \cdot \mathbf{B}$ can be written when **A** and **B** are each referred to a right-handed orthogonal set of unit vectors as the basic coordinate system. Thus, if **i**, **j**, **k** are unit vectors so oriented that a rotation of **i** into **j** appears counterclockwise when viewed from the terminus of **k** and if the same can be said for rotations of **j** into **k** and **k** into **i** when viewed from the termini of **i** and **j**, respectively, the ordered triple $[\mathbf{i}, \mathbf{j}, \mathbf{k}]$ forms a right-handed orthogonal set. If the components of **A** and **B** in the **i**, **j**, and **k** directions are denoted respectively by A_x, A_y, A_z, and B_x, B_y, B_z, then since $\mathbf{i} \cdot \mathbf{i} = \mathbf{j} \cdot \mathbf{j} = \mathbf{k} \cdot \mathbf{k} = 1$ and $\mathbf{i} \cdot \mathbf{j} = \mathbf{i} \cdot \mathbf{k} = \mathbf{k} \cdot \mathbf{j} = 0$, we find

$$\begin{aligned}\mathbf{A} \cdot \mathbf{B} &= (A_x\mathbf{i} + A_y\mathbf{j} + A_z\mathbf{k}) \cdot (B_x\mathbf{i} + B_y\mathbf{j} + B_z\mathbf{k}) \\ &= A_xB_x + A_yB_y + A_zB_z.\end{aligned}$$

2. Vector Product

Definition 6: The vector product $\mathbf{A} \times \mathbf{B}$ of two vectors **A** and **B** is a vector perpendicular to the plane of **A** and **B** and so oriented that the ordered triple $[\mathbf{A}, \mathbf{B}, \mathbf{A} \times \mathbf{B}]$ forms a right-handed orthogonal set. The magnitude of $\mathbf{A} \times \mathbf{B}$ is defined by $A\,B \sin (\mathbf{A}, \mathbf{B})$, where $0^\circ \leq (\mathbf{A}, \mathbf{B}) \leq 180^\circ$.

We note first, in the special case when $\mathbf{A} \parallel \mathbf{B}$, that $(\mathbf{A}, \mathbf{B})$ is 0° or 180° and hence that $\mathbf{A} \times \mathbf{B} = 0$. Thus, we may say that two non-zero vectors are parallel if and only if their cross-product vanishes.

From figure 125, it is immediately evident that the magnitude of $\mathbf{A} \times \mathbf{B}$ is represented geometrically by the area of the parallelogram determined by **A** and **B**. Also, if the order of **A** and **B** is reversed in $\mathbf{A} \times \mathbf{B}$, that is to say, if one considers the product $\mathbf{B} \times \mathbf{A}$, then to preserve the right-handedness of the triple $[\mathbf{B}, \mathbf{A}, \mathbf{B} \times \mathbf{A}]$ the direction of $\mathbf{B} \times \mathbf{A}$ must be opposite to that of $\mathbf{A} \times \mathbf{B}$. Thus,

$$\mathbf{A} \times \mathbf{B} = -\mathbf{B} \times \mathbf{A}$$

and we see that cross multiplication is not commutative. As we shall see below, cross multiplication is not associative either; that is,

$$(\mathbf{A} \times \mathbf{B}) \times \mathbf{C} \neq \mathbf{A} \times (\mathbf{B} \times \mathbf{C}),$$

but it is distributive with respect to addition:

$$\mathbf{A} \times (\mathbf{B} + \mathbf{C}) = \mathbf{A} \times \mathbf{B} + \mathbf{A} \times \mathbf{C}.$$

With A and B referred to a right-handed orthogonal coordinate system $[\mathbf{i}, \mathbf{j}, \mathbf{k}]$, we may derive a formula for

$$\mathbf{A} \times \mathbf{B} = (A_x\mathbf{i} + A_y\mathbf{j} + A_z\mathbf{k}) \times (B_x\mathbf{i} + B_y\mathbf{j} + B_z\mathbf{k})$$

by use of the distributive law and the relations

$$\mathbf{i} \times \mathbf{i} = \mathbf{j} \times \mathbf{j} = \mathbf{k} \times \mathbf{k} = 0,$$
$$\mathbf{i} \times \mathbf{j} = \mathbf{k}, \quad \mathbf{j} \times \mathbf{k} = \mathbf{i}, \quad \mathbf{k} \times \mathbf{i} = \mathbf{j}.$$

The result is

$$\mathbf{A} \times \mathbf{B} = (A_y B_z - A_z B_y)\mathbf{i} + (A_z B_x - A_x B_z)\mathbf{j} + (A_x B_y - A_y B_x)\mathbf{k}.$$

A more convenient form for remembering the latter is

$$\mathbf{A} \times \mathbf{B} = \begin{vmatrix} \mathbf{i} & \mathbf{j} & \mathbf{k} \\ A_x & A_y & A_z \\ B_x & B_y & B_z \end{vmatrix},$$

the determinant being expanded by minors according to the elements of the first row.

3. THE SCALAR TRIPLE PRODUCT, $\mathbf{A} \times \mathbf{B} \cdot \mathbf{C}$, is first of all a scalar since it is obtained by finding the dot product of the vectors $\mathbf{A} \times \mathbf{B}$ and $\mathbf{C}$. One can easily show that, when $\mathbf{C}$ has components C_x, C_y, C_z, the product $\mathbf{A} \times \mathbf{B} \cdot \mathbf{C}$ is given by the formula

$$\mathbf{A} \times \mathbf{B} \cdot \mathbf{C} = \begin{vmatrix} A_x & A_y & A_z \\ B_x & B_y & B_z \\ C_x & C_y & C_z \end{vmatrix}.$$

Geometrically, the numerical value of $\mathbf{A} \times \mathbf{B} \cdot \mathbf{C}$ represents the volume of the parallelopiped having $\mathbf{A}$, $\mathbf{B}$, $\mathbf{C}$ as concurrent edges. More precisely, it represents $\pm$ Volume according as the triple $[\mathbf{A}, \mathbf{B}, \mathbf{C}]$ is or is not a right-handed set. Indeed, from figure 126, we have

$$\begin{aligned} \mathbf{A} \times \mathbf{B} \cdot \mathbf{C} &= |\mathbf{A} \times \mathbf{B}|\,|\mathbf{C}| \cos\theta \\ &= (\text{area of base parallelogram})\ (\pm\ \text{Altitude}) \\ &= \pm\ \text{Volume}. \end{aligned}$$

Since cyclic permutation of the letters in $\mathbf{A} \times \mathbf{B} \cdot \mathbf{C}$ does not alter the parallelopiped we note that

$$\mathbf{A} \times \mathbf{B} \cdot \mathbf{C} = \mathbf{B} \times \mathbf{C} \cdot \mathbf{A} = \mathbf{C} \times \mathbf{A} \cdot \mathbf{B}.$$

From this we conclude that a given scalar triple product is left unchanged by interchanging the dot and the cross.

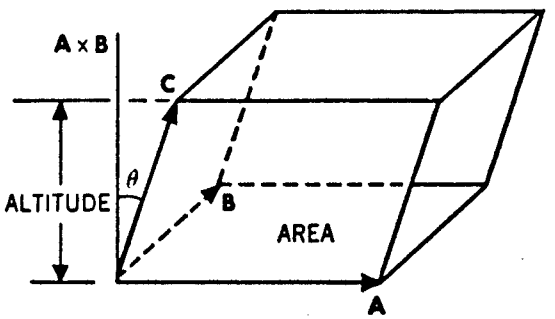

Figure 126. — Scalar Triple Product

4. THE VECTOR TRIPLE PRODUCT, $(\mathbf{A} \times \mathbf{B}) \times \mathbf{C}$ is a vector perpendicular to $\mathbf{A} \times \mathbf{B}$ and hence is coplanar with $\mathbf{A}$ and $\mathbf{B}$. It is easily verified that

$$(\mathbf{A} \times \mathbf{B}) \times \mathbf{C} = (\mathbf{A} \cdot \mathbf{C})\,\mathbf{B} - (\mathbf{B} \cdot \mathbf{C})\,\mathbf{A},$$

and

$$\mathbf{A} \times (\mathbf{B} \times \mathbf{C}) = (\mathbf{A} \cdot \mathbf{C})\,\mathbf{B} - (\mathbf{A} \cdot \mathbf{B})\,\mathbf{C}.$$

This shows, incidentally, that cross multiplication is not associative.

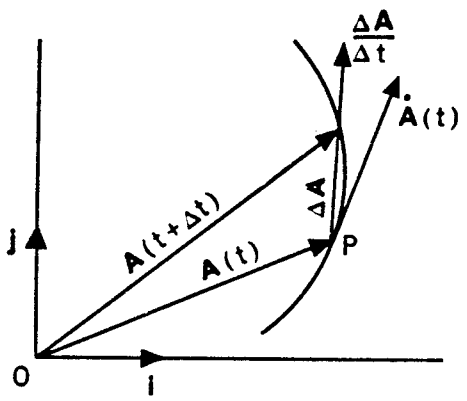

Figure 127. — Vector Differentiation

A.3 Vector Calculus—The Derivative

The derivative of a variable vector $\mathbf{A}(t)$ with respect to the scalar variable t is defined by

$$\dot{\mathbf{A}}(t) = \frac{d\mathbf{A}}{dt} = \lim_{\Delta t \to 0} \frac{\Delta \mathbf{A}}{\Delta t}$$

Where $\Delta \mathbf{A} = \mathbf{A}(t+\Delta t) - \mathbf{A}(t)$ is the increment vector representing the change in $\mathbf{A}(t)$ occasioned by a change Δt in t. The difference quotient $\frac{\Delta \mathbf{A}}{\Delta t}$, shown in figure 127, is then simply the secant vector which is $\frac{1}{\Delta t}$ times as long as $\Delta \mathbf{A}$. The limiting vector $\dot{\mathbf{A}}(t)$ is then tangent to the path traced by the terminus of $\mathbf{A}(t)$ as t varies.

If $\mathbf{A}(t) = A_x(t)\,\mathbf{i} + A_y(t)\,\mathbf{j}$, then the derivative with respect to the $|\mathbf{i}, \mathbf{j}|$ frame of reference, in which A_x and A_y are variable components, is

$$\dot{\mathbf{A}}(t) = \dot{A}_x(t)\,\mathbf{i} + \dot{A}_y(t)\,\mathbf{j}.$$

When $\mathbf{A}(t)$ is interpreted as the position vector of a moving point P and t as the time, then $\dot{\mathbf{A}}(t)$ and $\ddot{\mathbf{A}}(t)$ are respectively the velocity and acceleration of P. We note also that if $\mathbf{A}(t)$ is fixed in magnitude but variable in direction, then $\dot{\mathbf{A}}(t)$ will be perpendicular to $\mathbf{A}(t)$. Moreover, $\dot{\mathbf{A}}(t)$ will be given by the formula

$$\dot{\mathbf{A}}(t) = A(t)\omega\mathbf{T}$$

where ω is the angular speed of the rotating vector $\mathbf{A}$, and $\mathbf{T}$ is a unit vector perpendicular to $\mathbf{A}$ and advanced 90° from $\mathbf{A}$ in the direction of increasing angle θ (see figure 128). This follows from

$$\dot{\mathbf{A}}(t) = \frac{d\mathbf{A}}{d\theta} \cdot \frac{d\theta}{dt} = A\frac{d\mathbf{u}}{d\theta}\omega = A\omega\mathbf{T},$$

where $\mathbf{u}$ is a unit vector in the direction of $\mathbf{A}$, since $\frac{\Delta \mathbf{u}}{\Delta \theta} \to 1$ when $\Delta\theta \to 0$, as is well known from the calculus.

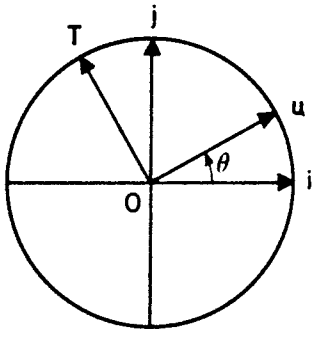

Figure 128. — Unit Vector and Its Derivation

The angular velocity of vector $\mathbf{A} = A\mathbf{u}$ denoted by $\boldsymbol{\omega}$, is a vector of magnitude $\omega = \dot{\theta}$ and of direction $\mathbf{u} \times \mathbf{T}$. Thus, the angular velocity of a rotating vector is another vector perpendicular to the plane in which the rotation takes place. Hence,

$$\text{(A.1)} \quad \boldsymbol{\omega} = \omega(\mathbf{u} \times \mathbf{T}) = \mathbf{u} \times \omega\mathbf{T} = \mathbf{u} \times \dot{\mathbf{u}}.$$

From Formula (A.1) it is easily established, upon taking the vector product of both sides with $\mathbf{u}$, that

$$\text{(A.2)} \quad \dot{\mathbf{u}} = \boldsymbol{\omega} \times \mathbf{u}.$$

Formula (A.2) is equally valid in the following, slightly more general, case:

Consider a rigid body rotating about a fixed axis passing through the fixed point O. Then if P is a fixed point of the rigid body not situated on the axis of rotation, the velocity of P is obtained by replacing $\mathbf{u}$ in (A.2) by the vector $\overrightarrow{OP}$. Thus,

$$\frac{d}{dt}(\overrightarrow{OP}) = \boldsymbol{\omega} \times \overrightarrow{OP},$$

where $\boldsymbol{\omega}$ is now the angular velocity of the rigid body about the fixed axis. This is seen to be an immediate consequence of (A.2) upon resolving $\overrightarrow{OP}$ into components along and perpendicular to the axis of rotation and then differentiating. The derivative of the component along the axis is obviously zero while the derivative of the component perpendicular to the axis is then found from (A.2).

A.4 Time Derivative of a Vector Referred to a Rotating Frame of Reference

The following theorem* in mechanics, here assumed without proof, is fundamental to our discussion:

THEOREM: If O is any point of a free rigid body, the velocities of its points are the same as if they were compounded of an instantaneous translation $\mathbf{V}$ and an instantaneous rotation $\boldsymbol{\Omega}$ about an axis through O; and $\boldsymbol{\Omega}$ is the same for any choice of O.

*See "Vectorial Mechanics" by Brand; John Wiley & Sons; p. 497.

Unlike the motion described in A.3., where the axis of rotation was fixed, here the axis of rotation passing through O varies from instant to instant. If P is another fixed point of the rigid body different from O, then at each instant the velocity of P relative to O is given by

$$\text{(A.3)} \quad \frac{d}{dt}(\overrightarrow{OP}) = \boldsymbol{\Omega} \cdot \overrightarrow{OP}.$$

Differentiating (A.4) we have

$$\dot{\mathbf{A}}(t) = \dot{A}_x\mathbf{i} + \dot{A}_y\mathbf{j} + \dot{A}_z\mathbf{k} + A_x\frac{d\mathbf{i}}{dt} + A_y\frac{d\mathbf{j}}{dt} + A_z\frac{d\mathbf{k}}{dt}.$$

Identifying $\overrightarrow{OP}$ in (A.3) successively with $\mathbf{i}$, $\mathbf{j}$, and $\mathbf{k}$, we obtain

$$\frac{d\mathbf{i}}{dt} = \boldsymbol{\Omega} \times \mathbf{i}\,; \quad \frac{d\mathbf{j}}{dt} = \boldsymbol{\Omega} \times \mathbf{j}\,; \quad \frac{d\mathbf{k}}{dt} = \boldsymbol{\Omega} \times \mathbf{k}.$$

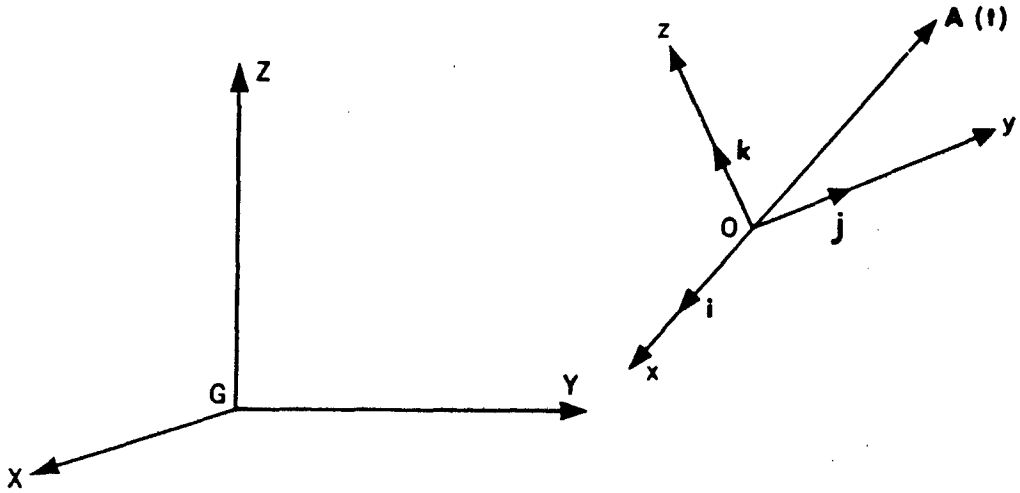

Figure 129. — Time Derivation of a Vector Referred to a Rotating Frame

In figure 129, let G-XYZ be a fixed system of coordinate axes and O-xyz a moving system, being rotated and translated relative to G-XYZ. Let $\mathbf{A}(t)$ be a vector which is at times to be referred to both systems of axes. We seek a formula for $\dot{\mathbf{A}}(t)$.

Let the vector $\mathbf{A}(t)$ in component form be

$$\text{(A.4)} \quad \mathbf{A}(t) = A_x\mathbf{i} + A_y\mathbf{j} + A_z\mathbf{k}.$$

Combining the above steps and simplifying, we find

$$\dot{\mathbf{A}}(t) = \dot{A}_x\mathbf{i} + \dot{A}_y\mathbf{j} + \dot{A}_z\mathbf{k} + \boldsymbol{\Omega} \times (A_x\mathbf{i} + A_y\mathbf{j} + A_z\mathbf{k}),$$

or,

$$\text{(A.5)} \quad \dot{\mathbf{A}} = \dot{A}_x\mathbf{i} + \dot{A}_y\mathbf{j} + \dot{A}_z\mathbf{k} + \boldsymbol{\Omega} \times \mathbf{A}.$$

When $\mathbf{A}(t)$ is fixed in magnitude, (A.5) reduces to (A.3).

Appendix B

CONVERSION TABLES

B.1 Introduction

Throughout this book it has been necessary to employ military terminology and for that reason it is convenient to have conversion tables which change military units to standard units and vice versa. Several such tables are listed in this appendix.

Table B.1

Conversion Table — Knots to MPH to FT/SEC

$$1 \text{ knot} = \frac{6080}{5280} \text{ MPH} = \frac{6080}{3600} \text{ FT/SEC}$$

$$1 \text{ knot} = 1.151515 \text{ MPH} = 1.688889 \text{ FT/SEC}$$

KNOTS	MPH	FT/SEC	KNOTS	MPH	FT/SEC	KNOTS	MPH	FT/SEC
200	230	338	350	403	591	500	576	844
210	242	355	360	415	608	510	587	861
220	253	372	370	426	625	520	599	878
230	265	388	380	438	642	530	610	895
240	276	405	390	449	659	540	622	912
250	288	422	400	461	676	550	633	929
260	299	439	410	472	692	560	645	946
270	311	456	420	484	709	570	656	963
280	322	473	430	495	726	580	668	980
290	334	490	440	507	743	590	679	996
300	345	507	450	518	760	600	691	1013
310	357	524	460	530	777	610	702	1030
320	368	540	470	541	794	620	714	1047
330	380	557	480	553	811	630	725	1064
340	392	574	490	564	828	640	737	1081

Table B.2

Conversion Table — MPH to FT/SEC to KNOTS

$$1 \text{ MPH} = \frac{5280}{3600} \text{ FT/SEC} = \frac{5280}{6080} \text{ KNOTS}$$

1 MPH = 1.466667 FT/SEC = .868421 KNOTS

MPH	FT/SEC	KNOTS	MPH	FT/SEC	KNOTS	MPH	FT/SEC	KNOTS
200	293	174	400	587	347	600	880	521
210	308	182	410	601	356	610	895	530
220	323	191	420	616	365	620	909	538
230	337	200	430	631	373	630	924	547
240	352	208	440	645	382	640	939	556
250	367	217	450	660	391	650	953	564
260	381	226	460	675	399	660	968	573
270	396	234	470	689	408	670	983	582
280	411	243	480	704	417	680	997	591
290	425	252	490	719	426	690	1012	599
300	440	261	500	733	434	700	1027	608
310	455	269	510	748	443	710	1041	617
320	469	278	520	763	452	720	1056	625
330	484	287	530	777	460	730	1071	634
340	499	295	540	792	469	740	1085	643
350	513	304	550	807	478	750	1100	651
360	528	313	560	821	486	760	1115	660
370	543	321	570	836	495	770	1129	669
380	557	330	580	851	504	780	1144	677
390	572	339	590	865	512	790	1159	686

Table B.3

Conversion Table — FT/SEC to MPH to KNOTS

$$1 \text{ FT/SEC} = \frac{3600}{5280} \text{ MPH} = \frac{3600}{6080} \text{ KNOTS}$$

1 FT/SEC = .681818 MPH = .592105 KNOTS

FT/SEC	MPH	KNOTS	FT/SEC	MPH	KNOTS	FT/SEC	MPH	KNOTS
300	205	178	600	409	355	900	614	533
320	218	189	620	423	367	920	627	545
340	232	201	640	436	379	940	641	557
360	245	213	660	450	391	960	655	568
380	259	225	680	464	403	980	668	580
400	273	237	700	477	414	1000	682	592
420	286	249	720	491	426	1020	695	604
440	300	261	740	505	438	1040	709	616
460	314	272	760	518	450	1060	723	628
480	327	284	780	522	462	1080	736	639
500	341	296	800	545	474	1100	750	651
520	355	308	820	559	486	1120	764	663
540	368	320	840	573	497	1140	777	675
560	382	332	860	586	509	1160	791	687
580	395	343	880	600	521	1180	805	699

Table B.4

Conversion Table — DEGREES to MILS

$$1 \text{ DEGREE} = \frac{\pi}{180}(1000) \text{ MILS} = 17.453293 \text{ MILS}$$

(The Fire Control Mil)

Degrees						Minutes		Seconds	
0	0.0000	60	1047.1976	120	2094.3951	0	0.0000	0	.0000
1	17.4533	61	1064.6508	121	2111.8484	1	0.2909	1	.0048
2	34.9066	62	1082.1041	122	2129.3017	2	0.5818	2	.0097
3	52.3599	63	1099.5574	123	2146.7550	3	0.8727	3	.0145
4	69.8132	64	1117.0107	124	2164.2083	4	1.1636	4	.0194
5	87.2665	65	1134.4640	125	2181.6616	5	1.4544	5	.0242
6	104.7198	66	1151.9173	126	2199.1149	6	1.7453	6	.0291
7	122.1730	67	1169.3706	127	2216.5682	7	2.0362	7	.0339
8	139.6263	68	1186.8239	128	2234.0214	8	2.3271	8	.0388
9	157.0796	69	1204.2772	129	2251.4747	9	2.6180	9	.0436
10	174.5329	70	1221.7305	130	2268.9280	10	2.9089	10	.0485
11	191.9862	71	1239.1838	131	2286.3813	11	3.1998	11	.0533
12	209.4395	72	1256.6371	132	2303.8346	12	3.4907	12	.0582
13	226.8928	73	1274.0904	133	2321.2879	13	3.7815	13	.0630
14	244.3461	74	1291.5436	134	2338.7412	14	4.0724	14	.0679
15	261.7994	75	1308.9969	135	2356.1945	15	4.3633	15	.0727
16	279.2527	76	1326.4502	136	2373.6478	16	4.6542	16	.0776
17	296.7060	77	1343.9035	137	2391.1011	17	4.9451	17	.0824
18	314.1593	78	1361.3568	138	2408.5544	18	5.2360	18	.0873
19	331.6126	79	1378.8101	139	2426.0077	19	5.5269	19	.0921
20	349.0659	80	1396.2634	140	2443.4610	20	5.8178	20	.0970
21	366.5191	81	1413.7167	141	2460.9142	21	6.1087	21	.1018
22	383.9724	82	1431.1700	142	2478.3675	22	6.3995	22	.1067
23	401.4257	83	1448.6233	143	2495.8208	23	6.6904	23	.1115
24	418.8790	84	1466.0766	144	2513.2741	24	6.9813	24	.1164
25	436.3323	85	1483.5299	145	2530.7274	25	7.2722	25	.1212
26	453.7856	86	1500.9832	146	2548.1807	26	7.5631	26	.1261
27	471.2389	87	1518.4364	147	2565.6340	27	7.8540	27	.1309
28	488.6922	88	1535.8897	148	2583.0873	28	8.1449	28	.1357
29	506.1455	89	1553.3430	149	2600.5406	29	8.4358	29	.1406
30	523.5988	90	1570.7963	150	2617.9939	30	8.7266	30	.1454
31	541.0521	91	1588.2496	151	2635.4472	31	9.0175	31	.1503
32	558.5054	92	1605.7029	152	2652.9005	32	9.3084	32	.1551
33	575.9587	93	1623.1562	153	2670.3538	33	9.5993	33	.1600
34	593.4119	94	1640.6095	154	2687.8070	34	9.8902	34	.1648
35	610.8652	95	1658.0628	155	2705.2603	35	10.1811	35	.1697
36	628.3185	96	1675.5161	156	2722.7136	36	10.4720	36	.1745
37	645.7718	97	1692.9694	157	2740.1669	37	10.7629	37	.1794
38	663.2251	98	1710.4227	158	2757.6202	38	11.0538	38	.1842
39	680.6784	99	1727.8760	159	2775.0735	39	11.3446	39	.1891
40	698.1317	100	1745.3293	160	2792.5268	40	11.6355	40	.1939
41	715.5850	101	1762.7825	161	2809.9801	41	11.9264	41	.1988
42	733.0383	102	1780.2358	162	2827.4334	42	12.2173	42	.2036
43	750.4916	103	1797.6891	163	2844.8867	43	12.5082	43	.2085
44	767.9449	104	1815.1424	164	2862.3400	44	12.7991	44	.2133

Table B.4 — Continued
Conversion Table — DEGREES to MILS

$$1 \text{ DEGREE} = \frac{\pi}{180}(1000) \text{ MILS} = 17.453293 \text{ MILS}$$

(The Fire Control Mil)

Degrees						Minutes		Seconds	
45	785.3982	105	1832.5957	165	2879.7933	45	13.0900	45	.2182
46	802.8515	106	1850.0490	166	2897.2466	46	13.3809	46	.2230
47	820.3047	107	1867.5023	167	2914.6999	47	13.6717	47	.2279
48	837.7580	108	1884.9556	168	2932.1531	48	13.9626	48	.2327
49	855.2113	109	1902.4089	169	2949.6064	49	14.2535	49	.2376
50	872.6646	110	1919.8622	170	2967.0597	50	14.5444	50	.2424
51	890.1179	111	1937.3155	171	2984.5130	51	14.8353	51	.2473
52	907.5712	112	1954.7688	172	3001.9663	52	15.1262	52	.2521
53	925.0245	113	1972.2221	173	3019.4196	53	15.4171	53	.2570
54	942.4778	114	1989.6753	174	3036.8729	54	15.7080	54	.2618
55	959.9311	115	2007.1286	175	3054.3262	55	15.9989	55	.2666
56	977.3844	116	2024.5819	176	3071.7795	56	16.2897	56	.2715
57	994.8377	117	2042.0352	177	3089.2328	57	16.5806	57	.2763
58	1012.2910	118	2059.4885	178	3106.6861	58	16.8715	58	.2812
59	1029.7443	119	2076.9418	179	3124.1394	59	17.1624	59	.2860
60	1047.1976	120	2094.3951	180	3141.5927	60	17.4533	60	.2909

Table B.5
Conversion Table — MILS to DEGREES

$$1 \text{ MIL} = \frac{180}{\pi} 10^{-3} \text{ DEGREES} = .057296 \text{ DEGREES}$$

Decimal Values of Degrees

	1000 Mils	100 mils	10 mils	mils	$\frac{1}{10}$ mil
1	57.2958	5.7296	.5730	.0573	.0057
2	114.5916	11.4592	1.1459	.1146	.0115
3	171.8873	17.1887	1.7189	.1719	.0172
4	229.1831	22.9183	2.2918	.2292	.0229
5	286.4789	28.6479	2.8648	.2865	.0286
6	343.7747	34.3775	3.4377	.3438	.0344
7	401.0705	40.1070	4.0107	.4011	.0401
8	458.3662	45.8366	4.5837	.4584	.0458
9	515.6620	51.5662	5.7566	.5157	.0516

Degrees, Minutes, and Seconds

	1000 mils	100 mils	10 mils	mils	$\frac{1}{10}$ mil
1	57°17′44.8″	5°43′46.5″	0°34′22.6″	0°3′26.3″	0°0′20.6″
2	114°35′29.6″	11°27′33.0″	1°8′45.3″	0°6′52.5″	0°0′41.3″
3	171°53′14.4″	17°11′19.4″	1°43′07.9″	0°10′18.8″	0°1′01.9″
4	229°10′59.2″	22°55′05.9″	2°17′30.6″	0°13′45.1″	0°1′22.5″
5	286°28′44.0″	28°38′52.4″	2°51′53.2″	0°17′11.3″	0°1′43.1″
6	343°46′28.8″	34°22′38.9″	3°26′15.9″	0°20′37.6″	0°2′03.8″
7	401°4′13.6″	40°6′25.4″	4°0′38.5″	0°24′03.9″	0°2′24.4″
8	458°21′58.4″	45°50′11.8″	4°35′1.2″	0°27′30.1″	0°2′45.0″
9	515°39′43.3″	51°33′58.3″	5°9′23.8″	0°30′56.4″	0°3′05.6″

Table B.6

CONSTANTS

VALUES		RECIPROCALS	
π	3.14159 26535 89793	$\frac{1}{\pi}$	0.31830 98861 83791
$\frac{\pi}{2}$	1.57079 63267 94897	$\frac{2}{\pi}$	0.63661 97723 67582
2π	6.28318 53071 79586	$\frac{1}{2\pi}$	0.15915 49430 91895
π^2	9.86960 44010 89359	$\frac{1}{\pi^2}$	0.10132 11836 42338
$\sqrt{\pi}$	1.77245 38509 05516	$\frac{1}{\sqrt{\pi}}$	0.56418 95835 47756
$\sqrt{\frac{\pi}{2}}$	1.25331 41373 15500	$\sqrt{\frac{2}{\pi}}$	0.79788 45608 02865
$\sqrt{2\pi}$	2.50662 82746 31001	$\frac{1}{\sqrt{2\pi}}$	0.39894 22804 01433
e	2.71828 18284 59045	$\frac{1}{e}$	0.36787 94411 71442
e^2	7.38905 60989 30650	$\frac{1}{e^2}$	0.13533 52832 36613
$\sqrt{e}$	1.64872 12707 00128	$\frac{1}{\sqrt{e}}$	0.60653 06597 12633
$\log 10^e$	0.43429 44819 03252	$\log_e 10$	2.30258 50929 94046

$g = 32.174$ ft/sec^2 = 10.725 yds/sec^2
$\rho = .07513$ lbs/ft^3 = .002335 slugs/ft^3
1 statute mile = 5280 ft. 1 nautical mile = 6080 ft.

1 radian = 57.29577 95130 82321 degrees.
1 degree = 0.01745 32925 19943 radians.

The Speed of Sound

Temperature C	Speed of Sound FT/SEC	Speed of Sound MPH
0°	1088	742
20°	1129	770
100°	1266	863
500°	1814	1237
1000°	2297	1566

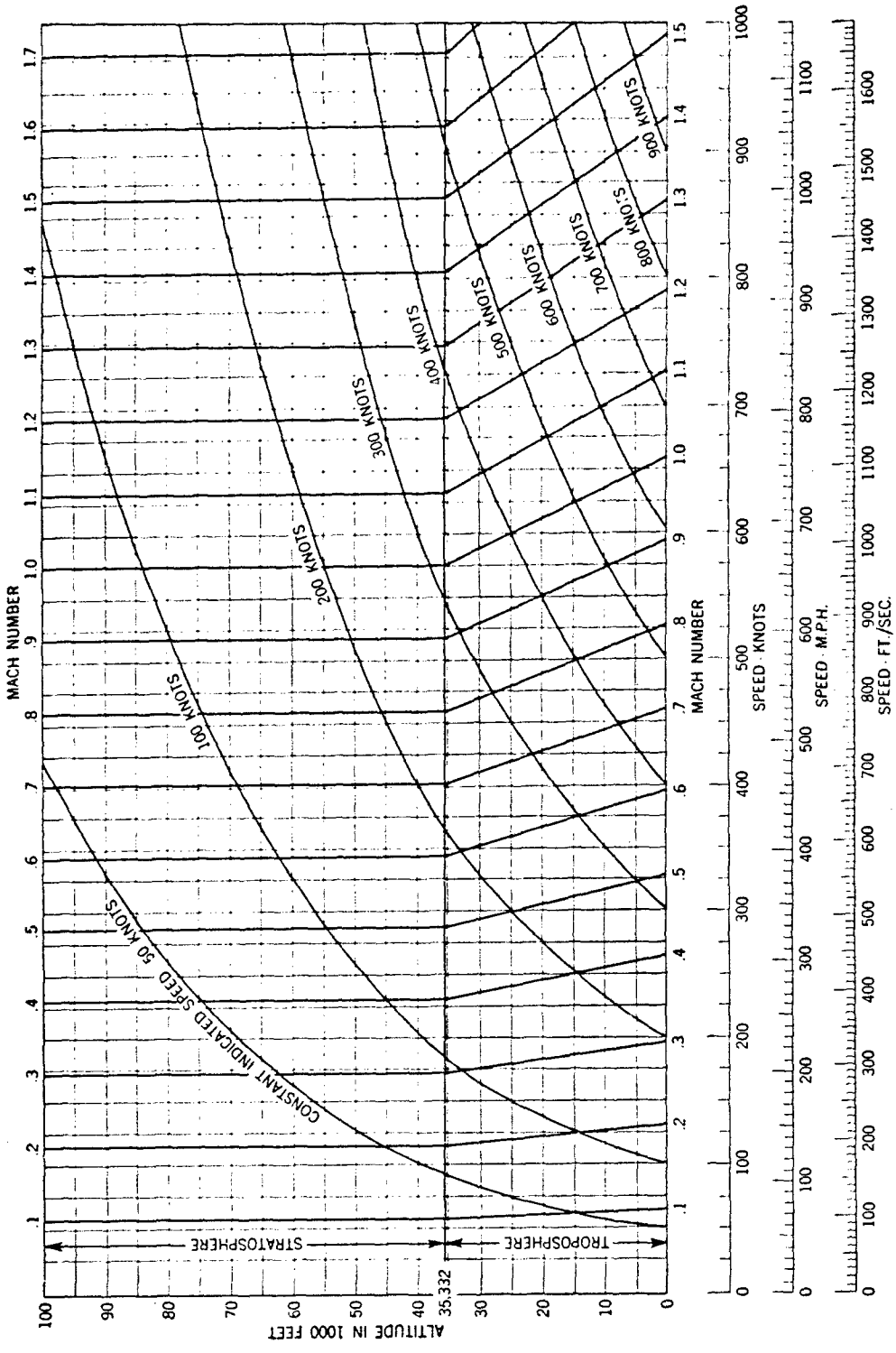

Figure 130. — Airspeed vs. Altitude

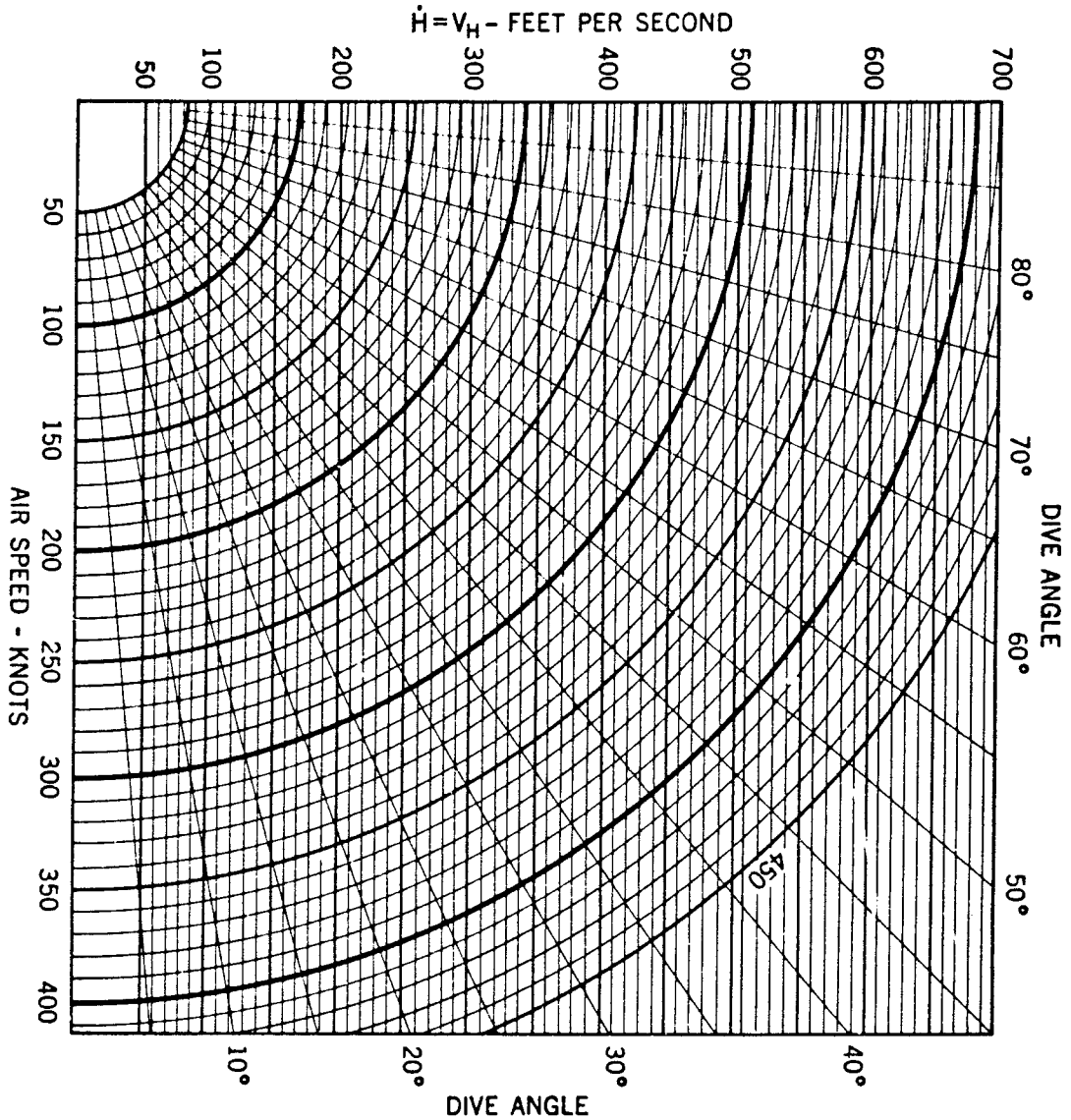

Figure 131. — Nomogram for Calculating Rate of Decrease of Altitude in a Dive

BIBLIOGRAPHY

(1) Bliss, G. A.; "Mathematics for Exterior Ballistics," John Wiley & Sons, Inc., New York, 1944.

(2) Fowler, R. H., Gallop, E. G., Lock, C. N. H., Richmond, H. W.; "The Aerodynamics of a Spinning Shell," Phil. Trans. Royal Society of London (A) Vol. 221, (1920) pp. 295 387.

(3) Hayes, T. J.; "Elements of Ordnance," John Wiley & Sons, Inc., New York, 1938, Chapter X.

(4) Hermann, E. E.; "Exterior Ballistics," U. S. Naval Institute, Annapolis, Maryland, 1935.

(5) Moulton, F. R.; "New Methods in Exterior Ballistics," University of Chicago Press, Chicago, 1926.

(6) Nielsen, K. L. and Synge, J. L.; "On the Motion of a Spinning Shell," Quarterly of Applied Mathematics, Vol. IV, No. 3, October, 1946. pp. 201-226.

(7) Handelman, G. H.; "Aerodynamic Pursuit Curves for Overhead Attacks," Journal of the Franklin Institute, March, 1949.

(8) Bonguer; "Sur de nouvelles courbes auxquelles on peut donner le nom de liques de poursuite" (Novel Curves Known as Pursuit Curves), Memoires de Math. et de Phys. de l'Academie Royale des Sciences (1732), pp. 1-14.

(9) Maupertius; "Sur les courbes de poursuite" (Pursuit Curves), Memoires de Math. et de Phys. de l'Academie Royale des Sciences (1732), pp. 15-17.

(10) Teixeira, G.; "Obras sobre mathematica" (Pure Mathematics), Vol. 5 Coimbra (1909), pp. 254 258.

(11) Loria, G.; "Ebene Kurven" (Two-Dimensional Curves), Second Edition, Vol. 2, Leipzig and Berlin (1911), pp. 241-247.

(12) Nobile, V.; "Sullo Studio intrensico delles curve di caccia" (Study on the transition of a Pursuit Curve), Rend. Circ. Mat. Palermo, Vol. 20, (1905), pp. 73 82.

(13) Mechler, E. A.; Russel, J. B.; Preston, M. G.; "The Absis for the Optimum Aided Tracking Time Constant"; Journal of the Franklin Institute, October, 1949.

(14) Morse, P. M.; Kimball, G. E.; "Methods of Operations Research"; OEG Report 54, Office of the Chief of Naval Operations, 7 May 1946.

(15) Davidson, Martin; "The Gyroscope and Its Applications"; Hutchinson's Scientific and Technical Publications; London, January, 1946.

(16) Brand, Louis; "Vectorial Mechanics"; John Wiley & Sons, February, 1930.

(17) Ordnance Pamphlet #649; "Theory and Operation of Bombsight Mark XV"; (Unclassified); U. S. Navy Bureau of Ordnance, October, 1941.

(18) Rosser, J. B.; Newton, R. R.; Gross, G. L.; "Mathematical Theory of Rocket Flight." McGraw-Hill Book Company, Inc., New York, 1947.

DISTRIBUTION

Requests for copies of NAVORD REPORT 1493 should be submitted on NAVEXOS 158, Stock Forms and Publications Requisition, through the District Publications and Printing Office by which requestor is serviced. *Catalog of Naval Shore Activities, Edition No. 18:*

List A2

Naval Material (5 copies)
Naval Research (5 copies)
Industrial Relations (5 copies)

List A3

CNO (5 copies)
Naval Records and Library (5 copies)

List A5

BuAer (10 copies)
BuPers (10 copies)
BuOrd (10 copies)
BuShips (2 copies)
BuSandA (2 copies)

List A6

(5 copies)

List B2

Senior Naval Member, Research & Development Board (2 copies)
Chief, Armed Forces Special Weapons Project (2 copies)

List B3

All (3 copies)

List B5

(2 copies)

List C1

Aberdeen (2 copies)
Guided Missiles School — Fort Bliss, Tex. (3 copies)
General Staff College, Fort Leavenworth, Kans. (3 copies)
U. S. Army Field Forces, Ft. Monroe, Va. (3 copies)
U. S. Army General School, Ft. Riley, Kans. (3 copies)
U. S. Military Academy, West Point (5 copies)

List C2

Air Material Center, Dayton, Ohio (3 copies)
Air Force Technical School, Keesler, Miss. (2 copies)
Tactical Air Command, Langley, Va. (2 copies)
Air Command Staff School, Maxwell, Ala. (3 copies)
Offutt Air Force Base, Nebr. (3 copies)
Air Tactical School, Panama City, Fla. (2 copies)

Experiment and Test Stations (10 copies)

Naval Engineering Experiment Station, Annapolis, Md.
David W. Taylor Model Basin, Carderock, Md.
Naval Aviation Ordnarce Test Station, Chincoteague, Va.
Naval Proving Ground, Dahlgren, Va.
Naval Ordnance Test Station, Inyokern, China Lake, Calif.
Naval Air Development Center, Johnsville, Pa.
Navy Mine Countermeasures Station, Panama City, Fla.
Naval Air Test Center, Patuxent River, Md.
Naval Air Missile Test Center, Pt. Mugu, Port Hueneme, Calif.
Naval Unit, White Sands Proving Grounds, Las Cruces, N. Mex.

Laboratories (6 copies)

Navy Underwater Sound Lab, Fort Trumbull, New London, Conn.
Naval Civil Eng. Resch and Eval Lab, Port Hueneme, Calif.
Special Devices Center, Office of Naval Research, Sands Point, Port Washington, L. I., N. Y.
Navy Electronics Laboratory, San Diego, Calif.
Naval Research Laboratory, Office of Naval Research, Anacostia, Washington, D. C.
Naval Ordnance Laboratory, White Oak, Md.

Schools (6 copies)

Naval Postgraduate School, Annapolis, Md.
Naval School General Line, Monterey, Calif.
Naval School, Academy and College Preparatory, Newport, R. I.
Marine Corps School, Quantico, Va.
Fleet Sonar School, San Diego, Calif.
Naval School Mine Warfare, Yorktown, Va.

G5A, G5D, K5A, K5B, K5D, J60, J95 (all 5 copies) except NOPI (100 copies)

U. S. Army, Washington, D. C. (5 copies)

U. S. Air Force, Washington, D. C. (10 copies)

U. S. Bureau of Standards, Washington, D. C. (3 copies)

Commercial Activities having Navy Contracts (1 copy)

Franklin Institute, 20th and Benjamin Franklin Pkwy., Philadelphia, Pa.
Specialties Ins., Skunks Misery Road, Syosset, L. I., N. Y.
M. ten Bosch, Inc., 80 Wheeler Ave., Pleasantville, N. Y.
Farrand Optical Co., Bronx Blvd. and E. 238th St., New York, N. Y.
Columbia Research & Development Corp., 4608 Indianola Ave., Columbus, Ohio
Librascope Inc., 1607 Flower St., Glendale 1, Calif.
Kearfott Co., Inc., Little Falls, N. J.
Poitras & Taplin, 198 Highland St., Holliston, Mass.
Jacobs Instrument Co., 4718 Bethesda Ave., Bethesda, Md.
Stavid Engineering, Inc., 312 Park Ave., Plainfield, N. J.
Arma Corp., 254 38th St., Brooklyn, N. Y.

American Hydromath Corp. (Attn. Mr. R. M. Kristal), 145 West 57th St., New York 19, N. Y.
Bendix Aviation Corp., 4855 4th Ave., Detroit 1, Mich.
Electric Indicator Co. (Attn. Mr. A. Block), Stamford, Conn.
Consolidated-Vultee Aircraft Corp., San Diego, Calif.
Emerson Electric Mfg. Co., 8100 Florissant Ave., St. Louis 21, Mo.
Melpar, Inc. (Attn. Mr. Tom Meloy), 452 Swann Ave., Alexandria, Va.
Norden Laboratories Corp., 121 Westmoreland Ave., White Plains, N. Y.
Minnesota Electronic Corp., 47 West Water St., St. Paul, Minn.

10 Aug. 51/2M/1

☆ U. S. GOVERNMENT PRINTING OFFICE : O—1952